THE SYNTHESIS OF LUBRICANT ADDITIVES FROM WASTE COMMODITY POLYMERS

GREGORY JAMES HUNT

THE SYNTHESIS OF LUBRICANT ADDITIVES FROM WASTE COMMODITY POLYMERS

BY

GREGORY JAMES HUNT

THE SYNTHESIS OF LUBRICANT ADDITIVES FROM WASTE COMMODITY POLYMERS

Thesis submitted for the degree of:

"Doctor of Philosophy", PhD

From work conducted in the Department of Chemistry at the University of Durham and at the BP Technology Centre, BP PLC.

The work was funded by the Engineering and Physical Sciences Research Council, UK, and BP PLC, UK, by a CASE doctoral training award.

Further financial support was generously provided by:

Collingwood College at the University of Durham

Royal Society of Chemistry

RSC | Advancing the Chemical Sciences

Macro Group UK

STATEMENT OF COPYRIGHT

DECLARATION

The work reported in this thesis was carried out in the Department of Chemistry at the University of Durham, Durham, UK and the BP Technology Centre, Pangbourne, UK between October 2006 and March 2010. All the work was carried out by the author unless otherwise stated, and has not previously been submitted for a degree at this or any other University.

Acknowledgements

Firstly, I must express my deepest gratitude to Prof. Neil Cameron who has always been on hand to guide, discuss and encourage with his expertise and for allowing me to attend an array of meetings and conferences. Neil's limitless patience in the writing of this Thesis also requires acknowledgement.

Having benefited from working in CG169 and CG234 there are many to thank; Dr. Matt Gibson (Gibbo) for setting me straight during my Masters project and for his organic chemistry skill. Dr's Fransico-Fernadez Trillo, Jon Fay and Sebastian Spain for all their insights into organic and polymer chemistry. David Ward Johnson (the Johnson) for many interesting conversations and being the butt of so many jokes. Kimmins for his enthusiasm and many a good night out in the New Inn or Spice Lounge. Paco, Gerledine and the Germans are thanked for the multitude of language lessons by the fume cupboards. Dr. Alison Parry for all her expertise and help, not to mention her impressive whistling skills. Dr. Ross Carnachan is thanked for providing so many memories, most notably the iPod/laptop incident and being the sole consistent member of the group during my time in Durham. Caroline is thanked for spicing up the dynamics of the lab, as is Lauren Cowie for her enthusiasm and wit.

Dr Lian Hutchings is thanked for all his discussions regarding SEC, and for not getting too mad after running it dry. Dr. Richard Thompson for running the Ion beam experiments. All the analytical staff, Alan, Ian, Mike, Jackie and Aileen.

Special mention should be made to Scott, Jon, Johnson and Lauren for providing me with friendship and encouragement which made weekend chemistry fun!

Dr. Gordon Lamb is thanked for all this patience and encouragement of new ideas and for making my time in Pangbourne so enjoyable. Dr. Andrew Smith for all his insights into chemistry.

I must thank my parents Eileen and Robert for all their help and support.

Finally, I must thank my fiancée Rachel; I couldn't have done it without you!

Table of Contents

INTRODUCTION: ASPECTS OF POLYMER SCIENCE; SYNTHESIS, DEGRADATION AND LUBRICATION. 1

AIMS AND OBJECTIVES 2

FUNDAMENTALS OF POLYMER SCIENCE 2

What is a polymer? *2*

How are polymers classified? *3*

What are the common features of a polymer? *4*

Classification according to method of manufacture *5*

POLYMER DEGRADATION 13

Methods of degradation *14*

Thermal Degradation *16*

Chemical Degradation *19*

Catalytic Degradation *19*

Superacids *22*

Biological Degradations *23*

Photodegradation[47] *25*

Microwave degradation *26*

Ultrasonic degradation[46, 48] *26*

Mechanical degradation[48] *27*

Use of Reactors *27*

LUBRICANT FORMULATION 29

Basics of Lubrication *29*

Lubricant Additives *37*

The Final Lubricant *47*

GENERATION OF FUNCTIONAL MATERIALS FROM WASTE PLASTIC 48

INTRODUCTION 49

RESULTS AND DISCUSSION 50

Initial investigation: the use of microwave assisted pyrolysis with a CEM Discover Microwave Reactor *50*

Biotage Initiator 60 Microwave pyrolysis system 59
Recycling of expanded polystyrene using Biotage Initiator 60 Microwave pyrolysis system 72
CONCLUSIONS 78
EXPERIMENTAL SECTION 79
General 79
Methods 80
LUBRICANT COMPONENTS FROM WASTE POLYSTYRENE AND CONVENTIONAL SOURCES 83
INTRODUCTION 84
Copolymerisation of maleic anhydride and styrene 85
RESULTS AND DISCUSSION 93
Effect of maleic anhydride on the fragmentation of cumyl dithiobenzoate. 99
Maleic anhydride addition to a Macro-RAFT agent. 104
Stearyl methacrylate copolymers 114
Polymerisation with N-maleimides 119
Coupling reactions 122
Reactions with degraded polystyrene 126
Microwave assisted synthesis of maleimides. 129
EXPERIMENTAL SECTION 131
General 131
Monomer synthesis 132
Macro-monomer synthesis. 133
Chain Transfer agent synthesis. 133
Polymer Synthesis 136
Post synthetic functionalisations 139
CONCLUSIONS 142
TESTING OF LUBRICANT COMPONENTS FROM WASTE POLYSTYRENE AND CONVENTIONAL SOURCES 144

INTRODUCTION 145
RESULTS AND DISCUSSION 145
Solubility *147*
Dispersancy *150*
Viscosity characteristics *162*
Thermal and Oxidative stability *166*
EXPERIMENTAL 169
Rheological Testing *169*
Kinematic Viscosity *169*
Oxidation and thermal stability *169*
CONCLUSIONS 170
CONCLUSIONS AND FUTURE WORK 173
CONFERENCE PRESENTATIONS 178
CONFERENCE ATTENDANCE (NON-PRESENTER) 178
AWARDS AND BURSARIES 179
REFERENCES 180

Table of Figures

Figure 1: Examples of naturally-occurring and man-made polymers 3
Figure 2: Examples of polymer architectures 3
Figure 3: The basis of chain reactions 6
Figure 4: A deactivation/activation cycle for the control of dormant species where, P_n is the propagating radical, K_{deact} is the deactivation rate constant, K_{act} is the activation rate constant. X is a species/ligand capable of reactivation. M is available monomer, k_p is the polymerisation rate constant. 9
Figure 5: A reversible transfer mechanism. 9
Figure 6: RAFT Polymerisation mechanism 12
Figure 7: Patents granted with controlled radical polymerisation in claim. Data from Scifinder scholar patent search. 13
Figure 8: Structural types of degradation 15
Figure 9: Polyethylene terephthalate (PET) depolymerisation 16
Figure 10:Proposed mechanism for the depolymerisation of Polystyrene in the presence of a base catalyst. 22
Figure 11 X-ray structure of $H(CB_{11}Cl_{11})$ 23
Figure 12: Common monomers of polybutenes 36
Figure 13: Examples of synthetic base oils, polyphenyl ethers and polysiloxanes 36
Figure 14: Common antiwar component Zinc dialkyldithiophosphates 39
Figure 15: Representation of an overbased detergent micelle 42
Figure 16: Typical polyisobutylene end groups 46
Figure 17:Diels-Alder reaction of maleic anhydride with butene type end groups 47
Figure 18:Alder ene reaction of maleic anhydride with propylene type end group 47
Figure 19:Schematic of the apparatus for the microwave bond cleavage process. A) Microwave generator. B) Supported catalyst dispersed in C) Hydrocarbon sample D) cold trap for liquid products E) Gas burette. 51

Figure 20: Proposed degradation pathway for polyethylene from reference[7]. 52
Figure 21: Graphical representation of the microwave degradation performed at a power of 300W over time. The relative percentage of each fraction is displayed. 55
Figure 22: Proposed Thermal degradation mechanism by Grassie and Scott ... 56
Figure 23: Typical ^{1}H NMR spectra from residual solid component from the microwave degradation of polystyrene 58
Figure 24: Photograph of Biotage Initiator 60 with modifications in place pre-vial selection 60
Figure 25: Photograph of Biotage Initiator 60 with modifications in place with vial loaded. 61
Figure 26: Vial failure 63
Figure 27: Graph of Pressure vs time for microwave degradations performed with Biotage initiator 60 microwave with a fixed power of 300W. The active carbon content was varied. Tmax = maximum temperature recorded. 64
Figure 28: Temperature vs time for microwave degradation of polystyrene with varying active carbon content. 65
Figure 29:Temperature vs time for degradation of polystyrene in diphenoxybenzene and 1,3-phenoxybenzene. 67
Figure 30: Reduction in M_n with time for virgin polystyrene M_n 170K. 68
Figure 31:Comparison of SEC trace at 30, 45 & 60 minutes of reaction. Power: 400W Solvent: naphthalene. 69
Figure 32: ^{1}H NMR spectra for 1) The waste polystyrene mixture prior to degradation 2) the residual waste product at 160minutes. 70
Figure 33:Polystyrene degradation reactions leading to terminal olefin formation 71
Figure 34: ^{1}H NMR Stack plot between 4.5-7.4ppm 1) Polystyrene 2) Degradation residue after 30minutes 3) Degradation residue after 60 minutes 4) Degradation residue for virgin polystyrene after 60 minutes. 73

Figure 35: Photograph of the waste residues post filtration in THF. left = 60 minutes, middle = 30 minutes, right = virgin polystyrene 60 minutes..... 74
Figure 36:a)Intramolecular Hydrogen Transfer b)unzipping c)intermolecular hydrogen transfera)Intramolecular Hydrogen Transfer b)unzipping c)intermolecular hydrogen transfer. 76
Figure 37: General expression of the reversible activation process 86
Figure 38: RAFT agent structure 87
Figure 39: Accepted Mechanism of RAFT polymerisation..... 90
Figure 40: Repeat units of Maleic anhydride and styrene ii) N-phenylenediamine maleimide and iii) stearyl methacrylate chain ended with maleic anhydride and styrene 93
Figure 41*: Schematic comparison of RAFT polymerisation and free radical polymerisation with identical conditions and the addition of maleic anhydride to the polymerisation at a given time. This demonstrates the advantages of using RAFT to place molecules or a defined number of molecules accurately both within a polymer chain and at the end of the chain.* 96
Figure 42*: RAFT copolymerisation of styrene and maleic anhydride.* 96
Figure 43*: ^{1}H NMR Stack Plot for the RAFT Polymerisation of Styrene with maleic anhydride (5mol%) added at t=0 and 150 minutes. Notice the disappearance of the maleic protons at 6.9ppm.* 97
Figure 44*: SEC chromatographs of the RAFT polymerisation of styrene and Styrene – maleic anhydride copolymer at sampling times of 300, 150, 90 minutes.* 98
Figure 45*: Photographs of the RAFT polymerisation of cumyl dithobenzoate with styrene and styrene maleic anhydride. Notice the colour difference over time. LHS = styrene only, RHS = Styrene and maleic anhydride.* 100
Figure 46*: Kinetic plots for the RAFT Polymerisation of styrene-alt-maleic anhydride, styrene, and styrene with maleic anhydride added at 30min.* 101
Figure 47: Kinetic plots for the RAFT Polymerisation of styrene-alt-maleic anhydride, styrene, and styrene with maleic anhydride added at 60 min. Time ajusted for the first 60minutes of reaction with maleic anhydride present 102

Figure 48*: Kinetic plots for the addition of maleic anhydride at t=0 and t=150 min, conversion was determined by offline ^{1}H NMR spectroscopy.* 103
Figure 49*: Kinetic plots for the addition of maleic anhydride at t=150 min. Conversion was determined by offline ^{1}H NMR spectroscopy.* 103
Figure 50*: RAFT polymerisation of styrene* 104
Figure 51*: Conversion vs Molecular weight (M_n) from table 8.* 106
Figure 52:Molecular weight vs conversion for the RAFT polymerisation of styrene in toluene, bulk and chloroform at 70°C. 106
Figure 53*: Temperature effects upon the inital rate of the RAFT Polymerisation of Styrene.* 108
Figure 54: Proposed reaction of RAFT Polystyrene with maleic anhydride to produce end capped polystyrene with maleic anhydride 108
Figure 55*: Comparison of the 125MHz ^{13}C NMR spectra showing 180-110ppm; top spectrum: RAFT polymerisation of styrene. Middle spectrum: RAFT polymerisation of styrene with maleic anhydride addition after 48h. Bottom spectrum: maleic anhydride monomer.* 109
Figure 56*: Disappearance of maleic anhydride over time by ^{1}H NMR spectroscopy.* 110
Figure 57: MALDI-MS data: Top: RAFT Polystyrene with maleic anhydride. Bottom: RAFT polymerisation of styrene 111
Figure 58: SEC chromatographs for the RAFT polymerisation of styrene (light-blue) macro-RAFT with maleic anhydride incorporation (red), macro-RAFT polymerisation with maleic anhydride followed by reaction with hexyl-1,6-diamine(green) and macro-RAFT polymerisation with maleic anhydride followed by reaction with hexyl-1,6-diamine then dithiotreitol (dark blue). . 112
Figure 59*: Possible reaction pathways for the observed doubling of molecular weight in the SEC experiment.* 113
Figure 60: RAFT polymerisation of stearyl methacrylate. 115
Figure 61: RAFT polymerisation of stearyl methacrylate with styrene and maleic anhydride. 117

Figure 62: SEC chromatograms for RAFT Polymerisation of stearyl methacrylate over time, note the addition of styrene after 270 minutes. 118
Figure 63: RAFT polymerisation of stearyl methacrylate block styrene 120
Figure 64: A plot of molecular weight vs conversion for the RAFT polymerisation of styrene and maleiomide. 121
Figure 65: N-phenylenediamine 122
Figure 66*: Coupling(polystyrene) end functionalised (maleic anhydride) with polyisobutylene-amine to form a coupled PIB-PS copolymers* 123
Figure 67: The functional groups that correspond to the functional groups in table 14 124
Figure 68: Examples of potential end group structures on the degraded polystyrene 126
Figure 69: 1H NMR stack plot for the addition of maleic anhydride to degraded polystyrene. 1) addition of maleic anhydride at t=O, 2) After 24 hours, 3) degraded polystyrene only 127
Figure 70*: Maleic anhydride functionalised waste polystyrene* 127
Figure 71: Coupling of maleic anhydride functionalised waste polystyrene with PIBamine 128
Figure 72*: Proposed mechanism of N-maleimide formation* 130
Figure 73*: Three methods to place maleic anhydride within a chain.* 143
Figure 74:The repeating groups for different dispersant types outlined in table 17 146
Figure 75: Rotational viscosity flow graph for candidate dispersants at a treat rate of 0.5wt% 153
Figure 76: Rotational viscosity flow graph for candidate dispersants at three different treat rates. 155
Figure 77: The relationship between dynamic viscosity and candidate dispersant concentration..... 155
Figure 78: Comparison of G' between 60-115^{o}C for the reference oil and the candidate dispersants 156
Figure 79: The effect of heating upon the viscous modulus 157

Figure 80: Comparison of the phase angle with temperature for reference and candidate dispersants 158
Figure 81: Wet mode ESEM images of reference oil. Soot agglomeration is clearly visible 160
Figure 82: wet mode ESEM images of the fresh oil 160
Figure 83: wet mode ESEM of reference oil with addition of 0.5wt% candidate dispersant 1. 161
Figure 84: wet mode ESEM of reference oil with addition of 0.5wt% candidate dispersant 4. 161
Figure 85: Oxidation induction time measurement. 167
Figure 86: Candidate dispersant 4 repeating group structure 170
Figure 87: Candidate dispersants 1 and 5 indicating the repeating group structure 171
Figure 88: Different N-malomides with potential interest 177
Figure 89: Example of self health polymer system from an end functionalised maleic amine thiol 177

Introduction: Aspects of Polymer Science; Synthesis, Degradation and Lubrication.

1

Aims and Objectives

This research aims to produce lubricant additives from waste commodity polymers while also exploring conventional lubricant additive synthesis and performance testing of synthetically derived additives. A synthetic strategy is sought to change from waste commodity polymer to useful lubricant additive. To set the scene for this research an introduction to the pertinent aspects of polymer science, polymer degradation and lubricant formulations is provided.

Fundamentals of Polymer Science

What is a polymer?

A polymer or macromolecule is a material of high molecular weight that is composed of constituent molecules - termed monomers - linked together, usually by covalent bonds[1]. For the vast majority of cases, these are long linear chains, however, they can be branched, hyperbranched, crosslinked, cyclic or even dentritic in nature. As with most concepts in chemistry, nature was the first to exploit the potential of high molar mass materials. The use of high molar mass materials as energy storage in the case of sugar into starch or glycogen is an example of polymerisation: the process of linking monomers together to make a polymer. The excellent stress stability of cellulose, which guarantees the shape and stability of so many of plant cells, is another of nature's examples. Bakelite (polyoxybenzylmethylenglycolanhydride), was one of the first manmade or synthetic polymers created and successfully commercialised. Formed from phenol formaldehyde resin, Bakelite found use in the manufacture of a large range of materials and is still used as a porcelain replacement material today[2].

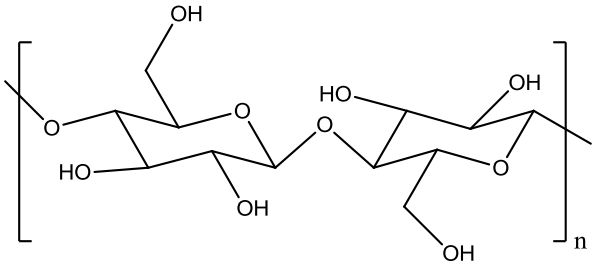

Cellulose
Naturally occuring polymer

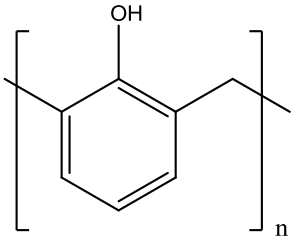

Phenol Formaldehyde Resin
(Bakelite)
Man made polymer

Figure 1: Examples of naturally-occurring and man-made polymers

How are polymers classified?

Three of the most common ways to describe and categorise polymers are their response to temperature - thermosets and thermoplastics; their method of manufacture – step or chain growth; and their structural type - linear, branched or network. Each classification has its own use to describe a situation or to aid with understanding[3].

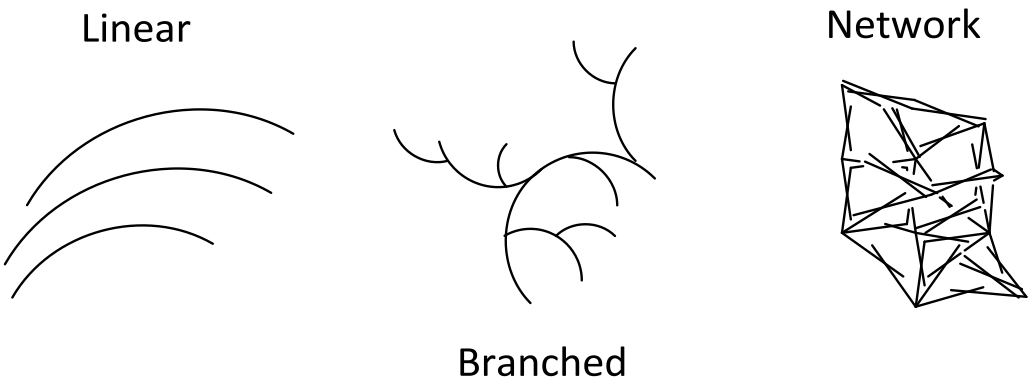

Figure 2: Examples of polymer architectures

What are the common features of a polymer?

As mentioned earlier it is the high molar mass of polymers that give them properties not observed with low molecular weight species; but that is only part of the story. Polymers are generally not discrete molecules and consist of mixtures of macromolecules of similar structure but different degrees of polymerisation and consequently molecular weight. The nomenclature used to describe the molecular weight of a polymer is based upon the molecular weight distribution.

The terms number average molecular weight (M_n), weight average molecular weight (M_w) and polydispersity index (PDI) are the most frequently used expressions for the comparison of different macromolecules. They describe the distribution of chain lengths within a macromolecule and are used to explain how the properties of a polymer are related to the average size of the molecules present.

M_n is defined as:

$$M_n = \frac{\sum N_i M_I}{\sum N_i}$$

where M_i. is the molar mass of the molecular species i and N_i is the number of molecules of i in the sample.

M_w is defined as:

$$M_w = \frac{\sum N_i M_i^2}{\sum N_i M_i}$$

with the polydispersity index or Inhomogenity ratio (PDI):

$$PDI = \frac{M_w}{M_n}$$

Classification according to method of manufacture

As mentioned previously, polymers can be classified according to their method of manufacture[4]. Generally there are two type of process.

Chain Growth Polymerisation

Chain growth polymerisations require an activated species (initiator or active centre) to enable polymerisation. Once an active species is created, monomers add one molecule at a time with the terminus of each added monomer becoming an active centre, enabling the process to continue. Species capable of generating active centres involve compounds which create radicals via homolytic bond cleavage, and are considered in the initiating step. From this point, chain growth can start as a cascade reaction with repetition of monomer addition and re- establishment of the active centre (propagation). Propagation of an individual macromolecule is arrested by either termination or transfer. In an anionic polymerisation an active chain end which bears an ionic charge, either positive (cationic) or negative (anionic) is required. Monomers suitable for polymerization by each of these mechanisms must be able to stabilize the charge for polymerisation to proceed[5, 6].

Termination leads to irreversible loss of the active centre, resulting in a dead chain. Usually termination occurs either by recombination, whereby a pair of propagating chains react to form a single chain of their combined lengths, or by disproportionation whereby one propagating chain abstracts a hydrogen from another resulting in two terminated chains, one with an unsaturated end-group, the other saturated. Transfer results in the growth of a second chain while the first one is terminated (transfer of the active centre to another molecule which is able to initiate further growth) and is conceptually the same

as the unsaturated chain created from disproportionation. Although the "dead" polymer is usually set to remain as such, the chain can continue to grow only when activated in a subsequent transfer step; this re- activation does not in general occur at the dead chain end, but somewhere else in the chain, with branched or cross-linked products the result. Although these stages are often written separately they all occur simultaneously soon after the beginning of the polymerisation[7].

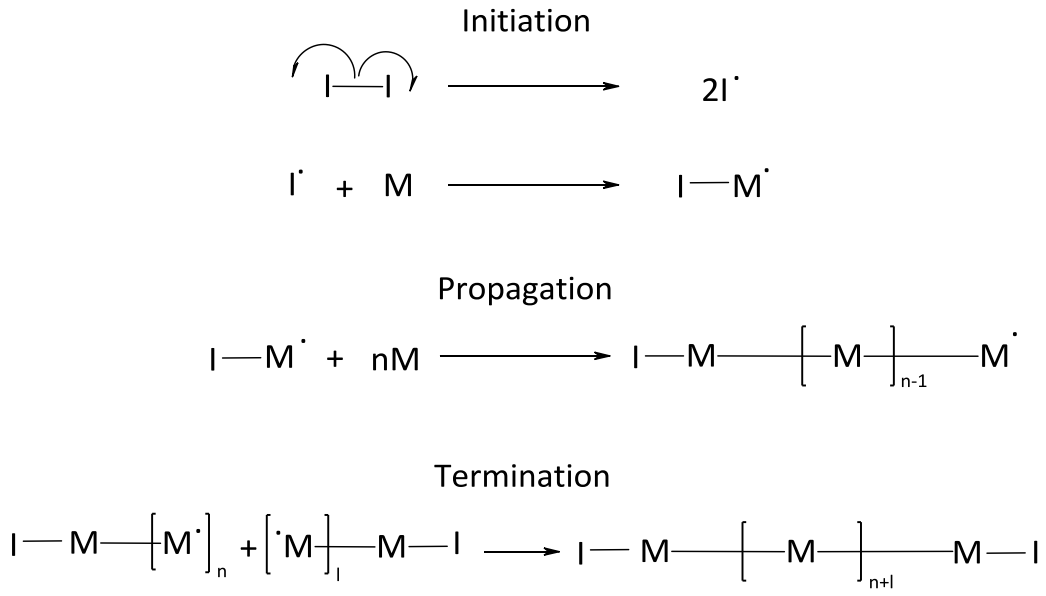

Figure 3: The basis of chain reactions

In summary, chain growth polymerisations require an activated species (initator or active centre) to enable polymerisation and the nature of the active centre leads to more classification, with chain growth polymerisations classified as radical, ionic (anionic & cationic) or transition metal mediated (coordinative, insertion) polymerisations[8].

Free Radical Polymerisation

Free-radical chain polymerisation, with its ability to polymerise a multitude of monomers in a wide range of polymerisation conditions and tolerance to

impurities and functional groups, has enabled the technique to become one of the most significant industrial polymerisation methods in use today.

As a chain growth polymerisation method, free radical (highly reactive unpaired electrons) polymerisations follow the same polymerisation mechanism: initiation, propagation and termination. Initiation in a free radical polymerisation is a two stage process involving the production of active radical centres. This formation of free radicals is achieved in several ways including thermal, redox and photochemical reactions. The primary radicals are produced by homolytic bond cleavage, typically of an azo or peroxide compound to form a pair of radicals. The second step is then the addition of this radical centre to a monomeric species to create an initial propagating radical. In this process homolytic cleavage is usually slow compared to addition to the monomeric species and is therefore considered to be rate limiting.

Propagation is the successive addition of monomer molecules to a radical that is not initiator derived. Each addition results in a radical identical to the previous one except that the chain is longer by one monomer unit. Propagation is extremely rapid, especially compared to initiation, and thereby results in long chain lengths even at low monomer conversion.

Termination is the irreversible reaction of the propagating polymer chain resulting in the loss of its radical.

The type of terminal group, average molecular weight and the molecular weight distribution are all affected by the proper choice of reaction conditions or the addition of low molecular weight compounds to the polymerisation. For example, an increase in the reaction temperature or the concentration of initiator in a radical polymerisation causes an increase in the number of growing radicals. The consequence of this is that because the rate of propagation is first order with respect to the concentration of growing radicals

and the rate of termination is second order, the average molecular weight distribution will be reduced. Although these properties can be controlled to a degree, targeted and narrow molecular weight polymers are difficult to achieve. Various techniques have been developed to improve free radical polymerisations, however the nomenclature used to describe processes that provide solutions to some of the limitations of free radical polymerisation are the subject of debate within IUPAC[9].

Controlled Free Radical (CRP) Polymerisation.

Controlled Free Radical Polymerisation, which is likely to be recommended to be referred to as reversible-deactivation radical polymerization[9] (RDRP), can trace its theoretical conception back to Szwarc *et al[10]* –who first observed a living polymerisation - a polymerisation that is free from termination or chain transfer. Although a controlled free radical polymerisation cannot claim to be free from termination or chain transfer, the superior product attributes associated with living polymerisations, namely molecular weight control; narrow molecular weight distribution; end-group control; and the ability to chain extend can also be achieved with controlled free radical polymerisations.

Controlled radical polymerisation introduces the concept of deactivation and activation of the propagating radicals. The reversible termination of a propagating radical species creates a dormant chain end. The dormant chain end is only active for a very short time to allow for monomer insertion into a labile bond. The establishment of a dynamic equilibrium between propagating radical and dormant species is the key aspect to control the polymerisation.

Dormant radicals are controlled in two similar ways, either in the form of a deactivation/activation cycle[11] shown in Figure 4, or by a reversible transfer mechanism, Figure 5.

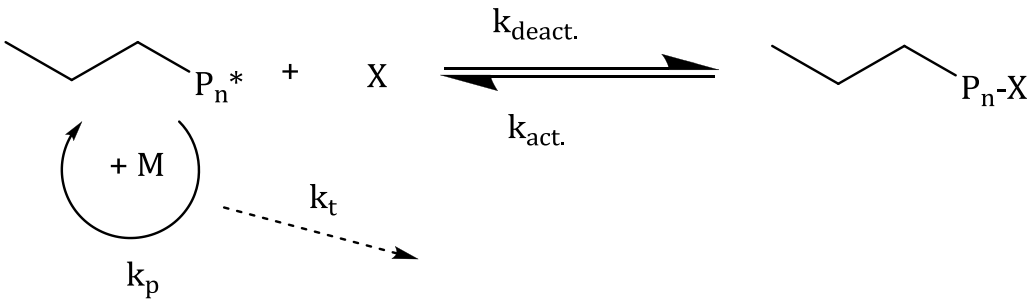

Figure 4: A deactivation/activation cycle for the control of dormant species where, P_n is the propagating radical, K_{deact} is the deactivation rate constant, K_{act} is the activation rate constant. X is a species/ligand capable of reactivation. M is available monomer, k_p is the polymerisation rate constant.

In a deactivation/activation cycle, propagating radicals are trapped by a species or ligand capable of reactivation. The reaction between the propagating radical and the reactivation species or ligand inhibits termination with each other. The deactivated species can be regenerated in a variety of ways, and the polymers produced using this method are end capped with this ligand or functional group.

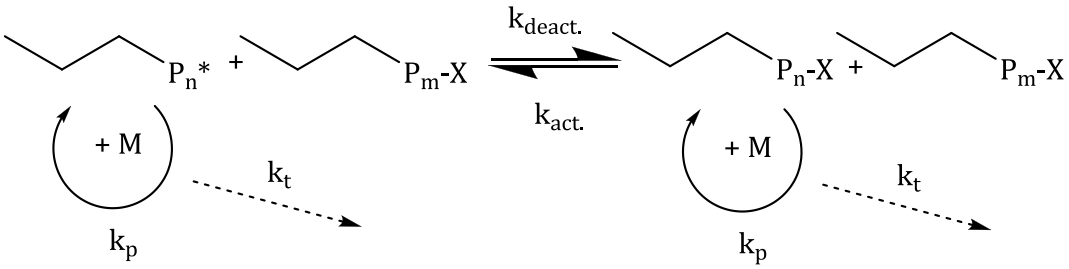

Figure 5: A reversible transfer mechanism.

A reversible or degenerative transfer mechanism is similar but has subtle differences to the deactivation/activation cycle. A chain transfer agent is used that acts as the deactivating species. Again, the propagating radicals are deactivated and reactivated by the transfer agent, creating control over the polymerisation reaction.

In all instances, the selectivity and control of the reaction relies on the ability of the propagating radicals to react with only a few monomer units before deactivation. It is the balance of k_p (propagation rate constant) and the kinetics of the deactivation mechanism and k_t (termination rate constant) which provide the control in these polymerisations.

In conventional radical polymerization, new chains are continually formed through initiation while existing chains are destroyed by radical-radical termination. The steady state concentration of propagating radicals is approximately 10^{-7} M and an individual chain will have a lifetime of only 1-10s before termination[12]. A consequence is that long chains are formed early in the process and (in the absence of other influences) molecular weights decrease with monomer conversion due to the depletion of monomer. In controlled free radical polymerization all chains are initiated at the beginning of the reaction and grow until all monomer is consumed unlike conventional radical polymerisations, the polymer chains are continually changing their molecular weight and chain length distributions with time. Therefore molecular weight increases linearly with conversion and the molecular weight distribution is narrow because the propagating species maintain the majority of chains in a dormant form which means the incidence of termination can be reduced relative to propagation.

Reversible Addition-Fragmentation Chain Transfer Polymerisation (RAFT)

In RAFT polymerisation no radicals are formed or destroyed during the chain equilibrium process as this is based upon transfer reactions. Therefore RAFT is an example of a reversible transfer mechanism. During the reaction, chains are alternatively converted from a propagating radical to polymeric transfer agents and vice versa, this process generating an equilibrium which enables incremental growth. The choice of the RAFT agent (the transfer agent) is crucial

for the success of the polymerisation. RAFT agents should have a high transfer constant for the monomeric species being polymerised, i.e. a high rate of addition and suitable leaving group. RAFT polymerisation has been shown to have a broad range of tolerance to polymerisation conditions. RAFT agents are chosen with the monomer in mind with a variable Z group in Figure 6. One of the great benefits of RAFT Polymerisations are relatively tolerant to moisture, and a wide range of reaction conditions however they are not tolerant towards oxygen[13].

Some disadvantages of RAFT polymerisations include the requirement to synthesize specific RAFT agents, in some cases requiring long synthetic strategies. The presence of sulfur at the polymer chain imparts a pink colouration into the polymers and can also be troublesome following post polymerisation transformations, i.e sulphur smells strongly.

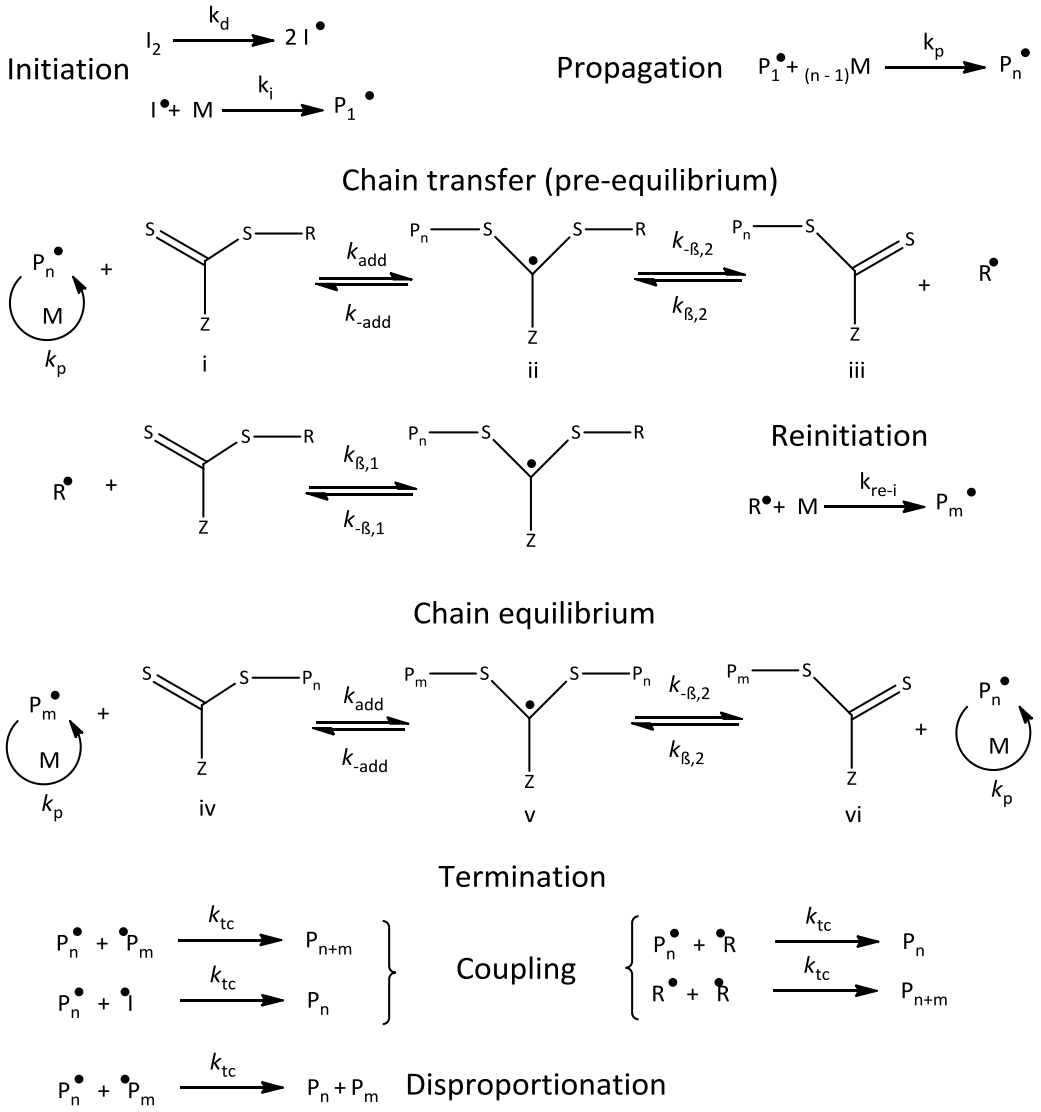

Figure 6: RAFT Polymerisation mechanism

RAFT and other controlled radical polymerisation process have attracted significant attention over the last decade, with figure 7 showing the number of patents granted involving controlled radical polymerisation.

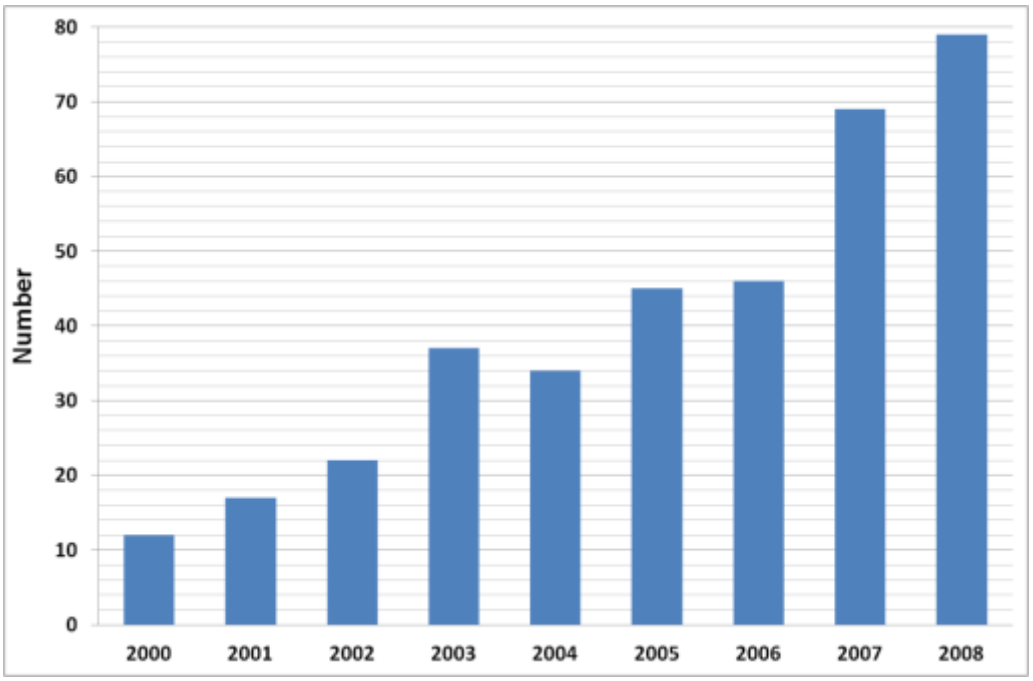

Figure 7: Patents granted with controlled radical polymerisation in claim. Data from Scifinder scholar patent search.

Polymer Degradation

Polymer degradation encompasses a series of events during which the physical, chemical and mechanical properties of a polymer change. Polymer degradation denotes changes in physical properties caused by chemical bond scission in the backbone of the macromolecule or by reaction with other chemical species. Scission and chemical reaction of pendent groups of linear polymers affect the physical properties only to a minor degree - relative to backbone scission - and for this reason are not considered as a degradation pathway.

Polymers are produced on an enormous scale globally and find use in a wide range of applications depending upon their structure and production cost. A study in 2000 commissioned by the Association of Plastics Manufactures in Europe (APME) and in 2011 by Plastics Europe found that 40% of all plastic produced is used for packaging[14]. Factor this into other short term applications in which plastics are used and this leads to a considerable amount

of plastic waste, which at present is not dealt with adequately. The majority of plastic waste is either incinerated - generating toxic substances - or placed in landfill sites where it can take many decades to decompose. It is estimated that 22% of the total volume of all landfill sites are occupied by waste plastics[15].

Clearly this cannot continue indefinitely, and so solutions must be found. A starting point is to increase our understanding and knowledge of how polymers degrade so, potentially, we can offer carbon friendly ways of dealing with plastic waste. There are both environmental and legal arguments that compel the study of polymer degradation: not least recent legislation by the European Union which requires plastics packaging in the EU to be at least 15% recyclable, a percentage which will only increase.

Conversion of waste to valuable chemicals has environmental and economic appeal and can be an alternative to incineration. However, the problems faced by the industry need to be addressed before significant amounts of chemical or tertiary recycling can enter the mainstream recycling sector. Economies of scale are vital and the process should be as economical as possible. The role of Government can improve the situation by indirect and direct means: educating people about the need for recycling; increasing the cost of landfill and incineration; reducing the tax burden of recycling companies and offering financial incentives such as grants.

Methods of degradation

In principle, all organic polymers are degradable; differing only in degradation mode and time. In practice, however, nearly all bulk polymers are inert materials. Polymer degradation refers to the scission of a chemical bond in the backbone of a macromolecule leading to a reduction in molecular weight. This broad definition encompasses a range of possibilities of how this can occur, so

for practical reasons it is useful to subdivide bond scission into the modes of initiation: thermal, chemical, photochemical, and biological degradation.

In addition to the mode of degradation it is worth noting the structural types of degradation; backbone scission, side or branching group scission and cross linker scission.

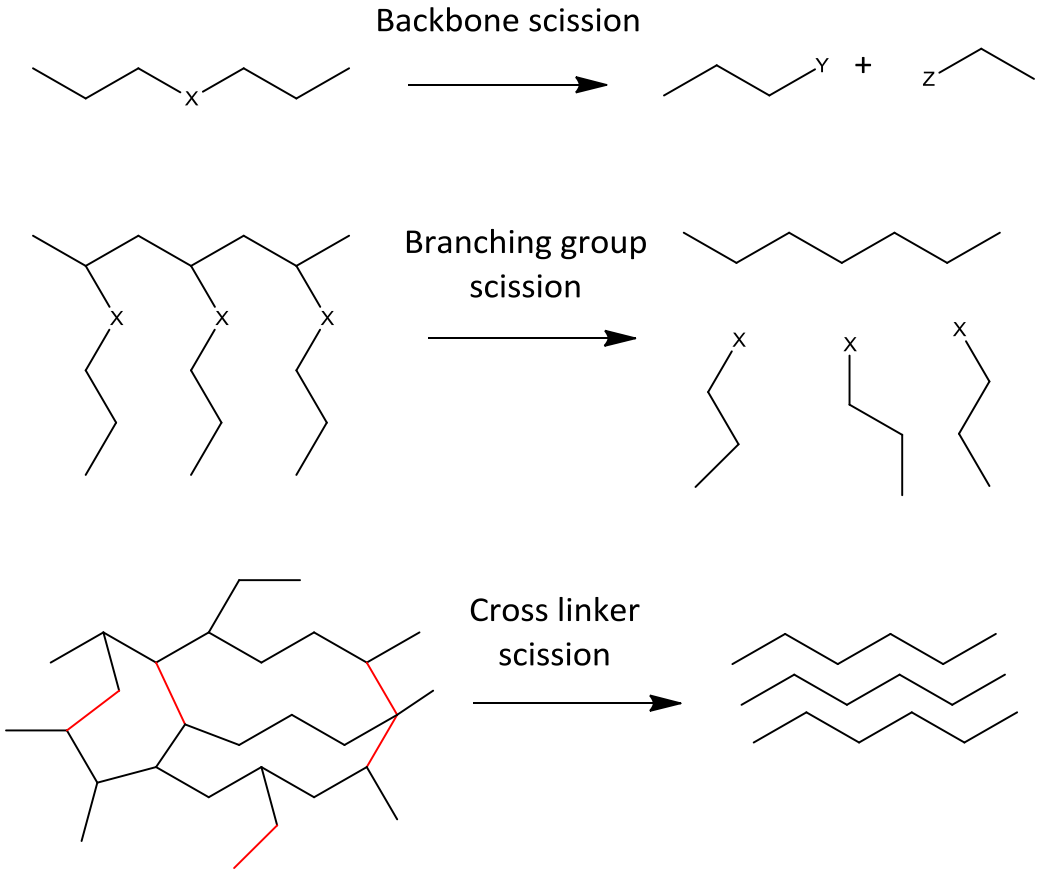

Figure 8: Structural types of degradation

Condensation polymers such as PET and polyamides can be broken down into their monomer units by depolymerisation processes[16]. In contrast, chain growth addition polymers (vinyl) such as polyethylene and polypropylene are very difficult to decompose to monomer, with the notable exception of poly(methyl methacrylate)[17] whereby depolymerisation is initiated by scission of head-to-head bonds, scission of the β-bond to chain end unsaturation and

also from main chain scission. The step growth addition polymerisation of urethane is also difficult to decompose to monomer.

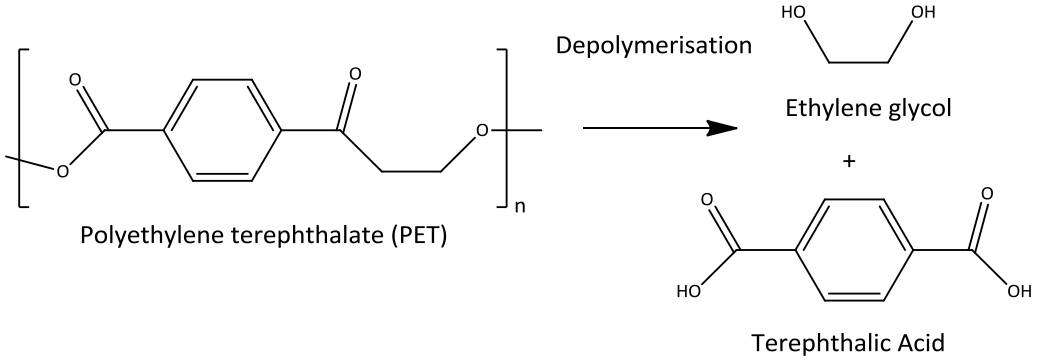

Figure 9: Polyethylene terephthalate (PET) depolymerisation

Thermal Degradation

Thermal degradation traditionally refers to the case where the polymer, at an elevated temperature, starts to undergo chemical changes without the simultaneous involvement of another compound. It should be noted that for most polymers, in the strictest sense, it is not possible to distinguish between thermal and thermo-chemical degradation, due to very few polymers being chemically “pure”. Impurities or additives are often present in virgin materials and recycled polymers will most certainly contain high concentrations of these species or will have suffered some degradation themselves. It is important to stress that thermal degradations carried out in an inert atmosphere (pyrolysis[18]) proceed via a different method than those in air (thermolysis[16]). Thermolysis is often considered exclusively as a thermal process in the literature although it is associated with chemical degradation. Thermal degradations are often carried out concurrently with other methods of initiation.

The scissions of chemical bonds under the influence of heat (and any other method of initiation) are a result of overcoming bond dissociation energies. Bond scission at room temperature is not feasible because at ambient temperature, thermal energies correspond to ~2.4kJ/mol. Typical single bond dissociation energies for combinations of C, O, H are in the order of 150-400kJ/mol. However, one should consider that vibrational energy is rapidly dissipated throughout all the molecules and all bonds and if the energy distribution is Maxwellian, then a certain fraction of bonds in some molecules will be in a highly excited vibrational state in comparison with bonds of the average energy state. Because the fraction of highly vibrationally excited bonds increases with increasing temperature, occasionally a repulsive energy level is reached and that bond breaks. Usually this occurs at temperatures between 400-600^{o}C, with bond scission between 150-300^{o}C less frequent[19]. However, at this temperature initiation of chemical processes such as oxidation which proceeds more rapidly at these temperatures can occur. This gives thermolysis a lower degradation temperature than pyrolysis.

Degradation is observed by molecular weight decrease and evolution of low molecular weight gaseous products. Intramolecular reactions such as cyclisation and elimination frequently occur, but for many linear polymers intramolecular crosslinking can also occur, observed by an increase in molecular weight. Depolymerisation is also possible but this depends on the structure of the polymer[20].

Thermolysis begins via an initiation step which produces the radical precursors.

$$PH \rightarrow P\bullet + H\bullet \qquad (1)$$

or

$$Polymer \rightarrow P\bullet + P\bullet \qquad (2)$$

The radical species produced can either be primary, secondary or tertiary carbon and depends specifically on the polymer's structure.

With oxygen present, a peroxy radical intermediate is produced during the propagating step:

$$P\bullet + O_2 \rightarrow POO\bullet \quad (3)$$

The highly reactive POO• is then able to abstract a labile hydrogen from another polymer molecule giving rise to the hydroperoxide species, along with another polymer radical.

$$POO\bullet + PH \rightarrow POOH + P\bullet \quad (4)$$

For most linear saturated hydrocarbon polymers hydrogen abstraction occurs preferentially from tertiary carbon atoms as they are the most able to stabilise the subsequent radical[21]. However, hydrogen abstraction can also take place at secondary and primary carbon atoms but with lower reaction rates. For polymers that contain unsaturation, the allylic position is the most likely place for hydrogen abstraction to occur due to the allylic C-H bond being weaker than the C-H bonds in ordinary sp^3 carbon centres and therefore more reactive.

Termination or deactivation:

$$POO\bullet + POO\bullet \rightarrow POOOOP (\rightarrow POOP + O_2) \quad (5)$$

$$POO\bullet + P\bullet \rightarrow POOP \quad (6)$$

$$P\bullet + P\bullet \rightarrow PP \quad (7)$$

In most polymers the rate of this step in the chain reaction determines the overall rate of oxidation[22]. This method is often referred to as autoxidation. Oxyl radicals, PO*, also play a deleterious role with respect to main chain scission, (β-scission).

Chemical Degradation

In its strictest sense, chemical degradation refers exclusively to processes which are induced under the direct influence of chemicals brought into contact with the polymer. This is a spontaneous event, however the rate of this reaction is strongly associated with temperature and certain chemical degradations will only occur at elevated temperature because of the high activation energy.

Catalytic Degradation

The catalytic cracking of polymers has attracted great interest in the last 20 years, partly because of the poor selectivity of thermal degradation. Methods of selective degradation of carbon-carbon bonds - particularly at ambient temperature - are scarce at best, so some degree of thermal cracking is required in the process. The use of catalysts does not only increase selectivity, it reduces the pyrolysis temperature; lowers the activation energy; increases the process efficiency; reduces the energy consumption and increases the quality of the products produced. This leads to more consistent hydrocarbon products.

Catalysts with acidic surface sites and proton-donating ability enhance the isomerisation of degradation products which increases the octane rating and the quality of the fuel in feedstock recycling[23-26]. However, strong acid sites and large pore sizes both lead to faster deactivation of the catalyst. Catalytic

methods are often combined with pyrolysis techniques in high temperature reactors. It is preferable to use catalysts with mild acidity and long life because pyrolysing with a catalyst leads to the formation of coke, which in turn deactivates the catalyst over time.

There are considerable differences in the selectivities of catalysts[27]. Zeolite catalysts are microporous materials having a maximum pore size of approximately 0.75 nm[28]. HZSM-5, a zeolite acid catalyst with large external surface area and strong acid sites, promotes the end chain scission reactions of polyolefins, which results in mainly short chain hydrocarbon species[29, 30]. Heavier products are produced using the mesoporous HMCM-41 because of its larger pore size and mild acidity combination resulting in random scission[31]. HZSM-5 promotes the cracking of polyethylene with high yields into both gaseous and aromatic hydrocarbons; whereas REY zeolite leads to a mixture of hydrocarbons with boiling points within the range of commercial gasolines in the catalytic conversion of a heavy oil feed, obtained by a previous polyethylene thermal cracking. This fact is responsible for the appearance of steric hindrances in the cracking of bulky polymeric molecules; it has also been found in the catalytic cracking of polypropylene over HZSM-5 zeolite[32]. One major drawback in the use of zeolites in polymer degradation of mixed plastic waste is their sensitivity to HCl, which causes destruction of the catalyst in concentrations above 200ppm.

Many approaches involve a transition metal species capable of activation of a hydrocarbon via oxidative addition of C-H to the co-ordinately unsaturated metal centre.

Clays of layered silicate framework with metal ions inside have also been used as effective cracking catalysts. Manos *et al*[30]., showed that two natural clays were able to decompose polyethylene into ~ 70% heavy liquid fraction. The

authors attribute this to the mild acidity of the clays, because in comparison to other more acidic catalysts, overcracking occurs.

Malherbe *et al*.[28] have reported three types of base catalysts which are centred on layered double hydroxides (LDH). LDH is a class of ionic lamellar solids with positively charged layers with two kinds of metallic cations and exchangeable hydrated gallery anions in the interlamellar space. LDHs are attractive catalysts due to the relative ease of their synthesis. In comparison to other catalysts LDHs produce heavier fractions from polymer degradation than with the zeolite HY. LDHs also show less coking than HY which is due to the non-occurrence of secondary hydrogen transfer reactions - HY produces a high level of isobutane which is indicative of a high level of secondary reactions. Recently the solvent-free synthesis of Zn–Al layered double hydroxides, Zn–Al LDH(Cl), by grinding solid ZnO and $AlCl_3.6H_2O$ and then autoclaving at 150^{o}C for 1 day without the addition of water and alkaline solution, has been reported by Chitrakar *et al*[33].

Zhang *et al*[34] used solid base catalysis to degrade polystyrene rather than more conventional methods of acid catalysis[35]. BaO was found to be the most effective for recovery of monomer and dimer. They conclude that the degradation of polystyrene was via a depolymerisation mechanism, the role of the base catalyst being the generation of carbanions in the initial stage of the degradation. They propose that the rate-determining step is the elimination of a hydrogen atom to generate carbanions, because the depolymerisation should proceed at a constant rate regardless of catalyst used. The rate of degradation is faster with base than acid catalysts. Little work has be carried out with regards to the mechanism of degradation of polystyrene using this catalytic method, however degradation is purposed to occur via the formation of the carbanion from the elimination of hydrogen atom from the backbone of the polymer. This allows for the carbanion to undergo further decomposition via β-scission to afford monomer[34].

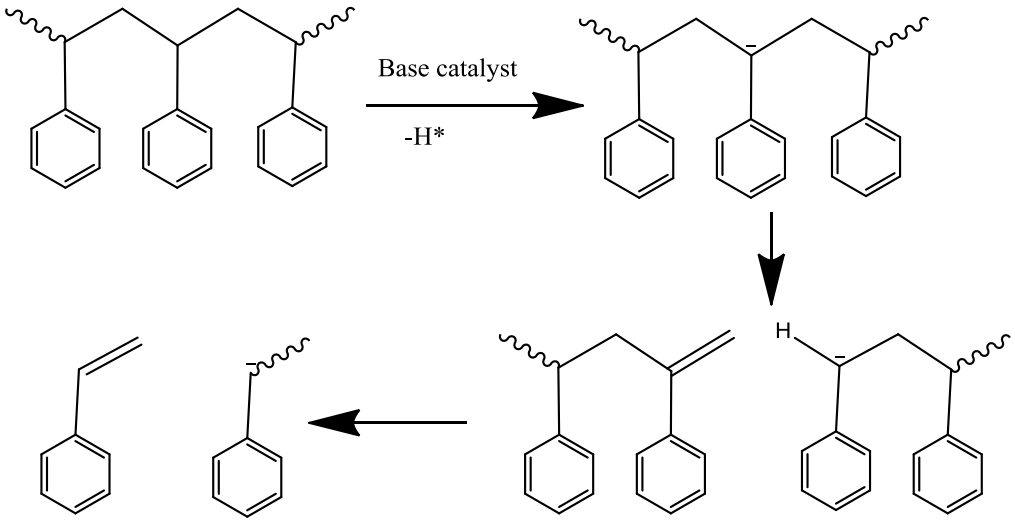

Figure 10:Proposed mechanism for the depolymerisation of Polystyrene in the presence of a base catalyst.

Superacids

A superacid is defined by an acidity greater than that of 100 wt% concentrated sulfuric acid[36]. Commercially available superacids include trifluoromethanesulfonic acid (CF_3SO_3H), also known as triflic acid, and fluorosulfuric acid (FSO_3H), both of which are about a thousand times stronger than sulfuric acid. The strongest superacids are prepared by the combination of two components: a strong Lewis acid and a strong Brønsted acid.

Carborane acids are a new type of superacid[37], described as soft but gentle[38]. For example conventional superacids[39] (e.g.$HFSO_3/SbF_5$) decompose fullerenes even at low temperatures, whereas carborane acids e.g. $H(CHB_{11}H_5Cl_6)$ cleanly protonate C_{60} at room temperature to give the isolable salt $[HC_{60}]$ $[CHB_{11}H_5Cl_6]$. As a class, carborane acids are stronger than previously known Lewis-free Brønsted acids (CF_3SO_3H, FSO_3H, etc.), and the carborane acid having 11 chlorine substituents on the boron cluster, $H(CHB_{11}Cl_{11})$, is presently the strongest and most robust[40]. It is estimated to have an acidity

many times that of magic acid[41], the first commonly named superacid. There is potential for these acids to be used in polymer degradation.

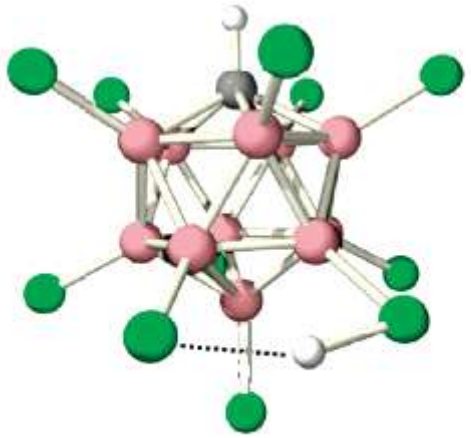

Figure 11 X-ray structure of $H(CB_{11}Cl_{11})$

$HF\text{-}BF_3$ superacid-catalyzed hydrocracking of tar has been reported by Strausz *et al*[42]. Although this is not polymer degradation, it does also offer a potential method of degradation for polymers. The proposed method of degrading/upgrading the tar involves an ionic mechanism, which is different to the mostly free radical methods of degradation discussed so far, and as the authors report it leads to different products from the upgrading process. However, there are one or two drawbacks with this method. Firstly, it requires a special reaction vessel because of the $HF\text{-}BF_3$ gas and it does leave fluorine incorporated into the mixture, albeit in very small amounts.

Biological Degradations

The terms biological and biodegradation have been used to include events occurring in both the natural environment and in the living human body. The degradation of polymers in a biological medium is a complex physio-chemical process, comprising the diffusion of the medium components in the bulk polymer and the transformation of chemically unstable bonds. Because

polyolefins have crystalline structures the degradation usually occurs on the surface of the material.

Micro-organisms produce a great variety of enzymes which are capable of reacting with natural and synthetic polymers. Biologically initiated degradation is strongly similar to chemical degradation in terms of the enzymatic attack of polymers, a chemical process which is induced in order to obtain food for the organism (with the polymer as a carbon source).

Although commercial chain polymers are normally resistant to biodegradation, when PE containing transition metals is peroxidised at 40-50^{o}C it can be used as a carbon source by thermophillic fungi[43]. It has been reported that fragmented PE in conjunction with fertilisers has had a beneficial effect on the growth rate of vegetables.

It should be noted that enzymes can be inactive on high molecular weight material and become active at later stages of degradation when the chain fragments become small and soluble in the surrounding fluids.

Nocardia sp. H17-1, an oil-degrading bacterium, has potential to be used in polymer degradation. Alkane hydroxylase, the enzyme responsible for attaching alcohol functionalities to alkanes, could potentially attach alcohol functionality to polyolefins to allow them to be further degraded. More information is known about this process than many other biological degradations as the enzyme is encoded by alkB gene. It is composed of a membrane bound non-heme iron monooxygenase structure[44].

Acinetobacter sp M-1 strain has been accredited as consuming n-alkanes up to C44, without the addition of other detergents. The authors also report that the emulsification of n-alkanes is one of the most important factors in microbial

degradation, postulating that increasing the elumisfication of n-alkanes would lead to longer n-alkane chains being an available food source[45].

Albertsson[46] believes that the future of this field remains uncertain while the definitions and nomenclature remain vague and not generally accepted. The experimentation is difficult and often imperfect because the work relates to very complex biological processes with multiple variables.

Polymer degradation by biological methods will most likely increase in the future, as there is currently a great deal of focus by plastic manufactures to replace current commodity polymers with degradable polymers. The problems faced are in meeting the properties of the current commodity polymers while reducing their functioning life. For example, if polyethylene were to be replaced in the packaging of food with biodegradable alternatives, then the environmental damage of deforestation and increased energy utilisation would result because twice the weight of polyethylene is required to package the same foodstock. It is clearly not a cost free option, and as world oil reserves begin to decline some tough decisions by governments around the world will need to be taken.

Photodegradation[47]

Photodegradation concerns the physical and chemical changes brought about by irradiation of polymers with UV or visible light. In order for this process to occur light must be absorbed by a substrate, so the presence of chemophoric groups is a prerequisite for this type of initiation. Absorption in a macromolecule consists of a specific interaction of a certain chemophoric group with a photon of given energy. The remainder of the macromolecule is unaffected during this absorption, therefore tailored degradations can potentially be achieved if we know the structure of the polymer and where the chemophoric groups lie. The use of lasers to induce photodegradation has

grown in the last 10 years; these emit coherent and monochromatic light. Prior to the use of lasers, mercury lamps were used because of their high emission intensities.

Saturated compounds containing sp^3 carbon-carbon, carbon-hydrogen and carbon-halogen bonds absorb light at $\lambda \leq 200nm$. Sp^2 carbons and carbonyls absorb above $\lambda = 200nm$, with a maximum between 200-300 nm. Although sp^2 double bonds absorb light, the chance of inducing chemical scission or change depends on the photophysical processes that follow that absorption[48].

Kemp *et al.* [49] applied UV irradiation to a 150 µm film of polystyrene for 500h. The FTIR results gave a broad absorption in the carbonyl region with a maximum at ca. 1743 cm^{-1}.

Microwave degradation

Microwave radiation has been shown to offer a means of degrading polymeric materials. The radiation is used in conjunction with a chemical species, frequently activated carbon [50, 51]. Tanner *et al*.[52] have shown methods for the selective degradation of long chain molecules and polyethylene to α-olefins. The method uses microwave power in conjunction with a catalyst and activated wood char. Selectivity for small molecules of up to 30% can be achieved[53, 54].

Ultrasonic degradation[46, 48]

Ultrasound is known to enhance chemical reactions as well as mass transfer at ambient temperatures and pressures. These effects are caused by cavitations, i.e. the collapse of microscopic bubbles in a liquid. The chemical effects of cavitation arise from the extreme conditions in the bubble (5000 K and 200

bar) and the high strain rates outside the bubble generated upon implosion. It has been shown that ultrasound-induced polymer breakage is a direct consequence of cavitation, because no degradation is observed under conditions that suppress cavitation. Ultrasound-induced polymer scission is a non-random process, as scission occurs approximately in the centre of the chain with scission processes stopping at a certain limiting molecular weight[55].

Mechanical degradation[48]

Mechanical degradation refers to macroscopic effects brought about by the influence of shear forces. It should be kept in mind that, under the influence of mechanical stress, low molecular weight organic materials generally exhibit different behaviour to polymers. Normally, low molecular weight molecules do not undergo chemical changes as a result of mechanical stress. For example, under shearing forces intermolecular interactions between certain molecules at certain sites in a specimen are disrupted and new interactions occur as a result of this displacement. This does not generally lead to the formation of free radicals, indicative of scission. However, in polymers, free radicals are generally detected after mechanical stress indicating ruptures of the chemical bonds.

Use of Reactors

Initial methods for the bulk degradation of polymers have been proposed by many companies and academics[23, 26, 56-67]. Thermal decomposition is the initial starting point for many investigations and technologies have been developed to upgrade plastic waste into valuable feedstock[68, 69]. The most developed technology is the bubbling fluidised bed reactor[70, 71] (FBR); with its main advantages of isothermicity, short residence times for the gaseous

stream and its ability to work effectively at ambient pressure. These give the FBR a significant advantage over rotary kilns[72, 73] and stirred tank reactors[74].

Prepared plastic feed is fed directly into the FBR which is heated to a temperature between 400-600^{o}C, usually in the absence of air. Under these conditions the plastics degrade or “crack” thermally to hydrocarbons that vaporise and leave the reactor with the fluidising gas. Impurities can be filtered out at this stage and the purified gas is cooled, to condense the hydrocarbon fractions. Generally, the lighter hydrocarbon gas is compressed, heated and returned to the reactor to act as the fluidising gas[74].

More recently however, new technologies have been developed to improve the solid-gas interface and avoid certain limitations of the FBR, which relate to the handling of sticky solid materials. The circulating fluidised bed reactor, circulated spear reactor and the tubular reactor are examples. It is also possible to connect two fluidised beds in series to further tailor the process and many such modifications of the FBR exist.

A major problem with catalysts in pyrolysis reactors is the formation of coke, which leads to deactivation of the catalyst. For this reason many systems position the catalyst outside the main reactor, for example in a secondary reactor where the pyrolysis oil is upgraded over a suitable catalyst. An example is REY (Ni-supporting rare earth metal exchanged Y-type zeolite)[75].

Rotary kilns have been used extensively because of their simple operation. However, they do have some drawbacks because of this simplicity: they suffer from poor heat and mass transfer and as a consequence temperature gradients exist within the reactor. This does not allow for consistent degradation of products[76-78]. They also require relatively long residence times, ca 20min., and coking is a problem for the reactor.

Lubricant Formulation

Basics of Lubrication

Lubrication is the use of a material to improve the smoothness of movement of one surface over another, with the material used being named the lubricant. The movement of one surface over another is resisted by a force, known as friction. If the friction is low and steady then there will be smooth easy sliding. However if the friction is great or uneven then the movement can become impossible, the surfaces can overheat, and/or be seriously damaged.

Lubricants, in addition to reducing or controlling friction, are usually expected to perform secondary functions such as reducing wear, preventing overheating and preventing corrosion. Modern engine development would have been impossible without advances in lubrication technology where the lubricant is required to lubricate, seal, control friction properties, prevent excessive wear and seizure of moving parts, protect against corrosion, keep surfaces and oil ways clear, cool and permit operation at extremes of temperature. Lubricants may be solids, liquids or gases: the most important property for a liquid lubricant being its viscosity.

Traditionally in engine oil formulation the approach has been to minimise or eliminate wear at the expense of a slight increase in average friction. Recently, however, the importance of reducing fuel consumption - especially in automotive engines - has lead to a change of emphasis. The target is now to achieve the lowest possible total friction. This is achieved with the use of less viscous lubricating oils. However, this requires the development of new additives to minimise the effects of increasing adhesive friction and wear.

Engine oil lubricants make up more than half of the world lubricant market and it is this section of the lubricant world that will be the focus of this report.

Base Oil Chemistry

The base oil or base stock is the largest component of a lubricant formulation by volume. Traditionally, the base oil is the neat mineral oil or refined petroleum fraction, however synthetic base oils have become popular because of their uniformity and reduction in cost over the last 10 years.

In motor oil lubrication the requirement of the base oil component of the lubricant has changed over time. Originally, the base oil required the correct viscosity and the absence of acidic components, changing to simply solvents or carriers for additives until it was recognised that some synthetic fluids with a uniform chemical structure offered superior performance to that of mineral base oils. However, the considerably higher price of these products hindered their introduction. This gave rise to semi-synthetic hydrocracked oils which matched the properties of synthetic hydrocarbons. Modern base oil development now focuses on the performance, environmental, and health and safety criteria. This leads to chemically more pure oils such as hydrocracked products, polyalphaolefins (PAOs) and esters.

There is still a wide range of mineral and synthetic motor oils available in domestic and world markets.

Mineral Oils

From the beginning of the petroleum industry, mineral oils have been used for lubricant base oils. Mineral oils are a complex mixture of hydrocarbons, mostly alkanes of various lengths, which are traditionally characterised by their

technical properties or by identification of groups of components with similar chemical character. For example, characterisation by carbon distribution in terms of the chemical bonds present: aromatic, naphthenic, and paraffinic. Other methods include the Aniline Point; a method for characterising the aromatic and paraffinic components of a base oil, and the Viscosity–Gravity Constant (VGC).

The process of converting crude oil into finished mineral base oil is referred to as refining. For mineral oils the actual refining process begins only after the distillation stages. In this context, refining is thus the term used to describe all the manufacturing stages after vacuum distillation.

Refining

The first stage of lubricant refining is fractional distillation, separating out compounds from the crude oil which approximately meet the viscosity grades ultimately required. This is a two step process involving atmospheric and vacuum distillation. The vacuum residue contains highly viscous hydrocarbons which distillation cannot separate from the asphalt that is present. An extraction process must be used to separate these highly viscous base oils. Extractive separation uses light hydrocarbons (propane to heptane), of which propane is the leading product for de-asphalting.

At this stage, the distillates still contain components which affect aging, viscosity, flowing characteristics, and components which are hazardous to health. To eliminate these disadvantages further refining methods have been developed, such as acid refining, solvent extraction and dewaxing, of which solvent refining has become the most accepted method over the past few decades.

Hydrogenation and Hydrocracking

Hydrogenation and hydrocracking influence the chemical structures of mineral oil molecules. Unstable molecules are chemically stabilized by the removal of heteroatoms (e.g. oxygen, sulfur, nitrogen) and hydrogenation converts aromatics into saturated naphthenic or paraffinic structures. In addition to the hydrogenation process, hydrocracking breaks -down or cracks larger molecules into smaller ones. Larger molecular structures can re-form from small fragments. The principal process criteria are temperature, pressure, catalyst and space velocity. If special conditions are met, a focal point of the process is the isomerization of paraffinic structures. Besides the saturation of aromatics, opening of the naphthene rings can occur.

It is clear that lubricant base oils can be much more easily tailored using these processes than is possible with simple solvent refining separation. The future of lubricant base oil production thus lies with hydrogenation and hydrocracking. An additional advantage of advanced hydrocracking is the lower dependence on the quality of the crude oil. Although the economic boundaries of solvent refining are set by yield (extract and paraffin quantities), altering hydrocracking process parameters can compensate for varying crude oil qualities.

Gas-to-Liquids (GTL)

Efforts to increase the value of natural gas have lead to the development of the chemical liquefaction of natural gas on the basis of the Fischer–Tropsch process. This process creates high-quality liquid products and paraffin wax. High-quality oils can then be obtained from natural gas by part oxidation, polymerization, and isomerisation.

The 80-year-old Fischer-Tropsch technology has attracted considerable attention in the last few years. The focus of this attention is the better utilization of natural gas. Syngas (CO and H_2) is made from methane, oxygen (air) and water vapor and this, in turn, is made into fluid and solid hydrocarbons in the Fischer-Tropsch reactor. The solid hydrocarbon waxes (> 99% paraffins) are hydrocracked, hydro-isomerisated and iso-dewaxed into super-clean base oils.

In principle, all carbon containing materials can be used for the production of liquid products and paraffin wax by Fischer–Tropsch process. Environmental concerns are addressed as with gasification and liquefaction of carbon, biomass, and even oil sands are of increasing interest. The advantage of lubricating base oils produced via the GTL process is the high quality at low (economic) cost. The oils produced using this process have excellent oxidation and thermal stability with tailor made viscosity grades.

Synthetic Oils

In contrast with mineral oils - which contain many different hydrocarbons and heteroatom-containing derivatives of these hydrocarbons, which require purification, refining and distillation - synthetic base oils are prepared by reaction of a few defined chemical compounds and tailored to their application by the choice of reaction conditions. Many of the synthetic base oils available today were developed decades ago, but their use on an industrial scale has increased only slowly because of their considerably higher cost than mineral oils. However, because of the rise in worldwide crude oil prices, synthetics have become economically more attractive and it is this, coupled with the desire of oil marketing companies to differentiate their products, rather than the chemical benefits which are leading to wider scale incorporation in lubricant formulation.

Originally, synthetic hydrocarbons were developed in Germany and the United States of America with the shortage of petroleum base stocks acting as the driving force. All synthetic hydrocarbons can be synthesized starting with ethylene. Ethylene itself is one of the most important petrochemicals and is mainly produced in steam crackers.

Polyalphaolefins (PAOs)

PAOs in a lubrication context are oligomers of ethylene, usually α-decene or a mixture of α-olefins containing, in general, between six and twelve carbon atoms. The oligomers are saturated (hydrogenated), and are aliphatic or branched paraffinic hydrocarbons. Oligomerization with Ziegler–Natta catalysts tends to yield a wide range of oligomers[79] that can be controlled more easily when a catalyst of the alkylaluminium halide–alkoxide–zirconium halide type is used[80, 81]. Boron trifluoride-based Friedel–Crafts oligomerization with alcohols as co-catalysts has also been achieved, however the mechanism is not fully understood. Free radical oligomerization of α--oolefins with peroxides as initiators is possible, however this method is not favoured because of the high activation energy, low yield, and poor quality of the PAOs produced. The next step of the manufacturing process comprises the catalytic hydrogenation of the unsaturated olefins. This is achieved with the aid of classical catalysts, e.g. nickel or palladium on alumina. In a third and final step the saturated oligomers are distilled.

PAOs satisfy some of the requirements of ideal hydrocarbon lubricants, namely that they should have linear chains, be completely saturated and crystallize at low temperatures. The viscosities, pour points and viscosity indexes of straight-chain alkanes increase with chain length. Branching gives increased viscosity and a decrease in pour point. The length and position of the side chains influence all three properties. When branching occurs in the middle of the main

chain, pour points are lower. Long side chains improve viscosity–temperature (V–T) characteristics. PAOs therefore have several advantages over mineral oils; narrow boiling ranges, very low pour points, and a viscosity index greater than 135 for all grades. The viscosity index of a fluid is an arbitrary measure of the change in viscosity with a rise in temperature. A high viscosity index fluid will indicate little or no change in viscosity with increasing temperature, where as a low viscosity index indicates a large change in viscosity with increasing temperature.

Comparison with equiviscous mineral oil in some oxidation tests without additives has shown some mineral oils seem superior to polyalphaolefins. This is because of the presence of natural antioxidants in the mineral oils that have survived the refining process. However, PAOs usually have low polarity, which leads to poorer solvency for very polar additives as well as causing problems with seals.

Other synthetic hydrocarbons

Polyinternalolefins (PIO) are rather similar to polyalphaolefins. Both kinds of hydrocarbon are prepared by the oligomerization of linear olefins. The difference is that polyinternalolefins are made from cracked paraffinic base stocks. Internal olefins are more difficult to oligomerize and the resulting products have VIs 10 to 20 units lower than the VIs of equiviscous polyalphaolefins .

Polybutenes (PBs) as synthetic consist mainly of isobutene and are, therefore, often also known as polyisobutenes (PIBs). They are produced by the polymerization of a hydrocarbon stream which contains isobutene and at least two other butenes and some butanes. It is a Lewis acid-catalyzed process which yields a copolymer with a backbone built mainly from isobutene units. At the end of the carbon chain there remains one double bond, which means

polybutenes are less resistant to oxidation than PAOs and PIOs. PIBs with molecular masses from about 300 to 6000 are important as VI improvers and are therefore included as an additive as well as a base stock.

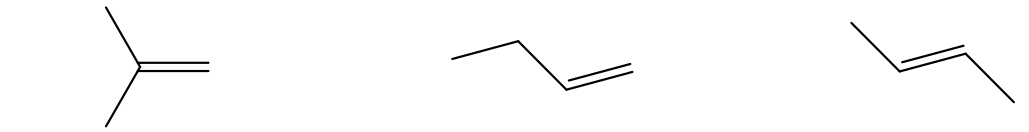

2-methylprop-1-ene or Isobutene | but-1-ene | (*E*)-but-2-ene

Figure 12: Common monomers of polybutenes

Alkylated aromatics are also used as base oils, often required for specialist lubrication formulations.

Other Synthetic base oils

The following are listed for completeness to this section, but are outside the scope of this review. There are many other types of synthetic base oils that are not hydrocarbon in nature, many of these were developed for specialist lubricant applications or as improvements over traditional base oils; synthetic esters (developed for the jet engine lubrication), polyols, polyethers, polyphenyl ethers and polysiloxanes.

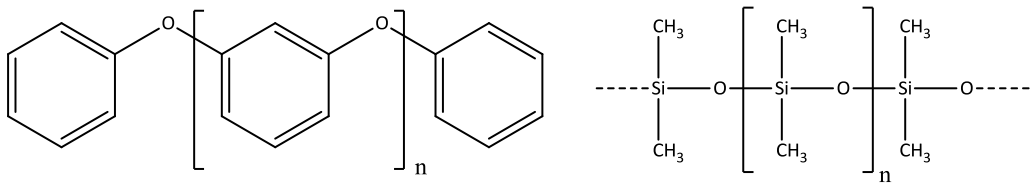

Polyphenyl Ethers | Polysiloxanes

Figure 13: Examples of synthetic base oils, polyphenyl ethers and polysiloxanes

Base Oil Summary

The choice of base oil used in a lubricant is determined by the balance of function, price and location. With the highest quality and highest cost base oils used in the European market, the lowest cost base oils are traditionally used in the US and Asian markets. Since modern lubricants are required to also act as a coolant, suppressing harmful deposit formation and controlling corrosion/oxidation the base oil alone would struggle to meet these demands. Therefore performance-enhancing additives in tailor-made formulations are added to the oil.

Lubricant Additives

An additive is a compound that enhances or imparts a new property to the base oil. Additives are required to perform the secondary functions of the lubricating oil. The development of modern engines and transmission technology would be impossible without lubricant additives. Additives are increasingly in demand by original equipment manufacturers (OEMs) as they move towards new designs and new materials technology to meet new legislation forcing lower emissions and longer service intervals. The development of new novel lubricants will be key to meeting these targets.

Additives are used at treat rates from just a few ppm, - antifoam agents -, up to 20 weight percent or more, - dispersants. Additives can be synergistic or antagonistic, with some even incorporated just to decrease the possibility of additives interfering with each other negatively. Naturally, additives impart a big influence on the performance of the overall lubricant, but there are some properties of the lubricant that cannot be influenced, e.g. thermal stability, compressibility, boiling point and volatility[82].

Antioxidants

The function of a lubricant is limited by aging of the lubricant base stock, which typically results in discolouration, burnt odour and in later stages significant rise in viscosity, due to the formation of lubricant and non lubricant derived decomposition structures agglomerating. Antioxidants can significantly delay the aging process. The aging process can be separated into two stages: the oxidation of the lubricant and the thermal decomposition at high temperature. In practice it is the oxidation of the lubricant which significantly influences the lifetime. Phenolic, aromatic, sulphur and phosphorus antioxidants act as radical scavengers; competing with lubricant molecules in the reaction with reactive radicals. The most famous example of this is the zinc dithiophosphates, because of their multifunctional uses. Organosulfur and organophosphorus componds act as peroxide decomposers, which convert hydroperoxides in the lubricant into non-radical products preventing chain propagation reactions.

Antifoam

The foaming of lubricants is undesirable and can lead to increased oxidation by the mixture with air, cavitation damage and poor transport of oil in circulation systems, leading to a lack of lubrication. Effective antifoam agents, such as liquid silicones, posses a lower surface tension compared to the base oil, which helps to prevent foaming.

Antiwear

Antiwear additives prevent the welding of moving parts when machinery starts to move before the hydrodynamic lubrication has built up. These additives have a polar structure that allows them to form layers on the metal surface by

adsorption or chemisorption. This guarantees their immediate availability[83-87].

Common antiwear compounds are phosphorus and sulphur containing compounds: ZDDP – zincdithiophosphates - are used because of the multifunctional abilities they possess[88-93]. They are able to act as many different additives simultaneously: antiwear[94], antioxidant[95, 96] and Extreme Pressure additives[95].

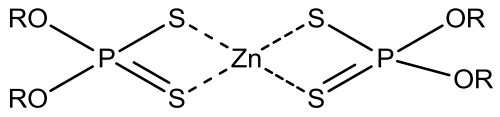

Zinc dialkyldithiophosphates (ZDDP)

Figure 14: Common antiwar component Zinc dialkyldithiophosphates

Pourpoint Depressants

Pour point depressants are also referred to as low-temperature flow improvers or wax crystal modifiers. Without the addition of these additives many lubricants would be too viscous to flow at low temperatures. Although paraffin crystallisation cannot be suppressed, the crystalline lattice and therefore the morphology of the paraffin crystals can be altered. Polymers are used to co-crystalise parrafinic components in the base oil and polymer chain. This interaction results in an alteration of the crystal. Instead of needle- like paraffin crystals which result in rapid gelation, densely packed round crystals are formed which hardly affect the flowing properties at temperatures below the pour point. Polyalkyl methylacrylates are normally used for mineral oil based formulations.

Demulsifiers

Water contamination is a problem for lubricant formulations: without demulsifiers lubricating oils can form stable water-in-oil emulsions. In principle, the majority of surface active substances are suitable demulsifiers, however polyethylene glycol coupled to phenol formaldehyde branched aliphatic species have proved successful at separating emulsions. The ethylene oxide portion increases the water solubility and provides a good barrier to stop corrosion.

Detergents

Detergents neutralise oxidation-derived acids whilst also helping to suspend polar oxidation products in the bulk lubricant[97-100]. This enables detergents to control rust, corrosion and resinous build-up. Generally, detergents contain a surface active polar functionality and an oleophilic hydrocarbon group with a connecting group bridging the two. Chemically, detergents are the metal salts of organic acids that usually contain excess base[101-104]. Sulfonates, phenates and carboxylates are the most common types of detergent molecules[105].

The excess base allows detergents to neutralise the acidic oxidation products to form salts. While this decreases the corrosive tendency of the acid, the solubility of the salt in the bulk lubricant still remains low. The organic part of the detergent can then associate with the salts to keep them suspended in the bulk lubricant. This is similar to how dispersants work, however their effectiveness is limited because of their lower molecular weight. The ability of detergents to associate is not solely limited to acidic products; alcohols, aldehydes and resins are also solubilised in this manner.

The most common detergent type is the alkylaromatic sulfonic acids (AAS), such as alkylbenzenesulfonic acids (ABS)[106-108]. This is made by reaction of

alkyl benzene with a sulfonating agent[109, 110]. The alkyl benzene starting material is made by alkylation of benzene with either an α-olefin or alkyl halide[111].

The detergency is then imparted by the chemical reaction between the acidic substrate and a metal hydroxide, to produce a neutral metallic detergent and water[112].

$RSO_3 – H \quad + \quad K – OH \rightarrow \quad RSO_3K \; + \quad H_2O$

This neutral salt of an acidic detergent substrate is also referred to as the soap or surfactant. In general, the soap is the stoichiometric reaction product of one equivalent of an acid substrate plus one equivalent of metal base. As mentioned above, detergents are usually basic and these are produced in a similar manner to neutral detergents except the metal hydroxides used are typically divalent in character: for example, calcium or magnesium.

Finally, detergents can also be overbased – where up to 30 times more metal is contained than the neutral detergents. The purpose of this overbasing is to reduce the amount of detergent required in an oil formulation without compromising the detergency capability of the formulation. There is also no valence restriction on the metal for the formation of overbased detergents[113]. To produce overbased detergents the correct choice of promoters, catalysts, solvents, substrate and excess of metallic base is required. In essence an overbased detergent is a stable colloidal suspension of calcium carbonate in oil. In order to achieve this the detergent must produce a reverse micelle reaction vessels for the overbasing and to provide oil solubility/stability to the metal carbonate particles that are formed during overbasing[114, 115]. The reactants are heated together at temperatures above 100^{o}C for several hours and prior to filtration, reaction with an inorganic

acid or acid anhydride (most commonly, CO_2) is used to increase the amount of metal base colloidally dispersed in the product.

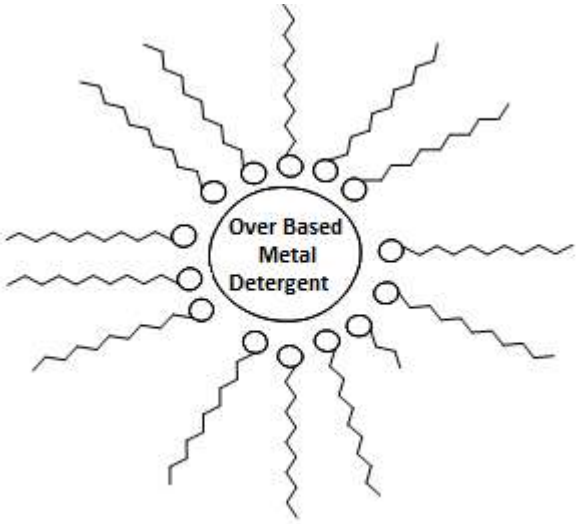

Figure 15: Representation of an overbased detergent micelle

The spontaneous dissolutions of a normally insoluble substance by a relatively dilute solution of a surfactant is called Solubilisation. Solubilisation is a micellar phenomenon that occurs only at concentrations above the critical micelle concentration (CMC). Knowledge of the CMC is vital to prevent unnecessary additional amounts of expensive ingredients from being used in a formulation. Surface tension and light scattering measurements are used to measure the CMC of detergents.

The level of overbasing is defined by the amount of total basicity contained in the product, for example a 100TBN (total base number) magnesium phenate. Base number is defined in terms of equivalent amount of potassium hydroxide contained in the material. A 100 TBN calcium sulfonate contains base equivalent to 100 milligrams of potassium hydroxide per gram, or more simply, 100 mg KOH/g.

Viscosity Modifiers

Viscosity modifiers are added to reduce the viscosity-temperature dependence of the base oil. In the simplest case, desired viscosities can be achieved by mixing fluids with corresponding viscosity indexes. Viscosity modifiers are added to meet harder lubricant specifications. Viscosity modifiers have a polymeric nature. The molecules are often chain-like, with solubility dependent on chain length, structure and chemical composition[116]. As a general rule, the base oil solubility of viscosity modifiers decreases as the temperature falls and improves with increasing temperature. An explanation of this effect is offered by Selby *et al.[117]*: because of the low solubility at low temperature the chain- like viscosity modifier molecules form coils of small volume. As the temperature is increased these molecules expand and unravel, resulting in an increasing benefit on high temperature viscosity.

The common types of viscosity modifiers are olefin copolymers (OCPs), polyalkyl(meth)acrylates (PAMA), polyisobutylene (PIB) and hydrogenated styrene-butadiene copolymers (SBR).

Dispersants

Dispersants are typically the highest treat additives in engine oil formulation. Their function is to control the deleterious effects of oil insoluble products resulting from incomplete combustion: typically keeping sludge, resin, varnish, soot particles and hard deposits in the bulk lubricant. Their addition in the formulation is vital to minimising particulate- related abrasive wear and viscosity increase. Dispersants are structurally very similar to detergents, and are often referred to as ashless detergents[118]. They have a polar head and oil soluble hydrocarbon tail, are metal free (unlike detergents), have little or no acid neutralising ability and are larger molecules[119-121].

Dispersants suspend deposits in a variety of ways: including undesirable polar species into micelles; associating with colloidal particles - preventing them from agglomerating and falling out of solution; suspending aggregates in the bulk lubricant; modifying soot particles so as to prevent aggregation which would lead to oil thickening; and lowering surface/interfacial energy of polar species in order to prevent their adherence to metal surfaces.

Dispersants are believed to prevent agglomeration via two mechanisms: steric[122, 123] and electrostatic stabilisation[122, 124]. In steric stabilisation, following the polar head groups' adsorption onto the surface of the dirt particle, the tail provides a physical barrier to attraction. This separates the small particles and prevents them from coming into contact with others and increasing in size[125, 126].

The second mechanism involves an induced charge on the dirt particle. Dispersants that contain basic amine sites interact with acidic groups on contaminants such as sludge to form salts. Agglomeration is then inhibited by electrostatic repulsion of the negatively charged dirt particles[106, 126, 127].

Desirable dispersant properties include thermal and oxidative stability, good low temperature properties and good solubilising ability.

Dispersant structure

Dispersants generally consist of three groups: a hydrocarbon group, a polar group and a connecting group.

The hydrocarbon group is polymeric in nature and leads to a classification into polymeric dispersants (3-7000 g mol^{-1}) and dispersant polymers (~25000 g mol^{-1}). A wide range of olefins are used to make polymeric dispersants, but the most common are polyisobutylene derived dispersants[125]. Dispersant

polymers are also known as dispersant viscosity modifiers (DVMs) and dispersant viscosity index improvers (DVIIs). High molecular weight olefin-copolymers[128] such as ethylene-propylene copolymers (EPRs), ethylene-propylene-diene copolymers (EPDMs) and styrene-diene rubbers (SDRs) are commonly used as polymer substrates for this class of dispersant.

The polar head group is either nitrogen or oxygen derived. Nitrogen is usually derived from basic amines and oxygen from neutral alcohols. In the case of dispersant polymers, the polar head group is introduced either by direct grafting, copolymerisation or by introduction of a reactive functionality. Compounds used for this include monomers such as 4-vinylpyridine, unsaturated anhydrides and acids, most commonly maleic anhydride. Frequently used connecting groups are succinimide, phenol and phosphate, with succinimide being the most common.

Polyisobutylene derived dispersants

These dispersants contain a polyisobutylene backbone with a succinic linker group with various head groups. They are the most common type of dispersant produced commercially[129]. Polyisobutylene is prepared using cationic polymerization, however depending on the co-initiator used one of two routes is followed for the reaction with maleic anhydride.

Cationic polymerisation is a chain growth polymerisation mechanism with a positively charged propagation centre, initiators used in cationic polymerisations are often Lewis acids such as BF_3 (boron triflouride), $SnCl_4$ (tin tetrachloride) or $AlCl_3$ (aluminium chloride) for the initiation of various vinyl monomers with electron-donating side groups. This group is required as this type of substituent stabilises the propagating charge on the living chain end, electron withdrawing side groups destabilise the propagating charge and inhibit polymerisation by this mechanism.[5] Currently cationic polymerisation

of isobutylene is the only commercial synthetic route to polyisobutylene due to the monomer reactivity.

Polyisobutylene made using aluminium tri-chloride ($AlCl_3$) provides mostly tri- or tetra- substituted end groups while the use of boron tri-fluoride (BF_3) as a catalyst gives products favouring formation of vinylidene end groups. Depending upon the end group present on the polyisobutylene conversion to the succinic anhydride end group is achieved either by a Diels-Alder or ene process.

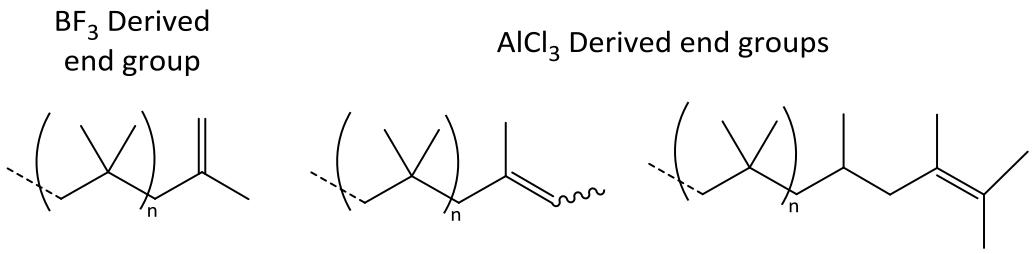

Figure 16: Typical polyisobutylene end groups

When high levels of vinylidene end groups are present, then at high temperatures excess maleic anhydride is added to force an ene reaction with the less substituted vinyldiene double bond to give the desired product. The alternative route is to set up a facile Diels-Alder reaction with the maleic anhydride to form the desired product. This requires an equivalent of chlorine and maleic anhydride per double bond and this results in the elimination of two equivalents of hydrogen chloride which produce a diene via double bond substitution of the major olefin end group. These two routes give subtle differences to the head group architecture which can provide different performance advantages depending on the application.

Further reaction to produce the dispersant is done simply by reaction with an amine or alcohol functionality to give the desired product.

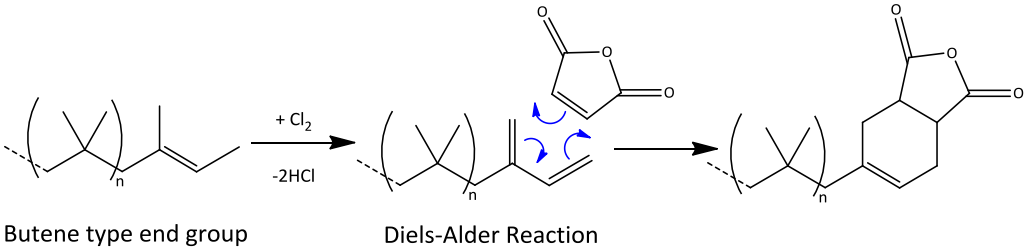

Figure 17:Diels-Alder reaction of maleic anhydride with butene type end groups

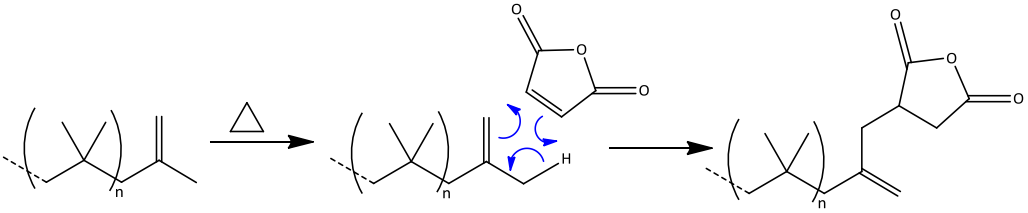

Figure 18:Alder ene reaction of maleic anhydride with propylene type end group

The Final Lubricant

The composition of any lubricant combines the correct choice of base oil and additive chemistry as the variables of base oil, additive composition and concentration have large impacts on the final lubricant fluid's physical and chemical properties. Careful selection of the additive chemistry determines the difference between a lubricants use in engine or gear box. A modern lubricant will contain many different components often working both synergistically and antagonistically.

2

Introduction

Potential methods for the degradation of plastic into another form or physical state have already been outlined in chapter 1. In order to investigate further and incorporate the degraded waste product into a synthetic strategy a number of priorities need to be established: 1) which desired functionalities can be easily obtained; 2) to what extent the material can be degraded; 3) how easily can the material be incorporated into a synthetic strategy for the preparation of a lubricant additive.

To try to achieve these aims the process of feedstock recycling was investigated[130-139]. The different processes for feedstock recycling have focused on the type of equipment used, and have mainly been carried out with "virgin" or homogenous waste plastic streams. Much of the currently published research has centred on the use of fluidized beds[23, 62, 64, 140-156], rotary kilns[23, 46, 64, 140, 153], rotating reactors, and most recently microwave pyrolysis systems[157-159]. Microwave radiation brings the benefit of access to high temperatures and high rates of heating with excellent efficiencies for the conversion of electrical energy into heat (80-85%) and for heat transfer to the stream. A typical process involves mixing the plastic stream, usually transparent to microwaves, with an absorbent material. This absorbent material has two functions, firstly to act as a substance absorbs the microwave radiation and secondly to dissipate this absorbed energy as heat. This material is usually carbon. Upon exposure to microwave radiation the carbon can reach temperatures of up to 1000^{o}C in a matter of minutes with the energy transferred to the plastic by conduction. This provides a very efficient energy transfer, enabling a reducing chemical environment[50, 51, 160].

Results and Discussion

Two different microwave systems were employed to investigate the effectiveness of using a microwave assisted degradation pathway to produce waste material with the desired carbon-carbon double bonds required for the upgrading of waste material. For clarity they are discussed separately.

Initial investigation: the use of microwave assisted pyrolysis with a CEM Discover Microwave Reactor

The initial investigation into the degradation process for waste plastic using a microwave generator was based on the work of Tanner *et al[54]*. This process involves a method for the cleavage of a hydrocarbon compound in the liquid phase. The application of microwave radiation with absorbent material and catalyst can generate shorter chain unsaturated hydrocarbons and hydrogen gas. Scheme 2.0 shows the set up of the Tanner process[53]. The liquid slurry was exposed to a fixed power of microwave radiation for varying lengths of time under a supply of nitrogen gas. The same apparatus as shown in figure 19 was adopted and distillation equipment was custom designed to fit into the microwave cavity of a loaned CEM Discover Microwave reactor.

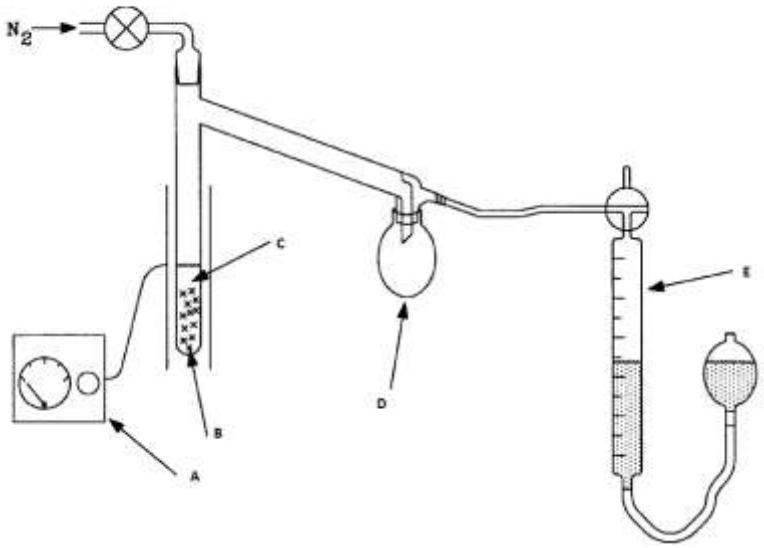

Figure 19:Schematic of the apparatus for the microwave bond cleavage process. A) Microwave generator. B) Supported catalyst dispersed in C) Hydrocarbon sample D) cold trap for liquid products E) Gas burette.

Because commodity polymers are usually solid in their native state the method was applied with a modification to the polymers. The commodity polymers were mechanically ground into a powder and mixed with activated charcoal, thus providing a solid matrix with sample and activated charcoal acting as both a microwave absorbent material and a source of catalytic metals, as demonstrated by Tanner *et al*. The sample was then irradiated at a fixed power for a variable period of time.

Polyethylene (PE)

Polyethylene is not known to depolymerise or unzip to monomer[161]. The thermal degradation of polyethylene has been studied at great length, mainly due to its abundance in everyday products. The majority of studies on the thermal degradation of polyethylene have concluded that propene and 1-hexene are the most abundant chemicals produced from thermal scission. The

rationale is based on the hypothesis that scission is initiated at the weak link sites along the polymer main chain. Once this thermally induced scission has occurred a reaction of a radical with the hydrogen atom on the 5th carbon should be geometrically favourable because the transition state is a 6-membered ring. This radical species can then undergo chain scission producing two degradation pathways leading to propene and 1-hexene. This all occurs at temperatures between 400-650^{O}C[162].

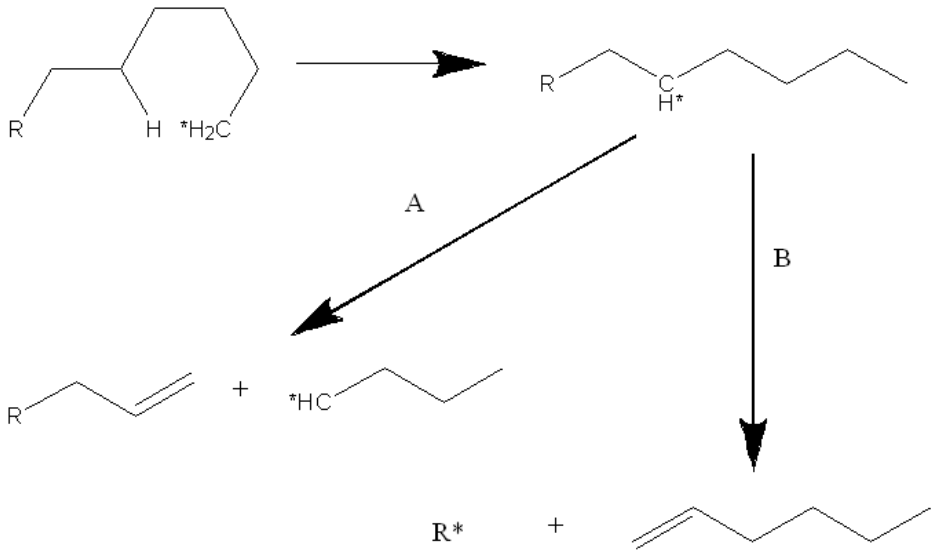

Figure 20: Proposed degradation pathway for polyethylene from reference[7].

A ratio of 4 parts polyethylene to 1 part activated charcoal was used. A flow of nitrogen was then passed over the sample and the sample exposed to microwave irradiation for the requisite time. The exiting gas was passed through a cold finger held at -78^{o}C to condense any liquid fractions. The gas was not collected. The liquid fractions were collected and analysed by GC-MS. Table 1 provides the raw data for the degradations while table 2 displays the percentage of each fraction produced post degradation. Figure 21 displays this information graphically.

Table 1: Summary of microwave reactions involving polyethylene.

Time (min)	Liquid (g)	Gas (g)	Power (W)	Most abundant liquid product (from GC-MS)
0	0	0	300	-
1	0	0.49	300	-
2	0.1	0.4	300	hexene
3	0.1	0.88	300	hexene
4	0.1	1.12	300	hexene
7	0.26	1.35	300	hexene
10	0.28	1.49	300	hexene
0	0	0	200	-
1	0	0	200	-
2	0.01	0.2	200	-
3	0.02	0.33	200	-
4	0.08	0.61	200	-
7	0.11	1.1	200	heptene
10	0.16	1.31	200	heptene

From table 1 the most abundant liquid product at lower power is heptane, rather than the expected hexane, suggesting that the thermally induced scission has occurred with the hydrogen atom on the 6th carbon and proceeded through a 7-membered ring rather than through the more geometrically favourable 6-membered ring transition state. The Entropic costs between the two postulated transition states are likely to be significant. The difference in microwave heating rates could therefore be the cause for the difference in the major degradation product as at higher temperatures the 6-membered ring transition state would be more favourable.

For a given reaction time, the greater the power of the microwave the greater the proportion of both liquid and gaseous fraction produced relative to the residual solid component, this is unsurprising as increasing the temperature will favour the decomposition of the PE. However the composition of liquid products is considerably different at the early stages of the degradation with a tenfold difference in the liquid fraction produced in the first 3 minutes of the reaction at 300W compared to 200W.

Table 2:Relative percentagesc of solid, liquid and gas fractions from the degradation o f Polyethylene

Time (min)	Liquid (%)	Gas (%)	Solid (%)	Power (W)
0	0	0	100	300
1	0.04	19.6	80.36	300
2	4	16	80	300
3	3.96	35.2	60.84	300
4	4	44.8	51.2	300
7	10.4	54	35.6	300
10	11.2	59.6	29.2	300
0	0	0	100	200
1	0.04	0	99.96	200
2	0.4	8	91.6	200
3	0.8	13.2	86	200
4	3.2	24.4	72.4	200
7	4.4	44	51.6	200
10	6.4	52.4	41.2	200

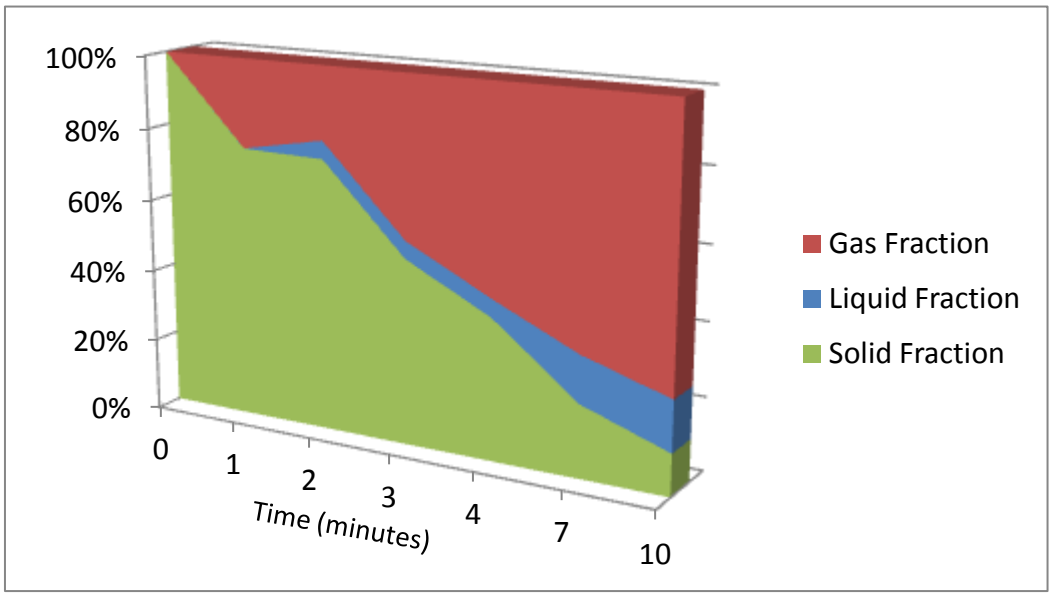

Figure 21: Graphical representation of the microwave degradation performed at a power of 300W over time. The relative percentage of each fraction is displayed.

During the reaction constant distillation was observed with a steady increase in temperature up to 280^{o}C which was achieved after approximately 180s for 300W power and 220s for 200W power. This temperature was then maintained until the end of the reaction. With increasing time the amount of both gaseous and liquid fractions increase, with the gaseous fraction being the largest component by mass. However the composition of this fraction was not collected and therefore not analysed. The liquid fraction appears to stay constant with time over the 2-4 minute period with an increase in the relative amount up to 10 minutes. This appears to suggest that even though the temperature reached is the same, that the time taken to get to the required temperature effects the degradation product distribution.

The solid residue was insoluble in all available solvents for GC-MS, this suggests that the solid residue is a mixture of activated carbon and un-reacted polyethylene. High Temperature (110^{o}C) ^{1}H and ^{13}C NMR was attempted however the same issue with solubility was encountered and resulted in very poor spectra.

Polystyrene (PS)

Unlike polyethylene, polystyrene is known to unzip or depolymerise at high temperature back to its constituent monomer. In 1935 Staudinger and Steinhofer proposed one of the first thermal degradation mechanisms for PS, reporting that a chain scission mechanism was responsible for the formation of monomer, dimer, trimer, tetramer and pentamer. Grassie and Scott later proposed a mechanism that begins after thermal scission which produces two primary radical species. The reaction continues with the production of dimer by intramolecular radical transfer. This can be described as unbuttoning of the polymer, see figure 22.

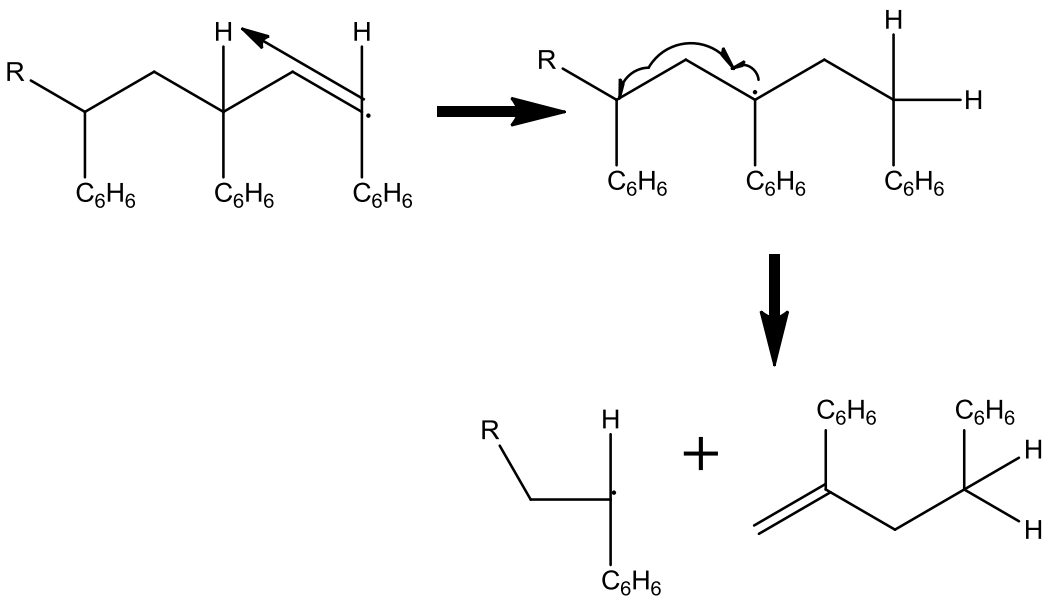

Figure 22: Proposed Thermal degradation mechanism by Grassie and Scott

PS degradation under nitrogen proceeds in a single step and is characteristic of typical depolymerisation mechanism with the rate- limiting step being the unbuttoning initiated by random scission. Nishizaki *et al[163]* reported that approximately 50% of polystyrene is converted into styrene by simple thermal degradation at 723K.

The same experimental procedure was followed with polystyrene as with polyethylene. Table 3 displays the summary of degradation reactions with Polystyrene. The most abundant fraction produced was styrene, with dimer and trimer also produced in the liquid fraction. These results are broadly consistent with what has been published in the literature previously using thermal methods[163-165].

Table 3: Summary of reactions involving polystyrene. Power at 300W.

Time (min)	Liquid (g)	Gas (g)	Most abundant in liquid fraction	Other compounds
0	0	0	-	
2	0.04	0.2	-	
3	0.1	0.22	Styrene	
5	0.17	1.01	Styrene	dimer,trimer
10	0.31	1.44	Styrene	dimer

The product distribution is different from polyethylene: less gas is evolved in the process and the liquid fraction has a greater percentage of the overall product distribution. Again the gaseous fraction was not collected. The liquid fraction was passed through a GC-MS and the most abundant fraction was found to be styrene. This is consistent with the literature for the thermal degradation of polystyrene. However, the advantage of using polystyrene as a candidate material is found with its solubility in common solvents. Therefore size exclusion chromatography (SEC) analysis was performed on both the virgin polystyrene and the residual solid from the degradation process to look at any molecular weight differences between the two materials. Table 4 highlights the molecular weight change. From the data in table 4 it is clear there is a large

decrease in molecular weight with irradiation time. Again as with polyethylene the temperature remained at 280^{o}C.

Table 4: Molecular weight change in residual polystyrene

Time (min)	Solid (%)	M_n	PDI	Reduction in M_n (%)
0	100	170,000	2.4	-
2	90.4	170,000	2.4	0
3	87.1	170,000	2.5	0
5	52.8	120,000	4.1	29
10	29.8	7,800	6.5	94

To look for the presence of any functional groups present in the solid residue samples were analysed using Nuclear Magnetic Resonance spectroscopy (NMR) and infrared spectroscopy. The results of the proton spectra are shown below in figure 23.

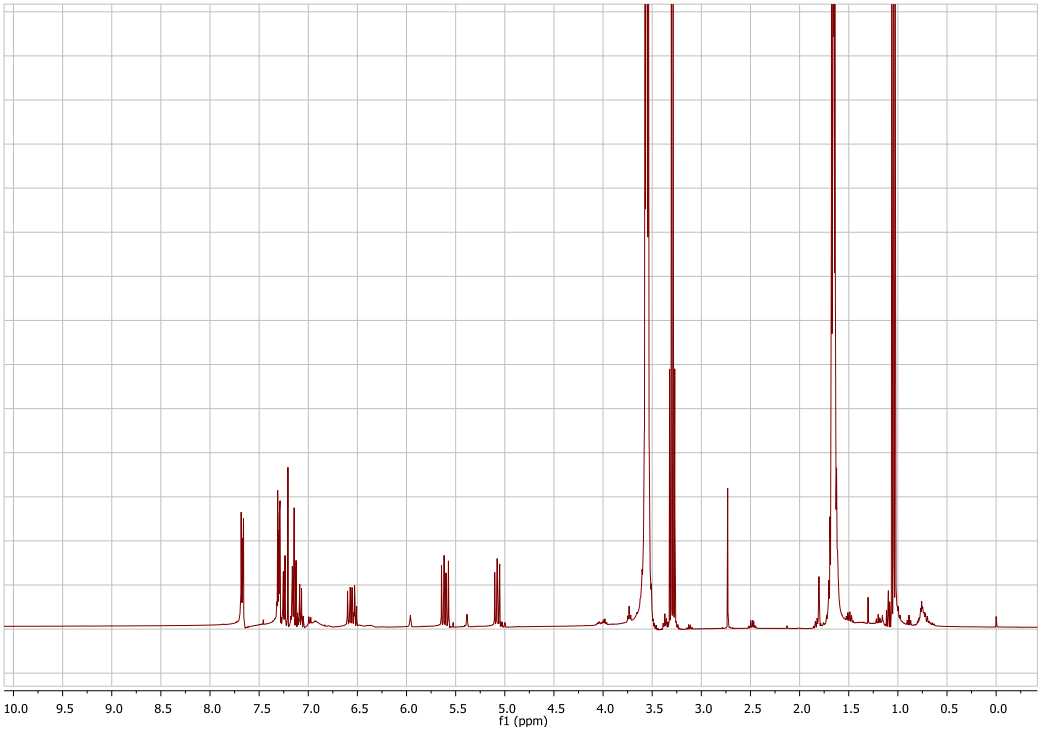

Figure 23: Typical 1H NMR spectra from residual solid component from the microwave degradation of polystyrene

The proton spectrum indicates the presence of unsaturated carbon-carbon bonds in the solid residue. The resonances at 5.1, 5.5 and 6.5ppm are consistent with styrenic protons[166, 167] expect for the fact the splitting patterns do not directly correspond with styrene. It is likely that the multiplet at 5.1 and 5.5ppm are three sets of doublets indicating three separate species present in the residue. Additionally, there are two singlets at 5.4 and 5.9ppm which are indicative of unsaturated carbon-carbon double bonds. FTIR analysis of the residue confirms the presence of different double bond species; weak absorbance's observed at 1590 and 1638 cm^{-1} and at 1612 and 1639 cm^{-1} are indicative of unsaturated C-H stretching in vinyl substituted aromatics[168].

Initial conclusions

From the initial investigation there are two options to focus on. Firstly, considering the liquid products from either degradation pathway, the 1-hexene could be a candidate to produce a group IV base oil (PAO) and the styrene is a useful monomer. However, both of these products are taking the degradation of the waste plastic back to or almost to the monomer basis.

Secondly, the analysis of the solid residue from the degradation of the polystyrene offers the potential for functionalised oligomeric species. This has the added benefit of being akin to the head group of a dispersant. From a commercial viewpoint this is the more valuable route to follow.

Biotage Initiator 60 Microwave pyrolysis system

Due to the CEM Microwave being recalled from its loan agreement, the established method was transferred to a closed vessel system. The major differences with the Biotage microwave are its cavity size, its closed vessel

arrangement and the automation. Because of these differences it isn't possible to set up distillation apparatus in the same manner as previously described and adaptation is required. Air is able to penetrate into the system, therefore this method isn't performed under pyrolysis conditions.

In order to replicate the degradation process the Biotage Initiator 60 microwave was adapted in the following ways: 1) cooling the microwave cavity to ~ -78^{o}C; and 2) adapting the vial to vent to the atmosphere by penetrating the lid with a 5cm needle, making sure to just break the surface. Figures 24 and 25 show the overview of the microwave system.

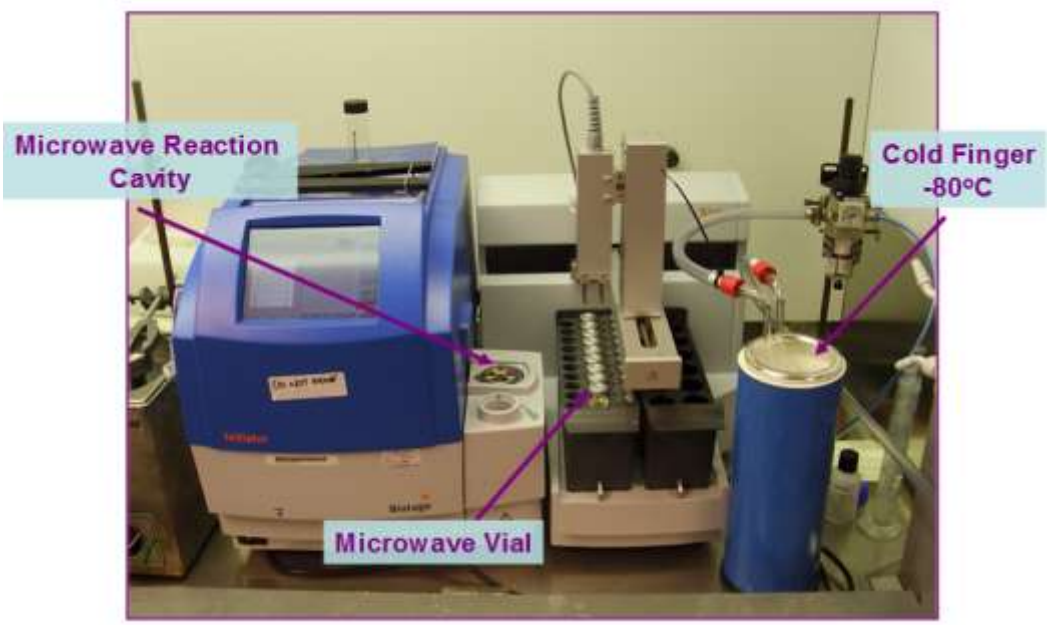

Figure 24: Photograph of Biotage Initiator 60 with modifications in place pre-vial selection

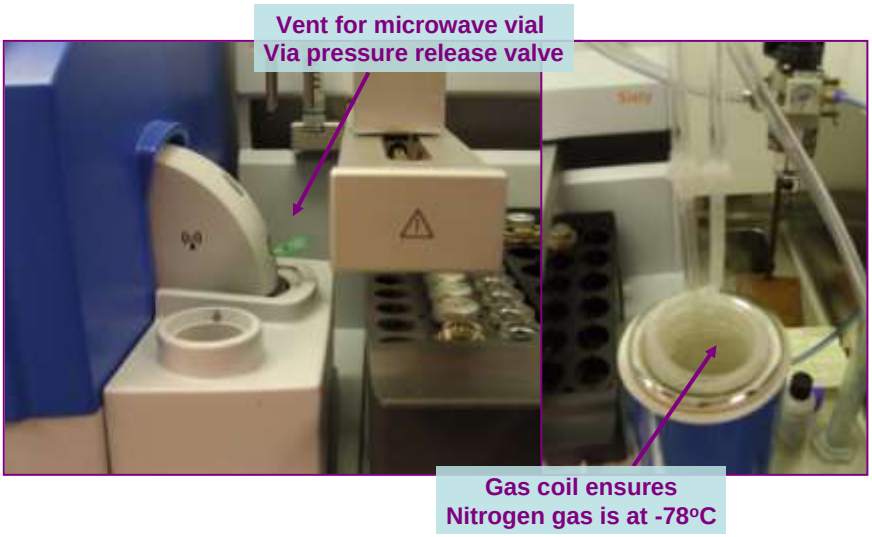

Figure 25: Photograph of Biotage Initiator 60 with modifications in place with vial loaded.

To replicate the desired conditions for degradation with this microwave setup a number of compromises and deviations from the initial method were established. Due to the Biotage system's various inbuilt features, careful manipulation of conditions was required. For example, it isn't possible to perform the degradation in a totally enclosed environment as the pressure build-up rate becomes too great for the built in monitoring system and the microwave simply powers down. Similarly, without cooling of the microwave vial the rate of temperature change was detected to be outside the acceptable limits and again the microwave would power down. Both of these issues occur at a very early stage in the degradation, well before the onset of depolymerisation.

To optimise the conditions a fixed power setting was used and the following parameters were investigated: active carbon ratio, solvent and time. The same batch of polystyrene for the CEM degradation was used.

Effect of Absorbent Material

The ability of microwaves to heat a material depends upon the materials shape, size, dielectric constant and the nature of the microwave equipment employed along with the time of exposure[169-171]. When a material containing permanent dipoles is subject to a varying electromagnetic field in the microwave frequency range (2450MHz), the dipoles of that material find themselves unable to follow the rapid reversals in the field. This results in a phase lag with the incident radiation and the energy is dissipated into the material as thermal energy. This heat will be lost from the dipolar material by convection and radiation.

The absorbent material used here is activated carbon, this material contains an abundance of different metal ions and oxides at very low concentrations (1-50ppm) which provide the permanent dipoles needed to interact with the microwave radiation. The carbon acts as an effective thermal conductor to dissipate the energy of the system. By mixing the activated carbon with the waste plastic an effective thermal cracking process is established once microwave radiation is applied to the system.

The same batch of activated carbon was used for all microwave degradations ensuring that the same ratio of metals with permanent dipoles to activated carbon was maintained.

The ratio of waste plastic to activated carbon was varied from 1:1 (w/w) to 10:1 (w/w), see table 5. The ratio of 5:1 was found to be the most suitable ratio. A ratio less than 5:1 waste:activated carbon resulted in runaway of the reaction, and failure of the microwave vial (Figure 26). Conversely, a ratio greater than 8:1 does not provide sufficient absorbent material to heat the system to a temperature where degradation would occur within the experimental

conditions. A ratio of 5:1 (w/w) was found to be an efficient compromise and was easy to weigh out within the size limitation of the vial.

Figure 26: Vial failure

Table 5: The results when varying the activated carbon (microwave absorber) to sample ratio. Polystyrene at 0.50g, power at 400W.

Activated Carbon (g)	Ratio	Lower M_n Product (%)	Gas Product (%)	Comment
0.5	1:1	-	6.3	Vial failure
0.4	1.25:1	-	4.7	Vial failure
0.3	1.67:1	-	5.9	Vial failure
0.2	2.5:1	-	7.2	Vial failure
0.1	5:1	2.6	94.1	-
0.08	6.25:1	1.6	92.3	-
0.06	8:1	-	15.7	-
0.05	10:1	-	-	-

Figure 27 shows the increase in pressure when performing the degradation in a closed vessel environment with different ratios of activated carbon. With a closed system, the pressure build up is rapid, especially at higher concentrations of activated carbon. The consequence of this rapid pressure build up is the initiation of one of the built-in safety systems in the Biotage initiator 60. An automatic shutdown procedure is triggered as the system believes that the reaction is running out of control. In addition the temperature change in the reaction vessel is rapid, changing from RT to 120^{o}C in 20s.

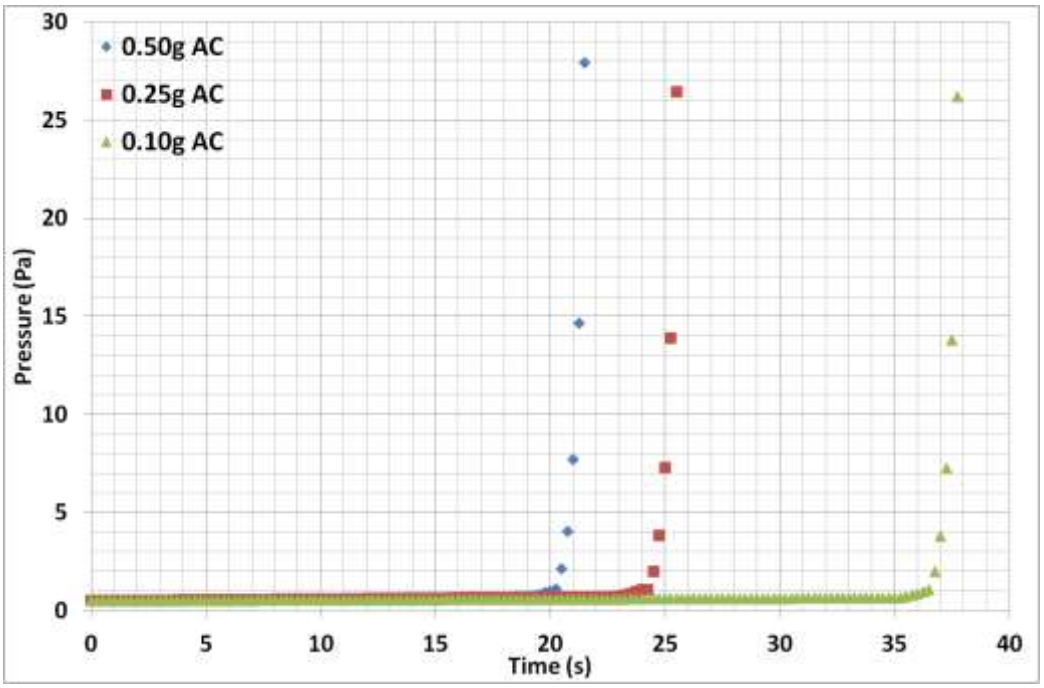

Figure 27: Graph of Pressure vs time for microwave degradations performed with Biotage initiator 60 microwave with a fixed power of 300W. The active carbon content was varied. Tmax = maximum temperature recorded.

Figure 28 shows the increase in temperature with time for when the pressure sensor is disabled; as expected similar temperatures are reached in comparable times with the pressure sensor on, however under these conditions the microwave also initiates an automated shutdown on the basis of the temperature ramp. Unfortunately there is no way to disable this auto

shutdown feature on the microwave. A solution to this situation is to operate the microwave in an open vessel mode and pulse the microwave radiation into the vessel.

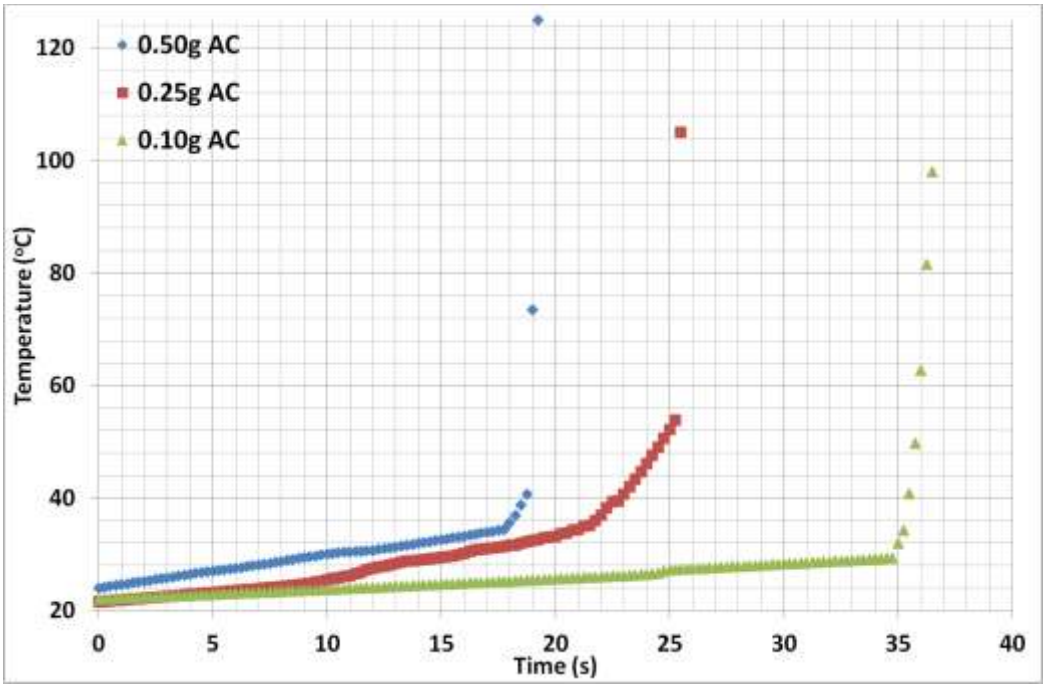

Figure 28: Temperature vs time for microwave degradation of polystyrene with varying active carbon content.

Effect of Solvent

Due to the different arrangement of the Biotage system the use of a solvent was trialled. The addition of solvent increases the dissipation of energy within the system and is the only way to reduce the formation of hotspots. 1,3-diphenoxybenzene (similar structure to a group IV base oil –similar structure to polyphenylethers) and naphthalene were chosen as suitable solvents due to their high boiling points and relative low cost. The results are shown in table 6. No noticeable difference was found between the solvents: naphthalene is therefore favoured due to its availability in large quantities and relatively low

cost. The active carbon was not soluble in the solution and therefore addition of a very small magnetic flee was required to agitate the solution.

Table 6: Solvent effect on the degradation of 0.50g of polystyrene at 400W power.

Solvent	Ratio Active carbon: PS	Lower M_n Product (%)	Gas Product (%)
Naphthalene	5:1	5.7	78
Naphthalene	5:1	5.8	77
1,3-dihydroxybenzene	5:1	2.7	93
1,3-dihydroxybenzene	5:1	2.6	94

Although there is no noticeable difference between naphthalene and 1,3-diphenoxybenzene, there is a significant difference between the heating rates of 1,3-phenoxybenzene and naphthalene with those of diphenoxybenzene. Figure 29 shows the heating rate differences. The time taken to reach the temperature set by the microwave takes much longer with diphenoxybenzene, indicating that this solvent has lower thermal conductivity than 1,3-phenoxybenzene and naphthalene.

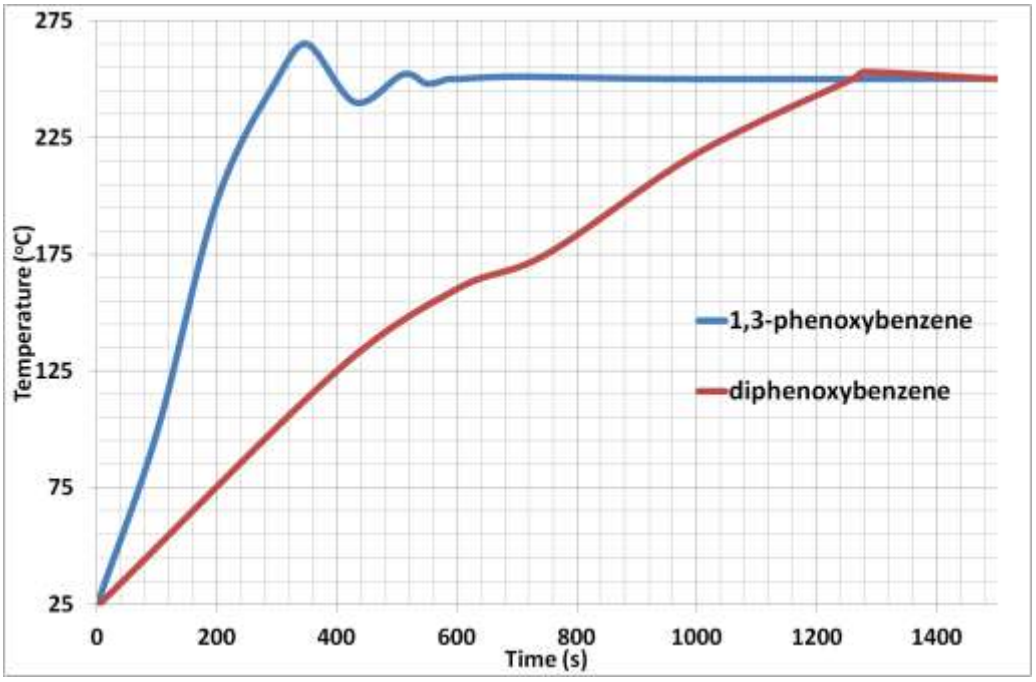

Figure 29:Temperature vs time for degradation of polystyrene in diphenoxybenzene and 1,3-phenoxybenzene.

Time

The length of time the sample is exposed to the conditions inside the microwave directly relates to the degradation of the material, assuming all other variables are kept constant. By using naphthalene as the solvent and using a ratio of activated carbon to polystyrene of 5:1 various degradations were carried out using the same power (400W). Figure 30 shows the reduction in molecular weight as characterised by Size Exclusion chromatography (SEC) for the recovered solid portion of degradations held at constant temperature from 0 to 90 minutes. Although the linear fit for the data is poor (R^2 = 0.8383), it does show a decrease in molecular weight with time. The residence time is much longer than those previously reported for similar degradation processes[16, 32, 63, 64, 70, 143, 145-149]; however, there is no direct comparison with literature results for two reasons; the lower operating

temperature of this method and the fact there is no analysis focusing on the waste residue from other degradation methods, as the established research has focused entirely on the generated liquid or gaseous fraction, without consideration for the solid residue, as this has been negligible with very little or no remaining solid fraction at the much higher thermal degradation temperatures.

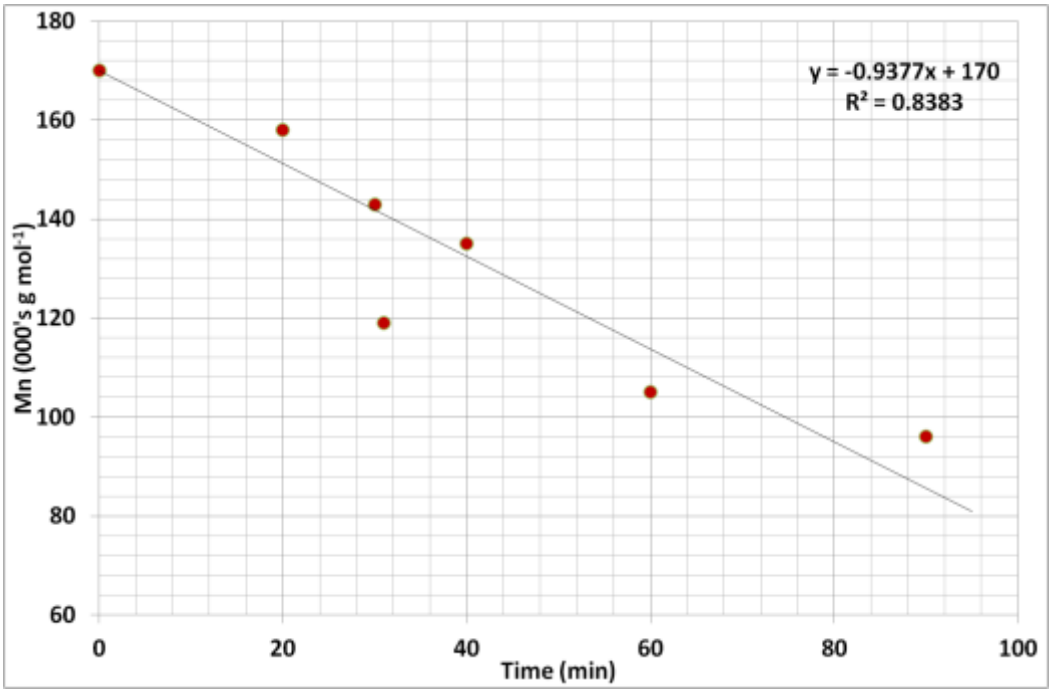

Figure 30: reduction in Mn with time for virgin polystyrene Mn 170K.

Figure 31 shows the observation by SEC that under 400W power and naphthalene as the solvent the relative amount of un-reacted polystyrene decreases with time, note this is not due to a concentration effect as each chromatogram corresponds to the same concentration of 2.0 mg/mL.

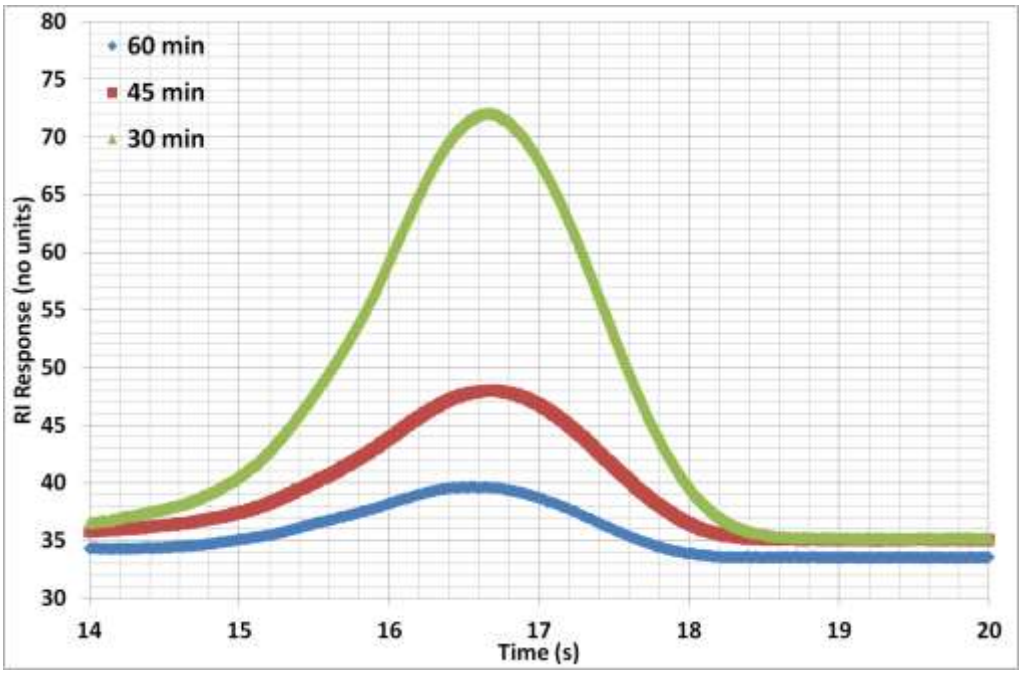

Figure 31:Comparison of SEC trace at 30, 45 & 60 minutes of reaction. Power: 400W Solvent: naphthalene.

The reduction in molecular weight caused by the degradation conditions was investigated further. ^{1}H NMR spectroscopy was performed on the residue, and a typical spectrum of the degradation product and the original polystyrene sample is shown in Figure 32. Notice the formation of unsaturated species as indicated by the peaks at 4.5-6.6ppm in the degraded fraction. These products are similar to the peaks formed from the original CEM degradations of polystyrene (figure 23). Also notice the absence of such peaks from the original polystyrene and naphthalene mixture before degradation, no evidence for un-saturation is observed.

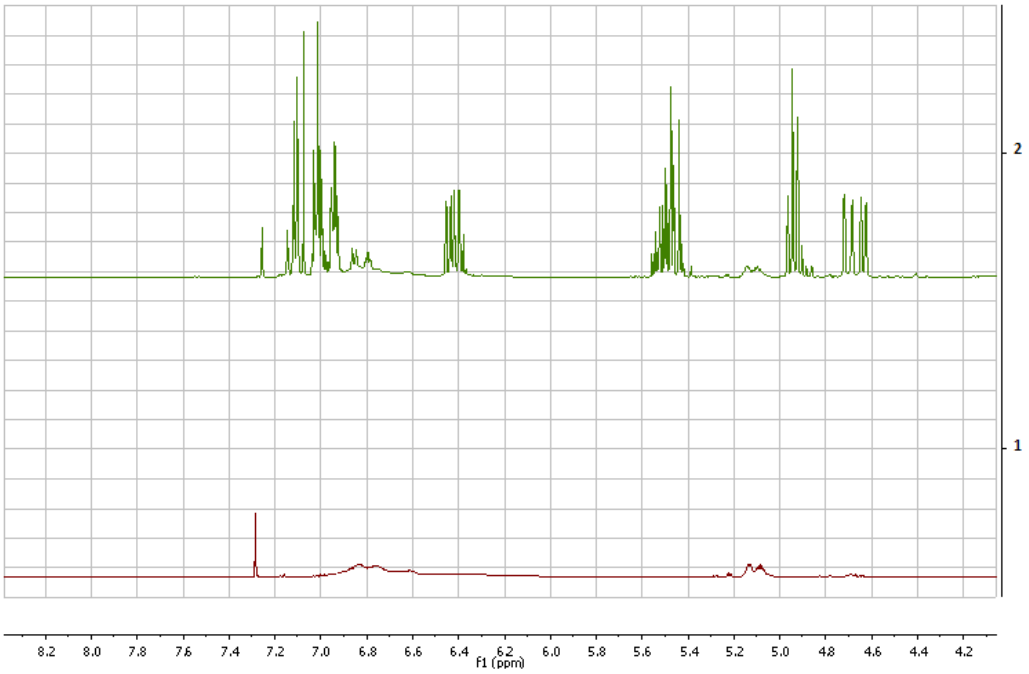

Figure 32: ^{1}H NMR spectra for 1) The waste polystyrene mixture prior to degradation 2) the residual waste product at 160minutes

There is also a distinct difference between the aromatic regions of the two spectra at 7-7.2ppm. The degraded mixture appears to have significant fine structure, by that you can clearly see well defined peaks corresponding to aromatic hydrogens where as the original polystyrene spectra shows little fine structure. This difference is explained by the decrease in the relative concentration of the polystyrene (which is consumed in the degradation process and is observed as a broad hump at 6-7ppm) and the formation of oligomeric and monomeric styrene. Additionally there is an increase in the relative concentration of the naphthalene which will contribute to the aromatic region between 7-7.2ppm. Due to the complex multiplet splitting patterns in the region 4.5-6ppm Figure 33 shows some proposed end groups which could be formed in the degradation process leading to terminal olefins.

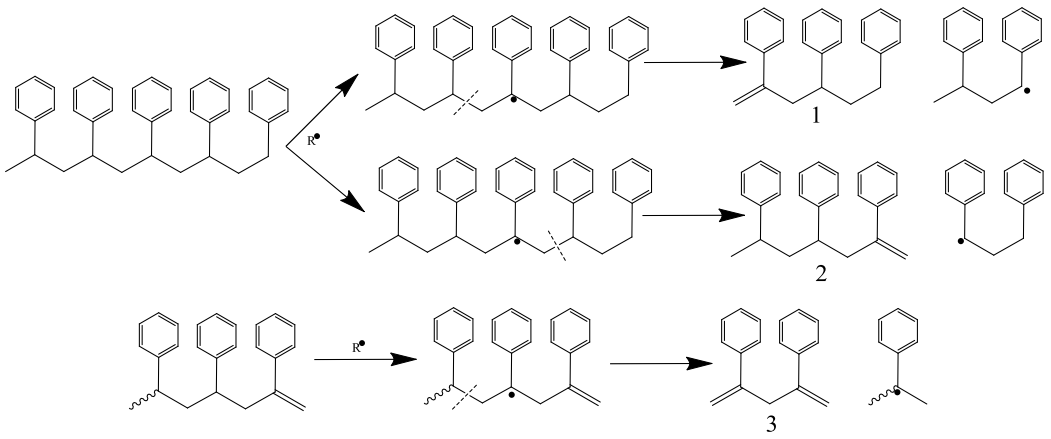

Figure 33:Polystyrene degradation reactions leading to terminal olefin formation

The terminal double bonds in figure 33 can be generated by β scission of tertiary radicals formed by hydrogen abstraction by secondary terminal radicals. On the other hand, saturated end groups will be generated by hydrogen abstraction reactions of secondary terminal radicals formed by β scission of tertiary radicals. An approximation of the number of double bonds per average degraded polystyrene molecule is done using ^{1}H NMR spectroscopy. The calculation of the number of double bonds per average degraded polystyrene (DBPS) was done by comparing the sum of integrals which correspond to potential double bonds (I_o) to the sum of the integral of saturated species (I_s) plus the sum of the integrals for potential double bonds.

$$\int DBPS = \left(\frac{\sum I_o}{\sum I_o + \sum I_s}\right)$$

The calculated value for the number of double bonds per average degraded polystyrene varies depending upon degradation time, but is within the range 0.04-0.09. This figure indicates that the number of terminal olefins present in the degraded polystyrene is between 4-9%. This calculation assumes that all the degraded chains are linear and no telechelic oligomers; oligomers with terminal double bonds at both ends of the polymer chain are formed.

Recycling of expanded polystyrene using Biotage Initiator 60 Microwave pyrolysis system

The application of the optimised conditions from the degradation of virgin polystyrene was transferred to the degradation of expanded polystyrene from a fridge-freezer container. The expanded polystyrene was dissolved in THF and precipitated in methanol to give polystyrene particles. SEC provided the M_n, 240,000 g mol^{-1}. The sample was then treated in the same manner as the virgin polystyrene samples. Results for the degradation reaction are shown in table 7. The aim here was to degrade the polystyrene so that at least a portion was left as oligomers or small polymers with terminal double bonds present.

Again ^1H NMR Spectroscopy was employed to look for the presence of double bonds in the degraded polystyrene. Figure 34 shows the ^1H NMR Stack for plot for the degradation after 30, 45 & 60minutes.

Table 7: Results from the degradation of 0.50g virgin polystyrene with 0.10g activated carbon (ratio 5:1). Power 400W.

Time (min)	Lower M_n Product (%)	Gas Product (%)
30	5.7	78
30	5.8	77
60	2.7	93
60	2.6	94

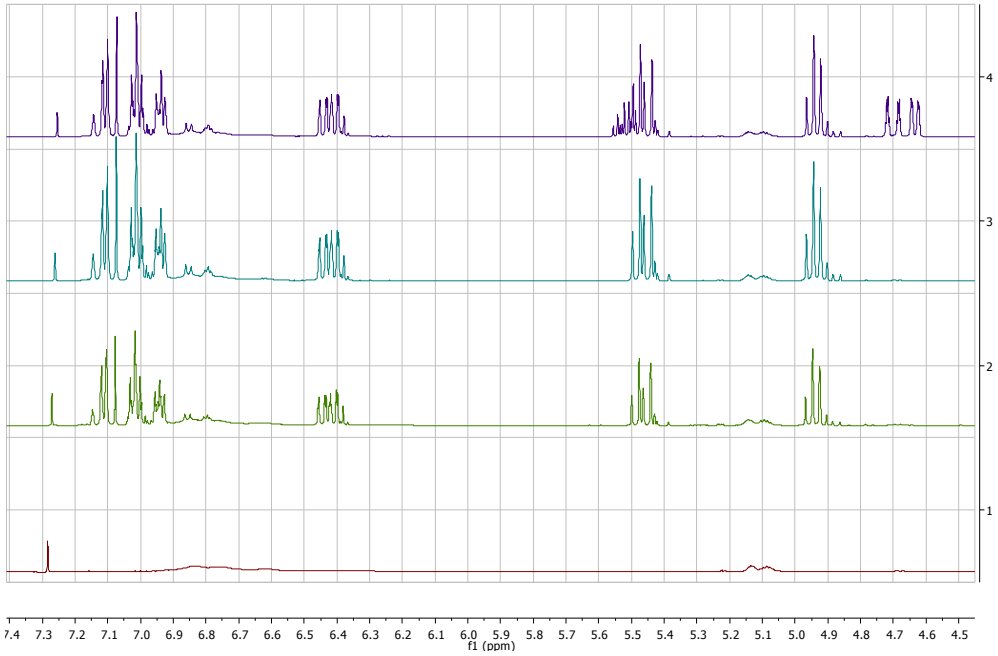

Figure 34: 1H NMR Stack plot between 4.5-7.4ppm 1) Polystyrene 2) Degradation residue after 30minutes 3) Degradation residue after 60 minutes 4) Degradation residue for virgin polystyrene after 60 minutes.

Notice the difference between the virgin polystyrene degradation at 60 minutes and the degradation of the expanded polystyrene at 60 minutes, additional peaks are observed at 4.6ppm in the virgin polystyrene indicating that a different terminal group is formed in this degradation. The expanded polystyrene likely includes the presence of various radical stabilisers and other chemical additives which could lead to inhibition of the proposed degradation route (figure 33) and stop the formation of a terminal end group which would otherwise be formed in the degradation of virgin (un-additised) polystyrene, and hence account for differences in the ^{1}H NMR data. Another source for the difference may arise from the sample preparation; the real world expanded polystyrene is dissolved in THF and precipitated into methanol, other impurities could potentially be concentrated up in this step and therefore play a larger role in the different products formed.

There is little difference in the concentration of the double bonds formed between 30 and 60 minutes for the expanded polystyrene. The number of

double bonds per average chain was found to be lower than the virgin polystyrene at 1-2%. The difference is due to the different molecular weights of the two polymers; the virgin polystyrene's molecular weight is almost 50% less than the expanded polystyrene and will therefore contribute to higher average of double bonds per average chain length.

Alternative theories for the differences arise from the age of the expanded polystyrene and the method of manufacture, both of which are unknown. It is possible that there is a greater onset of degradation for the expanded polystyrene relative to the virgin polystyrene, however this is unlikely to be significant as there would be evidence for the degradation when the expanded polystyrene sample was analysed by SEC, FTIR or NMR spectroscopy.

Figure 35 is a photograph of the three samples, notice the colour difference between the virgin and expanded polystyrene at 60 minutes.

Figure 35: Photograph of the waste residues post filtration in THF. left = 60 minutes, middle = 30 minutes, right = virgin polystyrene 60 minutes.

Kinetics of degradation

The kinetics of degradation is important from a number of different viewpoints, including the recovery of raw materials from recycling or the evolution of harmful substances from waste incineration. Mechanistically, free radical reactions can be distinguished from ionic reactions. However, kinetic differences are more important and, therefore, degradation reactions are classified either as single step reactions or chain reactions.

In step reactions the reaction rate is directly proportional to the rate of initiation, for example where one main chain bond is ruptured per absorbed photon. In chain reactions, the initiation reaction yields products that are then able to undergo spontaneous reaction with un-degraded molecules. Under continuous initiation the reaction rate is accelerated.

There are three types of reactions that can occur during depolymerisation; intramolecular hydrogen transfer, unzipping and intermolecular hydrogen transfer, see figure 36. Intramolecular hydrogen transfer involves the transfer of a hydrogen atom within a single polymer chain. Decomposition mechanisms based upon intramolecular hydrogen transfer are often known as random chain scission mechanisms. Intermolecular hydrogen transfer occurs between two different polymer chains, where the radical on one chain abstracts a hydrogen from the other polymer chain. This newly formed radical then breaks up into an unsaturated polymer and a radical. Unzipping, depolymerisation, depropergation is the reverse of polymerisation. The mechanism that prevails is dependent upon the structure of the polymer in question, if hydrogen abstraction is impeded then unzipping is likely to occur[172].

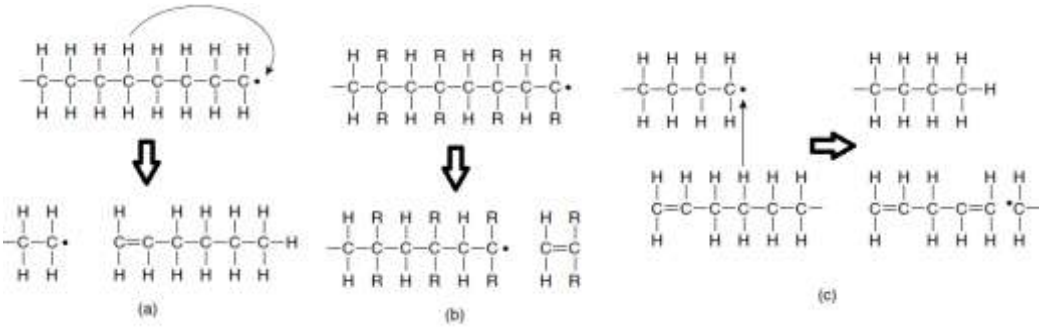

Figure 36:a)Intramolecular Hydrogen Transfer b)unzipping c)intermolecular hydrogen transfera)Intramolecular Hydrogen Transfer b)unzipping c)intermolecular hydrogen transfer.

The mechanism of thermal decomposition of many polymers can be summarized into the formal degressive rate expressions:

$$r = \left(\frac{d\alpha}{dx}\right) = k(T)\,(1-\alpha)^n$$

where, α = the degree of conversion, $\alpha = (m_0 - m)/(m_0 - m_\infty)$, with m_0 being the initial mass, m the actual mass, m_∞ the final mass, *k* is the rate coefficient and n the apparent order of the overall decomposition reaction. The temperature dependant term *k*(*T*) can be described by the Arrhenius relationship:

$$k(T) = A\,exp\left[\frac{-E_a}{RT}\right]$$

Where E_a is the activation energy of the process in (kJ mol^{-1}), A is the pre-exponential and R is the universal gas constant. Substituting in the Arrhenius relationship the formal degressive rate expression becomes:

$$r = \left(\frac{d\alpha}{dx}\right) = A\exp\left[\frac{-E_a}{RT}\right]\,(1-\alpha)^n$$

Dynamic and Isothermal methods that are used to investigate the kinetics of degradation mechanisms often reveal inconsistent results. Dynamic measurements are more influenced by heat transfer limitations than

isothermal methods, and so the thickness of the sample used has more impact on the global kinetic data than under isothermal conditions. When investigating the global kinetics of degradation it is important to select the correct heating method, for example the choice of dynamic or isothermal rates on the degradation of PS has little impact because of its relatively simple degradation mechanisms, but on more complex degradation pathways such as those in PE or PP then isothermal methods should be utilised.

Conclusions

The adapted microwave assisted degradation system shows good correlation with already established degradation processes[15, 16, 18-20, 24, 27-30, 32, 34, 50, 51, 70, 71, 73, 160-164, 173, 174]. A comparison to the literature for the liquid degradation products from polyethylene and polystyrene are in good agreement[34, 35, 48, 50, 71], however, whilst the majority of studies have focused on the liquid and gaseous products generated from the degradation of polystyrene, few have considered the remaining solid fraction. This work demonstrates how unsaturated double bonds were formed in the remaining solid fraction or residue of the waste polystyrene when using the adapted Biotage microwave assisted method. The control of the process has been demonstrated by the generation of different molecular weight materials containing unsaturated non-aromatic carbon-carbon double bonds as demonstrated by the ^{1}H NMR spectroscopy experiments. An attempt was made to quantify the number of terminal double bonds present in the waste material and estimates give this in the range 4-9% of each polymer chain. Slight differences in the degradation products are observed between virgin polystyrene and real world expanded polystyrene.

The CEM microwave processes used here for thermal degradation of polystyrene correlated well with the established literature for the products produced in the liquid fraction, for example the generation of styrene, dimer and trimer in the liquid products.

Although plastic waste materials have been degraded on multiple separate occasions the ability to control polystyrene degradations using a microwave technique in this way has not been reported. Although the scale of the degradation reactions conducted are small in comparison to other more established processes, this methodology have the potential for significant scale up and application with other polymers.

Experimental Section

General

Polyethylene (99%), polypropylene (99%), polystyrene (99%), Activated Carbon, Azobisisobutylonitrile, were purchased from Aldrich. DMSO-d_6 (>99.9%D), Toluene-d_8 (>99.9%D), dioxane-d8 (>99.9%D), THF-d8 (>99.9%D), $CDCl_3$ (>99.9%D) were purchased from Apollo Scientific. THF (99%) and toluene (<99.5%) were purchased from Fischer Scientific and dried by passage through two alumina columns using an Innovative Technology Inc. solvent purification system and stored under N_2. Hexane (Fischer Scientific >99%) was dried over 3A molecular sieves. 3A molecular sieves (Aldrich) were activated in an oven at 200^{o}C before use. All other chemicals were used as received. Microwave degradations were performed using a CEM Discover Labmate operating in open vessel mode at 2450 Mhz. NMR spectra (500MHz, DMSO-d_6, Toluene-d_8, dioxane-d_8, THF-d_8, $CDCl_3$, ^{1}H, ^{13}C) were obtained on a Varian Inova-500. High resolution NMR was performed on a Varian VNMRS 700 any nucleus spectrometer. Mass spectral analyses were performed on a Micromass LCT using positive or negative electrospray mode by either Dr Mike Jones or Miss Laura Turner. Mass spectral analyses of polymer samples were performed on Applied Biosystems Voyager-DE STR using MALDI Ionization mode operated by Dr. David Parker. Infrared spectroscopy was conducted on a Nicolet Nexus FT-IR as a KBr disc. Liquid samples were analysed by direct injection of the reaction medium into a liquid cell with KBr windows. Elemental analyses were conducted on an Exeter analytical E-440 elemental analyser. Molecular weight analysis was carried out by size exclusion chromatography (SEC) on a Viscotek TDA 302 with refractive index, viscosity and light scattering detectors. A value of 0.185 (obtained from Viscotek) was used for the dn/dc of polystyrene. 2 x 300 mm PLgel 5 µm mixed C columns (with a linear range of molecular weight from 200-2,000,000 g mol^{-1}) were employed; THF was used as the eluent with a flow rate of 1.0 ml/min at a temperature of 30^{o}C. The coupling reactions were monitored and further analysed by SEC using a Viscotek 200 with a refractive index detector and 3 x 300 ml PLgel 5 µm 104 Å high-resolution columns (with

an effective molecular weight range of 10,000-600,000 g mol^{-1}), THF was used as the eluent at a flow rate of 1.0 ml/min. UV-Vis spectroscopy was performed on a Unicom UV/Vis spectrometer.

Methods

CEM Microwave reaction with Polyethylene

Polyethylene (2.5 g) was mechanically ground and then mixed together with activated charcoal (0.5 g) inside a custom microwave tube. The tube containing the mixture was weighed and then placed inside the microwave cavity and the distillation apparatus was assembled. A flow of nitrogen gas was passed over the sample for 15minutes prior to being subjected to microwave radiation for 2-10 minutes at the desired power: 300W or 200W. Typically after 30 s the stream of gas evolution would change from colourless to silver/grey and would continue until reaction had begun to cool. Pre-weighed collection flasks were then held at -79^{O}C to collect any liquid fractions and the gas sample was vented into the fume hood scrubber. The sample of collected liquid was then reweighed to give the amount of liquid fraction collected. The solid residue was reweighed and the weight recorded. From the difference between the starting weight and the final weight the amount of gas component was calculated. The liquid fraction was then dissolved in DCM with a 1 in 10 dilution and passed through a GC-MS instrument. FT-IR was performed on the solid material. The gas sample was not analysed or collected. FTIR (KBr): 2920, 2859 (V_{CH} aliphatic); 1490,(V_{CH} aliphatic); 720(V_{CH} aliphatic). (typical GC-MS liquid fraction: (RT 6.1min, %=97, m/z = 84.1 (1-hexene)), yield: (liquid 11.2%, 0.28g), gas (60.1%, 1.50g) solid (28.7%, 0.71g).

CEM Microwave reaction with Polystyrene

Polyethylene (2.5 g) was mechanically ground and then mixed together with activated charcoal (0.5 g) inside a custom microwave tube. The tube containing

the mixture was weighed and then placed inside the microwave cavity and the distillation apparatus was assembled. A flow of nitrogen gas was passed over the sample for 15minutes prior to being subjected to microwave radiation for 2-10 minutes at the desired power: 300W or 200W. Typically after 30 s the stream of gas evolution would change from colourless to silver/grey and would continue until reaction had begun to cool. Pre-weighed collection flasks were then held at -79^{O}C to collect any liquid fractions and the gas sample was vented into the fume hood scrubber. The sample of collected liquid was then reweighed to give the amount of liquid fraction collected. The solid residue was reweighed and the weight recorded. From the difference between the starting weight and the final weight the amount of gas component was calculated. The liquid fraction was then dissolved in DCM with a 1 in 10 dilution and passed through a GC-MS instrument. FT-IR was performed on the solid material. The gas sample was not analysed or collected. FTIR (KBr): 3110, 2990(V_{CH} aromatic); 2933, 2820 (V_{CH} aliphatic); 1429(V_{CH} aromatic) 740(V_{CH} aliphatic). (GC-MS liquid fraction: (RT 4.8min, %=81, m/z = 104.1 (styrene),(RT 5.6min, %=10.4, m/z = 208.0 (dimer), RT 6.1min, % =4.4, m/z= 314.4 (trimer). yield: (liquid 15.5%, 0.31 g), gas (70.5%, 1.41 g) solid (14.0%, 0.28 g). ^{1}H NMR (500 MHz, $CDCl_3$) δ = 7.39-7.08 (broad,aromatic), 6.65-6.75 (m, HRC=CH-R), 5. 61-5.85 (m, HRC=CH-R), 4.9-5.1 (m, CH_2C=CH-R),1.6-2.6 (broad, R_2-C-H) 1.01-1.55 (broad, -CH_2-).

Optimised degradation conditions using Biotage Initiator 60 Microwave

Polystyrene (0.5 g, Mn =170,000 g mol^{-1}) and Activated Carbon (0.1 g) (5:1w/w) were dissolved in naphthalene (1.0 g) and placed in a 2-5mL microwave vial. The vial was then inserted into the microwave using the standard Biotage template. Upon closing of the microwave reaction cavity, a 5cm needle was carefully inserted into the top of the microwave vial via the pressure release valve. The reactants were cooled to ~-79^{o}C via the cooled nitrogen gas input, before being subjected to microwave radiation at 400W. The remaining char in the vessel was dissolved in THF and filtered through a pre-prepared small Celite (filteraid) column to remove the charcoal and then

analysed using size exclusion chromatography. Yield: (liquid 11%, 0.22 g), gas (81.0%, 1.61 g) solid (8.0%, 0.16 g). ^{1}H NMR (500 MHz, $CDCl_3$) δ = 7.39-7.08 (broad,aromatic), 6.65-6.75 (m, HRC=CH-R), 5. 61-5.85 (m, HRC=CH-R), 4.9-5.1 (m, CH_2C=CH-R), 4.55-4.71 (m, -HC=CR) 1.6-2.6 (broad, R_2-C-H) 1.01-1.55 (broad, -CH_2-).

Degradation of real world expanded polystyrene.

A sample of expanded polystyrene from freezer packaging was cut out and dissolved in THF. The polymer was then precipitated in methanol and cooled in ice to form white powder. The powder was dried on a vacuum line for 8 hours to remove any residual solvent. A sample of the expanded polystyrene powder was taken for SEC analysis. Expanded polystyrene (0.5g, Mn =240,000 g mol^{-1}) and activated carbon (0.1g) (5:1w/w) were dissolved in Naphthalene (1g) and placed in a 2-5mL microwave vial. The vial was then inserted into the microwave using the standard Biotage template. Upon closing of the microwave reaction cavity, a 5cm needle was carefully inserted into the top of the microwave vial via the pressure release valve. The reactants were cooled to ~-78^{o}C via the cooled nitrogen gas input, before being subjected to microwave radiation at 400W. The remaining char in the vessel was dissolved in THF and filtered through a pre-prepared small Celite (filteraid) column to remove the charcoal and then analysed using size exclusion chromatography. Yield: (liquid 17%, 0.34 g), gas (68.0%, 1.36 g) solid (15.0%, 0.30 g). ^{1}H NMR (500 MHz, $CDCl_3$) δ = 7.39-7.08 (broad,aromatic), 6.65-6.75 (m, HRC=CH-R), 5. 61-5.85 (m, HRC=CH-R), 4.9-5.1 (m, CH_2C=CH-R), 4.55-4.71 (m, -HC=CR) 1.6-2.6 (broad, R_2-C-H) 1.01-1.55 (broad, -CH_2-).

Lubricant Components from waste polystyrene and conventional sources

3

Introduction

The project aims to prepare novel lubricants and/or components for lubricants using commodity polymers as a feedstock. Before the functionalised waste material which was generated in chapter 2 can be incorporated into components for lubricants, a target lubricant component needs to be identified. An introduction to additive lubricant chemistry was provided in chapter 1. Following on from the success in degrading polystyrene the link between styrenic groups and soot (π-π interactions) was considered. To explore both this relationship and generate a lubricant component from the waste polystyrene the synthetic strategy focused on the synthesis of a dispersant type molecule. Because of the available expertise in polymer synthesis this idea was expanded to synthesise a dispersant viscosity modifier (DVM). The dispersant component in an engine oil formulation would typically account for 50wt% of the additive package, therefore making it an attractive investigation for the industrial partner alongside the scientific merit.

In general, dispersant molecules can be divided into three distinct parts: a dispersant head group; an oleophillic backbone; and a linker group. The rationale for this approach is that the waste polystyrene should act as the dispersant's head group with a new backbone and linker group being developed. Before launching into the incorporation of the waste polystyrene into the dispersant synthetic strategy a series of ideal materials were synthesised using a controlled free radical polymerisation technique known as Reversible Addition-Fragmentation chain Transfer (RAFT) Polymerisation. This endeavour led to the development of a method for the direct placement of linker groups within the backbone of a polymer chain and at the end of the chain. This ability to place a linker group within a chain is considered first in this chapter.

Maleic anhydride has been used extensively within the lubricant additive industry as a way of linking functional groups together. The traditional industry method has seen the radical grafting of maleic anhydride on to olefin copolymer backbones with little attention given to the position of that molecule on the polymer chain.

Copolymerisation of maleic anhydride and styrene

Alternating copolymerization permits the formation of a range of chain structures. Efforts have been directed to conventional radical chain copolymerizations involving maleic anhydride, which does not homopolymerize readily[6, 175]. Maleic anhydride is a strongly electron accepting monomer. Generally, strong electron donation in the comonomer will increase the tendency towards alternation. Mechanistic interpretations of a strong alternating tendency in conventional radical copolymerizations have been subjected to detailed investigations[176-183].

The use of controlled radical polymerisation methodologies in alternating polymerisation has been studied. A controlled radical polymerisation is governed by the establishment of a rapid dynamic equilibrium between a small number of growing chains and a large excess of dormant species[184]. In order to achieve this, initiation should be fast in order to rapidly provide a constant concentration of growing polymer chains. Secondly, the majority of the growing chains are dormant species which still have the ability of further growth due to a dynamic equilibrium that is established between the dormant species and the growing radicals. By keeping the concentration of active species low throughout the polymerisation, bimolecular radical-radical termination is suppressed. A general expression for this reversible activation process is shown below, figure 37, where K_a and K_{-a} are activation and deactivation rate constants[185].

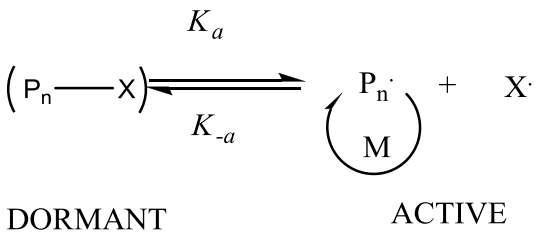

Figure 37: General expression of the reversible activation process

One of the first investigations into the use of controlled radical polymerisation methodologies for the alternating polymerisation of maleic anhydride and styrene was the use of nitroxide mediated polymerization. However, due to the high temperature (>110˚C) required to operate the nitroxide method, the alternating character of the polymer was not determined[186].

Attempts with atom transfer radical polymerisation (ATRP) for the copolymerisation of maleic anhydride and styrene have been reported in the literature. ATRP involves the use of a transition metal catalyst (usually copper halide) in combination with a suitable ligand to establish the reversible activation process[184, 187]. Although ATRP has become a method which is tolerant to a number of functionalities, acidic monomers are very difficult to polymerise directly. This is due to interactions of carboxylic acid functionality with the catalyst. It was postulated that carboxylic acids react with Cu(II) species by displacing the halogen atom, resulting in the formation of metal carboxylates which inhibit polymerization.

Maleic anhydride is similar to carboxylic acids, and if hydrolysed a dicarboxylic acid is produced. Attempts in the literature have failed to produce maleic anhydride copolymers by ATRP due to poisoning of the Cu catalyst[188]. The option for protecting group chemistry is not helpful in this case because maleic anhydride would need to be ring-opened, and then the ester or acid groups protected. This increases the steric hindrance on the double bond, lowering the reactivity of the monomer and making copolymerization difficult.

The development of RAFT Polymerisation by researchers at CSIRO in Australia in the late 1990s sowed the seeds for the first truly alternating controlled radical polymerisations of maleic anhydride and styrene[189-191]. Over the last 10 years the RAFT process has been reviewed and the understanding of the mechanism developed. RAFT polymerization is generally performed under standard free radical conditions with the involvement of a highly efficient chain transfer agent (CTA) of the general structure, figure 38, known collectively as RAFT agents.

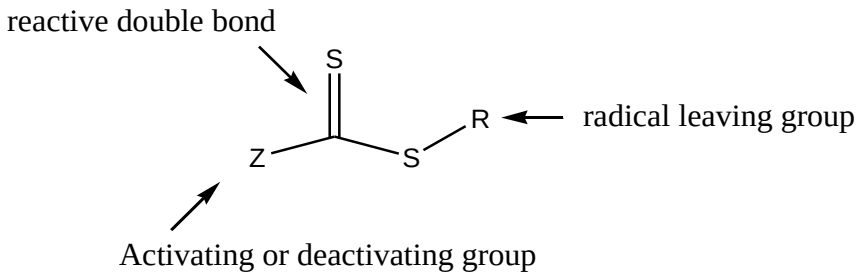

Figure 38: RAFT agent structure

RAFT agents are usually thiocarbonylthio compounds such as dithioesters, dithiocarbamates, trithiocarbonates and xanthates. For historical reasons, with the use of xanthates the process is referred to as MADIX: MAcromolecular Design through the Interchange of Xanthates[192].

When a radical polymerisation is carried out in the presence of a suitable thiocarbonylthio compound, a controlled behaviour can result. Figure 39 reports the mechanism of the RAFT polymerisation as it is understood today[193-196] and shows that, besides the elementary reactions of a classic (or conventional) radical polymerisation (i.e. initiation, propagation and termination – see Chapter 1 for a detailed overview) the RAFT process involves:

i. addition of a propagating radical P_n* to the RAFT agent (i) to give adduct radical (ii), which in turn fragments to yield thoicarbonylthio compound (iii) and

a new radical R* (chain transfer); as usual, the chain transfer constant to the RAFT agent (C_{tr}) is given by the ratio of the rate constant for chain transfer (k_{tr}) to that for propagation[197] (k_p);

$$C_{tr} = \frac{k_{tr}}{k_p} \qquad (1.1)$$

Which describes the reactivity of the propagating radical and the expelled radical respectively. Both Z-group and R-group influence the stability of the agents through electronic and steric effects. Lone pair electron donating heteroatoms of Z-group show a remarkable stabilizing effect while electron withdrawing substituents, either in Z- or R-group, tends to destabilize the agent[198, 199]. The rate of addition to the thiocarbonyl group (i) should not be dramatically affected by the nature of the group R since that group is remote from the C=S double bond and not directly conjugated with it. Therefore the magnitude of the transfer coefficient should reflect the partitioning of the intermediate between starting materials and products and the relative leaving group ability of R and the propagating radical[196].

A consequence of the addition-fragmentation mechanism is that, k_{tr} is a composite term of a number of rate constants defined in Figure 39

$$k_{tr} = \frac{k_{add} + k_{\beta,2}}{k_{-add} + k_{-\beta,2}} \qquad (1.2)$$

ii. re-initiation of the polymerisation by R* to give a new propagating macro-radical P_m*;

iii. repeated addition-fragmentation steps which set up an equilibrium between the propagating radicals P_m* and P_n*, and the dormant polymeric thiocarbonylthio compounds (iv) and (vi) through the intermediate radical iv

(chain equilibrium). This implies that, in the presence of a monomer, all chains will have the same probability of growth[200].

iv. From a mechanistic point of view, the reversible activation reaction at the core of the RAFT process is an example of degenerative chain transfer[185]. Low polydispersity products are obtained through a sensible choice of the general experimental conditions[201] (e.g. temperature, radical flux) as well as the reagents[202] and their relative concentration[203]. To begin with, a low radical flux must be used to start and maintain the polymerisation. According to the mechanism in figure 39 in fact, the total number of polymer chains produced by the RAFT process will be equal to the number initiated by the leaving group R* plus the number initiated by initiator derived radicals. As a consequence, a number of chains equal to the number of R* will possess a thiocarbonylthio end-group. Thus, the proportion of dead chains (Dc) in the final polymer will be equal to the ratio of effective initiator derived radicals to the number of RAFT agent molecules plus the number of effective initiator derived radicals (assuming that all RAFT agent molecules take part in the process with a 100% efficiency)[184, 204]. In reality however, it is unlikely the process is complete at 100% efficacy, as all termination steps are not stopped they are merely reduced.

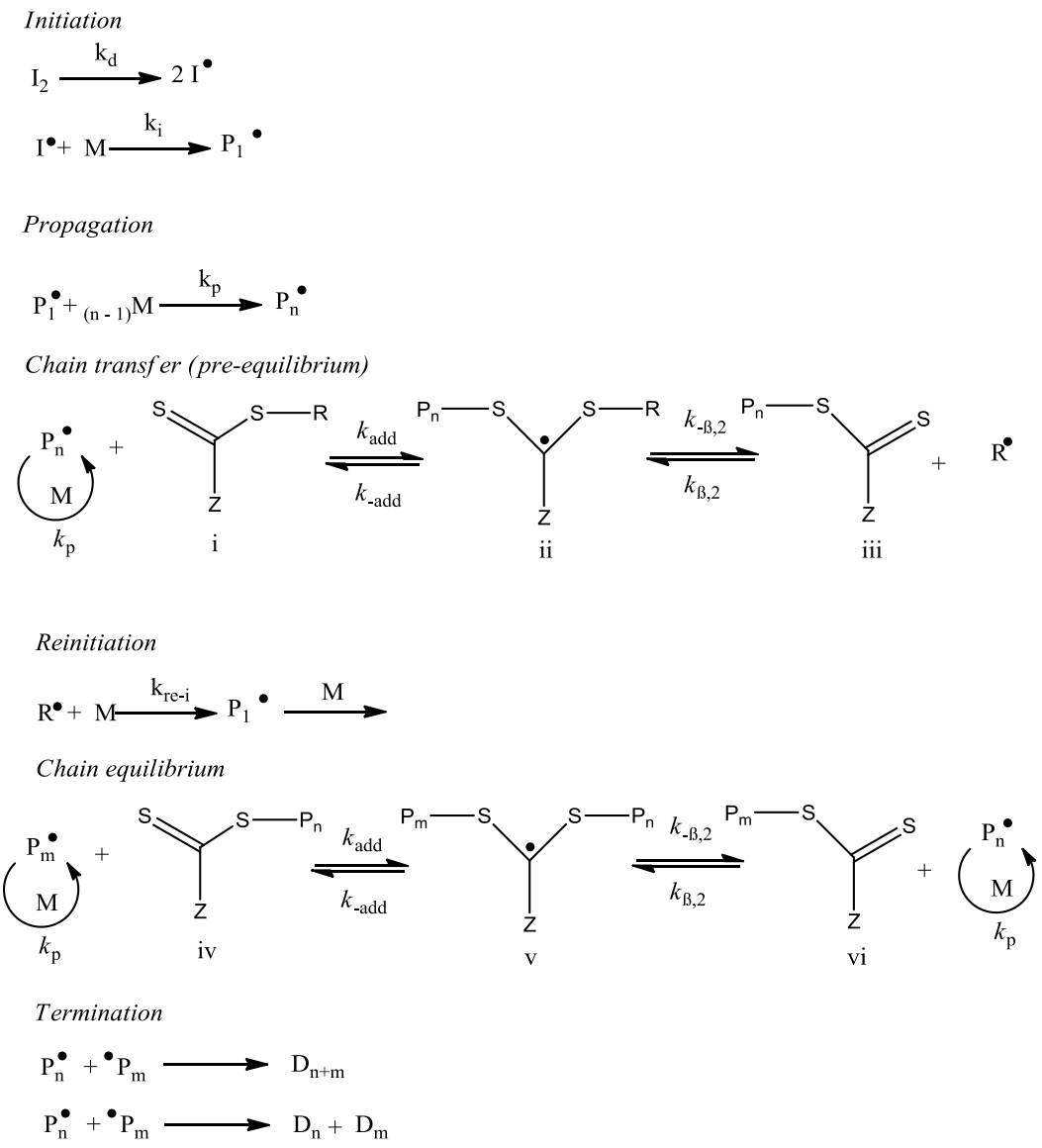

Figure 39: Accepted Mechanism of RAFT polymerisation

The concentration of initiator derived radicals and the contribution of disproportionation to the overall termination process needs to be considered with time and the initiator efficiency. Termination by disproportionation produces two dead chains, while termination via combination produces only one[204, 205].

Finally, most of the chains must be initiated in a short time window and chain transfer to the RAFT agent (i) and to the thiocarbonylthio compounds (iv) and

(vi) must be fast with respect to propagation reaction (i.e. $k_{tr}>>k_p$). This way, chain growth will be controlled by the equilibrium with the thiocarbonylthio compounds (iv) and (vi); all chains will grow at a similar rate and for a given reaction time, and will achieve similar molecular weights. If the fraction of initiator-derived chains is small, the average molecular weight will increase with conversion according to the equation:

$$M_n = M_m X \left(\frac{[M]_o}{[RAFT]_o}\right) + M_{RAFT}$$

where M_m and M_{RAFT} are the molecular weights of monomer and RAFT agents respectively, X is conversion and $[M]_o$ and $[RAFT]_o$ are the initial concentrations of monomer and RAFT agent.

To summarise, the mechanism of RAFT polymerization involves a reversible addition-fragmentation sequence of transfer of the S=C(Z)S- moiety between active and dormant chain ends. Provided that the exchange reaction is rapid compared to propagation and that each chain contains one end group derived from the RAFT reagent, then the theoretical molar mass at any conversion can be calculated from the equation above[206].

A distinguishing feature of RAFT polymerization is its applicability to a wide range of monomers, containing for example acid groups, acid salts, hydroxyl groups or tertiary amino groups, which have proved to be difficult with other CRP methods[207]. The process is similarly tolerant of the functionality in the RAFT reagent and the initiator, which allows the synthesis of a wide range of polymers with end group or side chain functionality in one step without the need for protecting group chemistry[208]. However, RAFT polymerisation does have some limitations and disadvantages. RAFT agents are generally not commercially available and the synthesis of a suitable RAFT agent often requires a complex synthetic strategy. The pairing of a RAFT agent with a suitable monomer is required, which can make the production of block

copolymers difficult depending upon the monomers being paired. The occurrence of bimolecular termination becomes significant at high targeted molecular weights (>100,000 g mol^{-1})[209].

Results and Discussion

The work reported here was directed towards the copolymerization of i) maleic anhydride and styrene; ii) *N*-phenylenediamine maleimide with styrene. In addition, the more complex architecture of iii) stearyl methacrylate homopolymer chain ended with maleic anhydride and styrene, see figure 40.

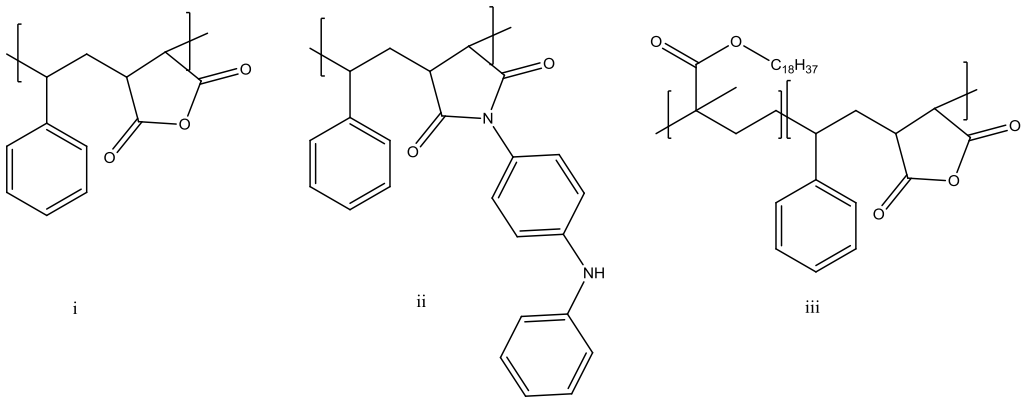

Figure 40: Repeat units of Maleic anhydride and styrene ii) N-phenylenediamine maleimide and iii) stearyl methacrylate chain ended with maleic anhydride and styrene

The copolymerisation of styrene and maleic anhydride was carried out with and without cumyl dithiobenzoate. The concentration of cumyl dithiobenzoate (RAFT agent) was varied along with the initiator concentration. The addition of the RAFT agent improved the control over the molecular weight although a delay in initiation was observed. Varying the concentration of RAFT agent to monomer concentrations impacted the degree of polymerisation as expected, and in the same manner as with a homopolymerisation. The rate of copolymerisation was also greater than the rate of homopolymerisation of styrene, an explanation comes from maleic anhydride - a 1,2-disubsituted olefin which is both sterically and electronically suited to the copolymerisation with styrene. The copolymer equation below provides a means for calculating the amount of each monomer incorporated into the chain for a given feed, for the proposed classical reactions:

$$\sim M_1^{\cdot} + M_1 \xrightarrow{k_{11}} \sim M_1^{\cdot}$$
$$\sim M_1^{\cdot} + M_2 \xrightarrow{k_{12}} \sim M_2^{\cdot}$$
$$\sim M_2^{\cdot} + M_2 \xrightarrow{k_{22}} \sim M_2^{\cdot}$$
$$\sim M_2^{\cdot} + M_1 \xrightarrow{k_{21}} \sim M_1^{\cdot}$$

$$\frac{d[M_1]}{d[M_2]} = \left(\frac{[M_1]}{[M_2]}\right)\left\{\frac{r_1[M_1] + [M_2]}{r_2[M_2] + [M_1]}\right\}$$

Where $r_1 = \frac{k_{11}}{k_{12}}$ and $r_2 = \frac{k_{21}}{k_{22}}$

Small values of *r* imply rapid cross propagation reactions and represent a tendency towards alternation, however only if both r_1 and r_2 are less than unity and $r_1 = r_2 \ll 1$ can regular alternation be expected. In this case maleic anhydride $r_1 = 0$ and styrene r_2 = 0.0095.[210] The tendency to alternate stems from either steric or electronic differences in the electron donor-acceptor properties of the radical and the double bond of the incoming monomer. Maleic anhydride is a strong electron acceptor and an unstable radical formed on maleic anhydride will favour reaction with a resonance stabilised monomer such as styrene, and the resonance stabilised terminal radical on styrene will prefer to add to the more unstable maleic anhydride monomer relative to another styrene monomer. Self propagation of the maleic anhydride is also further hindered by the steric hindrance of the maleic anhydride monomer, a 1,2-disubstituted olefin.

The experiments in this section demonstrate the methodology used to place molecules or a defined number of molecules accurately both within a polymer chain and at the end of the chain. The inital starting point for this work was with the alternating RAFT polymerisation of styrene and maleic anhydride (figure 42). The rate of reaction differs depending upon the presence of maleic anhydride. Maleic anhydride has been shown previously to react preferentially

with the leaving group of the RAFT agent at the beginning of the reaction[211, 212]: the result of this is that each polymer chain started will contain the maleic anhydride at one end of the polymer chain. Secondly, once the induction period has passed and the entire RAFT agent has begun to fragment and add reversibly then addition of maleic anhydride at this point will form an exclusive alternating copolymer with styrene. This is observed by the rate change and also the disappearance of the maleic protons. Once all the maleic anhydride is consumed, the polymerisation will continue with just styrene - at a later point more maleic anhydride can be added to give another block. The degree of polymerisation is directly proportional to the [monomer]:[RAFT]. Utilising these relationships, complex architectures can be accomplished simply by the addition of a known amount of maleic anhydride at different stages in reaction. This synthetic strategy is similar to what has been performed with ATRP maleimide polymerisations with styrene[213] and nitroxide mediated styrene maleic anhydride copolymers[214]. Figure 41 summarises the advantages of this method to place molecules, or a defined number of molecules, accurately both within a polymer chain and at the end of the chain over that of conventional free radical polymerisation.

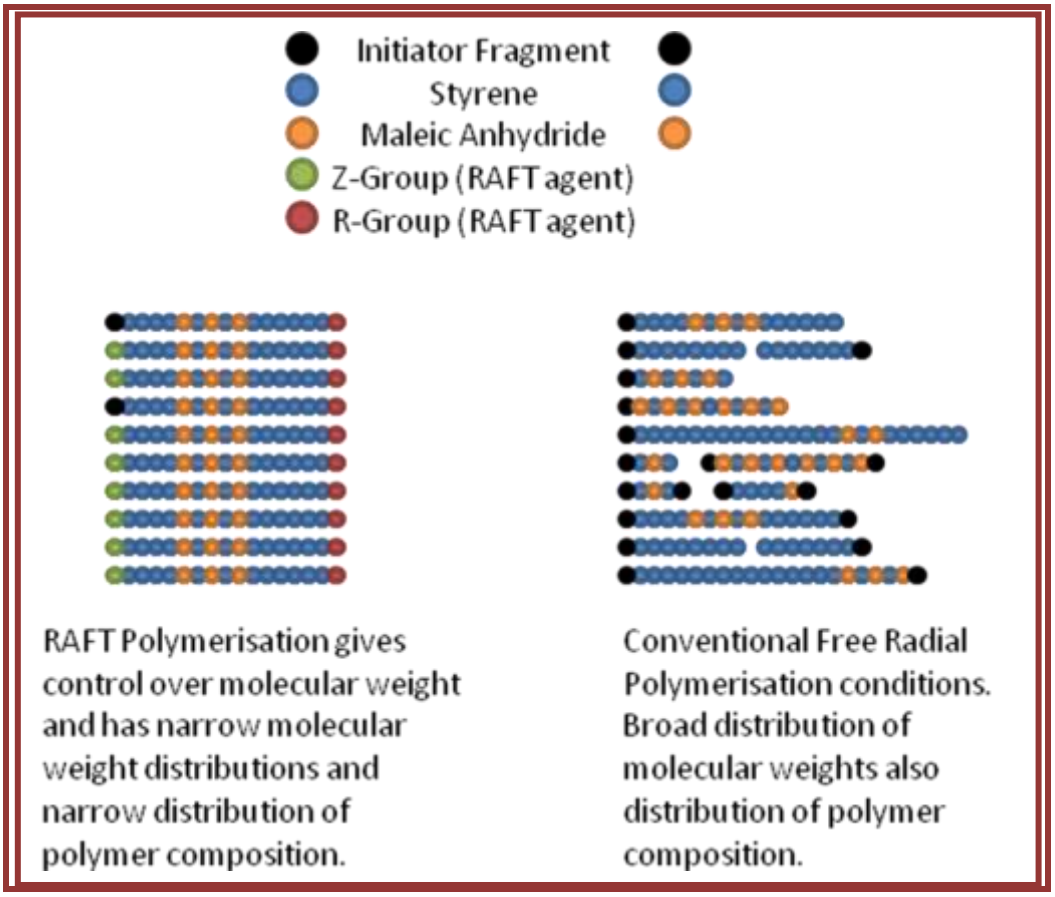

Figure 41*: Schematic comparison of RAFT polymerisation and free radical polymerisation with identical conditions and the addition of maleic anhydride to the polymerisation at a given time. This demonstrates the advantages of using RAFT to place molecules or a defined number of molecules accurately both within a polymer chain and at the end of the chain.*

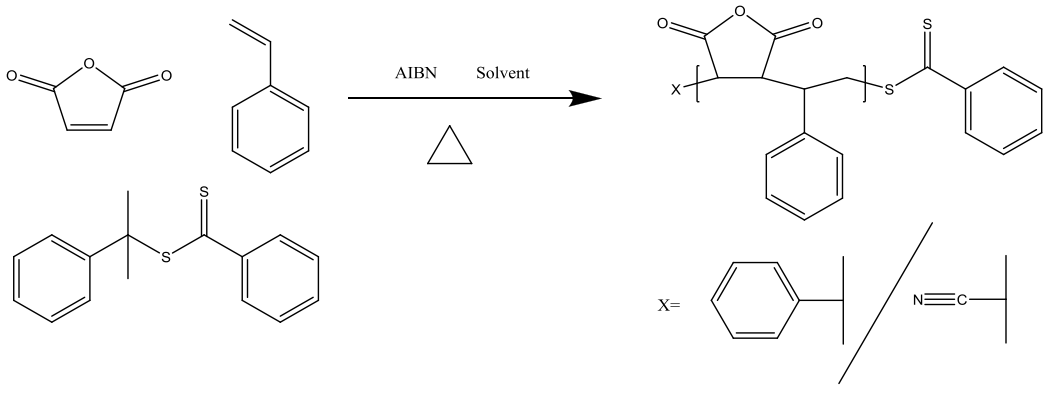

Figure 42*: RAFT copolymerisation of styrene and maleic anhydride.*

Evidence for this polymerisation strategy, figure 42, can be seen by the consumption of maleic anhydride as observed by offline ^{1}H NMR spectroscopy,

figure 43. Here in the RAFT Polymerisation of styrene with maleic anhydride (5mol%) added at t=0 and 150minutes, notice the steady disappearance of the maleic protons at 6.9ppm over time. After 120minutes all the maleic anhydride is consumed. Addition of a further batch of maleic anhydride at 150 minutes produces the same pattern, thus providing a method for selective placement of maleic anhydride alternating blocks within the chain. From this data a calculation can be performed to determine how many maleic anhydride monomers have been consumed in a single charge and with molecular weight data from SEC the number of average length of a maleic anhydride-alternating-styrene block can then be calculated. This allows for the the synthesis of macromolecules with well defined molecular weight and narrow PDI, but also of sequence within the polymer chain. This opens up the possibility to probe structure-performance relationships in much more detail than has been attempted before.

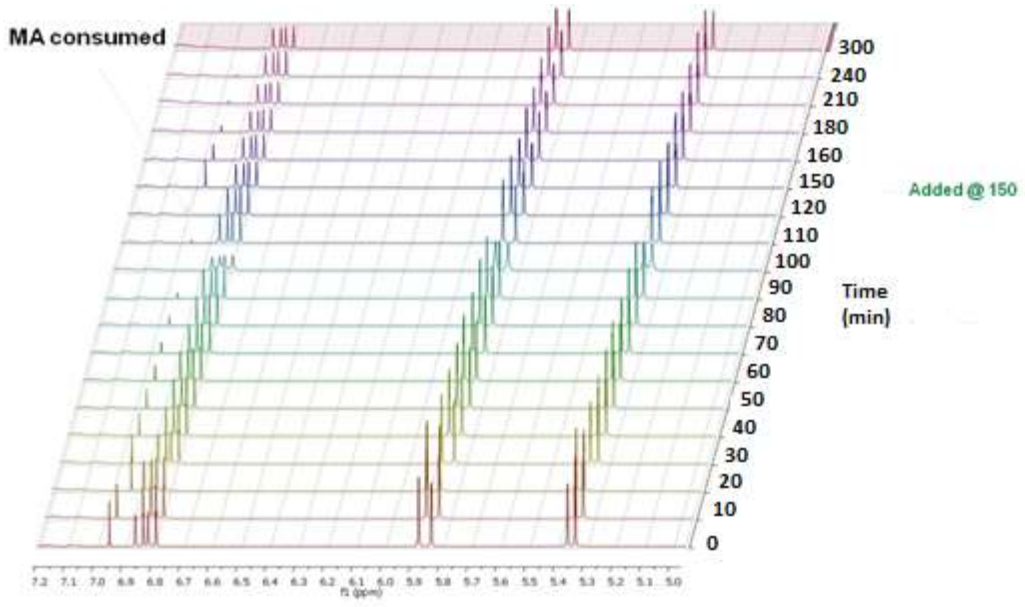

Figure 43: *^{1}H NMR Stack Plot for the RAFT Polymerisation of Styrene with maleic anhydride (5mol%) added at t=0 and 150 minutes. Notice the disappearance of the maleic protons at 6.9ppm.*

This offline ^{1}H NMR spectroscopy provides a means of determining the polymer sequence of the RAFT copolymerisation of styrene and maleic anhydride, enabling different length maleic anhydride blocks to be incorporated into a

polymerisation with styrene. This method could also be used for the free radical copolymerisation of styrene and maleic anhydride, however, monomer sequence could not be deduced as effectively without a controlled free radical method. SEC analysis was performed on the polymer at periodic intervals both before the addition of maleic anhydride to monitor the polymerisation. For each analysis a single distribution was observed that shifted towards higher molecular weight with increasing time. From the molecular weight data and the narrow PDI it infers that the second charge of maleic anhydride is consumed in the polymerisation.

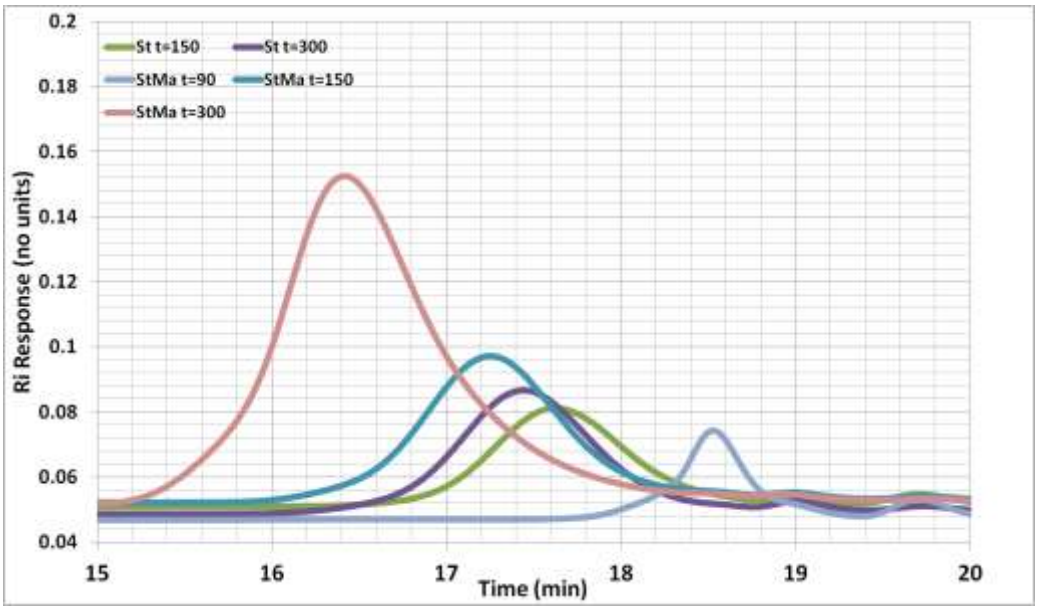

Figure 44*: SEC chromatographs of the RAFT polymerisation of styrene and Styrene – maleic anhydride copolymer at sampling times of 300, 150, 90 minutes.*

Table 8: Molecular weight data for the RAFT polymerisation of styrene and styrene maleic anhydride

Polymer	M_n	M_w	PDI
St 150 min	2000	2060	1.03
St 300 min	2700	2840	1.05
StMa 90 min	1400	1480	1.06
StMa 150 min	3400	3460	1.02
StMa 300 min	5000	5100	1.05

Looking at Table 8, the difference in molecular weights for the RAFT homopolymer and copolymer after the same period of time is explained by the difference in the rate of copolymerisation with maleic anhydride versus the rate of homopolymerisation of styrene. The next section explores these differences in the RAFT polymerisation of styrene and maleic anhydride.

Effect of maleic anhydride on the fragmentation of cumyl dithiobenzoate.

Many experimental parameters can have an effect on the rate of RAFT polymerisation: for example a high $[RAFT]_o/[initiator]_o$ ratio can result in a long induction time. However, some authors suggest that the initial induction period observed in most RAFT polymerisations stems from a slow fragmentation of the intermediate RAFT-radical in the pre-equilibrium and from a high value of the main equilibrium constant K. The effect of the leaving group is another parameter that can be studied, for example the variation in the reactivity of the C=S bond towards free radical addition should be small and the magnitude of the transfer coefficient should be dependent primarily on the leaving group ability of the free radical R*. Steric considerations suggest that oligomeric or polymeric radicals should be better leaving groups than monomeric radicals and for similar values of k(β,2) result in a higher chain transfer constant and reduced induction period. For a given initial monomer concentration, polymers

of decreasing length will be obtained by increasing the amount of RAFT agent added to the system, however this should not result in any kinetic difference.

The first visually observable effect of the presence of maleic anhydride from the beginning of the RAFT polymerisation is the clear colour change that happens early on in the polymerisation. This is associated with the fragmentation of the chain transfer agent.

Figure 45 shows the colour difference for the polymerisation of maleic anhydride and styrene and for the homopolymerisation of styrene, this indicates the fragmentation of the RAFT agent occurs sooner with the presence of maleic anhydride than with just the presence of styrene monomer. Notice that once the initial fragmentation of the RAFT agent has occurred in both polymerisations that the colour of the reaction is the same in both the homopolmyerisation and the copolymerisation.

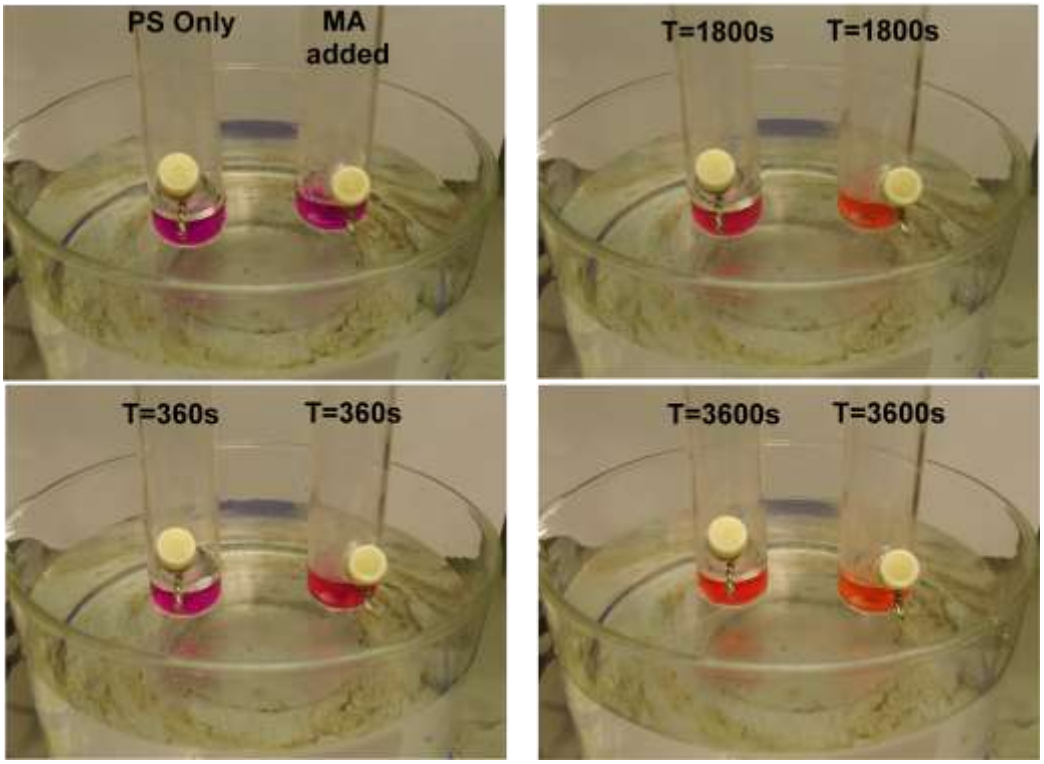

Figure 45*: Photographs of the RAFT polymerisation of cumyl dithobenzoate with styrene and styrene maleic anhydride. Notice the colour difference over time. LHS = styrene only, RHS = Styrene and maleic anhydride.*

Figure 46 shows the first order kinetic plots for the copolymerisation of styrene-alt-maleic anhydride, styrene with maleic anhydride added after 30 minutes and the homopolymerisation of styrene over the first 90 minutes of reaction. It is clear from this that maleic anhydride has an effect on the fragmentation of the cumyl dithiobenzoate chain transfer agent. The effect of maleic anhydride is a reduction in the lag or fragmentation time associated with RAFT polymerisation. In addition to this observation, there is a difference in the rate of polymerisation with the alternation having an increased rate over homopolymerisation of styrene.

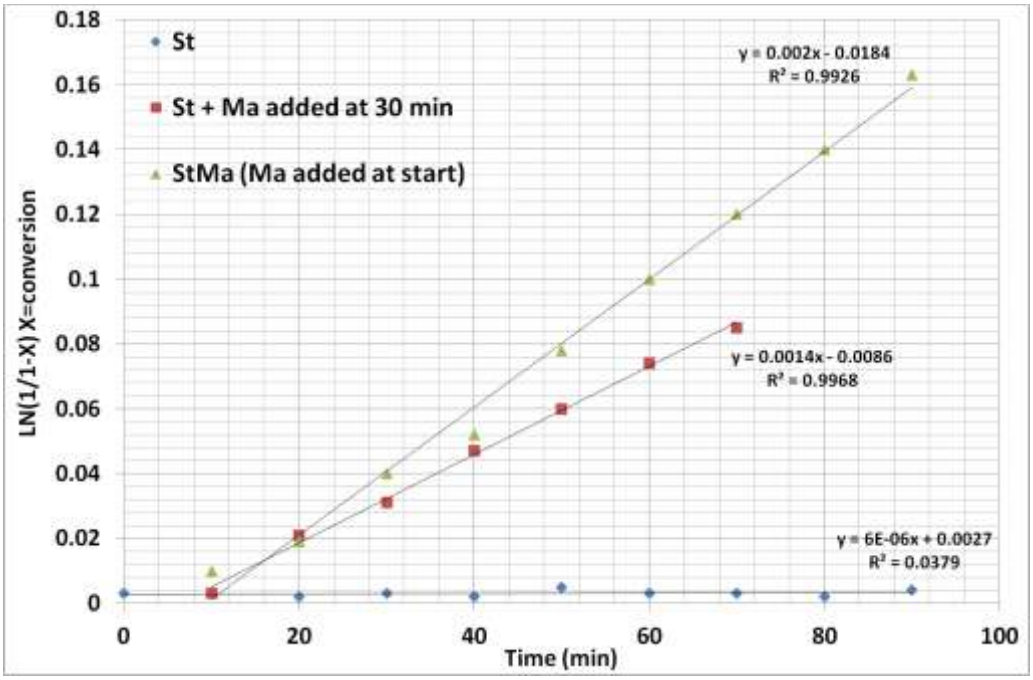

Figure 46*: Kinetic plots for the RAFT Polymerisation of styrene-alt-maleic anhydride, styrene, and styrene with maleic anhydride added at 30min.*

Figure 47 shows the normalised kinetic plots for the copolymerisation of styrene and maleic anhydride and the effect of adding maleic anhydride into the polymerisation of styrene at 60 minutes. The similar rate of polymerisation for the added maleic anhydride at 60 minutes and the styrene maleic anhydride copolymerisation can be used as an indication of the placement of

alternating maleic anhydride units into a styrene polymerisation. Furthermore this shows how repeatable the method is for determining the alternating polymerisation of maleic anhydride with styrene.

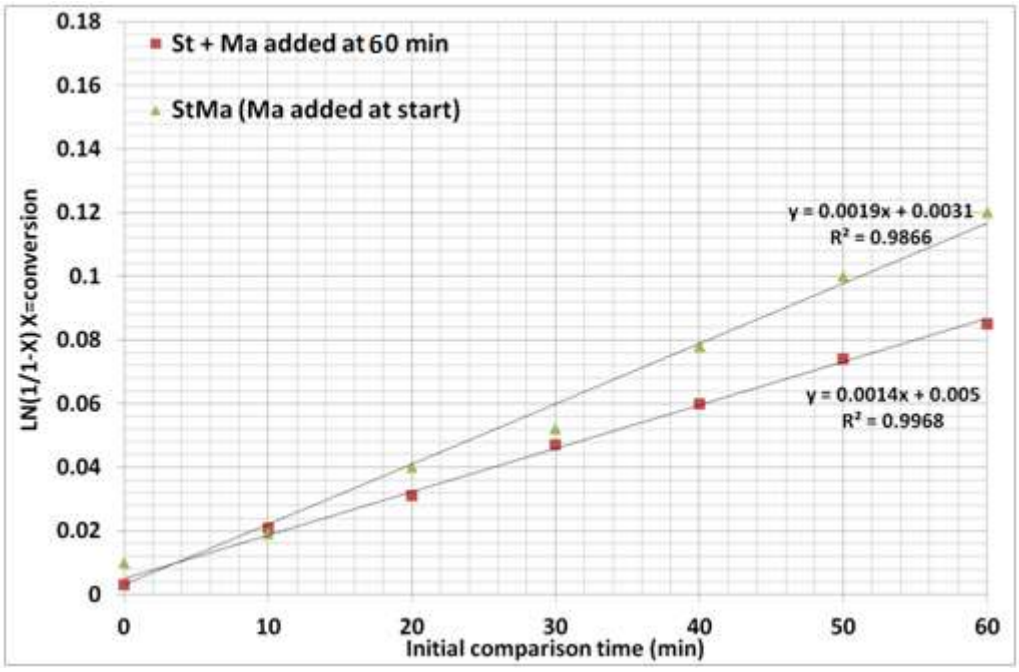

Figure 47: Kinetic plots for the RAFT Polymerisation of styrene-alt-maleic anhydride, styrene, and styrene with maleic anhydride added at 60 min. Time ajusted for the first 60minutes of reaction with maleic anhydride present

Figure 48 shows the difference in rate between maleic anhydride added at the beginning of the reaction and also after 150 minutes to the same reaction vessel following consumption of the first dose of maleic anhydride. This suggests that maleic anhydride is coupling with the RAFT agent in the pre-equilibrium stage due to the differences in the rate of polymerisation. Figure 49 shows the rate with maleic anhydride added once the homopolymerisation of styrene is under way, notice the similar slope to the plot for the addition at 150 minutes in figure 48. This further implies that maleic anhydride reacts preferentially with cumyl dithiobenzoate due to the similar polymerisation rates.

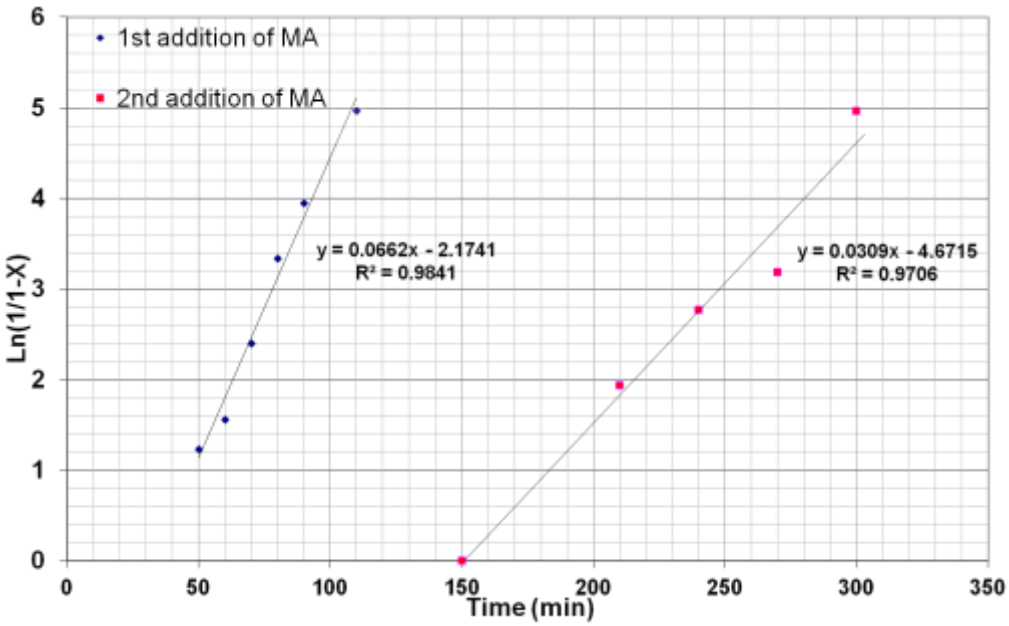

Figure 48: *Kinetic plots for the addition of maleic anhydride at t=0 and t=150 min, conversion was determined by offline ^{1}H NMR spectroscopy.*

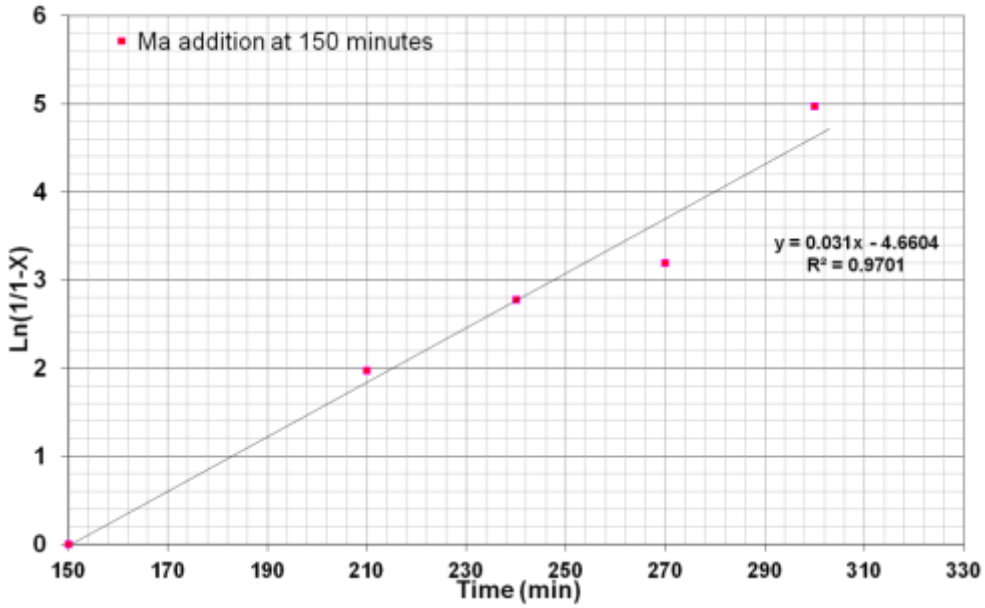

Figure 49: *Kinetic plots for the addition of maleic anhydride at t=150 min. Conversion was determined by offline ^{1}H NMR spectroscopy.*

If maleic anhydride is added to the early stages of a RAFT polymerisation of styrene with RAFT agent cumyl dithiobenzoate, then the pre-equilibrium stage of the RAFT polymerisation will begin immediately and the observed rate of maleic anhydride polymerisation is greater than if maleic anhydride is added to the polymerisation once the pre-equilibrium stage has passed. This effect can

also be whitnessed visually, by the change in colour when maleic anhydride is added into the early on in the polymerisation; where as once polymerisation has begun, no further colour change is observed.

Maleic anhydride addition to a Macro-RAFT agent.

The ability to place maleic anhydride within a block of polystyrene has been demonstrated; however of equal interest is the ability to place maleic anhydride at the end of the polymer chain, thereby end capping the polymer with maleic anhydride, which enabled further post polymerisation functionalisation of the polymer.

Polystyrene (various molecular weights) prepared from the RAFT polymerisation of styrene with cumyl dithiobenzoate (figure 51) was characterised by SEC and ^{1}H NMR spectroscopy.

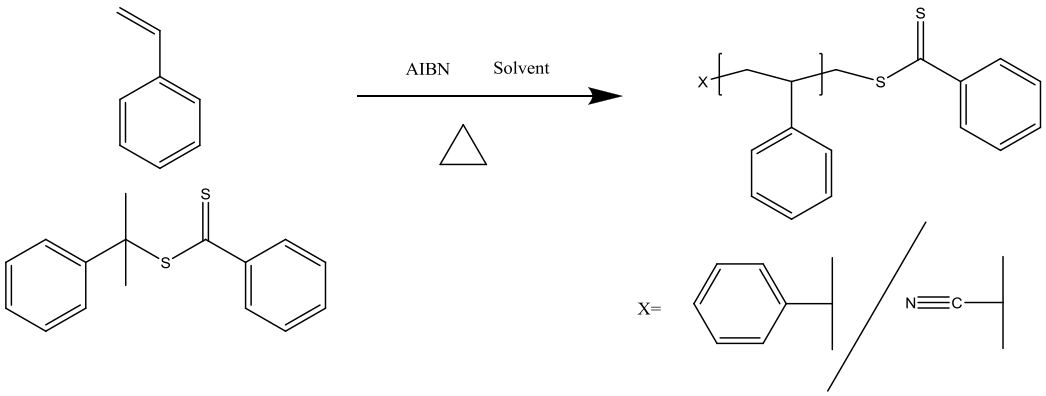

Figure 50*: RAFT polymerisation of styrene*

Table 9 shows the results from some initial polymerisation reactions carried out. A target molecular weight of 5000 was decided upon and Figure 51 shows the conversion against molecular weight for a typical polymerisation of styrene with cumyl dithiobenzoate upto 20% conversion. Figure 52 shows the kinetic plot and Figure 53 shows the effect of temperature on the initial kinetics.

Table 9*: Conditions and the results for various RAFT polymerisations of Styrene*

[M] : [RAFT]	[RAFT] : [I]	Temp (°C)	Solvent	Conversion[1] (%)	DP_n	$M_{n(Sec)}$[2]	PDI[2]
400	0	100	Bulk	58	235	24500	1.45
400	10	70	Bulk	77	300	32000	1.17
300	2	100	toluene	97	290	30500	1.21
300	2	90	toluene	96	290	30200	1.19
100	2	80	toluene	60	60	6300	1.12
100	2	80	toluene	69	70	7200	1.12
100	2	80	toluene	97	98	10400	1.1
200	10	65	$CDCl_3$	76	151	16000	1.3
200	2	65	$CDCl_3$	97	192	20500	1.11
50	2	75	toluene	95	48	4800	1.11
50[A]	2	75	toluene	97	49	5050	1.11
10	2	70	$CDCl_3$	97	10	1300	1.2
10	2	70	$CDCl_3$	97	10	1280	1.15

1. From ^{1}H NMR spectroscopy, 2. From light scattering measurements using SEC.

The RAFT polymerization of styrene in bulk and in solution (toluene, dueterated chloroform 50% v/v) (table 9) was carried out with cumyl dithiobenzoate as the RAFT agent and AIBN as the initiator. The first order reaction relationship between ln(1/1-X) (where X = conversion) and polymerization time is shown in figure 51 for the bulk, toluene and chloroform polymerisation at 70°C.

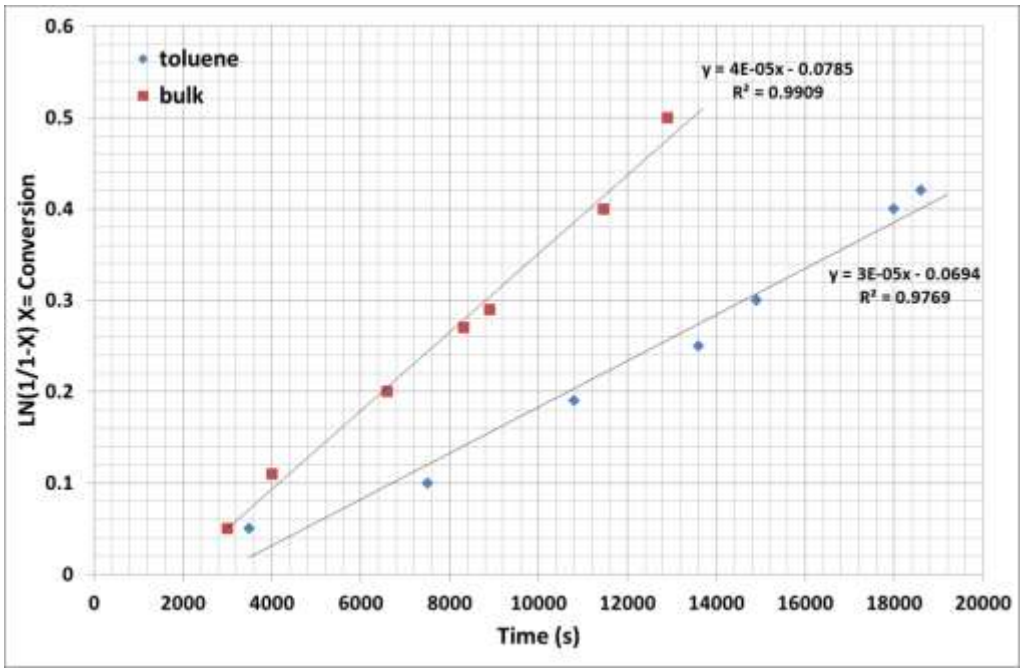

Figure 51*: Conversion vs Molecular weight (M_n) from table 8.*

The rate of the RAFT polymerisation of styrene in the bulk is faster than that in the solvent with the difference explained by the greater relative concentration of free radical to monomer in the bulk polymerisation.

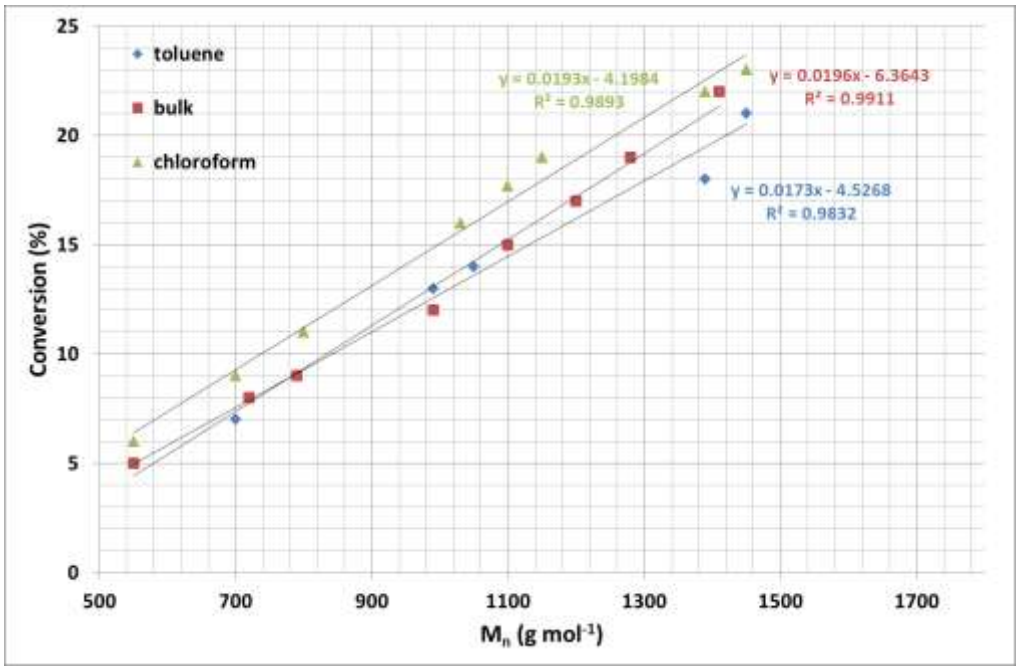

Figure 52:Molecular weight vs conversion for the RAFT polymerisation of styrene in toluene, bulk and chloroform at 70°C.

Figure 52 shows that M_n increases linearly with monomer conversion for both the bulk and solution polymerisation for the initial 25% of conversion and is in good agreement with already established literature on the RAFT polymerisation of styrene with cumyl dithiobenzoate RAFT agent[215]. At higher conversion the there is still a linear relationship for the RAFT polymerisation in solution, however for the bulk polymerisation this deviates from a linear relationship above 50% conversion. The PDI of the bulk polymerisation also increase with conversion, deviating from what theoretical estimations. The PDI difference for the bulk polymerisation is greater than the PDI difference for the solution polymerisation. This is counter intuitive as the presence of toluene which has high chain transfer constant for the polymerisation of styrene[216] would be expected to contribute to increases in PDI with time. The bulk RAFT polymerisation of styrene is more susceptible to the auto acceleration or Trommsdorf-Norrish effect[217, 218] which leads to a lack of control and therefore an increase in PDI due to the increased viscosity of the system although the RAFT process has been shown to suppress auto acceleration relative to a free radical polymerisation.

Figure 54 shows the effect that temperature has on rate of reaction at 80-100^{o}C for the RAFT polymerisation of styrene in toluene with online ^{1}H NMR spectroscopy used to measure the conversion of styrene into polystyrene. The higher the temperature the shorter the pre-equilibrium delay for the cumyl dithiobenzoate RAFT agent.

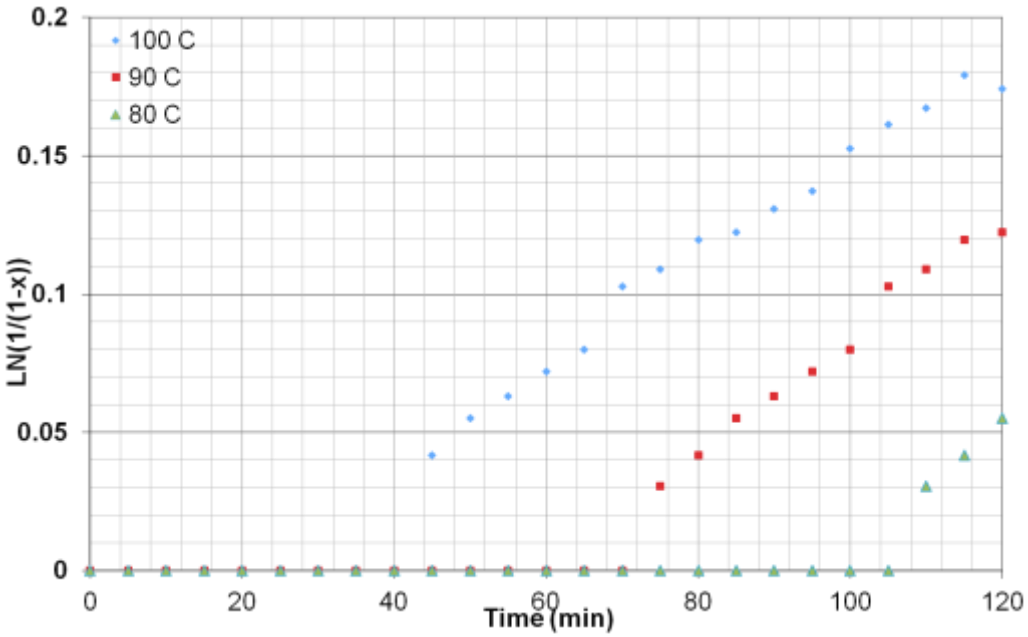

Figure 53*: Temperature effects upon the inital rate of the RAFT Polymerisation of Styrene.*

Once suitable RAFT polystyrene polymers had been synthesised, they were then subjected to further reaction with maleic anhydride and a second charge of AIBN, figure 55 with the aim of producing endcapped polystyrene with maleic anhydride.

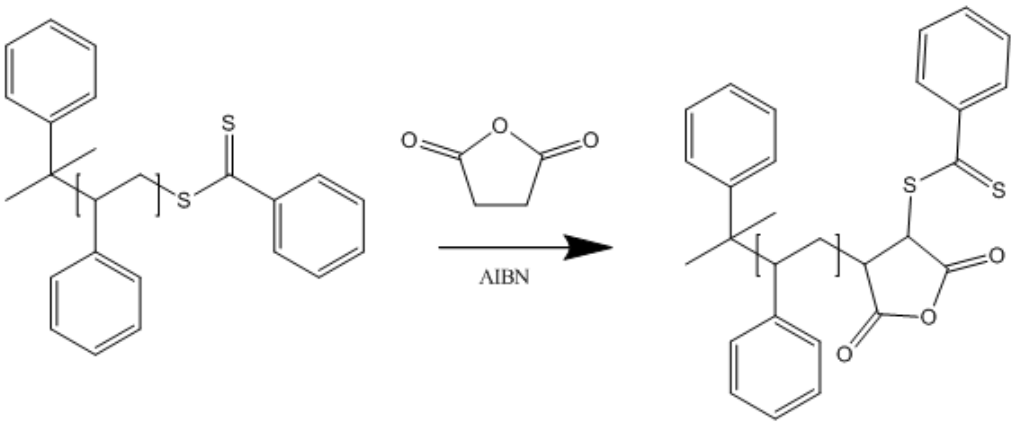

Figure 54: Proposed reaction of RAFT Polystyrene with maleic anhydride to produce end capped polystyrene with maleic anhydride

Prior to maleic anhydride addition, a sample was taken for offline ^{1}H & ^{13}C NMR spectroscopy & SEC analysis. Sampling of the reaction was then conducted at defined intervals. Figure 56 shows the comparison of the ^{13}C NMR

spectra for the initial polystyrene and the final product shows the appearance of the succinic carbons at 135ppm and the no presence for sp^2 carbons of maleic anhydride at 138ppm.

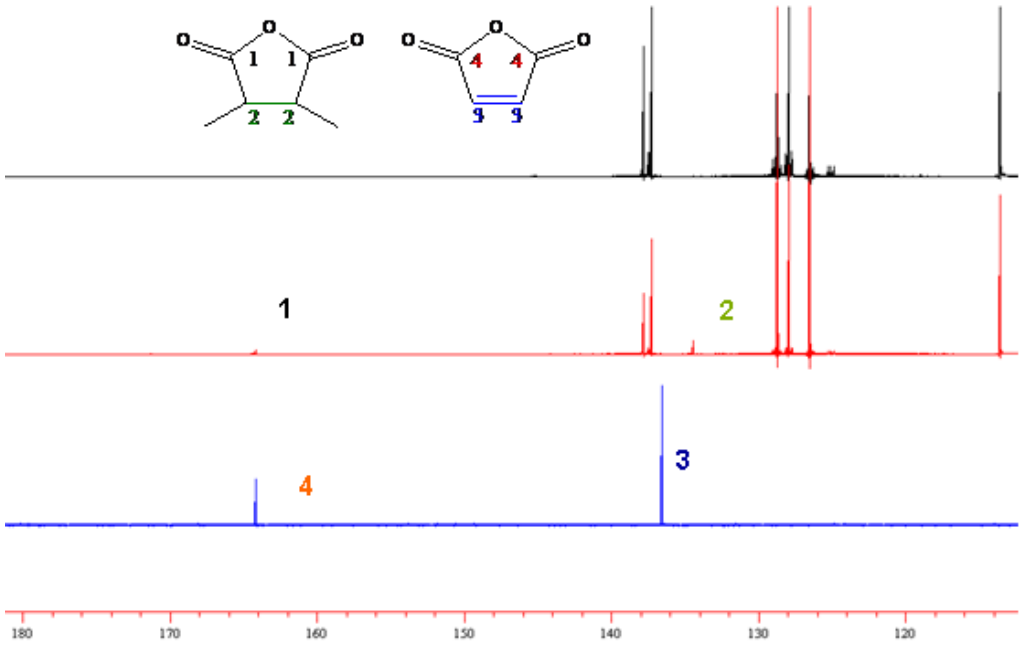

Figure 55*: Comparison of the 125MHz ^{13}C NMR spectra showing 180-110ppm; top spectrum: RAFT polymerisation of styrene. Middle spectrum: RAFT polymerisation of styrene with maleic anhydride addition after 48h. Bottom spectrum: maleic anhydride monomer.*

Again ^{1}H NMR spectroscopy (figure 57) was employed to look at the disappearance of the maleic anhydride protons. This analysis indicated that, after 48 hours, there was still residual maleic anhydride in the reaction mixture, indicating that the reaction had not proceeded to 100%. The reaction was left so long as to try to encourage as much maleic anhydride incorporation onto the end of the polystyrene as possible.

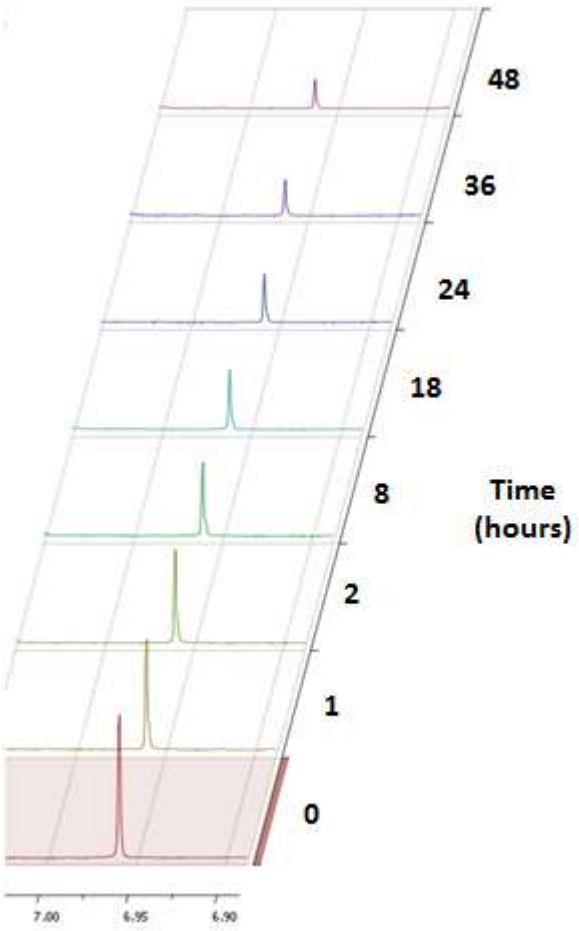

Figure 56*: Disappearance of maleic anhydride over time by ^{1}H NMR spectroscopy.*

MALDI-MS was used to investigate the incorporation of maleic anhydride, figure 58. Although, the analysis proved to be non trivial, even with the use of silver triflate solution the ionisation process provided low resolution data, however it does provide evidence that following the addition of maleic anhydride the molecular weight of the polymer distribution for the RAFT polystyrene has shifted to higher molecular weight by an increase of 99 mass units, which indicates that maleic anhydride has been successfully attached to the polymer chain. It is reasonable to assume that the maleic anhydride is attached at the end of the chain, as there is little option for the material to attach elsewhere under the conditions used, however MALDI cannot confirm the location of addition. It is possible to graft maleic anhydride onto a polymer backbone however this is achieved at temperatures in excess of 200^{o}C[219]. Although there is an increase in molecular weight, the whole distribution has

not shifted to higher molecular weight, which would be an indication that each polystyrene chain has been successfully end capped with maleic anhydride. This coupled with the ^{1}H NMR spectroscopy indicates that not every chain has reacted with the maleic anhydride.

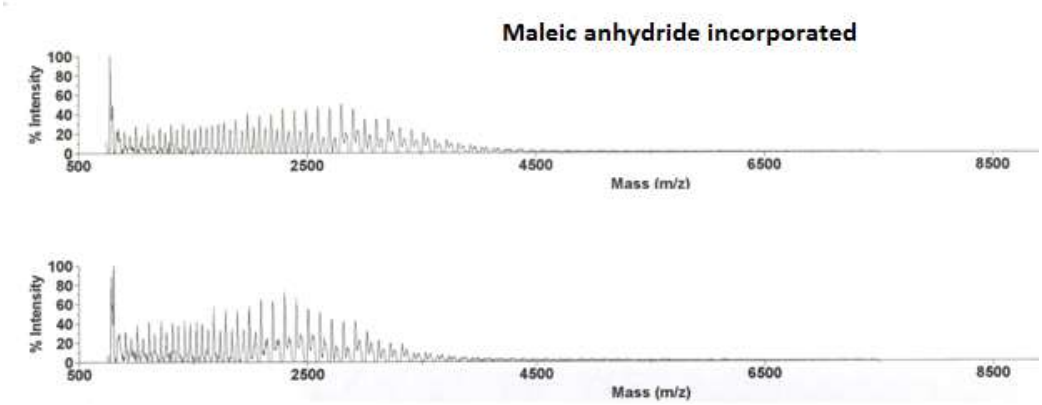

Figure 57: MALDI-MS data: Top: RAFT Polystyrene with maleic anhydride. Bottom: RAFT polymerisation of styrene

The low PDI (<1.15) for the RAFT polymerisation of styrene indicates that the RAFT polymerisation has been well controlled using cumyl dithiobenzoate, and would imply that the RAFT agent was still attached at the end of the chain. The lower than expected maleic anhydride incorporation is due to the second charge of initiator that will compete with maleic anhydride and maleic anhydride AIBN fragments with the polystyrene macroRAFT agent during fragmentation. This will result in some of the polystyrene chains being end capped with AIBN derived fragments.

Further proof for the attachment of maleic anhydride was sought and this led to the development of a chemical method to identify its incorporation by the use of SEC. Assuming maleic anhydride is present exclusively at the end of the chain, then reaction of this polymer containing maleic anhydride with a diamine (in low concentration) would lead to doubling of molecular weight of the polymer, observable by the SEC. Hexyl-1,6-diamine was chosen and a doubling in molecular weight was observed, Figure 59.

However, upon further consideration of the chemistry involved it is also possible that a cleavage reaction could occur between the amine and the dithioester end group of the RAFT agent. This would lead to free thiol groups at the end of the polymer which would then be able to combine via the formation of a disulfide bond, giving a corresponding doubling of molecular weight, see Reaction pathway B in Figure 60. This could also account for the observable doubling of molecular weight via SEC. Therefore, a further SEC experiment was conducted where the amine treated polymer was exposed to dithiothreitol and re-analysed via SEC. Dithiothreitol an effective reducing agent for disulfide bonds[220-222].

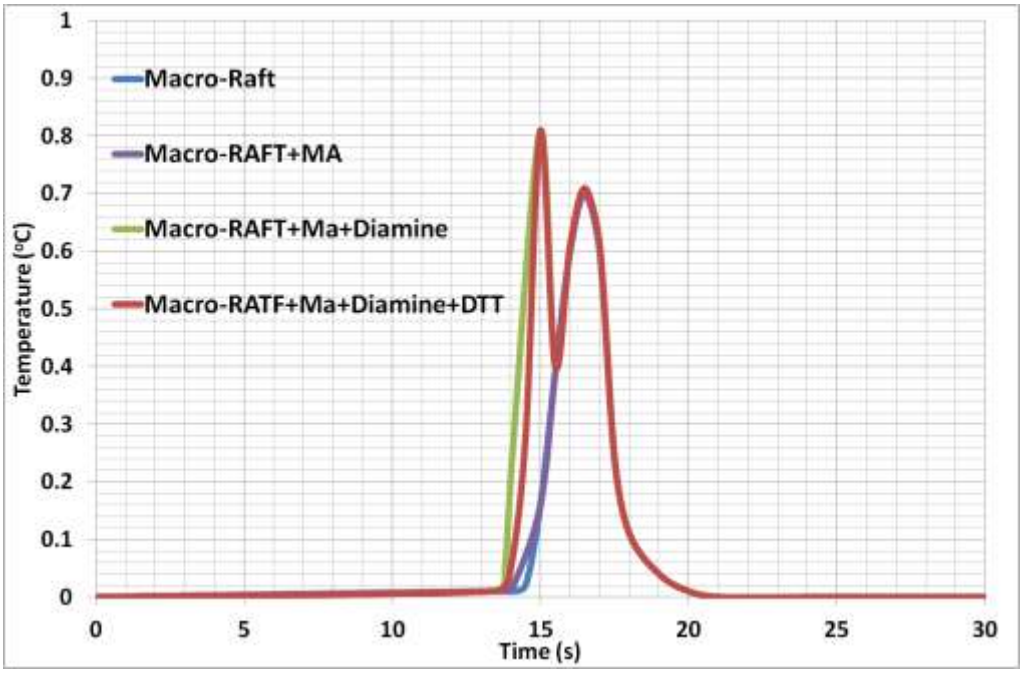

Figure 58: SEC chromatographs for the RAFT polymerisation of styrene (light-blue) macro-RAFT with maleic anhydride incorporation (red), macro-RAFT polymerisation with maleic anhydride followed by reaction with hexyl-1,6-diamine(green) and macro-RAFT polymerisation with maleic anhydride followed by reaction with hexyl-1,6-diamine then dithiotreitol (dark blue).

Figure 59 shows that no difference was observed in the SEC chromatograms between the diamine reacted polymer and the addition of dithiothreitol. Because dithiothreitol is known to cleave disulfide bonds, the doubling in molecular weight is inferred from the diamine coupling and not disulfide

formation. This confirms that the doubling in molecular weight is due to the coupling of the diamine with maleic anhydride attached at the end of the chain.

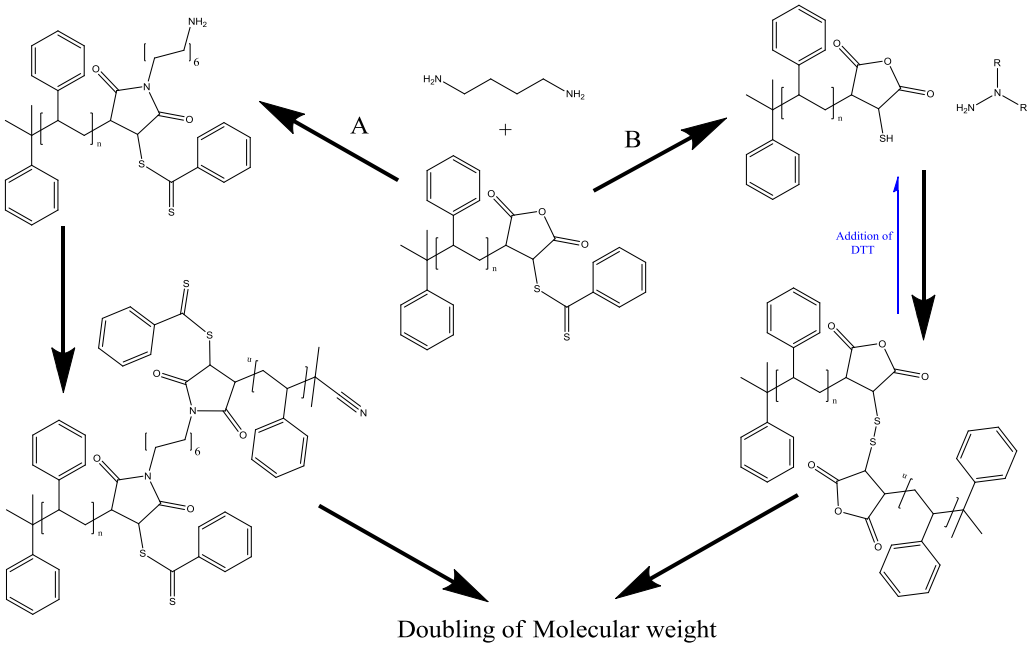

Figure 59*: Possible reaction pathways for the observed doubling of molecular weight in the SEC experiment.*

Table 10 summarises the molecular weight data obtained from the SEC chromatograms obtained in figure 59. Although this method gives credence to the incorporation of a single maleic anhydride unit onto the RAFT polystyrene, it doesn't give conclusive evidence that each polymer has been end capped with maleic anhydride; by comparison of the area under each chromatogram the amount of attached maleic anhydride is at least 54%, because the cross linking or coupling with the diamine will not achieve 100% conversion, and therefore there is still polystyrene end capped with maleic anhydride that has not cross linked, but has the other end of the diamine free in solution.

However, there is no conclusive evidence that all polystyrene chains have been end capped with maleic anhydride, but at least 54% of the chains are endcapped with maleic anhydride.

Table 10*: SEC data for the incorporation of maleic anhydride onto Macro-RAFT polystyrene.*

Polymer	M_n (g mol^{-1})	DP_n	PDI
Macro-RAFT	5000	48	1.15
Macro-RAFT+MA	5000	48	1.15
Macro-RAFT+MA+Diamine	9800	95	1.19
Macro-RAFT+MA+Diamine+DTT	9800	95	1.19

Stearyl methacrylate copolymers

The control of the RAFT polymerisation is related to the structure of the RAFT agent and its effect upon the series of equilibria in the RAFT mechanism. As mentioned previously, RAFT agents may be represented as Z-(C=S)-S-R, where the Z-group improves the stability of the radical intermediate and the R group is a fragment which reinitiates radicals. The choice of the Z-group affects the stability of the intermediate radical adduct, and therefore the stability of this group affects the reactivity of the C=S bond towards propagating radicals. If the Z group is the strongly stabilising group then the intermediate radical becomes too stable and no expulsion of an initiating radical is observed. This has been studied in depth and, in the majority of cases, a phenyl group has been found to be suitable. More recently, CTAs have been developed where the Z-group is bonded through a sulphur atom, giving rise to trithiocarbonates. In this case the C=S bond is reactive enough for intermediate formation but fragments quickly enough to give little or no induction period in the polymerisation.

The R-group has an effect upon the stability of the intermediate radical but its effect is less pronounced than the Z-group. Therefore the R-group's designated task is to be a good leaving group in comparison to the propagating polymer chain and also a re-initiating species for the monomer being polymerised.

The selection of the R-group is a compromise between a radical that is stable enough to be considered a good leaving group but reactive enough to re-initiate polymerisation.

The choice of stearyl methacrylate as a monomer offers the potential to produce polymers with good oil solubility due to the long C-18 linear side chain on the stearyl methacrylate monomer. The potential to couple stearyl methacrylate with another linker or block copolymer opens up synthetic routes to novel dispersant polymers.

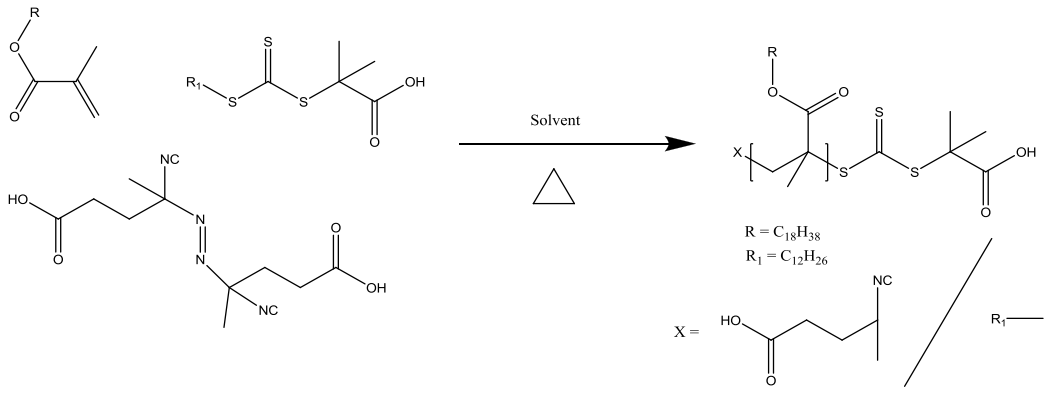

Figure 60: RAFT polymerisation of stearyl methacrylate.

For the RAFT polymerisation of stearyl methacrylate, Figure 61, (4-cyanopentanoic acid)-4-dithiobenzoate (CPADB) was initially used as the CTA, due to its ability to control the polymerisation of methacrylates, however, although the polymerisation of stearyl methacrylate was well controlled, the addition of maleic anhydride on this backbone was unsuccessful. Therefore 2-(dodecylthiocarbonothioylthio)-2-methylpropanoic acid (DDMAT), a trithiocarbonate RAFT agent, was chosen as a compromise between the ability to control the stearyl methacrylate polymerisation and to offer the further reaction with maleic anhydride and styrene.

DDMAT was synthesised according to the procedure by Skey *et al*.[223] with a yield similar to their reported yield of 62%.

Polymers with an overall target molecular weight of 10,000 g mol^{-1} and 50,000 g mol^{-1} were synthesised. The stearyl methacrylate block was synthesised first, filtered and purified before further polymerisation with styrene and maleic anhydride to make the block copolymers. There was good agreement between the theoretical molecular weights and the determined molecular weights using RALLS data from the SEC. Table 11 shows the overall molar percentage of each block in the corresponding copolymer.

Table 11:Copolymers formed using stearyl methacrylate. Molar percentage determined from NMR spectroscopy, degree of polymerisation from SEC.

Stearyl methacrylate block		Second Block		
Mol %	DP_n	Monomer 2	Mol %	DP_n
90	30	Styrene	10	10
90	30	Styrene/ maleic anhydride	25	25
75	25	Styrene	25	25
75	25	Styrene	25	25
75	25	Styrene/maleic anhydride	25	25
90	150	Styrene	10	50
75	125	Styrene	25	125

Stearyl methacylate copolymers with styrene[224] and maleic anhydride[225] have been reported using anionic polymerisation, however the RAFT block

copolymer of stearyl methacyrlate with styrene-alt-maleic anhydride, figure 62, has yet to be reported in the literature.

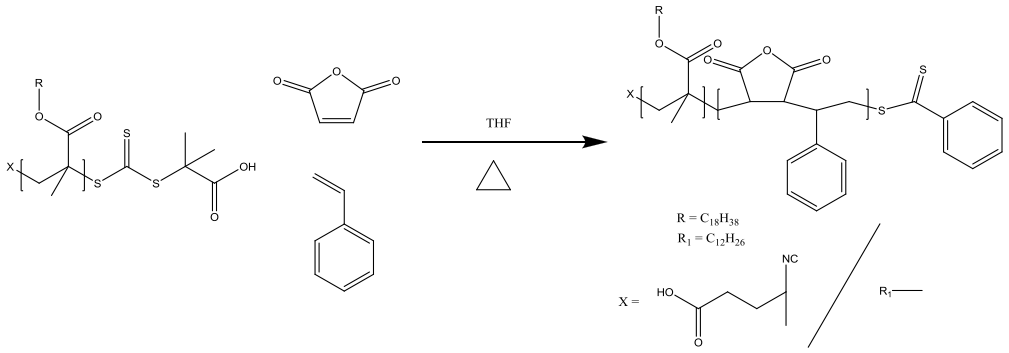

Figure 61: RAFT polymerisation of stearyl methacrylate with styrene and maleic anhydride.

Typical SEC trace for the polymerisation of stearyl methacylate block and the corresponding styrene block can be seen in figure 63. Notice that the addition of the styrene does not product a second distribution and the first distribution continues to grow. The PDI of the polymer increases with addition of the second block, which indicates that termination reactions have become more significant in the second block copolymer, than without the stearyl methacylate macro-RAFT agent present. The larger than expected PDI results from the Stearyl methacyrlates trithiocarbonate macro-RAFT agent's compatibility with styrene in order to control the polymerisation of the second block of styrene. The leaving group on the macro-RAFT agent is likely to be poor at reinitiating styrene monomer coupled with the different rate of fragmentation from the macroRAFT agent, in comparison to cumyl dithiobenzoate which provides good control over the RAFT polymerisation of styrene.

The other minor contributing factor to this increase in PDI is the number of dead chains from the stearyl methacrylate block; without the stearyl methacrylate block being end capped with trithioester RAFT agent then there isn't the possibility to produce the block copolymer from that chain.

Stearyl methacrylate copolymer with styrene-alt maleic anhydride, was also synthesised, table 11. There was also an increase in PDI similar to polystyrene

indicating again that the stearyl methacrylate macro-RAFT agent isn't the ideal choice for block polymerisation in this manner.

The RAFT polymerisation of stearyl methacrylate using the RAFT agent cumyl dithiobenzoate was attempted, however the polymerisation was uncontrolled and resulted in nonlinear rate plots along with large PDIs for the resulting polymer. No attempt was made to synthesis stearyl methacrylate block copolymers cumyl dithiobenzoate due to its poor control over the stearyl methacrylate block.

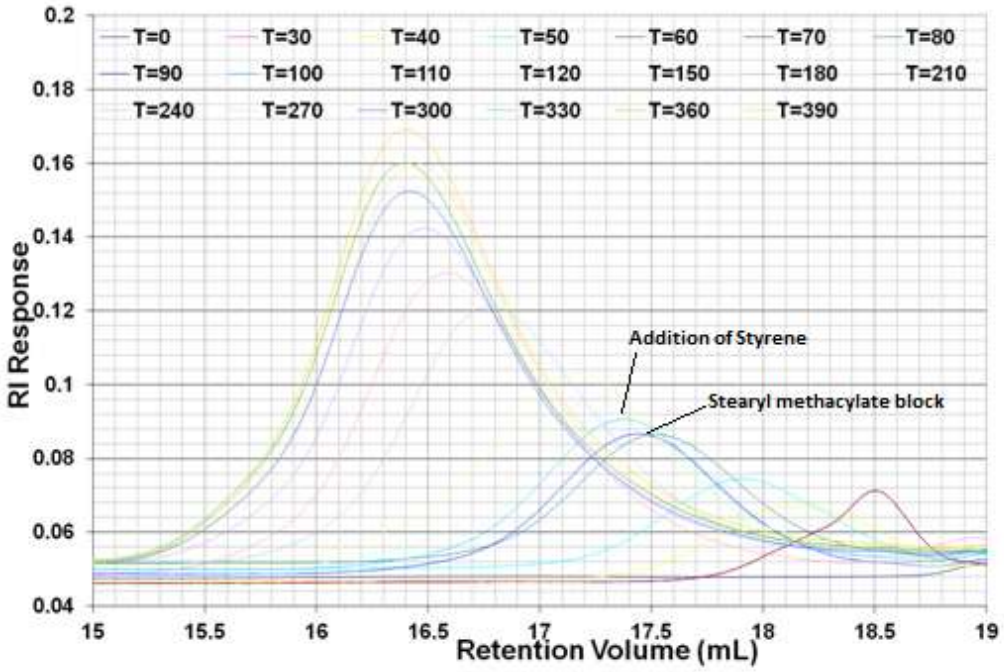

Figure 62: SEC chromatograms for RAFT Polymerisation of stearyl methacrylate over time, note the addition of styrene after 270 minutes.

This demonstrates the ability to produce block copolymers of stearyl methacrylate with blocks of styrene and styrene-alt-maleic anhydride in good yield with decent control. These polymer architectures allow for a fully polymeric version of the traditional dispersant viscosity modifier (DVM), a traditional DVM will contain an oil soluble tail, a linker and an active head

group. For example in the case of Poly(stearyl methacrylate-b-styrene), the stearyl methacrylate block acts as the oil soluble tail while the styrene block with its aromatic rings acts as a potential head group, with no need for a separate linker group.

Polymerisation with N-maleimides

The reaction between maleic anhydride and a primary amine results in the formation of N-maleimides, without compromising the double bond. This allows for polymerisation in the same way as with maleic anhydride. One advantage in producing N-maleimides is that upon polymerisation the amine functionality is incorporated into the polymer backbone. To achieve the same product with an alternating maleic anhydride polymer, a post polymerisation functionalisation step is required.

The RAFT polymerisation of styrene with N-phenylenediamine maleimide with cumyl dithiobenzoate was attempted, in a similar way to what has been reported with the ATRP polymerisation of styrene with N-substituted maleimides[226] and in an analogus way to the reported styrene-alt-maleic anhydride block styrene copolymers that have been synthesised above. The use of RAFT polymerisation to control the chain length and molecular weight distribution and monomer sequence offers the potential to produce once pot block copolymers of various architecture. In principal the polymerisation of styrene with another strongly electron accepting vinyl monomer should lead to the production of well defined block copolymers in one pot[186]. Figure 64 shows the reaction between styrene and N-phenylenediamine maleimide.

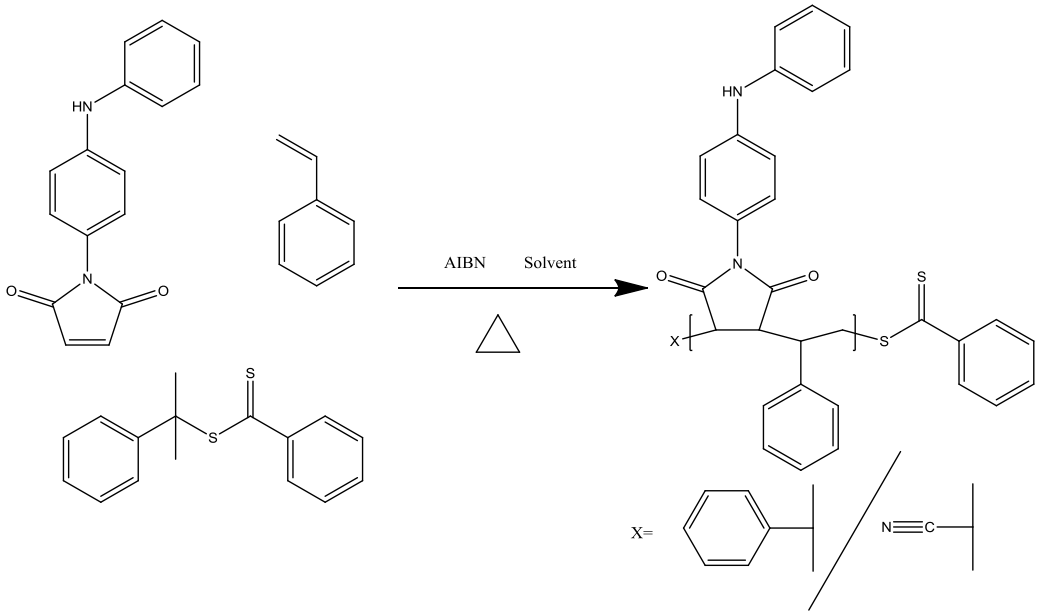

Figure 63: RAFT polymerisation of stearyl methacrylate block styrene

The molecular weight data for the polymerisation is shown in table 12.

Table 12: Reaction data for the RAFT Polymerisation of styrene (monomer 1) and N-maleimide (monomer 2), with the RAFT agent Cumyl dithiobenzoate.

[M]:[RAFT]	Conversion (%)	M_n	M_w	PDI
100	66	24000	35000	1.5
150	45	29000	37000	1.3
200	40	30500	38000	1.3
250	32	30000	41500	1.4
250	31	29500	48000	1.6

Figure 64 shows how the polymerisation has deviated from the expected molecular weight values at low conversion. Notice the larger than expected value for the PDI at low conversion indicating that there is a lack of control and that termination reactions are occurring more frequently than is desirable for a RAFT polymerisation.

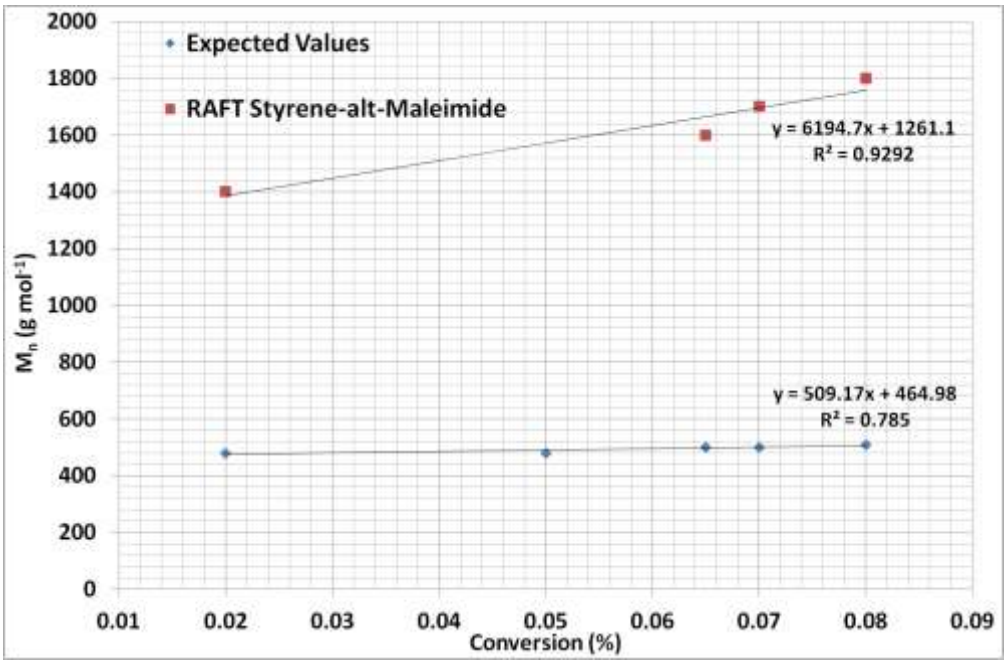

Figure 64: A plot of molecular weight vs conversion for the RAFT polymerisation of styrene and maleiomide.

Although it is known that N-maleimides will form alternating block copolymers with styrene, in the same way as maleic anhydride will, it is also possible to homopolymerise N-maleimides[223] unlike the homopolymerisation of maleic anhydride. Therefore it is likely that although there is a tendency towards alternation in this reaction, it is likely that this will also impact the PDI of the polymer.

Incorporation of head groups.

Having successfully introduced maleic anhydride into various polymer chains the requirement now for the dispersant synthesis is to attach a suitable head group onto the polymer. *N*-Phenylenediamine, depicted in Figure 65, was chosen.

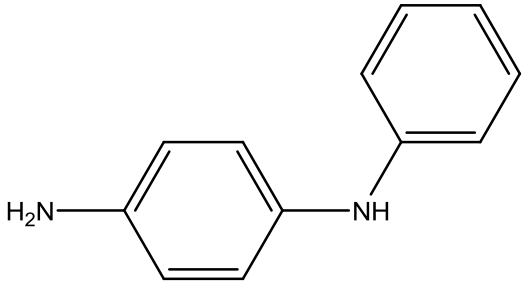

Figure 65: N-phenylenediamine

In order to produce a variety of dispersant type structures, copolymers and terpolymers were prepared. In these cases the polystyrene blocks would act as dispersant head groups while the oil soluble stearyl methacrylate block was intended to provide solubility. The alternating copolymers of styrene and maleic anhydride were reacted with a mixture of long chain amines and *N*-phenylenediamine to provide base oil solubility and dispersant group functionality, although it was hard to determine the exact ratio of amine attached.

Coupling reactions

Polyisobutylene amine reaction with polystyrene end capped with maleic anhydride.

Commercially available polyisobutylene-amine provided by BASF was used as a linker to attach polystyrene end functionalised with maleic anhydride via reaction of the succinic anhydride group of the polystyrene polymer to form a dispersant type molecule.

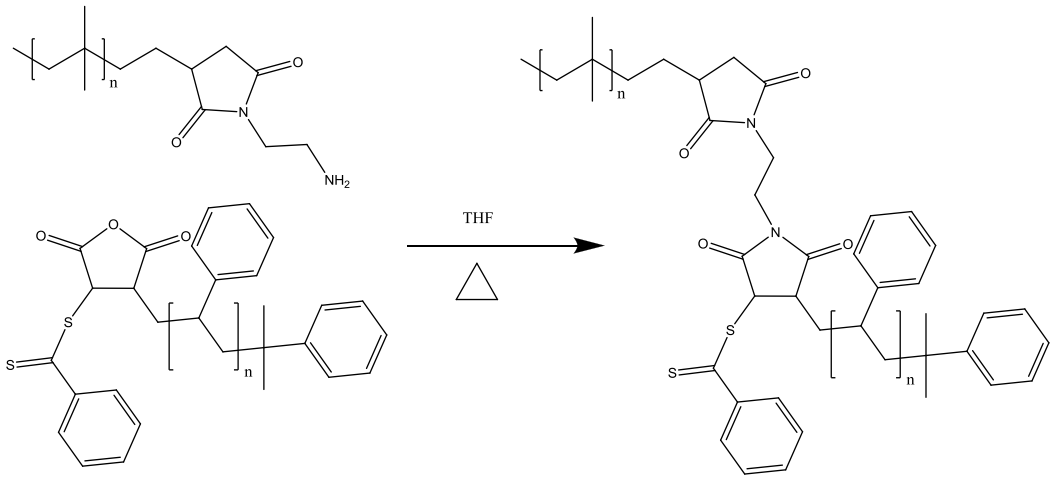

Figure 66: *Coupling(polystyrene) end functionalised (maleic anhydride) with polyisobutylene-amine to form a coupled PIB-PS copolymers*

The material was analysed by SEC and FTIR. Table 13 shows the molecular weight data for the coupling of end capped polystyrene with maleic anhydride with PIB-amine. There is a large increase in the PDI of the coupled product along with a broad chromatogram indicating that coupling has occurred.

Table 13: Molecular weight data for the coupling reaction between the RAFT polystyrene end capped with maleic anhydride and PIB amine.

Polymer	M_n (g mol^{-1})	M_w (g mol^{-1})	PDI
PS-end capped MA	5000	5750	1.15
PIB-amine	3200	4000	1.25
Coupled PS-MA-PIB-amine	4800	22000	4.58

FTIR analysis was used to determine the net absorbance rations of the different C=O structures present in each of the polymers that correspond with anhydride, amide and imide functional groups in order to determine the amount of coupling that has occurred. Table 14 shows the functional groups and the region in which they absorb, Figure 67 shows the functional groups.

Table 14: The Peak of interest in the FTIR spectrum and the corresponding wavenumber associated with the C=O stretch.

Peak	Wave number (cm^{-1})
Anhydride	1800-1760
Imide	1720-1690
Amide	1670-1650
Hydrocarbon	1600-1400

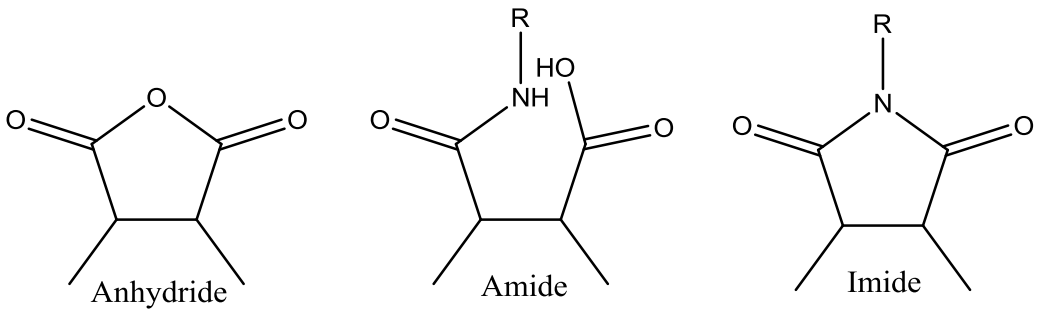

Figure 67: The functional groups that correspond to the functional groups in table 14

The net absorption ratio is recorded from the FTIR absorbance spectrum of the polymer of interest, the net absorbance ratio for the peak of interest is defined as:

The net absorbance ratio $= \frac{Net\ absorbance\ at\ \lambda 1}{Net\ absorbance\ at\ \lambda 2}$

Where λ1 = absorbance at the peak value, λ2 = absorbance at baseline peak value. All calculations were performed using thermo grams 32 software.

This method allows for comparison of the anhydride ratio to both the imide ratio and amide ratio within the same polymer and therefore comparison of these ratios for the two polymers that are being coupled, PIB-amine and PS end capped with maleic anhydride and the coupled product will indicate if the coupling reaction has occurred. An increase in the ratios of the imide:hydrocabon ratio and amide:hydrocarbon ratio and a decrease in the anhydride:hydrocarbon ratio relative the starting material will indicate the coupling has occurred, as the amine functionality of the PIB-amine will either form an amide or imide bond with the maleic anhydride unit at the end of the PS block. Table 15 shows the ratios obtained for this reaction.

Table 15:FTIR net absorbance ratios from for Anhydride: Hydrocarbon (Anh:HC), Amide:Hydrocarbon (Ami:HC), Imide:Hydrocarbon (Imi:HC), Anhydride:amide (Anh:Ami) and Anhydride:imide (Anh:Imi).

Polymer	Anh:HC	Ami:HC	Imi:HC	Anh:ami	Anh:Imi
PIB-amine	0.014	0.322	0.654	0.045	0.022
PS-end capped MA	0.214	0.001	0.002	159.925	142.867
Product	0.063	0.192	0.464	0.330	0.137
Theoretical 50:50 mix	0.114	0.162	0.328	0.707	0.349

*region used was selected from table 14, Hydrocarbon base line for all comparisons is 1460cm^{-1}

From table 15, the ratio of amide and imide to hydrocarbon for the product has increased relative to the theoretical values for the mixing of PIB-amine and PS-end capped with maleic anhydride. Furthermore the anhydride:hydrocarbon ratio is lower in the product than the mixed polymer system. This indicates that there is more amide and imide functionality present in the product and less maleic anhydride present than if PIB-amine and PS-end capped with maleic anhydride were just mixed together, consequently this means that the reaction between PIB-amine PS-end capped with maleic anhydride has occurred due to the relative increase in imide and amide functional groups in the product.

The large ratio in table 15 for the anhydride to imide and amide ratio for the end capped polystyrene is due to the lack of imide and amide present in the sample.

Reactions with degraded polystyrene

Maleic anhydride with degraded polystyrene.

Having already shown the ability to attach maleic anhydride to the end of a polymer chain by RAFT polymerisation, an attempt was made to repeat this with the degraded polystyrene. Figure 68, shows some of the potential end groups of the degraded polystyrene as inferred from the ^{1}H NMR and FTIR spectroscopy data presented in chapter 2.

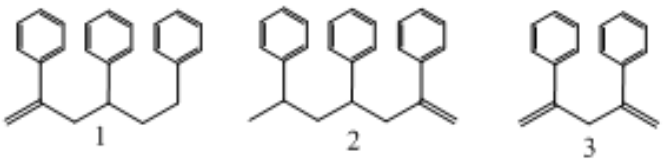

Figure 68: Examples of potential end group structures on the degraded polystyrene

SEC analysis indicated no change in the molecular weight of the polystyrene after reaction with maleic anhydride and ^{1}H NMR spectroscopy was again utilised to look at the disappearance of the maleic protons (Figure 69). Because maleic anhydride was added in excess, the disappearance of the maleic protons does not reach 100%, however there is a noticeable decrease in their abundance indicating that some reaction has occurred between the maleic anhydride and the degraded polystyrene. There is also a slight decrease in the

concentration the peaks at 4-6ppm. The idealised reaction scheme between maleic anhydride and the degraded polystyrene is shown in figure 70.

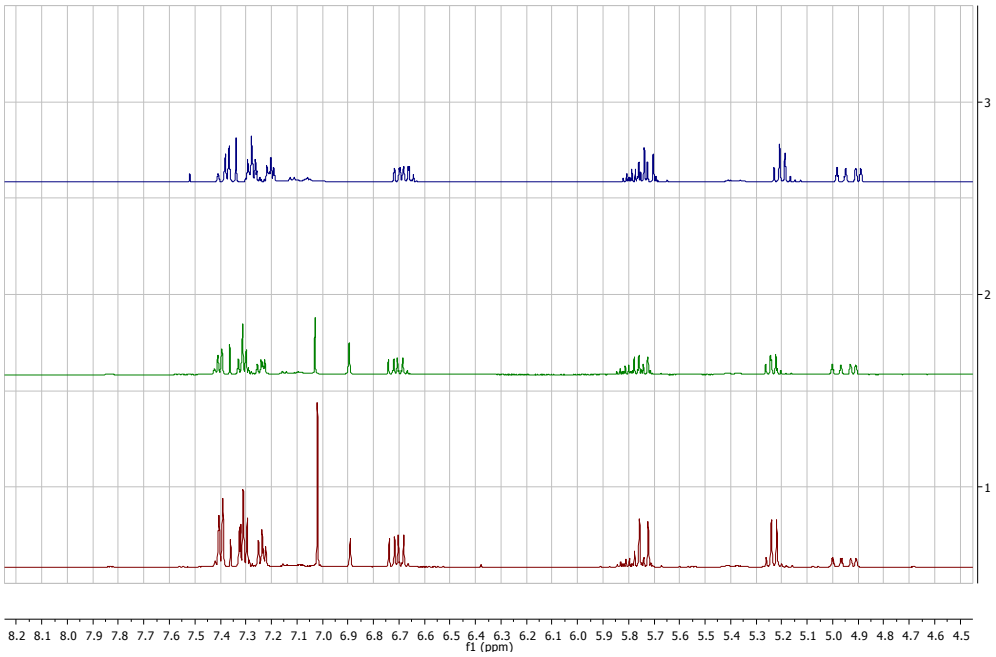

Figure 69: 1H NMR stack plot for the addition of maleic anhydride to degraded polystyrene. 1) addition of maleic anhydride at t=O, 2) After 24 hours, 3) degraded polystyrene only

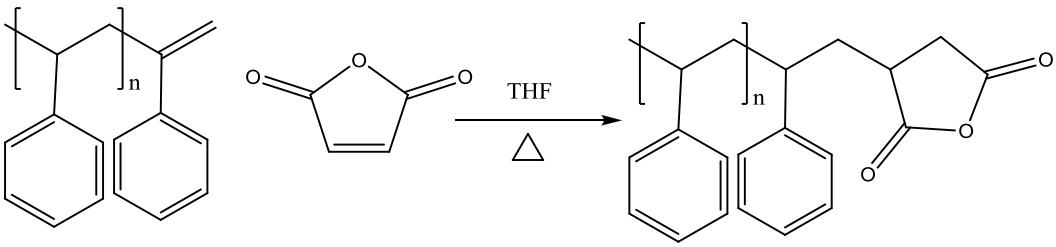

Figure 70*: Maleic anhydride functionalised waste polystyrene*

The functionalised waste polystyrene with maleic anhydride was reacted with PIB-amine in order to produce a dispersant structure (figure 71), with the PIB chain acting as the oil soluble tail.

SEC of the product produced a very large PDI, table 16. The gel-like material was soluble in THF and base oil.

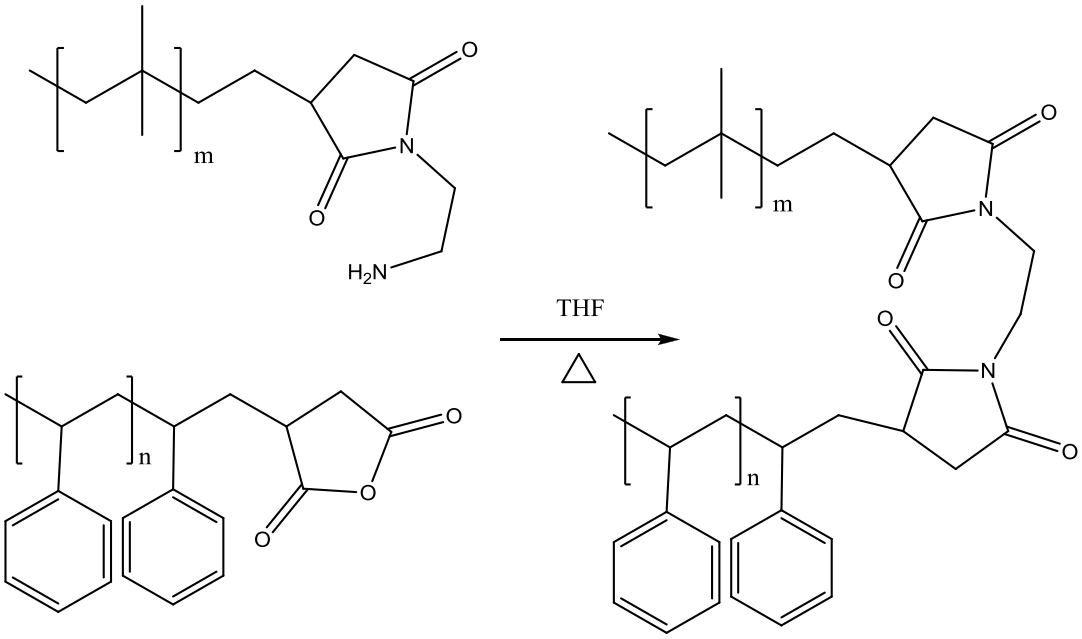

Figure 71: Coupling of maleic anhydride functionalised waste polystyrene with PIBamine

Table 16: Molecular weight data for PIB-amine and the coupled degraded polystyrene with maleic anhydride and PIB-amine.

Polymer	M_n (g mol^{-1})	M_w (g mol^{-1})	PDI
PIB-amine	3200	4000	1.25
Degraded PS-MA-PIB-amine	4400	27300	6.20

The large PDI observed and the gel like structure of the degraded polystyrene coupled with PIB-amine, indicates that the coupling reaction has been successful, however, such a large PDI and the fact that the product forms a gel implies that the idealised structure in figure 70, is not accurate. This data is consistent with cross-linking, this indicates that the maleic anhydride is not just coupled at the end of the degraded polystyrene chain; instead it suggests that the maleic anhydride is attached multiple times to individual degraded polystyrene chains.

Microwave assisted synthesis of maleimides.

Interest in the use of microwaves to assist organic reactions has grown in recent years and one of the contributing factors lies in the much faster reaction times that are observed for reactions heated via microwave dielectric heating rather than conventional heating. Microwave dielectric heating is a non-quantum mechanical effect and it leads to volumetric heating of the samples. Microwave energy is introduced into the reactor remotely and therefore there is no direct contact between the energy source and the sample undergoing heating. This, combined with much higher heating rates than those that can be achieved conventionally, may lead to very different temperature-time profiles for the reaction and as a consequence may lead to an alternative distribution of chemical products in the reaction.

Microwave dielectric heating resembles a flash heating process, where rapid heating and cooling is observed. The different profiles may therefore lead to significantly different products, particularly if the reaction product distribution is controlled by complex and temperature-dependent kinetic profiles.

N-(aryl/alkyl) maleimides were synthesised by adapting the microwave-assisted synthesis method of Ritter and Bezdushna[227]. Alternative methods for the synthesis of arylmaleimides have been reported in the past. The classical synthetic route to access N-arylmaleimides is the addition reaction of maleic anhydride to an aryl amine and subsequent dehydration of the N-arylmaleamic acid by treatment with a hot mixture of acetic anhydride and sodium acetate, resulting in a 80% yield[228]. Refluxing maleic anhydride and aniline in glacial acetic acid gave only a very poor yield of about 10% of arylmaleimide together with acetanilide and arlymaleamic acid. Additionally arylmaleimides have been prepared by the condensation of maleic anhydride and aniline in organic solvents with the presence of acid catalysts.

N-phenylenediaminemaleimide was prepared from maleic anhydride and N-phenylenediamine via microwave assisted synthesis. A power of 400W for 2 minutes was used followed by purification of the product by column chromatography (60:40 DCM: Methanol).

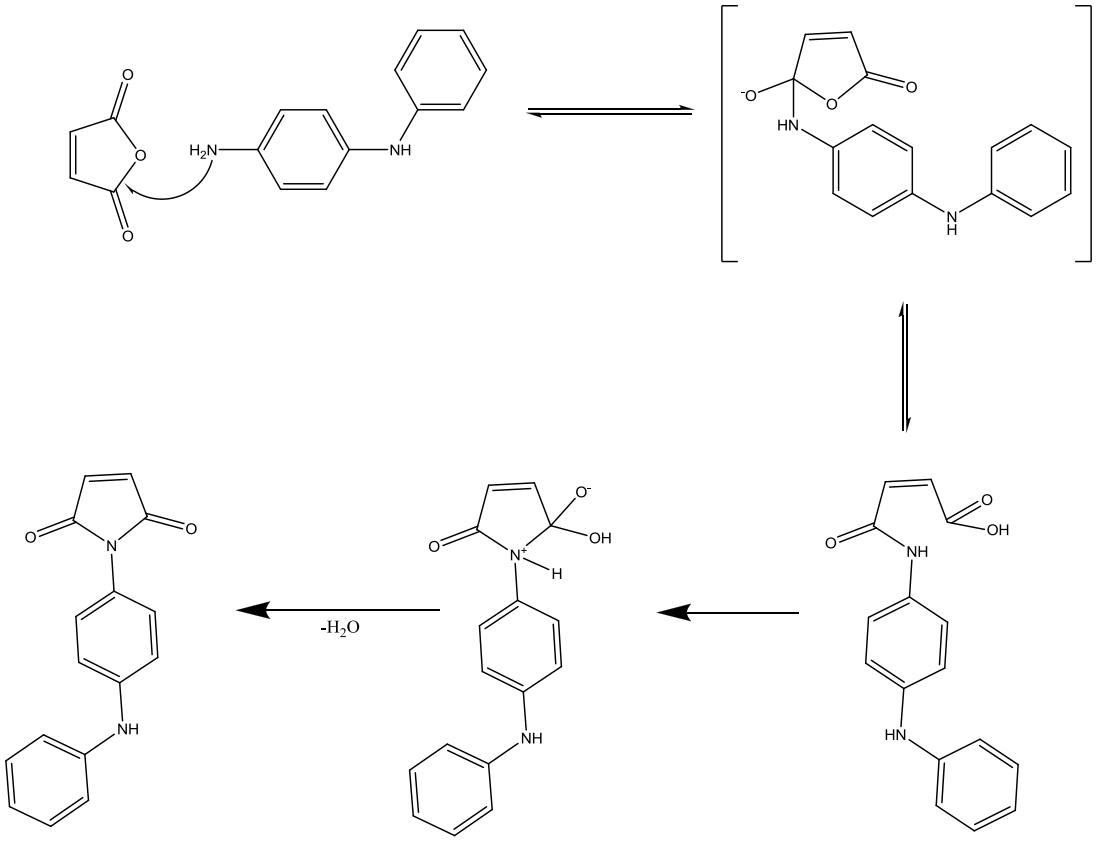

Figure 72*: Proposed mechanism of N-maleimide formation*

FTIR analysis was conducted on the product and indicated that the ratio of imide to amide ratio was approximately 40:1, indicating that the imide structure is formed over the amide salt.

Experimental Section

General

Maleic anhydride (>95%); 1-decene (>98%); 11-bromoundecanol (>99%); *N*-phenyl-p-phenylenediamine (>98%); dodecanol (99%); benzoyl peroxide (80%); poly(octadecene-alt-maleic anhydride); polyethylene (99%); polypropylene (99%); polystyrene (99%); 4,4-azobis-4-cyanopentanoic acid (99%); styrene (99%); azobisisobutylonitrile (>99%); alliquat 336; 1-dodecanthiol (99%); carbon disulfide (99%); dithiothreitol (99%); 4-bromostyrene (99%); isodecyl methacrylate (>97.5%); lauryl methacrylate (98%); stearyl methacrylate (>90%); acetone (>99%); bromoisobutyric acid (99%); 1-butanol (98%) and thioacetic acid (98%) were purchased from Aldrich. Octadecyamine (98%) and activated carbon were purchased from Fluka. Yubase4 and ExxonMobil AP/E core100 were supplied by Lubricants UK Ltd. Kerocom* PIBA 03 and Glissopal* SA were supplied by BASF. DMSO-d6 (>99.9%D); Toluene-d8 (>99.9%D); dioxane-d8 (>99.9%D); THF-d8 (>99.9%D); $CDCl_3$ (>99.9%D) were purchased from Apollo Scientific. THF (99%) and toluene (<99.5%) were purchased from Fischer Scientific and dried by passage through two alumina columns using an Innovative Technology Inc. solvent purification system and stored under N_2. Hexane (Fischer Scientific >99%) was dried over 3A molecular sieves. 3A molecular sieves (Aldrich) were activated in an oven at 200^{o}C before use. Styrene was passed through a short column packed with Al_2O_3 to remove the 4-tert-butylcatechol inhibitor. All other chemicals were used as received. Microwave degradations were performed using a CEM Discover Labmate operating in open vessel mode at 2450 Mhz. Alternatively, microwave degradations and polymerisations were performed on a Biotage initiator 60. NMR spectroscopy (500MHz, DMSO-d6, Toluene-d8, dioxane-d8, THF-d8, $CDCl_3$, ^{1}H, ^{13}C NMR recorded at ¼ of machine frequency) was performed on a Varian Inova-500 spectrometer. High resolution NMR spectroscopy was

performed on a Varian VNMRS 700 Any Nucleus spectrometer. Mass spectral analyses were performed on a Micromass LCT mass spectrometer using positive or negative electrospray mode. Mass spectral analyses of polymer samples were performed on Applied Biosystems Voyager-DE STR using MALDI Ionization mode. Infrared spectroscopy was conducted on a Nicolet Nexus FT-IR spectrometer using KBr disc samples. Liquid samples were analysed by direct injection of the reaction medium into a liquid cell with KBr windows. Elemental analyses were conducted on an Exeter analytical E-440 elemental analyser. Molecular weight analysis was carried out by size exclusion chromatography (SEC) on a Viscotek TDA 302 system with refractive index, viscosity and light scattering detectors. A value of 0.185 (obtained from Viscotek) was used for the dn/dc value of polystyrene. 2 x 300 mm PLgel 5 µm mixed C columns (with a linear range of molecular weight from 200-2,000,000 g mol^{-1}) were employed; THF was used as the eluent with a flow rate of 1.0 $mLmin^{-1}$ at a temperature of 30^{o}C. The coupling reactions were monitored and further analysed by SEC using a Viscotek 200 with a refractive index detector and 3 x 300 ml PLgel 5 µm 104 Å high-resolution columns (with an effective molecular weight range of 10,000-600,000 g mol^{-1}), THF was used as the eluent at a flow rate of 1.0 $mLmin^{-1}$. The theoretical number average degree of polymerisation ($D_{Pn,th}$) values of polymers prepared were calculated according to the following formula: $DP_{n,th} = x * ([M]_0/[RAFT]_0)$, where x = fractional conversion, $[M]_0$ = initial monomer concentration and $[RAFT]_0$ = initial RAFT agent concentration. UV-Vis spectroscopy was performed on a Unicom UV/Vis spectrometer.

Monomer synthesis

N-phenyl-p-phenylenediaminemaleimide

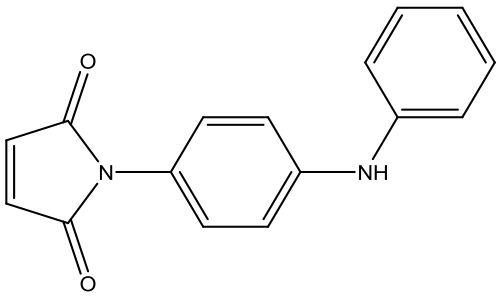

N-phenyl-p-phenylenediamine (1.87g 10.2mmol), maleic anhydride (1.0g 10.2mmol) and xylene 11.0mL were placed in a pressure-resistant microwave vial sealed with a septum and subjected to MW irradiation at a power of 85 W for 35 min. Expected C, 77.55% H, 4.98% N, 5.32%. Found: C,78.21% H,4.99% N 5.41%. FTIR (KBr): 3467 (V_{CN} imide) C-N 3070, 2980 (V_{CH} aromatic); 1670 (V_{CO} imide) 1460(V_{CH} aromatic) 730(V_{CH} aliphatic). ^{1}H NMR (500 MHz, $CDCl_3$) δ = 7.29-7.03 (9H,m,aromatic) 6.40 (2H, S,R-HC=CH-R) δC= 161, 144,140, 136, 128, 122,121 (EI)MS: Found 265, 263 g mol^{-1}

Macro-monomer synthesis.

Polystyrene dithiobenzoate

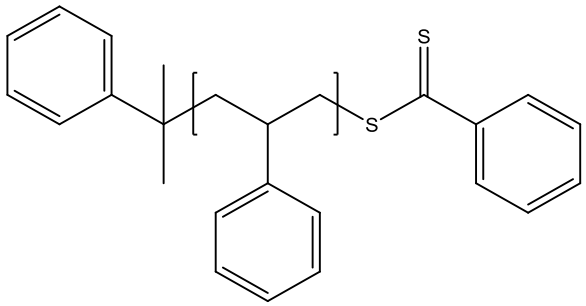

Styrene (2ml, 0.0175mol), cumyl dithiobenzoate (0.025g, 9x10^{-5} mol) and AIBN (0.0015g,9x10^{-5}mol) were placed with 5ml of toluene in a Schlenk tube and sealed with a Young's tap. The vessel was degassed by three freeze pump thaw cycles, filled with nitrogen gas, then placed in a preheated thermo-regulated oil bath at the desired temperature and left to react for 48 hours. Polystyrene was precipitated into methanol and dried on the high vacuum line for 8 hours, to leave a pink powder. (500 MHz, $CDCl_3$): 1.6-1.9 (b, CH2/CH), 2.81 (b, C-H) 7.2-7.59 (m, broad, Aromatic). GPC (THF): M_n= 2000 g mol^{-1}, PDI 1.19

Chain Transfer agent synthesis.

Synthesis of cumyl dithiobenzoate, CDB

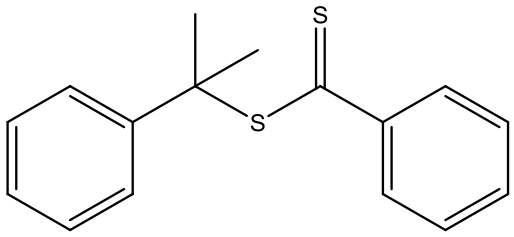

Benzoyl chloride (12.6g, 0.1moles) was added dropwise to a solution of elemental sulphur (6.4g, 0.2moles), 30% sodium methoxide solution in methanol (36g) and methanol (30mL). The resulting brown solution was then heated at 80^{o}C overnight. The mixture was filtered upon cooling to room temperature to remove the white solid and then methanol was removed via rotary evaporation. The resulting brown solid was redissolved in 100ml distilled water and washed with diethyl ether (3x 50ml). The final two layer system was acidified with HCl until the aqueous layer's brown colour disappeared and the ether layer changed to a deep purple. The ether layer was then dried over $CaCl_2$ filtered and the residual ether removed by rotary evaporation to leave the deep purple of the dithiobenzoic acid. The acid was then dissolved in hexane(10mL) and reacted with α-methylstyrene overnight in the presence of 1% paratoluenesulfonic acid (acid catalyst). The product was isolated via column chromatography. LRMS found m/z 272.2, (500 MHz, CDCl3): 1.71 (s, 6H, Me), 7.31 (m, 2H, Hmeta;arom:), 7.35 (m, 1H, Hpara;arom:), 7.43 (m, 2H, Hortho;arom:).

Synthesis of (4-cyanopentanoic acid)-4-dithiobenzoate (CPADB)

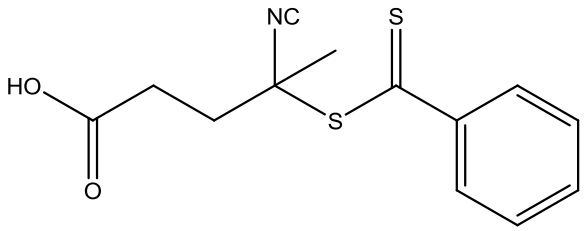

Di(thiobenzoyl) disulfide (pre-prepared by Sebastian Spain) and dry 4,4'-azobis(4-cyanopentanoic acid) in ethyl acetate were refluxed under nitrogen overnight. After cooling, the solvent was removed under reduced pressure. The product was purified by flash column chromatography (2:3 ethyl acetate:hexane) with the red fractions combined. Removal of the solvent gave

a red oil, which crystallised upon storage in the freezer. Recrystallisation in hot toluene afforded the product. Found: C, 55.68; H 4.57; N, 4.78; S, 22.98; $C_{13}H_{13}NO_2S_2$ requires C, 55.89%; H, 4.69%; N, 5.01%; S, 22.95%. FT-IR (NaCl plates) / cm^{-1}: 3350-2600 (broad, COO-H); 2234 (CN); 1710 (C=O); 1048 (C=S). (500 MHz, $CDCl_3$): 1.93 (s, 3H, Me), 2.35-2.78 (m, 4H, 2xCH_2), 7.38 (m, 2H, Hmeta;arom:), 7.55 (m, 1H, Hpara;arom:), 7.83 (m, 2H, Hortho;arom:).

Synthesis of 2-(dodecylthiocarbonothioylthio)-2-methylpropanoic acid (DDMAT)

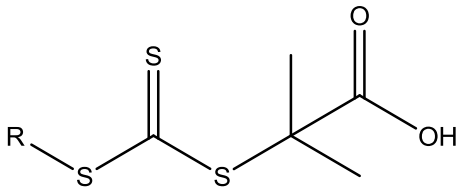

$R = C_{18}H_{38}$

1-Dodecanethiol (80.76 g, 0.40 mol), acetone (192.4 g, 3.31 mol), and Aliquot 336 (tricaprylylmethylammonium chloride, 6.49 g, 0.016mol) were mixed in a jacketed reactor cooled to 10°C under a nitrogen atmosphere. Sodium hydroxide solution (50%) (33.54 g, 0.42 mol) was added over 20 min. The reaction was stirred for an additional 15 min before carbon disulfide (30.42 g, 0.40 mol) in acetone (40.36 g, 0.69 mol) was added over 20 min, during which time the colour turned red. Ten minutes later, chloroform (71.25 g, 0.60 mol) was added in one portion, followed by dropwise addition of 50% sodium hydroxide solution (160 g, 2 mol) over 30 min. The reaction was stirred overnight. 600 ml of water was added, followed by 100 ml of concentrated HCl to acidify the aqueous solution. Nitrogen was purged through the reactor with vigorous stirring to help evaporate off acetone. The solid was collected with a Buchner funnel and then stirred in 1 L of 2-propanol. The undissolved solid was filtered off and was identified as S,S-C-bis(1-dodecyl)trithiocarbonate. The 2-propanol solution was concentrated to dryness, and the resulting solid was recrystallized from hexanes to afford 92.5 g of yellow crystalline solid; mp 62-3 °C. Found C, 56.18%; H, 8.75%; $C_{17}H_{32}O_2S_3$ required C, 56.00%; H, 8.85%; v max/cm^{-1} 2400-3200 (br), 2954, 2916, 2849, 1737, 1713, 1469, 1122, 1070,

815, 718; δH (400 MHz, $CDCl_3$) = 11.19 (1H, br s, COOH), 3.20 (2H, t, S-CH2-$(CH_2)_{10}$-CH_3), 1.66 (6H, s, C-$(CH_3)_2$), 1.60-1.11 (20H, t, S-CH_2-$(CH_2)_{10}$-CH_3), 0.80 (3H, t, SCH_2-$(CH_2)_1$0-CH_3); δC (400 MHz, $CDCl_3$) = 221.2, 179.3, 56.2, 39.7, 37.5, 32.3, 30.0, 29.7, 29.6, 29.5, 29.4, 28.9, 28.3, 25.6, 23.1, 14.5; m/z (EI) 365, 245, 169.

Polymer Synthesis

Typical Free Radical Polymerisation of Styrene

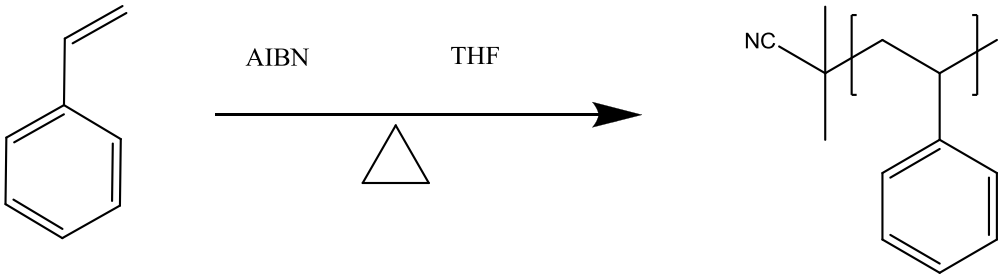

Styrene (2ml, 0.0175mol) and AIBN (0.015g ,$9x10^{-4}$mol) were placed in a Schlenk tube sealed with a Young's tap with 5ml of toluene. The vessel was degassed by three freeze-pump-thaw cycles, filled with nitrogen gas, placed in a preheated thermo-regulated oil bath at the desired temperature and left to react for the desired time. ^{1}H NMR 500MHz, toluene δ(ppm); 1.1-1.4 (3H, m, $H_{aliphatic}$), 7.07-7.42 (5H, broad, $H_{aromatic}$). δC= 150.0, 149.2 148.7, 141.4, 129.1, 128.5, 128.1, 121.6, 47.7, 46.7, 40.8, 35.0, 33.9, 32.4, 29.1, 28.7, 24.3,

Typical copolymerisation of styrene and maleic anhydride

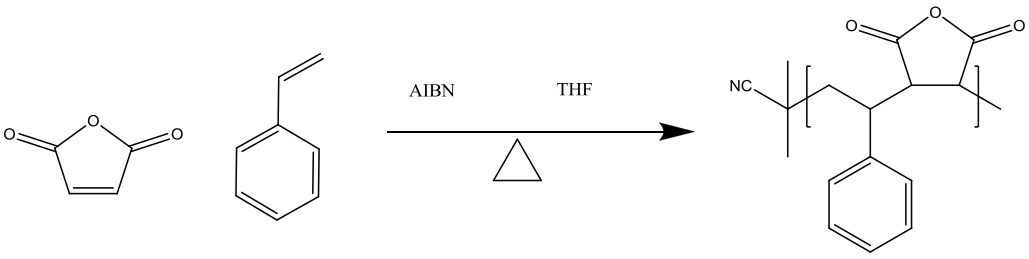

Maleic anhydride (6.70g, 0.069 mol), styrene (2.29g, 0.022 mol) and AIBN (0.01g, 1.1 mmol) were added to a mixture of acetone (12 ml) and toluene (60 ml). The mixture was stirred magnetically until a homogenous and transparent solution was formed. Then, the reaction mixture was degassed by three freeze-pump-thaw cycles under high-vacuum conditions, filled with nitrogen, and immersed in a thermo-regulated bath at 60°C for 60 min. The polymerization was evidenced by the formation of a milky white precipitate. The solvent was evaporated in a rotary evaporator, and the copolymer was re-dissolved in dry THF (65 ml), obtaining a viscous and transparent solution. This solution was poured over 200ml of hexane: the copolymer was precipitated in a white powder form. It was collected by filtration and vacuum dried at 70°C for 6h. ^{1}H NMR (DMSO) δ(ppm); 1.17-2.5 (3H, broad, H_a), 4.67 (2H, m H_b), 6.99-7.33(5H, broad, H_c). δC= 231, 177, 166, FTIR (KBr disc) cm^{-1}: 2926 (C-H), 2862 (C-H), 1851 (C=O), 1777 (C=O). SEC (THF): M_n= 121000 g mol^{-1}, PDI 2.48.

Typical RAFT Polymerisation of Styrene

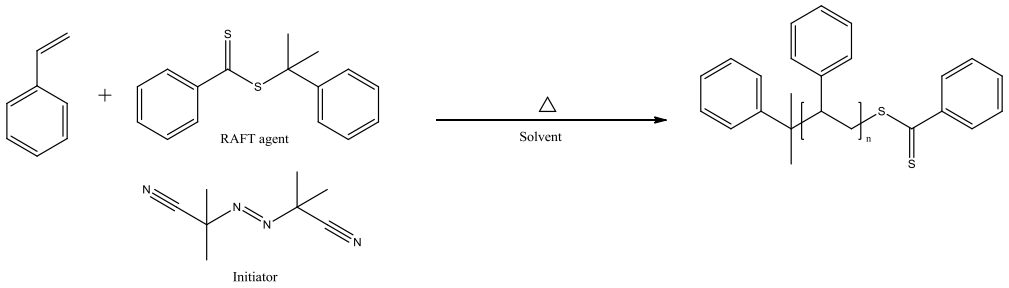

Styrene (2ml, 0.0175mol), cumyl dithiobenzoate (0.025g, 9x10^{-5} mol) and AIBN (0.0015g, 9x10^{-5}mol) were placed with 5ml of toluene in a Schlenk NMR tube sealed with a Young's tap. The vessel was degassed by three freeze-pump-thaw cycles, filled with nitrogen gas, placed in a preheated thermo-regulated oil bath at the desired temperature and left to react for the desired time (Scheme 2, Table 3). For the kinetic experiments, the reaction was run under the same conditions in a dry NMR tube fitted with a Young's tap, spectra being acquired every 234 seconds with a 36 second acquisition time.

Typical RAFT Polymerisation of Maleic anhydride and Styrene

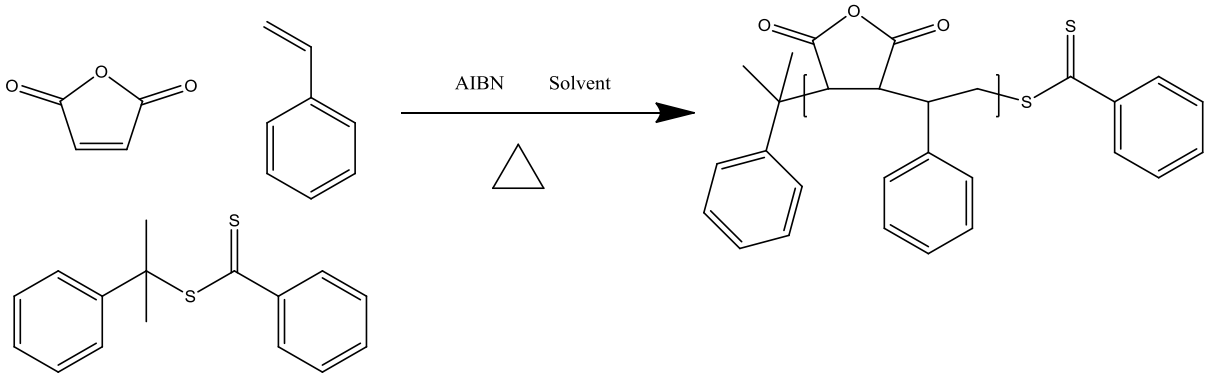

Maleic anhydride (2.0 g, 0.02 mol), styrene (2.13 g, 0.02 mol), AIBN (0.164 g, 0.001 mol) and cumyl dithiobenzoate (0.54 g, 0.002 mol) were placed in a Schlenk tube with 10ml of toluene, then subjected to three freeze-pump-thaw cycles, before being filled with nitrogen and placed in a thermo-regulated bath at 65^{o}C. The reaction mixture was sampled via extraction of 50uL of solution with a gas tight syringe. The resulting polymer was quickly precipitated into methanol, weighed and dried on the high vacuum line for 6 hours, to leave a pink powder. ^{1}H NMR (DMSO) δ(ppm); 1.17-2.5 (3H, broad, H_a), 4.67 (2H, m H_b), 6.99-7.33(5H, broad, H_c). FTIR (KBr disc) cm^{-1}: 3427, broad, (OH), 2922 (C-H), 2852 (C-H), 1851 (C=O), 1777 (C=O). GPC (THF): M_n= 9800g mol^{-1}, PDI 1.19

Typical polymerisation of stearyl methacrylate

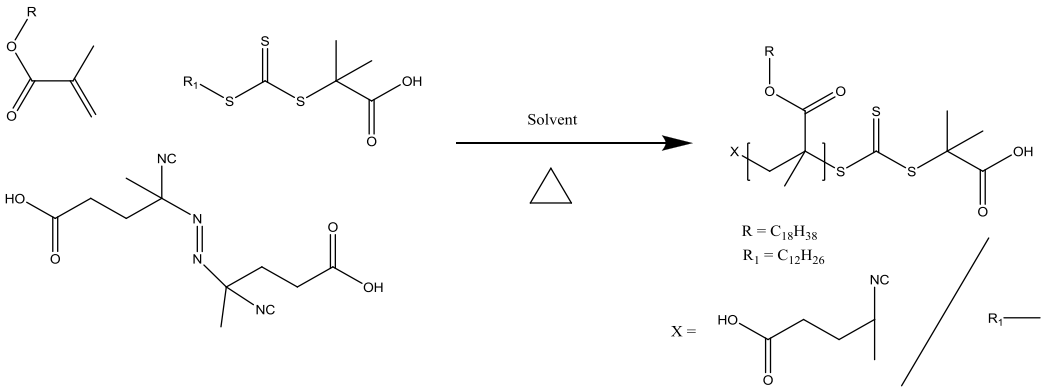

Stearyl methacrylate (2.0 g, 0.006 mol), 2-(dodecylthiocarbonothioylthio)-2-methylpropanoic acid (DDMAT) (0.1g, 0.003 mol), and AIBN (0.04 g, 0.0002) were placed in a Schlenk tube with 10ml of toluene, then subjected to three freeze-pump-thaw cycles, before being filled with nitrogen and placed in a thermo-regulated bath at 65°C. The reaction mixture was sampled via extraction of 50uL of solvent with a gas tight syringe. The resulting polymer was quickly precipitated into methanol, weighed and dried on the high vacuum line for 6hours, to leave a pink powder. SEC, NMR, IR were then performed on the polymer.

Post synthetic functionalisations

Functionalisation of poly(octadecene-alt-maleic anhydride) with N-phenyl-p-phenylenediamine

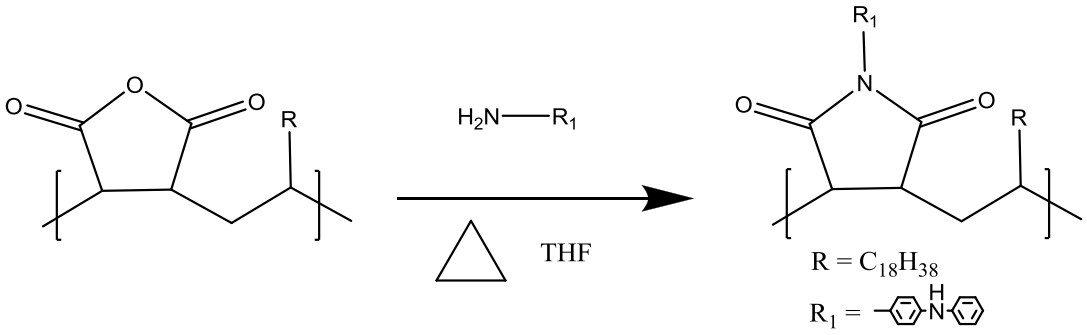

Poly(octadecene-alt-maleic anhydride) (30g, 0.085mol) and N-phenyl-p-phenylenediamine (5.0g, 0.02moles) were dissolved in THF, and heated to 50°C for 24 hours with vigorous stirring. The mixture was then precipitated into methanol to yield a dark green powder. ^{1}H NMR (DMSO) δ(ppm); 0.79 (3H, broad, H_a), 0.92-1.36 (33H, broad, H_b), 3.33 (2H, m H_b), 6.53-7.18 (9H, Broad, H_d). FTIR (KBr disc) cm-1: 3392, broad, (N-H), 2950 (C-H), 2921 (C-H),2851 (C-H), 1842 (C=O), 1773 (C=O). 1706 (C=O free acid), 1598 (C=O amide), GPC (THF): M_n=55,000 g mol^{-1} PDI =2.31.

Functionalisation of poly(octadecene-alt-maleic anhydride) with N-phenyl-p-phenylenediamine and octadecylamine.

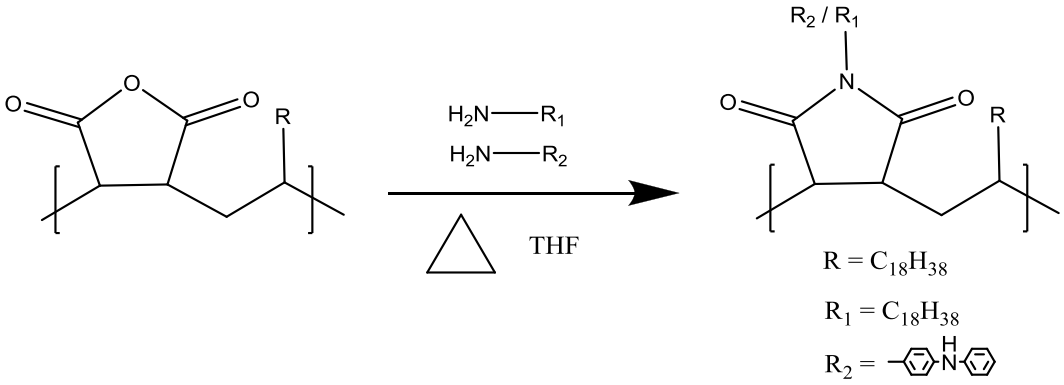

Poly(octadecene-alt-maleic anhydride) (30g, 0.085mol) and N-phenyl-p-phenylenediamine (2.5g, 0.02moles) and octadecylamine (2.5g 0.02moles) were dissolved in THF, and heated to 50^{o}C for 24 hours with vigorous stirring. The mixture was then precipitated into methanol to yield a dark green powder. ^{1}H NMR (DMSO) δppm; 0.79 (3H, broad, H_a), 0.92-1.36 (33H, broad, H_b), 3.33 (2H, m H_c), 6.53-7.18 (9H, Broad, H_d). FTIR (KBr disc) cm-1: 3392, broad, (N-H), 2950 (C-H), 2921 (C-H),2851 (C-H), 1842 (C=O), 1773 (C=O). 1706 (C=O free acid), 1598 (C=O amide), SEC (THF): M_n=55,000 g mol^{-1}. PDI = 2.47

Functionalisation of poly(octadecene-alt-(maleic anhydride-g-N-phenyl-p-phenylenediamine)) with 11-bromoundecanol

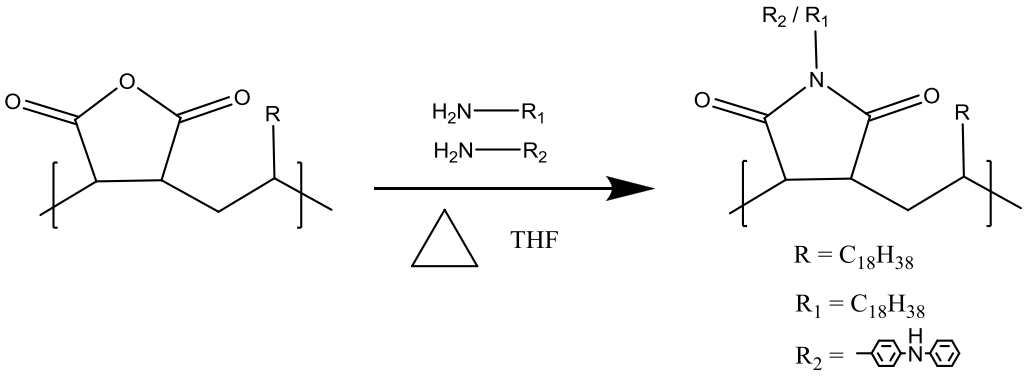

The copolymer (3.86g, 0.01 mol) and 4-dimethylaminopyridine (DMAP) (5.00g, 0.041 mol) were dissolved in 60ml of THF. The reaction mixture was

magnetically stirred until a homogenous solution was obtained. Then, the required amount of alcohol was added. The flask was attached to a reflux system and immersed in a thermo-regulated bath at 67^{o}C with constant agitation, precipitated from 25 ml of hexane, filtered, and vacuum dried at 60°C for 8 h, until total solvent extraction. ^{1}H NMR (DMSO) δppm; 0.79 (3H, broad, H_a), 0.95-1.39 (55H, broad, H_b), 3.33 (2H, m H_c), 3.68 (2H, m, H_e) 6.66-7.20 (9H, Broad, H_d). FTIR (KBr disc) cm^{-1}: 3392, broad, (N-H), 2950 (C-H), 2921 (C-H),2851 (C-H), 1842 (C=O), 1773 (C=O). 1705 (C=O free acid), 1598 (C=O amide), 696 (C-Br). GPC (THF): M_n=58,000 g mol^{-1} PDI = 2.14

Conclusions

The ability to place a linker unit within a polymer chain has been demonstrated by application of RAFT polymerisation and careful monitoring of the addition of maleic anhydride into a styrene polymerisation. The effect of maleic anhydride upon the initial fragmentation of cumyl dithiobenzoate has been explored and it has been shown that maleic anhydride reacts preferentially at the start of the polymerisation with cumyl dithiobenzoate, however, once all the fragmentation processes of the RAFT agent have occurred, secondary addition of maleic anhydride does not have the same impact: indicated by the differences in the rate of polymerisation. Three conceptually different ways of introducing maleic anhydride into a polymer chain are shown in Figure 74. Furthermore the reaction of styrene with N-phenylenedimaine maleimide has been shown to produce alternating one pot block copolymers in a similar manor to those reported by the ATRP polymerisation of N-maleimides with styrene by Lutz et al[229].

End capped RAFT polystyrene with maleic anhydride has been synthesised and successfully attached via the maleic anhydride linker to a polyisobutylene polymer chain. This allows for the testing of a fully polymeric dispersant viscosity modifier. A method for determining the ratios of anhydride, imide and amide by the use of FTIR spectroscopy was also demonstrated.

The functionalisation of degraded polystyrene has been shown with the reaction of maleic anhydride and then further functionalisation with PIB-amine. This reaction indicates that the number of maleic anhydride units attached to the degraded polystyrene is greater than 1 molecule per chain, due to the very large PDI and gel like characteristics of the product. However it doesn't confirm that maleic anhydride is attached to every degraded polymer chain.

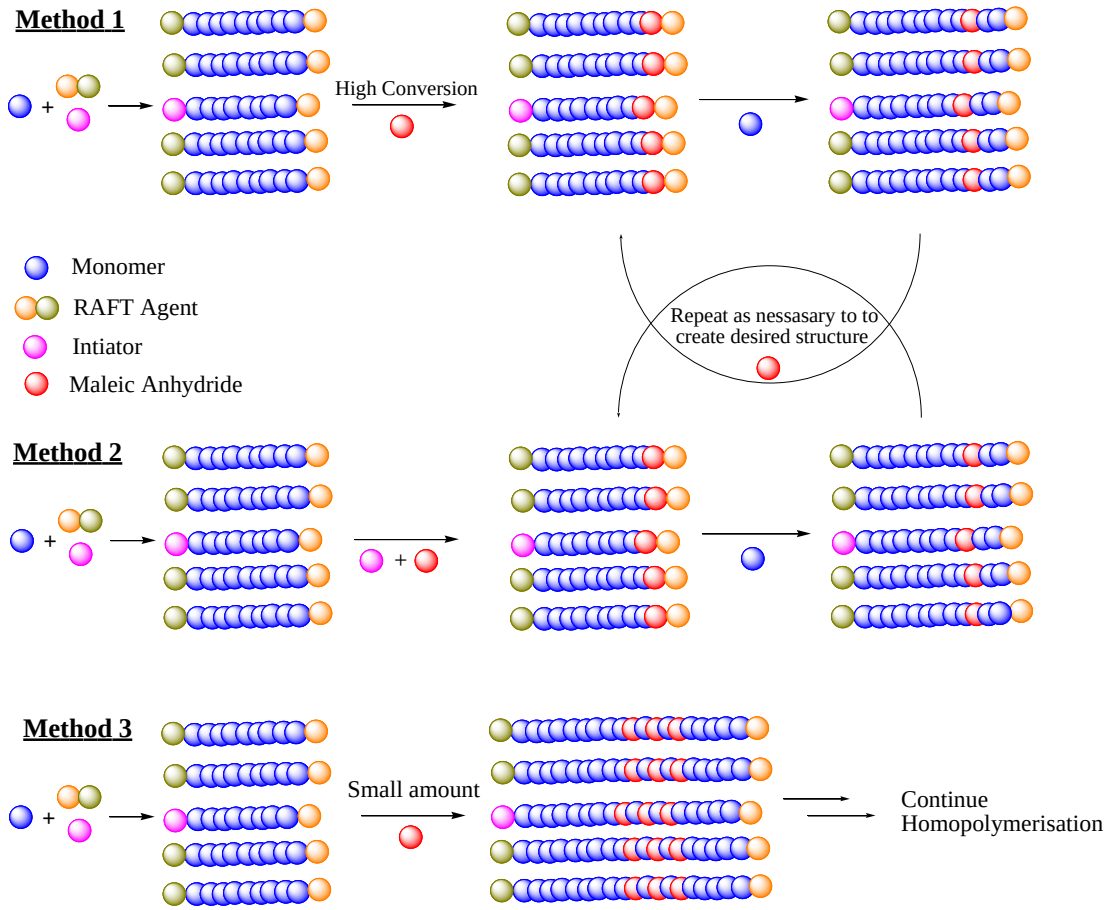

Figure 73: *Three methods to place maleic anhydride within a chain.*

The various polymer structures here will be tested to rate their potential effectiveness on soot dispersancy and also to assess their general properties for consideration into a lubricant formulation.

Testing of Lubricant Components from Waste Polystyrene and Conventional Sources

4

Introduction

Chapter 3 described the synthesis of potential engine oil dispersants. These prepared dispersants were subjected to tests to explore their effectiveness as engine oil dispersants. The ability of a dispersant to suspend by-products of combustion and lubricant degradation is the gold standard of measurement of performance. For engine oil dispersants soot, varnish, resin, lacquer and carbon deposits are all solid components produced in the crank case that need to be controlled by an engine oil dispersant. In addition to associating with such polar species, the dispersant must be thermally and oxidatively stable and contribute positively to the viscosity characteristics of the finished fluid. Other considerations are the seal performance characteristics, its environmental credentials and more recently its suitability within the REACH framework. The first key requisite for the testing of a dispersant is its solubility in the base or carrier fluid.

Results and Discussion

In order to aid in the discussion and to facilitate a simple compare and contrast, the candidate dispersants were classified into different groups. Table 17 contains the indentifying information for each group and figure 74 shows the repeating group structure of the candidate dispersants.

Table 17: Classification of candidate dispersant types.

Candidate	Type
1	Stearyl methacrylate-styrene copolymer
2	(Styrene-alt-maleic anhydride-block-styrene) terpolymer
3	(Stearyl methacrylate-alt-maleic anhydride) copolymer
4	(Stearyl methacrylate-block-styrene-alt-maleimide) copolymer
5	Poly(isobutylene-block styrene)
6	Poly(isobutylene-block-degraded polystyrene)

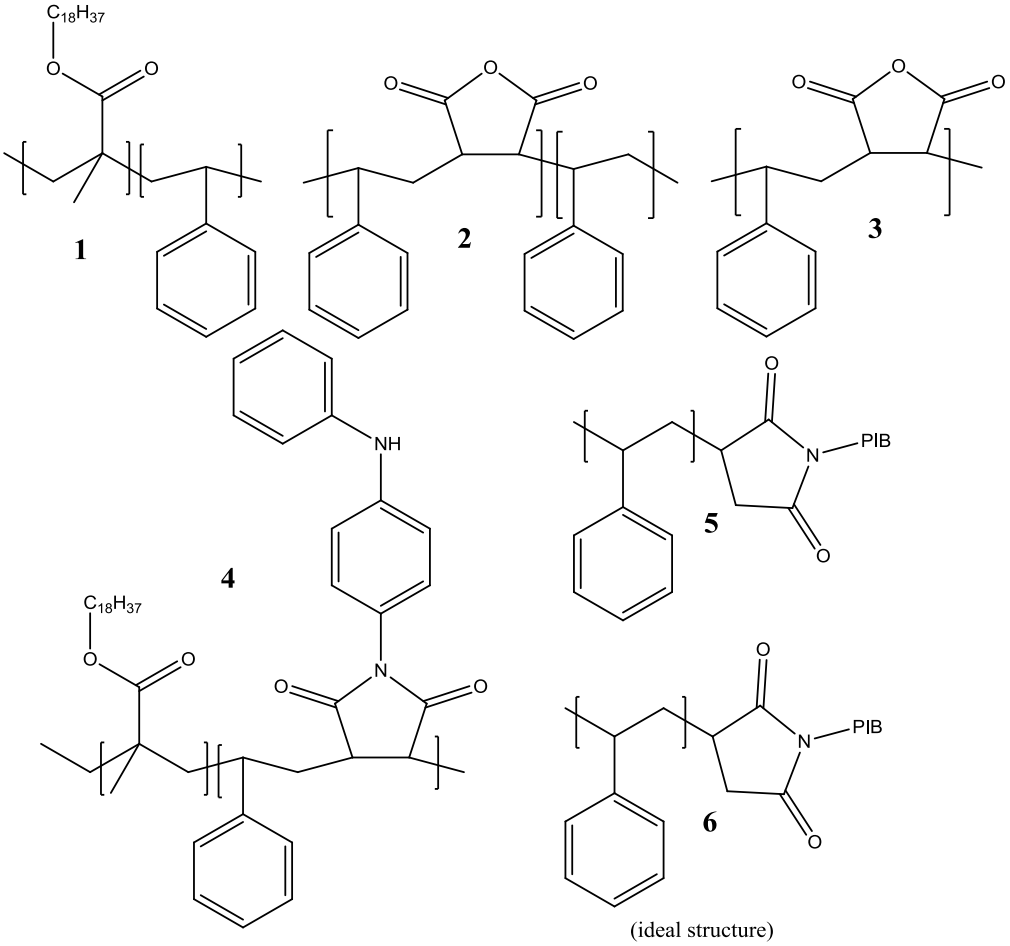

Figure 74:The repeating groups for different dispersant types outlined in table 17

Solubility

Base oils are, in volume terms, the most important component of lubricants[230]. As a weighted average of all lubricants, they account for more than 95% of lubricant formulations. Depending upon the application, the additive component of a lubricant can account for between less than 1% of the total lubricant (hydraulic and compressor oils) or up to 40% of the total lubricant (metalworking fluids, greases, or gear lubricants)[231]. With a dispersant being typically the largest component of an additive package, solubility in the carrier fluid is of paramount importance.

The candidate dispersants were formulated in the group III base oil, YuBase4. To aid dissolution they were heated to 67^{o}C and the solutions agitated with a mechanical stirrer. The solubility assessment was performed by inspection after cooling to room temperature. Table 19 contains the solubility data for the candidate dispersants.

Some of the candidates were insoluble in the group III base oil at all concentration levels tested. These were then tested for solubility in group V base oil, Priolube. This synthetic base oil is more polar than its group III counterpart, and therefore the expectation was greater solubility of the candidate dispersants in the oil. The same procedure was followed and table 20 contains the solubility data for the candidate dispersants in the group V base oil.

Table 18*: Solubility data for candidate dispersants in group III base oil, YuBase4 at 2.5, 5.0 and 10% by (w/w) solutions*

Group	First Block Mol%	Second Block Mol%	Target M_n	10wt%	5.0wt%	2.5wt%
1	90	10	10,000	yes	yes	yes
	75	25	10,000	yes	yes	yes
	90	10	50,000	yes	yes	yes
	75	25	50,000	yes	yes	yes
2	100	0	10,000	no	no	no
	90	10	10,000	no	no	no
	75	25	10,000	no	no	no
	50	50	10,000	no	no	no
3	50	50	10,000	no	no	no
4	90	10	10,000	yes	yes	yes
	75	25	10,000	yes	yes	yes
5	-	-	5000*	yes	yes	yes
	-	-	1000*	yes	yes	yes
6	-	-	-	yes	yes	yes

**refers to second block*

Table 19*: Solubility data for candidate dispersants in group V base oil, Priolube at 2.5, 5.0 and 10% by (w/w) solutions*

Group	First Block Mol%	Second Block Mol%	Target M_n	10wt%	5.0wt%	2.5wt%
2	100	0	10,000	no	no	no
	90	10	10,000	no	no	no
	75	25	10,000	no	no	no
	50	50	10,000	no	no	no
3	50	50	10,000	no	no	no

Groups 2 and 3 were found to be insoluble in both group III and V base oils. Although the group V base oil is more polar than the refined group III fluid it is still classed as a non-polar fluid.

Both the group 2 and 3 candidate dispersants are similar in their structure, both are based on alternating styrene maleic anhydride copolymers, with the group 2 polymers having a long styrene block at one end of the polymer chain. There structure also singles them out form the other candidate dispersants with the main difference coming from the lack of a large oil soluble chain like stearyl methacrylate or polyisobutylene which will affect their solubility in the base oils. The anhydride functionality will also affect the solubility as this structure is polar, especially if it is in its ring opened form. The larger styrene block in candidate 2 may associate in the solution and form orientated structure with π-π stacking of the styrene block, further reducing this candidate's solubility in group III and V base oils. No further lubricant testing was performed on candidate 2 and 3 dispersants.

In contrast the other candidate dispersants were all soluble in both base oils, indicating that the oil soluble sections are sufficient to keep the rest of molecule in solution.

Dispersancy

The overall performance of the dispersant depends upon all three components of its structure: the oleophilic chain, the linker group and the head group. The molecular weight of the oleophilic group determines the dispersant's ability to associate with polar species and suspend them in the bulk lubricant. For dispersants with the same linker and head group, the greater the molecular weight the higher the ability to suspend polar materials, but the lower the ability to associate with them. Therefore there is a trade-off between the two properties. The size affects the dispersant's affinity towards polar materials whilst the introduction of branching affects its solubility, both before association and after association. The linker group has to have sufficient oxidative and thermal resistance while the head group must be able to associate with insoluble particles. Dispersant polymers also have the additional attributes of high intrinsic viscosity and high thermal and oxidative stability, making their use advantageous because another component, the viscosity improver, can be removed from the formulation.

Soot Dispersancy Evaluation - Rheological Testing

The determination of a yield stress and apparent viscosity at low temperatures of engine oils is a good measure of the ability of an oil to be pumped in the field. In a similar manner the yield stress increases in an 'in-service' lubricant over time, where increasing soot levels lead to pumping difficulties albeit at elevated temperatures, resulting in oil starvation, reduced drain intervals and increased equipment down-time. Careful formulation with polymers containing dispersant active groups can go some way to aiding the control of viscosity under these regimes[232-234].

The effectiveness of candidate dispersants 1, 4, 5 & 6 (Table 17) in controlling soot-related viscosity increase was evaluated. A controlled stress rheometer was used in conjunction with rotational and oscillatory rheological methods

with the aim of assessing the candidate dispersants' chemistries. A Hookean solid deforms elastically where the resulting shear strain (ε) is proportional to the applied shear stress (γ). The elastic modulus (G'), the recoverable energy in an elastic solid, is the proportionality constant. A Newtonian fluid, on the other hand, exhibits a purely viscous response whereby resistance to flow, its viscosity (ή), is derived from applied shear stress divided by the shear rate (τ). The viscous modulus (G'') is the loss of energy through permanent deformation in flow. Viscoelastic materials fall in between the extremities of elastic solids and viscous fluids and can exhibit both properties characterised by the elastic modulus (G') and the viscous modulus (G"). Oscillatory rheometry was used to determine each test sample's response to a constantly changing shear stress in the form of a sinusoidal wave, with the sinusoidal strain measured. The elastic modulus (G') is derived from the difference in phase angle (θ) between the applied and resultant waves. A Hookean solid exhibits a zero phase angle whereas a Newtonian fluid is 90^{o}C out of phase. Viscoelastic materials lie in the range between zero and 90^{o}.

As mentioned above, used engine oil containing soot exhibits viscoelastic properties whereby the networks formed by agglomerated soot contribute to the elastic modulus and provide solid-like characteristics to the lubricant under prescribed shear stresses. Two important aspects for an 'in-service' lubricant are the maximum value of G' and the temperature at which the maximum is attained. A suitable dispersant chemistry should both minimize G' and have its maximum outside the operating temperature of the engine oil system. Therefore, a comparative study of the addition of the candidate dispersants and currently available dispersants to a reference fluid along with analysis of the reference fluid will allow the dispersant chemistry to be accessed.

A dispersant viscosity modifier-free, heavily sooted oil was produced from a Cummins M11 engine fitted with Engine Gas Recirculation (EGR) and supplied by the industrial partner. The soot content was found to be 7% using an IR

based soot meter. Preconditioning of the reference and each test sample is critical to the accuracy of the results. Fluids containing structure, be it from polymeric materials or agglomerated particles, e.g. soot, exhibit non-Newtonian behaviour and thus affect the applied shear viscosity. By conditioning samples using a standard method the shear history was removed as a variable. The rheological testing was performed on a Bohlin CVO50 controlled stress rheometer.

Rotational Viscometry

In order to measure absolute shear rates across the width of the rotating surface, a cone and plate geometry was used with a 4^{o} cone angle. The gap between the plate and cone was 70µm. A temperature of 100^{o}C was chosen to represent the conditions to which the oil is exposed to in a heavy duty diesel engine in service. The reference oil, containing only the poorly dispersed soot, displayed a yield point at low shear stresses, 0.1 – 1.2Pa. The combination of 7% soot and a low level of dispersant within the additive package lead to insufficient dispersancy, promoting agglomeration of primary soot particles. The absence of a yield stress at 100^{o}C for the fresh oil is expected due to the lack of particulate matter; whereas for the reference oil, a yield stress of 24,000 mPa.s was recorded. The effect of addition of the candidate dispersants is shown in figure 75 and 76.

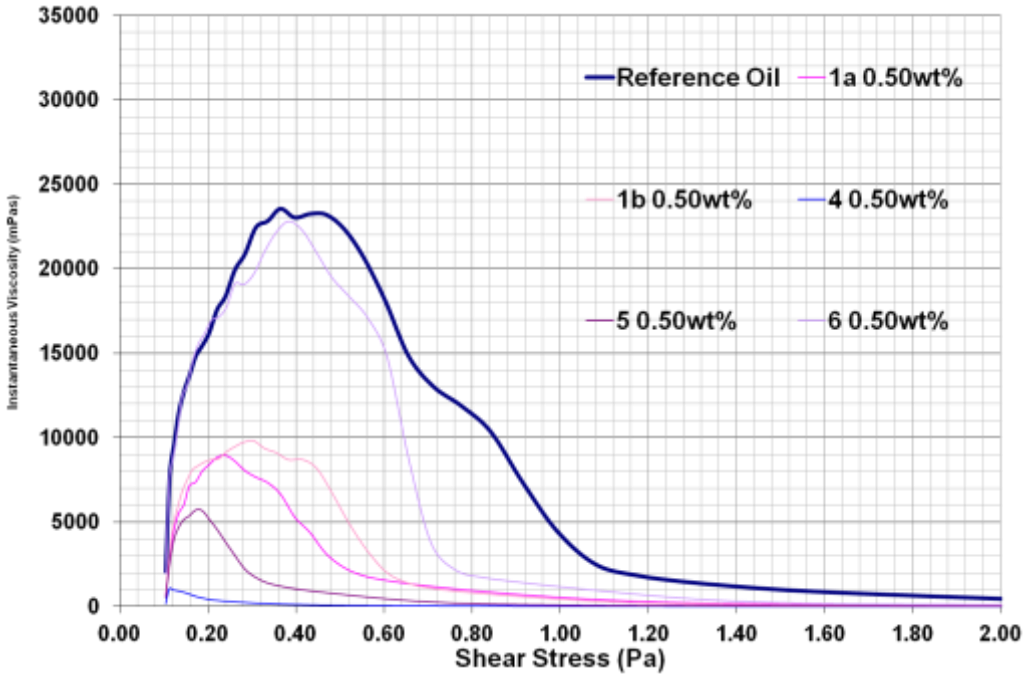

Figure 75: Rotational viscosity flow graph for candidate dispersants at a treat rate of 0.5wt%

The difference between the candidate dispersants is evident with chemistries that disperse the agglomerated soot, thereby lowering the yield stress and those that do not disperse and indeed worsen the situation, increasing the yield stress. Candidate dispersant 1 with different molecular weights (10,000 & 50,000) perform equally well, reducing the viscosity to 9800 mPa.s and 9600 mPa.s respectively. This suggests that, for the two molecular weights tested, there is little difference.

Candidate dispersant group 5 managed to reduce the yield stress to 5,000 mPa.s, while group 6 only managed to reduce the yield stress by 100 mPa.s to 23,900 mPa.s, this indicates that the waste polymer derived dispersant had little effect on dispersing the agglomerated soot particles in comparison to the other candidate dispersants. Although candidates 5 and 6 have a generic structure that is the same (table 19, figure 74), their actual structures will differ significantly (chapter 3).

The best performance was with candidate dispersant group 4 with a reduction in viscosity to 1,000 mPa.s. The stearyl methacrylate structure coupled with the alternating styrene N-phenylenedeiamine maleimide was very effective at reducing the viscosity of the fluid, the N-phenylenediamine moiety[235] is known to be an effective an head group for soot dispercency. The coupling of this functionality with the styrene and stearyl methacrylate makes for an effective dispersant.

Figure 76 shows the effect of treat rate on the instantaneous viscosity for the candidate dispersants. Interestingly, groups 1 and 5 additives at lower treat rate have a deleterious effect upon the yield stress. This suggests that at lower treat rate the addition of these additives increases agglomeration. Therefore below treat rates of 0.5wt% these molecules are contributing towards agglomeration. Candidate dispersant 6 was only tested at 0.5wt% treat rate due to a lack of material. Candidate 4's profile shows that at only at a treat rate below 0.2wt% does this material begin to be less effective than the next best candidate dispersant at 0.5wt%. Candidate 4 also has a greater impact on the viscosity at all treat levels. Figure 77 shows the relationship between dynamic viscosity and candidate dispersant concentration. Generally an increase in concentration of the candidate dispersant results in a reduction in the dynamic viscosity of the fluid.

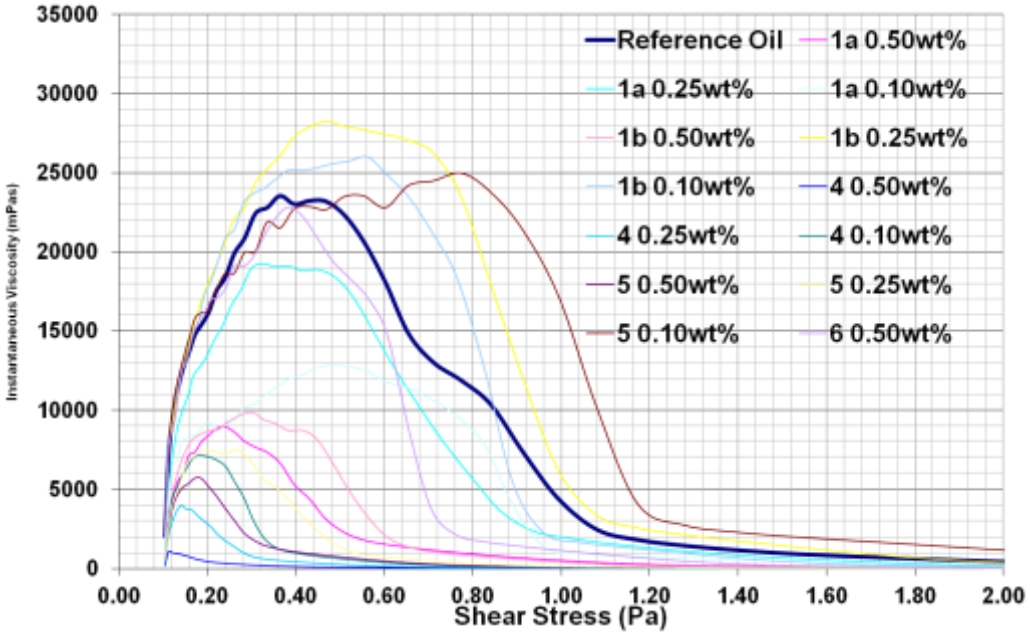

Figure 76: Rotational viscosity flow graph for candidate dispersants at three different treat rates.

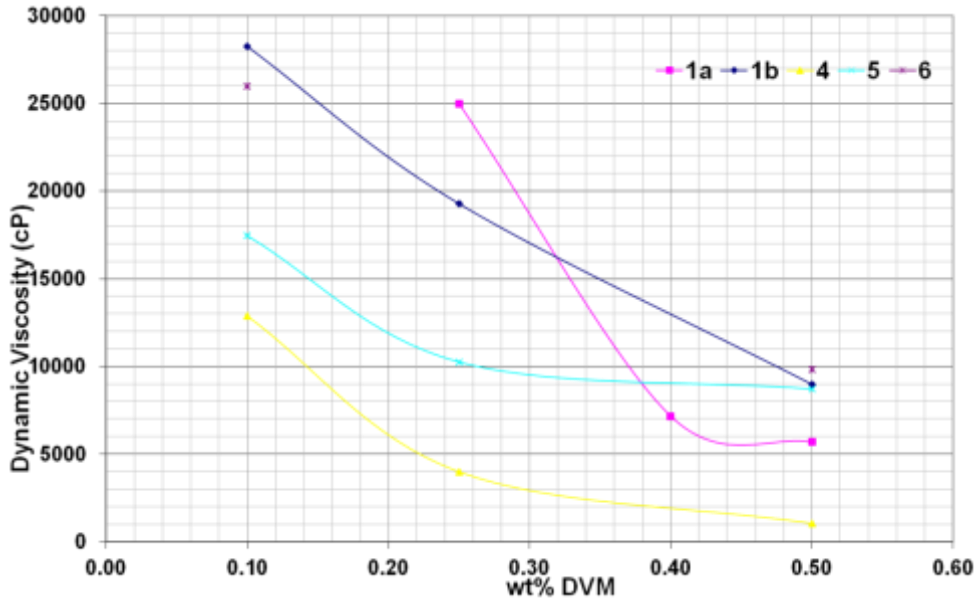

Figure 77: The relationship between dynamic viscosity and candidate dispersant concentration.

Oscillatory Viscometry

The effect of temperature over a range of 60-115°C on the used oil containing the candidate dispersants was evaluated using a parallel plate geometry and a

gap of 300µm. This geometry was used because of its lower sensitivity to thermal expansion over the temperature gradient employed, compared to a cone and plate geometry. The oscillation frequency of 1Hz is in the linear response range of the system. Other frequencies will produce the same oscillatory results for G' providing they are within the linear frequency response range.

The maximum value of the elastic modulus and the temperature at which this maximum is attained are of relevance to determining the effectiveness of a candidate dispersant. A good dispersant should minimize the elastic modulus and have its maximum outside the operating temperature of the lubricating system; for example above 100^{O}C for a heavy duty diesel engine.

Figure 78 shows the magnitude of G' for the reference oil and candidate dispersants. The fresh oil again shows the absence of any value of the elastic modulus G', indicating the absence of any particulate matter, which is expected. The elastic modulus of the reference oil indicates the high levels of soot present, with the elastic modulus being temperature dependent.

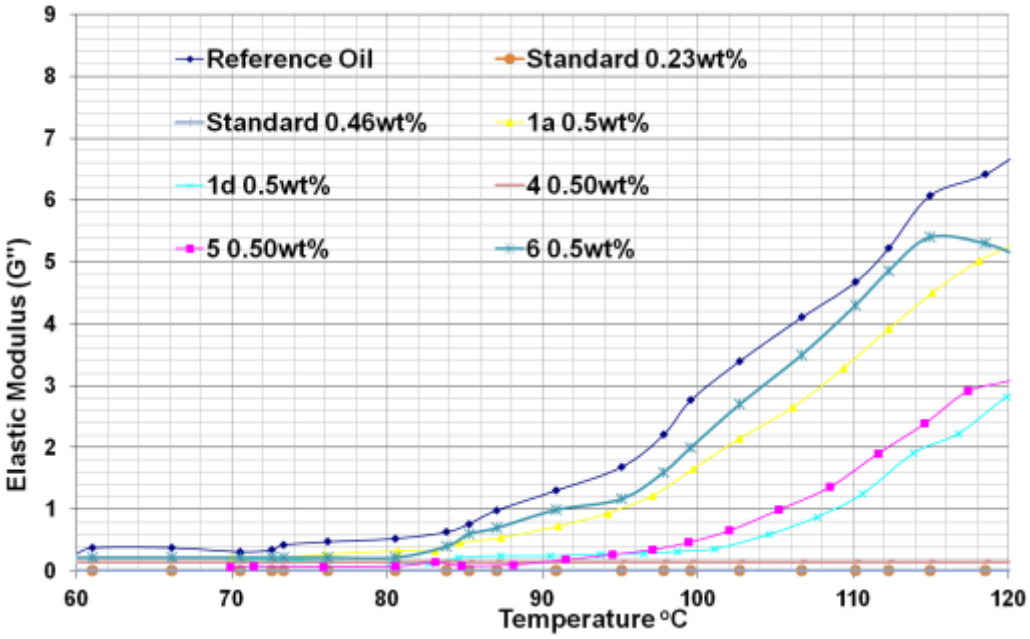

Figure 78: Comparison of G' between 60-115^{O}C for the reference oil and the candidate dispersants

The results for all candidate dispersants do suggest that the maximum of the elastic modulus has shifted to a lower value. No candidates were found to increase value of the elastic modulus with candidates 1b, 4 & 5 displaying the best results for the ability to control structure induced viscosity in this test. With the exception of candidate 6, the candidate dispersants indicate that the maximum value of the elastic modulus would occur at a temperature greater than 115^{o}C, outside of the operating condition of the rheometer.

The viscous modulus G" was also found to be temperature dependent. Paradoxically, the viscous modulus also increases for the reference fluid with temperature.

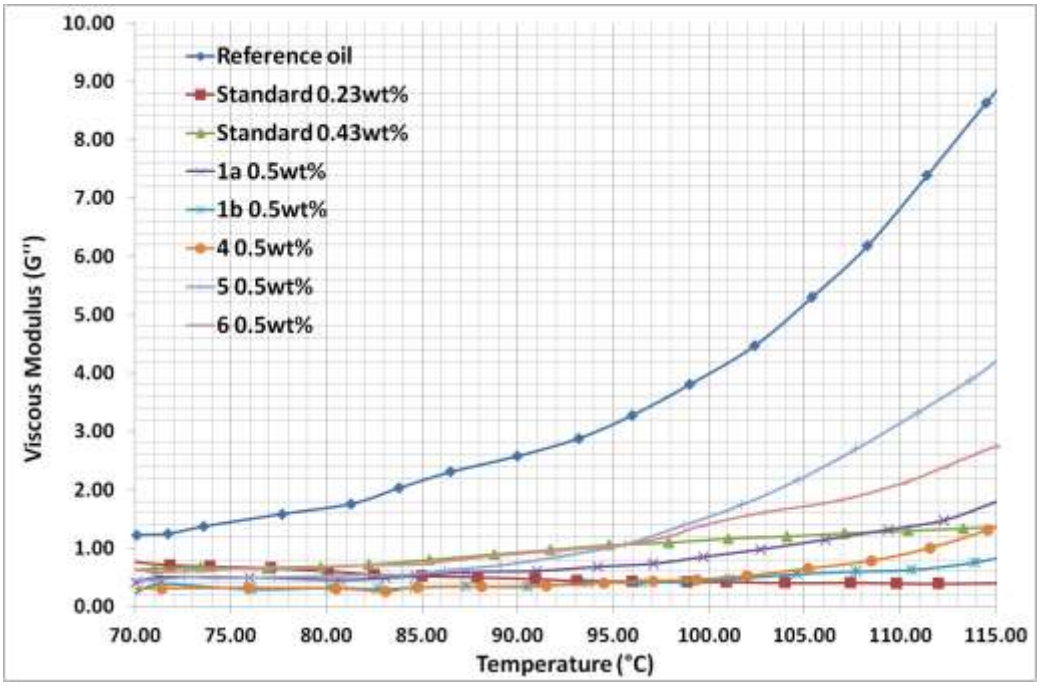

Figure 79: The effect of heating upon the viscous modulus

The elastic modulus is derived from the difference in phase angle between the applied and resultant sinusoidal waves. A comparison of the phase angle over the temperature range should also indicate the structure present in the

reference oil, and how the candidate dispersants affect that structure. Figure 80 shows the phase angle vs temperature.

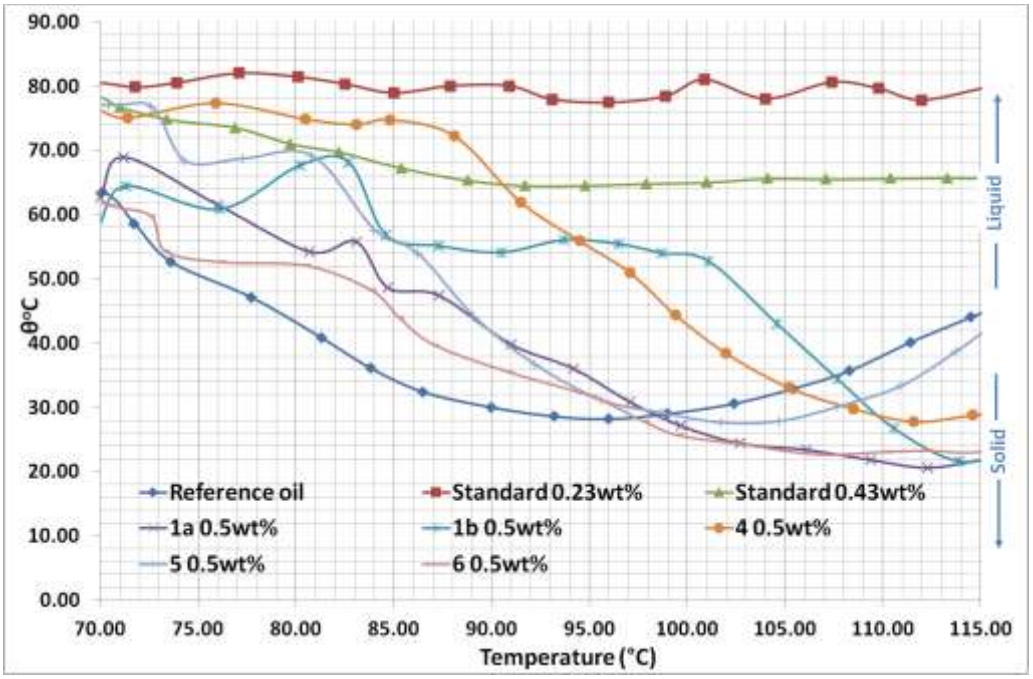

Figure 80: Comparison of the phase angle with temperature for reference and candidate dispersants

The closer the angle to 90^{o} the more the test fluid behaves like a Newtonian fluid, while an angle closer to 0^{O} indicates behaviour the more like a Hookean solid. From figure 80 the reference oil has a phase angle peak at 95^{o}C.

From the rheological evaluation, candidate dispersant 4 performed better than the rest of the candidates, with candidate 6 being the worst performer of the set. The structure of candidate 4 with the N-phenylenediamine head group clearly shows a preference for dispersing the agglomerated soot particles compared with the other candidate dispersants on test, however the results for candidate 4 are were compared to BP's library of results for this type of testing and the values obtained are comparable with commercially available dispersant acrylate copolymers, however, dispersant olefin-copolymers with

the N-phenylenediamine head group is one of the most effective dispersants when soot related viscosity increases is investigated in this way.

The exact structure of soot is unknown[94, 126, 236-239]; however it is known to contain a number of different functional groups, such as acid groups, aromatic groups and other heteroatom containing species[240-243]. With the exception of candidate dispersant 4, the head group of the candidate dispersants is styrene. The ability of styrene to disperse soot depends upon its chemical or physical interaction with the soot particle, the method of action is assumed to be through π-π interactions of the aromatic rings of the styrene and on the soot. Candidate 4's head group incorporates basic nitrogen along with two aromatic rings, this allows for two distinct differences, firstly the aromatic groups on candidate 4 have more freedom of movement relative to the blocks of styrene and there is relatively more aromaticity per head group, this allows for better and larger interactions with aromatic soot. Secondly, the basic nitrogen species allows for association with acidic groups on the soot, thereby offering two different modes of association.

Soot Dispersancy Evaluation – Environmental Scanning Electron Microscopy (ESEM).

The advantage of using the environmental scanning electron microscope (ESEM) in 'wet' mode is that it is not necessary to make nonconductive samples conductive. Materials samples do not need to be desiccated and coated with gold, for example, and this allows for the analysis of liquids.

The same reference and fresh oil used in the rheological investigation was imaged using wet-mode ESEM. The same preconditioning step was used. The images of the reference oil indicate numerous large particles present, see below in figure 81.

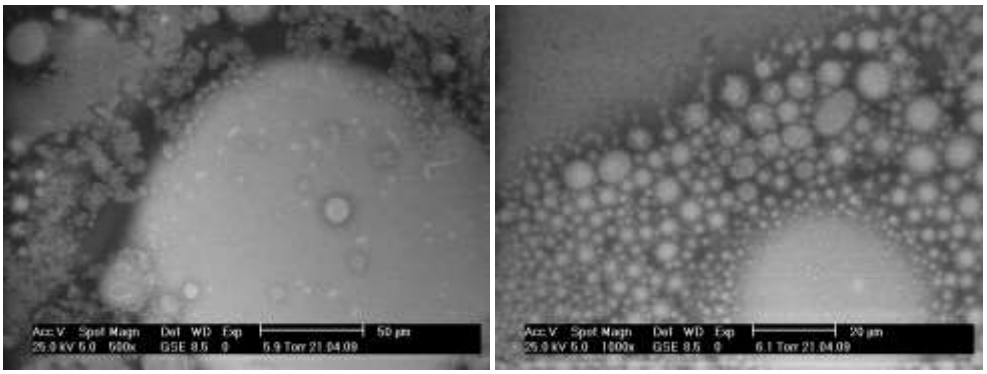

Figure 81: Wet mode ESEM images of reference oil. Soot agglomeration is clearly visible

The images in figure 81 show large differences in particle size and distribution, with a large particle surrounded by lots of smaller individual particles. From comparison to the rheological testing the presence of large particles would indicate the build up of structure in the fluid and therefore it is likely that the particles that have been imaged here are soot derived or related. The idea that some or all of the particles originate from the additive package or the original base oil is unlikely due to the images of the original fluid, figure 82, which show no structure or build up of particles.

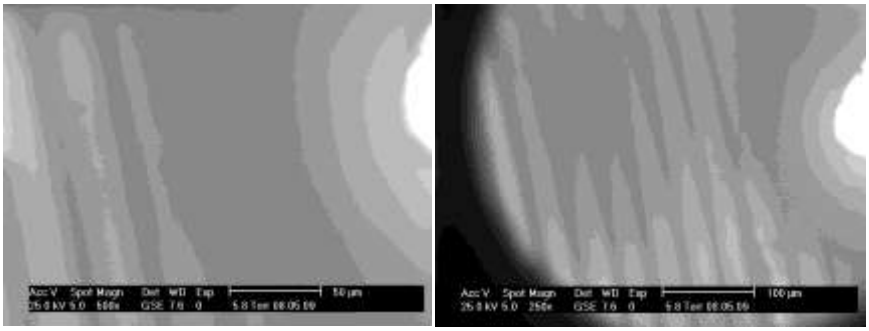

Figure 82: wet mode ESEM images of the fresh oil

The lines observed in figure 82 are from the grating on the bottom of the solution cell and are not from the fresh oil. Candidate dispersants 1 and 4 were added to the used oil sample and reimaged to look for any differences in the structure, Figure 83 shows the images for candidate 1 while figure 84 shows the structure for candidate 4.

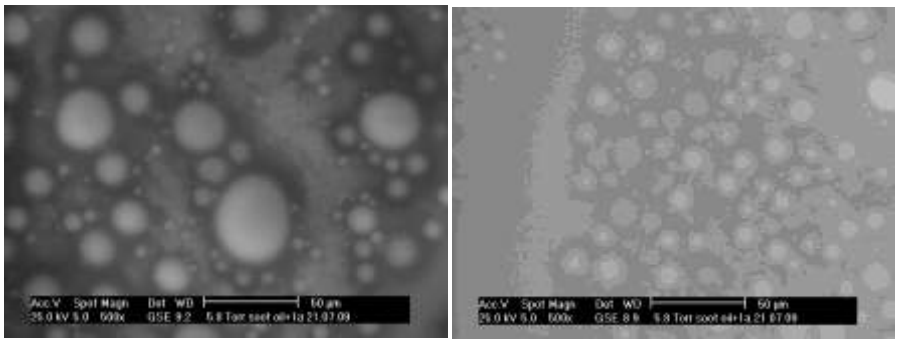

Figure 83: wet mode ESEM of reference oil with addition of 0.5wt% candidate dispersant 1.

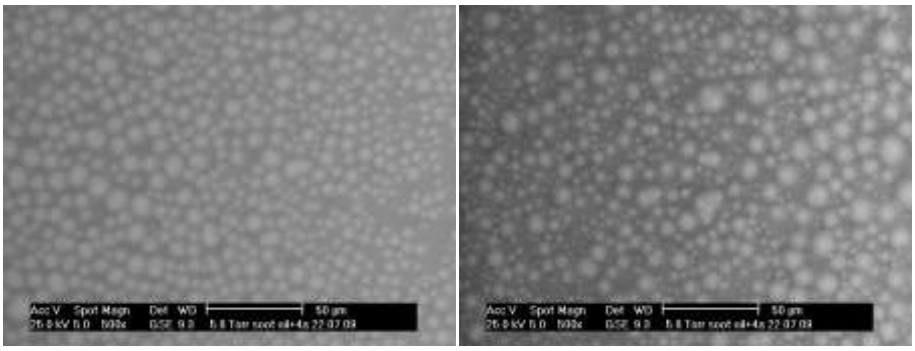

Figure 84: wet mode ESEM of reference oil with addition of 0.5wt% candidate dispersant 4.

Both candidate 1 and 4 disrupted the structure of the particles observed in the used oil. The average particle diameter was recorded using the calculation tool supplied with Gimp 2.6, see table 21. The addition of candidate 1, brought about a reduction in the average particle size from 31.2 µm to 20.4 µm. The addition of candidate 4 had a greater reduction in particle size to 9.5 µm. These reductions in particle size are in the same order as with the rheological testing that indicated candidate 4 was more effective at dispersing soot than candidate 1. The smaller particles that are observed indicate that the candidate dispersants are effectively breaking up the larger particle structure into smaller particles and/or micelles.

Table 20: Summary of particle sizes for reference oil, and candidate dispersants 1 and 4.

	Reference Oil	Candidate 1	Candidate 4
Average Particle diameter (µm)	32.1	20.4	9.5
Standard Deviation	12.6	8.1	2.4
Maximum diameter (µm)	147.9	41.7	13.3

The particle sizes as measured by ESEM are large and are more akin to particle sizes observed in emulsion polymerisation processes[244]. It has to be noted that these particles are imaged in a partial vacuum and that there is potential interference that will affect the validity of the actual size of the particles.

Viscosity characteristics

The candidates have been assessed on their potential to work as dispersants, However, the ability of a lubricant additive to impart a second beneficial property on an oil formulation is also of importance in modern formulations. Therefore the viscometric properties of the candidate dispersants is of equal interest. A candidate that performs well at soot dispersancy but also contributes towards the fluids viscosity profile is of real interest. Equally, however the candidates that performed poorly in the soot dispersancy testing may still be of interest if they provide interesting viscometric performance.

The typical treat rate of a dispersant in an engine oil lubricant varies between 4-8% by weight and usually the dispersant will be the largest component in an additive package. The dispersant can also be the highest molecular weight species present in the additive package depending upon the presence of a viscosity improver. Both these factors alter the physical properties of the fully formulated lubricant.

At high temperatures, the lubricant loses some of its viscosity and therefore its film forming ability is reduced leading to poor lubrication. The viscosity improver or dispersant viscosity modifier can lead to a boost in the viscosity of the lubricant at high temperatures; however this advantage can be a disadvantage at low temperatures, where an increase in viscosity is undesirable[234, 245]. The dispersant also contributes to the thickness of the lubricating film, which is of paramount importance when considering the efficiency and efficacy of lubrication. In general a thick film will provide good protection for the moving parts against wear and therefore durability will be good, however, due to the increased thickness, more energy will be required to keep the parts moving, therefore fuel economy will be impacted. Equally, if a thin lubricating film is used it will not offer high levels of protection and there will be increased wear and lower durability; however fuel economy will be much improved due to lower friction.

One way to characterise the effects of a dispersant upon the viscosity at both low and high temperatures is to calculate the viscosity index or VI[246]. The viscosity index is an arbitrary empirical number indicating the degree of change in viscosity of an oil within a given temperature range. It is determined by measuring the kinematic viscosities of the oil at 40^{o}C and 100^{o}C and then comparing these to reference fluid viscosities at the same two temperatures. A high viscosity index indicates a relatively small change of viscosity with temperature and vice versa[247].

In order to assess this change the candidate dispersants were formulated into a lubricant at a treat of 4wt% polymer concentrate. Group II base oil was used with an additive package of 9.7%, making a total additive pack including polymer concentrate of 14.7%. Table 21 shows the additive pack formulation used.

Table 21: Additive pack formulation for Research Formulation for additives

Additive Type	Product	%	Ad Pack treat (%)	
Dispersant	Infinium C9268	5	51.5	Blended as ad pack
Ca Sulfonate Detergent	LZ 6477C	2	20.6	
Ca Phenate Detergent	LZ6490	1	10.3	
AO - Phenolic	Irganox L-135	0.5	5.1	
AO - Aminic	Irganox L 57	1	10.3	
Total Pack treat		9.7	Total	100

Table 22 details both the research formulation and a baseline formulation. The formulated lubricant was blended at 67°C for 4 hours and allowed to cool. The kinematic viscosity was measured for each additive and the results are shown in Table 23.

Table 22: Research formulation.

	Baseline	1a	1b	4a	4b	5
Additive Pack	9.7	9.7	9.7	9.7	9.7	9.7
Motiva Star 6	85.3	81.3	81.3	81.3	81.3	81.3
SV261	5	5	5	5	5	5
Polymer concentrate	0	4	4	4	4	4
Total	**100**	**100**	**100**	**100**	**100**	**100**

Table 23: Kinematic viscosity results for formulations.

Tests	Baseline	1a	1b	4a	4b	5
KV100 (cSt)	13.03	12.8	12.79	14.98	17.16	12.98
KV40 (cSt)	96.09	92.84	93	109.34	123.3	94.26
VI	133	135	134	143	152	135

The viscometic data indicates little change in the viscosity index of the formulated lubricants for candidates 1 and 5. This indicates that candidates 1 and 5 do not act as effective viscosity modifiers in this solution, however they are not detrimental to the fluids performance. The lack of thickening ability from candidates 1 and 5 means these groups will not be considered as potential dispersant viscosity modifiers.

Candidate 4 has a larger viscosity index than the baseline formulation, indicating that there is some thickening of the fluid occurring at higher temperature with its presence. The increase in viscosity index by almost 15% means that candidate dispersant 4 offers potential as dispersant viscosity modifier. This thickening behaviour suggests that the polymer coil is expanding at higher temperature to a greater extent than candidates 1 and 5 and also to the base line formulation. Candidates 1 and 4 are more structurally similar to one another than they are to candidate 5. Both candidate 1 and 4 have large stearyl methacrylate blocks and therefore the differences in thickening must arise from the alternating styrene N-maleimide structure of candidate 4 in comparison to the polystyrene block of candidate 1. This alternating block must therefore be able to expand more at higher temperature than the styrene block on candidate 1, leading to increase in thickening ability at higher temperature. Therefore it suggests candidate 4 has a greater hydrodynamic volume at higher temperature than candidate 1 or 5.

Candidate 5 has a polyisobutylene chain coupled to a block of polystyrene. Assuming that candidate 5's polyisobutylene block has a similar thickening ability as the stearyl methacyrlate block of candidates 1 and 4, then the polystyrene block would be expected to behave in the same manner as for candidate 1, which it does.

Thermal and Oxidative stability

All three structural components of a dispersant will determine its thermal and oxidative stability. The oleophilic chain can oxidise in the same manner as the lubricant to form oxidation products that will contribute to the deposit forming species. Amine moieties in head groups are likely to oxidise at a faster rate than oxygen containing analogues because of the facile formation of an amine oxide functional group on oxidation. The reactivity towards other chemical species in the formulation also needs to be considered.

In order to assess the stability of the candidate dispersants, two different Pressure Differential Scanning Calorimetry (PDSC) experiments were conducted. The first was to determine the temperature at which oxidation of the formulated oil would occur at and involves heating the sample in oxygen with a heating ramp of 15^{o}C/min. The resulting exotherm indicates oxidation of the oil. The second experiment involves heating of the sample to 215^{o}C at 40^{o}C/min, and then holding the temperature constant and waiting for oxidation to occur. The Oxidation Induction Time is measured from the beginning of the second isothermal section (215°C) until the onset of the oxidation exotherm[247-249], see example in Figure 86.

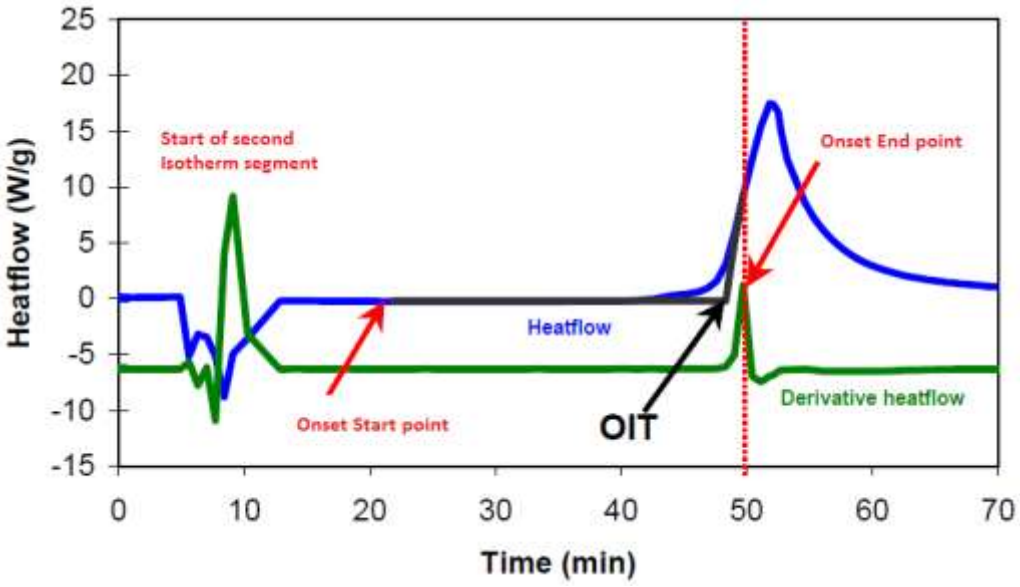

Figure 85: Oxidation induction time measurement.

The results for the thermal stability testing are shown in table 25. The oxidation onset temperature is similar for all candidate dispersants and the baseline formulation. This indicates that the candidate dispersants do not have a detrimental effect upon the oxidation stability of the fluid and are therefore not any less thermally stable than other components in the formulation.

Table 24: Results from the oxidation onset and oxidation induction PDSC tests for the candidate dispersants.

Tests	Baseline	1a	1b	4a	4b	5
Oxidation Onset temp (°C)	281.2	277.2	280.9	282.8	282.9	281.3
Oxidation Induction Time (mins)	35.5	42.1	41.8	45.0	45.1	43.5

The oxidation induction time is increased with the addition of all candidate dispersants. The oxidation induction time is used to assess a fluids ability to withstand the effects of oxidation upon a fluid. It is often linked to the presence of antioxidants and the ability of the dispersant and detergent to mitigate autooxidation mechanisms and degradation products formed in the oil

at high temperature. The implication here is that all the candidate dispersants have a favourable synergistic effect upon the oxidation induction time relative to the baseline formulation.

This increase in oxidation induction time is explained by the polymeric nature of these candidate dispersants. These large chain molecules will offer increased oxidation stability simply from the greater energy costs for the degradation of the candidate dispersants that are present in the fluid relative to a fluid that is absent from these polymers.

Experimental

Rheological Testing

Rheological testing was performed on a Bohlin CVO50 controlled stress rheometer. Temperature control was managed using a heater and chiller combination capable of operating between -30^{o}C and +115^{o}C. Rotational Viscometry; a cone and plate geometry was used with a 4^{o} cone angle to measure absolute shear rates across the width of the rotating surface. Gap = 70µm, temperature =100^{o}C. Oscillatory rheometry: Parallel plate 4cm diameter, GAP = 300µm, temperature 60-115^{o}C at 5^{o}C per min. Preconditioning: stress 3Pa for 30s with 60s equilibrium. Test condition: Frequency 1Hz, delay 0.5s, wait 30s, No. of measurements 30. Target strain 0.06Pa. All samples were pre-conditioned by sonication for 2 hours, to ensure thorough dissolution. Test samples were allowed to cool to room temperature before rheological evaluation.

Kinematic Viscosity

Kinematic viscosity at 40^{o}C and 100^{o}C was measured using a VH1 Automatic Houillon Viscometer, with a bath temperature stability of 0.01 ^{o}C. The sample is placed into 4 separate viscometer tubes and the time taken for the meniscus to pass from the first timing mark to the second timing mark is recorded to the nearest 0.01s. The kinematic viscosity is then calculated from the relationship. Kinematic viscosity (cSt) = constant * time (s).

Oxidation and thermal stability

Oxidation induction time and oxidation temperature were measured on a TA Instruments Q20P dedicated pressure DSC system. The instrument was calibrated to perform heat flow measurements on pressure sensitive materials from -130 to 725 °C, at pressures from 1 Pa (0.01 torr) to 7 MPa (1,000 psi). The pressure cell employs standard heat flux DSC technology and incorporates pressure control valves, a pressure gauge, and over-pressure protection.

Conclusions

The candidate dispersants were tested to assess their dispersancy and viscometric properties along with their oxidation and thermal stability behaviour in a fully formulated lubricant.

Candidate dispersant 4 (figure 86) was consistently the best performing candidate from the rheological and viscometric testing. The stearyl methacyrlate block coupled with the alternating styrene N-phenylenediamine maleimide was found to be most effective candidate dispersant at associating with soot and providing thickening at elevated temperatures.

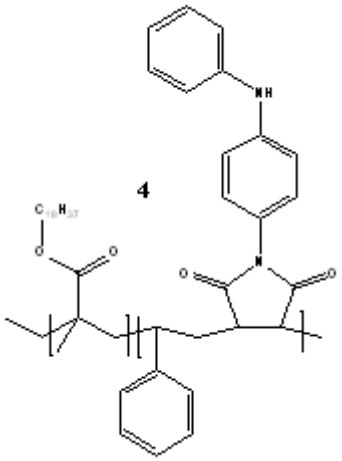

Figure 86: Candidate dispersant 4 repeating group structure

The ESEM images show the effect candidate 4 has on the particle size distribution of heavily sooted oil and indicates that candidate 4 is effective at disrupting the agglomerated soot in the fluid.

Candidates 1 and 5 (figure 87) have the same head groups (blocks of polystyrene) but differing oleophilic backbones; both materials performed similarly well in the dispersancy tests.

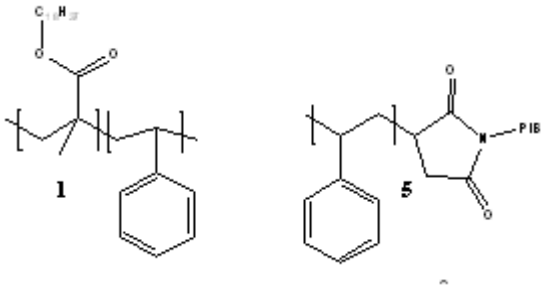

Figure 87: Candidate dispersants 1 and 5 indicating the repeating group structure

This indicates that the oleophillic backbone (stearyl methacrylate and polyisobutylene) had either little difference or equal effectiveness on their candidates ability to disperse soot. The polystyrene head group was in both cases found to have an interaction with the soot particles. For candidate dispersant 1, the molecular weight of the overall polymer influenced the performance of the dispersant. The higher molecular weight candidate 1 has a greater impact upon the elastic modulus than its lower molecular weight counterpart. The rationale for the molecular weight effect is an increase in the number of π-π interactions that can occur with a larger block of polystyrene.

Candidate 6 is possibly the most interesting candidate dispersant, synthesised from waste polystyrene and coupled with maleic anhydride to polyisobutylene this candidate is truly novel in terms of dispersant synthesis. However, the rheological testing suggested that candidate 6 was ineffective as a dispersant. The waste polystyrene structures proved to be ineffective in associating to the soot. One explanation for this could arise from multiple maleic anhydride groups attached to the polystyrene structure rather than just one maleic anhydride attachment per degraded polystyrene. The effect of this would be to create a cross-linked or highly branched polyisobutlene-polystyrene structure. The size of this structure may prevent the polystyrene aromatic nature from associate and dispersing the soot.

It should be noted that for all the results reported in the dispersancy evaluation, they only relate to soot derived from the M111 engine test. Other polar insoluble species derived from gasoline engines will have a different structure and therefore the candidate dispersants might perform differently with that reference fluid.

Table 25: summary of dispersant performance for candidate dispersants.

	Dynamic Viscosity (mPa.s)	G' (Pa)
Reference Oil	24,000	8
1a	9,800	4.1
1b	9,600	2
4	1,000	0.5
5	5,000	2.2
6	23,900	5.1

The candidate's dispersants performance in the rheological testing is summarised in Table 26.

ESEM was successfully carried out on both used and fresh oil samples with the inclusion of candidate dispersants 1 and 4. The images show the sooted structure of the used oil and how the candidate dispersants break up the structure once added to the fluid. This qualitative assessment of the structure present in used oil appears to correlate well to the data obtained by rheological evaluation of the soot and candidate dispersants.

The viscometric and thermal stability of the candidate dispersants was also assessed, with candidate 4 being the only candidate with potential for both dispersant and dispersant viscosity modifier characteristics.

Conclusions and Future Work

5

The objective of this Thesis was to produce lubricant additives from waste commodity polymers with particular attention paid to the method of degradation and the control of architecture in the synthesis of lubricant components. Background information pertinent to this research was provided in **chapter 1** and provides the basis for the rationale for this research. Much has been learned about the degradation of polystyrene and polyethylene in a microwave assisted degradation system, the ability to control complex polymer architectures using RAFT polymerisation of styrene, stearyl methacrylate, maleic anhydride and N-phenylenediamine maleimide. The testing of lubricant additives was also explored by evaluation of candidate dispersants.

The generation of functionalised waste polystyrene was achieved by the use of an adapted microwave assisted degradation system. This system shows good correlation with already established degradation processes and comparison to the literature for the liquid degradation products from polyethylene and polystyrene are in good agreement[34, 35, 48, 50, 71], however, whilst the majority of studies have focused on the liquid and gaseous products generated from the degradation of polystyrene, few have considered the remaining solid fraction. The work presented in this Thesis demonstrates how unsaturated double bonds were formed in the remaining solid fraction or residue of the waste polystyrene when using the adapted Biotage microwave assisted method.

Characterisation of the degradation products was achieved by the use of ^{1}H NMR and FTIR spectroscopy which described and quantified the number of terminal double bonds present in the waste material and estimates give this in the range 4-9% of each polymer chain. SEC analysis indicated the reduction in molecular weight.

Although plastic waste materials have been degraded on multiple separate occasions the ability to control polystyrene degradations using a microwave technique in this way has not been reported.

The degraded polystyrene was then shown to react with maleic anhydride via the double bonds generated in the degradation process. The target lubricant additive was achieved via reaction with PIB-amine, resulting in a gel like polymer that was then subjected to lubricant additive testing to determine its effectiveness as a dispersant and dispersant viscosity modifier. The rheological testing indicated that the proposed waste polymer derived lubricant additive was ineffective in associating to the soot and therefore a poor dispersant. However, the process proves that it is possible to produce lubricant additives from waste commodity polymers.

Various model dispersant and dispersant viscosity modifiers were prepared using RAFT polymerisation. An investigation into the initial kinetics of polymerisation with cumyl dithiobenzoate, styrene and maleic anhydride shows that the fragmentation and pre-equilibrium stage occurs faster with the presence of maleic anhydride than without. The ability to place a linker unit within a polymer chain at a specified place was also demonstrated with the RAFT styrene-maleic anhydride polymerisation.

Furthermore the RAFT polymerisation of styrene with N-phenylenedimaine maleimide has been shown to produce alternating one pot block copolymers in a similar manor to those reported by the ATRP polymerisation of N-maleimides with styrene by Lutz et al[229].

End capped RAFT polystyrene with maleic anhydride was also reported and further functionalisation of the polymer via the maleic anhydride group was demonstrated by the addition of a polyisobutylene polymer chain linked

through the maleic anhydride. The use of FTIR spectroscopy to determine the ratios of anhydride, imide and amide in the linked polymers was also shown.

Finally the model dispersants were tested to rate their potential effectiveness as dispersants. Candidate dispersant 4 (figure 86) is the best performing model dispersant, performing well in both the rheological and viscometric testing. The stearyl methacyrlate block coupled with the alternating styrene N-phenylenediamine maleimide is the most effective candidate dispersant at associating with soot and providing thickening at elevated temperatures and compares well with already available commercial technology.

It is hoped that the work begun in this thesis can be applied to develop new and interesting materials not limited to lubricant additives from waste commodity polymers but also to improve the options available for waste plastics.

Further optimisation and scale up of the microwave degradation process is needed to develop this technology as a method for degrading commodity polymers. An investigation into the degradation of mixed waste streams would be an interesting starting point, with the aim to investigate this effect upon product distributions and functional groups generated.

The polymerisation of N-maleimides I consider to be of great interest. Polymerisation with different N-maleimides would be an interesting exploration. The different electronic properties of N-maleimides might afford direct polymerisation without the need for copolymerisation. The synthesis of different N-maleimides and the copolymerisation of these would lead to many interesting structures that are currently unavailable to access.

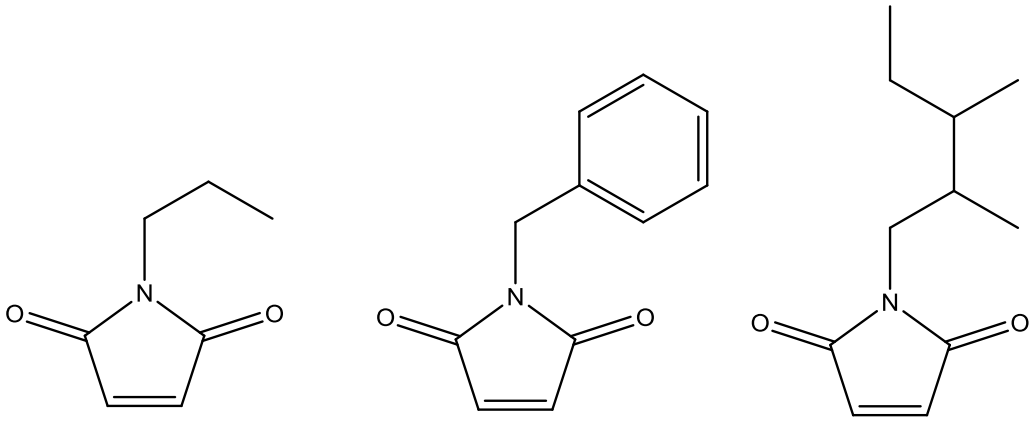

Figure 88: Different N-malomides with potential interest

The end functionalised polystyrene with maleic anhydride could be the basis for a self healing polymer study. Reaction of the maleic anhydride group with an aminothiol would afford the synthesis of a disulfide species. This species could then be oxidised and reduced to cleave and reform the disulfide bond, offering potential for a self healing polymer system. Similarly, the cleavage of the dithoiester moiety to a thiol would also offer potential in this manner.

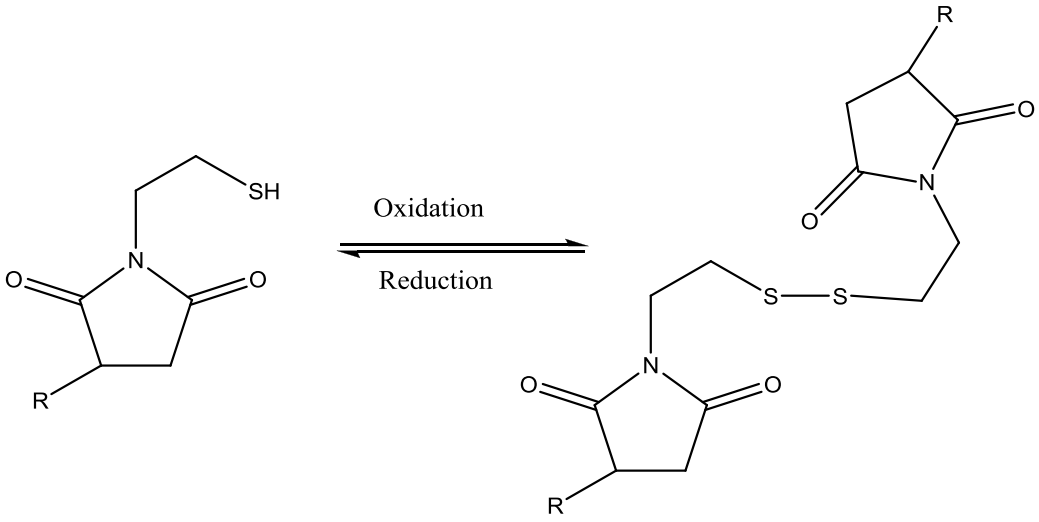

Figure 89: Example of self health polymer system from an end functionalised maleic amine thiol

Publications

1. G. J. Hunt; N.R. Cameron; G.D. Lamb; A. Smith; “Towards the synthesis of novel lubricants”, BP Invention disclosure document, April 2010.
2. M. I. Gibson; G. J. Hunt; N. R. Cameron; “Improved Synthesis of O-Linked, and First Synthesis of S- Linked, Carbohydrate Functionalised N-Carboxyanhydrides (GlycoNCAs)” Organic and Biomolecular Chemistry, 2007, 5, 2756-2757
3. In progress: G. J. Hunt; N.R. Cameron; G.D. Lamb; A. Smith; Generation of functional waste from commodity polymers.
4. In progress: G. J. Hunt; N.R. Cameron; G.D. Lamb; A. Smith; Synthesis of novel dispersant architectures via RAFT polymerisation.

Conference Presentations

1. September 2007, UK Polymer Showcase 2007 “Innovative Materials", London, UK
2. April 2008, Frontiers of Research and Young Researchers Meeting, Warwick, UK
3. June 2008, Macro2008: IUPAC 42nd World Polymer Congress, Taipei, Taiwan
4. September 2008, UK Polymer Showcase 2008 - "Polymers and Society”, York, UK
5. September 2009, Opening of the Wolfson Laboratories, Durham, UK

Conference Attendance (non-presenter)

1. January 2007, SCM3: International Symposium on Separation and Characterization of Natural and Synthetic Macromolecules, Rhône Congress Centre, Amsterdam, NL
2. March 2009, Bio-nanotechnologies, Durham, UK

3. April 2009, Additives 2009: Fuels and Lubricants for Energy Efficient and Sustainable Transport, York, UK

Awards and Bursaries

1. Recipient: DH Richards Memorial Bursary, Royal Society of Chemistry, Macro Group UK. Award to attend Macro2008: IUPAC 42nd World Polymer Congress, Taipei, Taiwan
2. Recipient: 2008 Collingwood College Special Projects and Travel Fund to assist with travel to Macro2008: IUPAC 42nd World Polymer Congress, Taipei, Taiwan.
3. Awarded 1st Prize for Best Poster at the Young Researchers Meeting of the Royal Society of Chemistry Macro Group UK meeting, Warwick, UK.
4. Royal Society of Chemistry bursary to attend Additives 2009: Fuels and Lubricants for Energy Efficient and Sustainable Transport, York, UK.

References

1. Young, R.J. and P.A. Lovell, *Introduction to Polymers*. 2nd ed. 1997: Chapman and Hall.
2. Crespy, D., M. Bozonnet, and M. Meier, Angew. Chem. Int. Ed, 2008. **47**: p. 3322.
3. Stevens, M.P., *Polymer Chemistry An Introduction*. 3rd ed. 1999: Oxford University Press.
4. Sperling, L.H., *Physical Polymer Science*. 4th ed. 2006: Wiley.
5. Kennedy, J.P., J.L. Price, and K. Koshimura, Macromolecules, 1991. **24**: p. 6567.
6. Cowie, J.M.G., *Polymers:Chemistry & Physics of Modern Materials*. 2 ed. 1991, London: CRC PRESS.
7. Ebdon, J.R., *New Methods of Polymer Synthesis*. 1991: Blackly and Sons.
8. Braun, D., et al., *Polymer Synthesis: Theory and Practice*. 4th ed. 2005: Springer.
9. Jenkins, A.D., R.G. Jones, and G. Moad, *Terminology for reversible-deactivation radical polymerization previously called "controlled" radical or "living" radical polymerization (IUPAC Recommendations 2010).* Pure and Applied Chemistry, 2010. **82**(2): p. 483-491.
10. Szwarc, M., M. Levy, and R. Milkovich, *POLYMERIZATION INITIATED BY ELECTRON TRANSFER TO MONOMER. A NEW METHOD OF FORMATION OF BLOCK POLYMERS1.* Journal of the American Chemical Society, 1956. **78**(11): p. 2656-2657.
11. Wang, J.-S. and K. Matyjaszewski, *Controlled/"Living" Radical Polymerization. Halogen Atom Transfer Radical Polymerization Promoted by a Cu(I)/Cu(II) Redox Process.* Macromolecules, 1995. **28**(23): p. 7901-7910.
12. Moad, G. and D.H. Solomon, *The Chemistry of Radical Polymerisation*. 2nd ed. 2006: Elsevier.
13. Mitsukami, Y., et al., Macromolecules, 2001. **34**: p. 2248.

14. PlasticsEurope, *Plastics - the Facts 2011*. 2011: Plastics Europe - Association of Plastic Manufacturers.

15. Ramdoss, P.K. and A.R. Tarrer, *High-temperature liquefaction of waste plastics.* Fuel, 1998. **77**(4): p. 293-299.

16. Buekens, A., *Introduction to Feedstock Recycling of Plastics*. Feedstock Recycling and Pyrolysis of Waste Plastics. 2006: John Wiley & Sons, Ltd. 1-41.

17. Greassie, N., Pure and Applied Chemistry, 1972. **30**: p. 119.

18. Cozzani, V., et al., *Influence of Gas-Phase Reactions on the Product Yields Obtained in the Pyrolysis of Polyethylene.* Industrial & Engineering Chemistry Research, 1997. **36**(2): p. 342-348.

19. Fawcett, N.C., *POLYMER DEGRADATION - PRINCIPLES AND PRACTICAL APPLICATIONS - SCHNABEL,W.* Journal of the American Chemical Society, 1984. **106**(8): p. 2486-2486.

20. Newborough, M., D. Highgate, and P. Vaughan, *Thermal depolymerisation of scrap polymers.* Applied Thermal Engineering, 2002. **22**(17): p. 1875-1883.

21. Rivaton, A., et al., *Basic Aspects of Polymer Degradation.* Macromolecular Symposia, 2005. **225**(1): p. 129-146.

22. Gryn'ova, G., J.L. Hodgson, and M.L. Coote, *Revising the mechanism of polymer autooxidation.* Organic & Biomolecular Chemistry, 2011. **9**(2): p. 480-490.

23. Aguado, J., D.P. Serrano, and J.M. Escola, *Fuels from Waste Plastics by Thermal and Catalytic Processes: A Review.* Industrial & Engineering Chemistry Research, 2008. **47**(21): p. 7982-7992.

24. Miskolczi, N., L. Bartha, and G. Deák, *Thermal degradation of polyethylene and polystyrene from the packaging industry over different catalysts into fuel-like feed stocks.* Polymer Degradation and Stability, 2006. **91**(3): p. 517-526.

25. Kodera, Y., Y. Ishihara, and T. Kuroki, *Novel Process for Recycling Waste Plastics To Fuel Gas Using a Moving-Bed Reactor.* Energy & Fuels, 2005. **20**(1): p. 155-158.

26. Nishino, J., et al., *Catalytic degradation of plastic waste into petrochemicals using Ga-ZSM-5.* Fuel, 2008. **87**(17-18): p. 3681-3686.

27. Serrano, D.P., J. Aguado, and J.M. Escola, *Catalytic Cracking of a Polyolefin Mixture over Different Acid Solid Catalysts.* Industrial & Engineering Chemistry Research, 2000. **39**(5): p. 1177-1184.

28. Tu, P., et al., *Degradation of Low-Density Polyethylene over Modified Zeolites.* Developments in Chemical Engineering and Mineral Processing, 2006. **14**(1-2): p. 203-218.

29. Manos, G., A. Garforth, and J. Dwyer, *Catalytic Degradation of High-Density Polyethylene over Different Zeolitic Structures.* Industrial & Engineering Chemistry Research, 2000. **39**(5): p. 1198-1202.

30. Manos, G., A. Garforth, and J. Dwyer, *Catalytic Degradation of High-Density Polyethylene on an Ultrastable-Y Zeolite. Nature of Initial Polymer Reactions, Pattern of Formation of Gas and Liquid Products, and Temperature Effects.* Industrial & Engineering Chemistry Research, 2000. **39**(5): p. 1203-1208.

31. Marcilla, A., A. Gómez-Siurana, and D. Berenguer, *Study of the influence of the characteristics of different acid solids in the catalytic pyrolysis of different polymers.* Applied Catalysis A: General, 2006. **301**(2): p. 222-231.

32. Durmus, A., et al., *Thermal-catalytic degradation kinetics of polypropylene over BEA, ZSM-5 and MOR zeolites.* Applied Catalysis B: Environmental, 2005. **61**(3-4): p. 316-322.

33. Chitrakar, R., et al., *A solvent-free synthesis of Zn-Al layered double hydroxides.* Chemistry Letters, 2007. **36**(3): p. 446-447.

34. Zhang, Z., et al., *Chemical Recycling of Waste Polystyrene into Styrene over Solid Acids and Bases.* Industrial & Engineering Chemistry Research, 1995. **34**(12): p. 4514-4519.

35. Ukei, H., et al., *Catalytic degradation of polystyrene into styrene and a design of recyclable polystyrene with dispersed catalysts.* Catalysis Today, 2000. **62**(1): p. 67-75.

36. Muller, P., *GLOSSARY OF TERMS USED IN PHYSICAL ORGANIC-CHEMISTRY.* Pure and Applied Chemistry, 1994. **66**(5): p. 1077-1184.

37. Stoyanov, E.S., et al., *The Structure of the Strongest Brønsted Acid: The Carborane Acid H(CHB11Cl11).* Journal of the American Chemical Society, 2006. **128**(10): p. 3160-3161.

38. Reed, C.A., et al., *Isolation of Protonated Arenes (Wheland Intermediates) with BArF and Carborane Anions. A Novel Crystalline Superacid.* Journal of the American Chemical Society, 1999. **121**(26): p. 6314-6315.

39. Metz, M.V., et al., *New Perfluoroarylborane Activators for Single-Site Olefin Polymerization. Acidity and Cocatalytic Properties of a "Superacidic" Perfluorodiboraanthracene.* Organometallics, 2002. **21**(20): p. 4159-4168.

40. Juhasz, M., et al., *The strongest isolable acid.* Angewandte Chemie-International Edition, 2004. **43**(40): p. 5352-5355.

41. Olah, G.A., *Crossing Conventional Boundaries in Half a Century of Research†.* The Journal of Organic Chemistry, 2005. **70**(7): p. 2413-2429.

42. Strausz, O.P., et al., *Upgrading of Alberta's Heavy Oils by Superacid-Catalyzed Hydrocracking.* Energy & Fuels, 1999. **13**(3): p. 558-569.

43. Weiland, M., A. Daro, and C. David, *Biodegradation of thermally oxidized polyethylene.* Polymer Degradation and Stability, 1995. **48**(2): p. 275-289.

44. Baek, K.H., et al., *Biodegradation of aliphatic and aromatic hydrocarbons by Nocardia sp H17-1.* Geomicrobiology Journal, 2006. **23**(5): p. 253-259.

45. Tanaka, A. and S. Fukui, *STUDIES ON UTILIZATION OF HYDROCARBONS BY MICROORGANISMS .13. EFFECT OF NONIONIC DETERGENTS ON*

ALKANE UTILIZATION BY YEASTS. Journal of Fermentation Technology, 1971. **49**(9): p. 809-&.

46. Hamid, S.H., *Handbook of Polymer Degradation*, ed. E.S. Pollution. 2000: CRC Press.
47. Geuskens, G., *Chapter 3 Photodegradation of Polymers*, in *Comprehensive Chemical Kinetics*, M.A.P.D.S.D.F.R.I.C.F.R.S. C.H. Bamford and P.D.D.S. C.F.H. Tipper, Editors. 1975, Elsevier. p. 333-424.
48. Schnabel W., *Polymer Degradation*. 1981, New York: Hancer International.
49. Kemp, T.J. and R.A. McIntyre, *Influence of transition metal-doped titanium(IV) dioxide on the photodegradation of polystyrene.* Polymer Degradation and Stability, 2006. **91**(12): p. 3010-3019.
50. Pringle, F.G., *MICROWAVE-BASED RECOVERY OF HYDROCARBONS AND FOSSIL FUELS* 2007, Mobilestream Oil, Inc: United States. p. 1-54.
51. Ludlow-Palafox, C. and H.A. Chase, *Microwave-induced pyrolysis of plastic wastes.* Industrial & Engineering Chemistry Research, 2001. **40**(22): p. 4749-4756.
52. Tanner, D.D., et al., *Reactions of microwave-generated O(P-3) atoms with unsaturated hydrocarbons.* Journal of Organic Chemistry, 1998. **63**(14): p. 4587-4593.
53. Tanner, D.D.D., Qizhu; Kandanarachchi, Pramod; Franz, James A., *Method of microwave bond cleavage of a hydrocarbon compound in a liquid phase*. 2000, Battelle Memorial Institute, Governors of the University of Alberta: United States. p. 1-19.
54. Tanner, D.D., et al., *The catalytic conversion of C-1-C-n hydrocarbons to olefins and hydrogen: Microwave-assisted C-C and C-H bond activation.* Energy & Fuels, 2001. **15**(1): p. 197-204.
55. Chakraborty, J., et al., *Ultrasonic degradation of polybutadiene and isotactic polypropylene.* Polymer Degradation and Stability, 2004. **85**(1): p. 555-558.

56. Hensel, J.D., R.A. Schwarz, and C.W. Grispin, *Sustainability in the Polymer Industry*. Clean Technology 2008: Bio Energy, Renewables, Green Building, Smart Grid, Storage, and Water, ed. M.R.B.L.D.L. Laudon. 2008. 363-366.

57. Aguado, J., et al., *Catalytic cracking of polyethylene over zeolite mordenite with enhanced textural properties.* Journal of Analytical and Applied Pyrolysis, 2009. **85**(1-2): p. 352-358.

58. Butterman, H.C. and M.J. Castaldi, *Syngas Production via CO(2) Enhanced Gasification of Biomass Fuels.* Environmental Engineering Science, 2009. **26**(4): p. 703-713.

59. Castaldi, M.J. and Jsme, *SOLID CARBON FEEDSTOCK GASIFICATION USING CO(2) SIMULATION AND EXPERIMENT*. Proceedings of the International Conference on Power Engineering 2009. 2009. 277-282.

60. Chang, Y.-M., et al., *Change in MSW characteristics under recent management strategies in Taiwan.* Waste Management, 2008. **28**(12): p. 2443-2455.

61. Fukushima, M., et al., *Toward maximizing the recycling rate in a Sapporo waste plastics liquefaction plant.* Journal of Material Cycles and Waste Management, 2009. **11**(1): p. 11-18.

62. Grause, G., et al., *Pyrolytic hydrolysis of polycarbonate in the presence of earth-alkali oxides and hydroxides.* Polymer Degradation and Stability, 2009. **94**(7): p. 1119-1124.

63. Hopewell, J., R. Dvorak, and E. Kosior, *Plastics recycling: challenges and opportunities.* Philosophical Transactions of the Royal Society B-Biological Sciences, 2009. **364**(1526): p. 2115-2126.

64. Kaminsky, W., C. Mennerich, and Z. Zhang, *Feedstock recycling of synthetic and natural rubber by pyrolysis in a fluidized bed.* Journal of Analytical and Applied Pyrolysis, 2009. **85**(1-2): p. 334-337.

65. Prechthai, T., M. Padmasri, and C. Visvanathan, *Quality assessment of mined MSW from an open dumpsite for recycling potential.* Resources Conservation and Recycling, 2008. **53**(1-2): p. 70-78.

66. Siddiqui, M.N. and H.H. Redhwi, *Pyrolysis of mixed plastics for the recovery of useful products.* Fuel Processing Technology, 2009. **90**(4): p. 545-552.

67. Thompson, R.C., et al., *Plastics, the environment and human health: current consensus and future trends.* Philosophical Transactions of the Royal Society B-Biological Sciences, 2009. **364**(1526): p. 2153-2166.

68. Brems, A., et al., *Thermogravimetric pyrolysis of waste polyethylene-terephthalate and polystyrene: A critical assessment of kinetics modelling.* Resources Conservation and Recycling, 2011. **55**(8): p. 772-781.

69. Krishna, S.V. and G. Pugazhenthi, *Properties and Thermal Degradation Kinetics of Polystyrene/Organoclay Nanocomposites Synthesized by Solvent Blending Method: Effect of Processing Conditions and Organoclay Loading.* Journal of Applied Polymer Science, 2011. **120**(3): p. 1322-1336.

70. Kaminsky, W. and H. Sinn, *Pyrolysis of Plastic Waste and Scrap Tires Using a Fluidized-Bed Process*, in *Thermal Conversion of Solid Wastes and Biomass*. 1980, American Chemical Society. p. 423-439.

71. Kaminsky, W., *Pyrolysis of Polymers*, in *Emerging Technologies in Plastics Recycling*. 1992, American Chemical Society. p. 60-72.

72. Hu, G., et al., *Effects of Geometric Parameters and Operating Conditions on Granular Flow in a Modified Rotating Cone.* Industrial & Engineering Chemistry Research, 2007. **46**(26): p. 9263-9268.

73. Westerhout, R.W.J., et al., *Recycling of Polyethene and Polypropene in a Novel Bench-Scale Rotating Cone Reactor by High-Temperature Pyrolysis.* Industrial & Engineering Chemistry Research, 1998. **37**(6): p. 2293-2300.

74. Scott, D.S., et al., *Fast pyrolysis of plastic wastes.* Energy & Fuels, 1990. **4**(4): p. 407-411.

75. Arandes, J.M., et al., *Valorization of Polyolefins Dissolved in Light Cycle Oil over HY Zeolites under Fluid Catalytic Cracking Unit Conditions.*

Industrial & Engineering Chemistry Research, 2003. **42**(17): p. 3952-3961.

76. Blanco, I., L. Abate, and M.L. Antonelli, *The regression of isothermal thermogravimetric data to evaluate degradation E(a) values of polymers: A comparison with literature methods and an evaluation of lifetime prediction reliability.* Polymer Degradation and Stability, 2011. **96**(11): p. 1947-1954.
77. Grause, G., et al., *TG-MS investigation of brominated products from the degradation of brominated flame retardants in high-impact polystyrene.* Chemosphere, 2011. **85**(3): p. 368-73.
78. Remili, C., et al., *The effects of reprocessing cycles on the structure and properties of polystyrene/Cloisite 15A nanocomposites.* Polymer Degradation and Stability, 2011. **96**(8): p. 1489-1496.
79. Vathauer, M. and W. Kaminsky, *Homopolymerizations of α-Olefins with Diastereomeric Metallocene/MAO Catalysts.* Macromolecules, 1980. **33**(6): p. 1955-1959.
80. Deng, H., et al., *Synthesis of High-Melting, Isotactic Polypropene with C2- and C1-Symmetrical Zirconocenes.* Macromolecules, 1980. **29**(20): p. 6371-6376.
81. Schumann, H., et al., *Oxygen-Stabilized Organoaluminum Compounds as Highly Active Cocatalysts for Ziegler−Natta Olefin Polymerization.* Organometallics, 1980. **22**(7): p. 1391-1401.
82. Owen Michael, J., *Foam Control*, in *Advances in Silicones and Silicone-Modified Materials*. 2010, American Chemical Society. p. 269-283.
83. Minfray, C., et al., *ALTERNATIVE TO ZDDP ADDITIVE: STUDY OF ZINC DIALKYLPHOSPHATE LUBRICANT PROPERTIES*. Proceedings of the Stle/Asme International Joint Tribology Conference 2008. 2009. 217-219.
84. Ozimina, D., M. Madej, and M. Styp-Rekowski, *Antiwear additives as retarding agents of elements with ceramic coatings wear.* Industrial Lubrication and Tribology, 2010. **62**(5): p. 275-278.

85. Meheux, M., et al., *Effect of lubricant additives in rolling contact fatigue.* Proceedings of the Institution of Mechanical Engineers Part J-Journal of Engineering Tribology, 2010. **224**(J9): p. 947-955.

86. de Castro Costa, R.P., et al., *Enhanced DLC Wear Performance by the Presence of Lubricant Additives.* Materials Research-Ibero-American Journal of Materials, 2011. **14**(2): p. 222-226.

87. Kar, P., P. Asthana, and H. Liang, *Formation and characterization of tribofilms.* Journal of Tribology-Transactions of the Asme, 2008. **130**(4).

88. Ahmad, I., et al., *Influence of some antioxidants on the oxidative stability of Rimula D lubricating oil.* Industrial Lubrication and Tribology, 2011. **63**(4): p. 234-238.

89. Berro, H., N. Fillot, and P. Vergne, *Molecular dynamics simulation of surface energy and ZDDP effects on friction in nano-scale lubricated contacts.* Tribology International, 2010. **43**(10): p. 1811-1822.

90. Morina, A., et al., *Role of friction modifiers on the tribological performance of hypereutectic Al-Si alloy lubricated in boundary conditions.* Proceedings of the Institution of Mechanical Engineers Part J-Journal of Engineering Tribology, 2011. **225**(J6): p. 369-378.

91. Mourhatch, R. and P.B. Aswath, *Tribological behavior and nature of tribofilms generated from fluorinated ZDDP in comparison to ZDDP under extreme pressure conditions-Part 1: Structure and chemistry of tribofilms.* Tribology International, 2011. **44**(3): p. 187-200.

92. Qiao, R., et al., *The tribological chemistry of the triazine derivative additives in rape seed oil and synthetic diester.* Applied Surface Science, 2011. **257**(9): p. 3843-3849.

93. Blanco, D., et al., *Use of ethyl-dimethyl-2-methoxyethylammonium tris(pentafluoroethyl)trifluorophosphate as base oil additive in the lubrication of TiN PVD coating.* Tribology International, 2011. **44**(5): p. 645-650.

94. Colclough, T., *Role of additives and transition metals in lubricating oil oxidation.* Industrial & Engineering Chemistry Research, 1987. **26**(9): p. 1888-1895.

95. Mahoney, L.R., et al., *Determination of the Antioxidant Capacity of New and Used Lubricants: Method and Applications.* Industrial & Engineering Chemistry Product Research and Development, 1978. **17**(3): p. 250-255.

96. Burn A, J., *Mechanism of Oxidation Inhibition by Zinc Dialkyl Dithiophosphates*, in *Oxidation of Organic Compounds*. 1968, AMERICAN CHEMICAL SOCIETY. p. 323-345.

97. Wang, Y. and W. Eli, *Recent Advances in Colloidal Lubricant Detergents.* China Petroleum Processing & Petrochemical Technology, 2010. **12**(4): p. 7-12.

98. Ahmed, N.S., A.M. Nassar, and A.-A.A. Abdel-Azim, *Synthesis and Evaluation of Some Detergent/Dispersant Additives for Lube Oil.* International Journal of Polymeric Materials, 2008. **57**(2): p. 114-124.

99. Wang, Y. and W. Eli, *Synthesis of Environmentally Friendly Overbased Magnesium Oleate Detergent and High Alkaline Dispersant/Magnesium Oleate Mixed Substrate Detergent.* Industrial & Engineering Chemistry Research, 2010. **49**(19): p. 8902-8907.

100. Fu, J., et al., *Temperature and acid droplet size effects in acid neutralization of marine cylinder lubricants.* Tribology Letters, 2006. **22**(3): p. 221-225.

101. Chen, Z., et al., *Calcium carbonate phase transformations during the carbonation reaction of calcium heavy alkylbenzene sulfonate overbased nanodetergents preparation.* Journal of Colloid and Interface Science, 2011. **359**(1): p. 56-67.

102. Frigerio, F. and L. Montanari, *Characterisation of the surfactant shell stabilising calcium carbonate dispersions in overbased detergent additives: Molecular modelling and spin-probe-ESR studies*, in *Computational Science - ICCS 2007, Pt 2, Proceedings*, Y.V.G.D.D.J.S.P.M.A. Shi, Editor. 2007. p. 272-279.

103. Besergil, B. and A. Celik, *Determination of synthesis conditions of alkali calcium sulfonate.* Industrial Lubrication and Tribology, 2004. **56**(2-3): p. 188-194.

104. Celik, A. and B. Besergil, *Determination of synthesis conditions of neutral calcium sulfonate, so-called detergent-dispersant.* Industrial Lubrication and Tribology, 2004. **56**(4): p. 226-230.

105. Beşergil, B., A. Akın, and S. Çelik, *Determination of Synthesis Conditions of Medium, High, and Overbased Alkali Calcium Sulfonate.* Industrial & Engineering Chemistry Research, 2007. **46**(7): p. 1867-1873.

106. Covitch, M.J., *Lubricant additive effects on engine oil pumpability at low temperatures-detergents and high ethylene olefin copolymer viscosity modifiers.* Tribology Transactions, 2007. **50**(1): p. 68-73.

107. Wang, Y., et al., *A Novel Method of Quantitative Carbon Dioxide for Synthesizing Magnesium Oleate (Linoleate, Isostearate, and Sulfonate) Detergents.* Industrial & Engineering Chemistry Research, 2011. **50**(13): p. 8376-8378.

108. Badulescu, R., et al., *Quantitative analysis of additives in lubricants.* Revista De Chimie, 2003. **54**(6): p. 519-521.

109. Gilbert, E.E. and E.P. Jones, *Sulfonation and Sulfation.* Industrial & Engineering Chemistry, 1959. **51**(9): p. 1148-1154.

110. Abou El Naga, H.H., et al., *Synthesis of basic and overbasic sulfonate detergent additives.* Industrial & Engineering Chemistry Research, 1993. **32**(12): p. 3170-3173.

111. Besergil, B. and B.M. Baysal, *Determination of sulfonation conditions of postdodecylbenzene.* Industrial & Engineering Chemistry Research, 1990. **29**(4): p. 667-669.

112. Cooper, J.E. and J.M. Paul, *Sodium alkylbenzenesulfonates from phenols.* Journal of Chemical & Engineering Data, 1970. **15**(4): p. 586-588.

113. Van Ess, P.R.S., H E, *LUBRICATING COMPOSITIONS CONTAINING HIGHLY BASIC METAL SULFONATES*. 1952: UNITED STATES.

114. Griffiths, J.A. and D.M. Heyes, *Atomistic Simulation of Overbased Detergent Inverse Micelles.* Langmuir, 1996. **12**(10): p. 2418-2424.

115. Tobias, D.J. and M.L. Klein, *Molecular Dynamics Simulations of a Calcium Carbonate/Calcium Sulfonate Reverse Micelle†.* The Journal of Physical Chemistry, 1996. **100**(16): p. 6637-6648.

116. Covitch, M., *Olefin Copolymer Viscosity Modifiers*, in *Lubricant Additives*. 2003, CRC Press. p. 293-327.

117. Selby, T.W. and P.C. Casey, *MARKETED ENGINE OILS - A COMPARATIVE-ANALYSIS OF PRODUCTS MADE FROM VIRGIN AND RE-REFINED BASE-STOCKS.* Abstracts of Papers of the American Chemical Society, 1992. **204**: p. 61-PETR.

118. Warrens, C., et al., *Effect of oil rheology and chemistry on journal-bearing friction and wear.* Proceedings of the Institution of Mechanical Engineers Part J-Journal of Engineering Tribology, 2008. **222**(J3): p. 441-450.

119. Gautam, M., et al., *Effect of diesel soot contaminated oil on engine wear - investigation of novel oil formulations.* Tribology International, 1999. **32**(12): p. 687-699.

120. George, S., et al., *Effect of diesel soot on lubricant oil viscosity.* Tribology International, 2007. **40**(5): p. 809-818.

121. Uy, D., et al., *Soot-additive interactions in engine oils.* Lubrication Science, 2010. **22**(1): p. 19-36.

122. Jones Timothy, G.J. and L. Hughes Trevor, *Drilling Fluid Suspensions*, in *Suspensions: Fundamentals and Applications in the Petroleum Industry*. 1996, American Chemical Society. p. 463-564.

123. Goodwin, J.W. and R.W. Hughes, *Particle Interactions and Dispersion Rheology*, in *Technology for Waterborne Coatings*. 1997, American Chemical Society. p. 94-125.

124. Norgren, M. and S. Mackin, *Sulfate and Surfactants as Boosters of Kraft Lignin Precipitation.* Industrial & Engineering Chemistry Research, 2009. **48**(10): p. 5098-5104.

125. Tomlinson, A., et al., *Interfacial Characterization of Succinimide Surfactants.* Langmuir, 1997. **13**(22): p. 5881-5893.

126. Shen, Y. and J. Duhamel, *Micellization and Adsorption of a Series of Succinimide Dispersants.* Langmuir, 2008. **24**(19): p. 10665-10673.

127. Baladincz, J., et al., *Interactions of additives in lubricating oil compositions.* Hungarian Journal of Industrial Chemistry, 1998. **26**(2): p. 155-159.

128. Kamigaito, M., T. Ando, and M. Sawamoto, *Metal-Catalyzed Living Radical Polymerization.* Chemical Reviews, 2001. **101**(12): p. 3689-3746.

129. Papke, B.L., *Irreversible Adsorption of Poly(isobutenyl)-succinimide Dispersants onto Calcium Alkylarylsulfonate Colloids*, in *Mixed Surfactant Systems*. 1992, American Chemical Society. p. 377-389.

130. Achilias, D.S., et al., *Recycling techniques of polyolefins from plastic wastes.* Global Nest Journal, 2008. **10**(1): p. 114-122.

131. Achilias, D.S., et al., *Chemical recycling of plastic wastes made from polyethylene (LDPE and HDPE) and polypropylene (PP).* Journal of Hazardous Materials, 2007. **149**(3): p. 536-542.

132. Gal, T. and B.G. Lakatos, *Thermal cracking of recycled hydrocarbon gas-mixtures for re-pyrolysis: Operational analysis of some industrial furnaces.* Applied Thermal Engineering, 2008. **28**(2-3): p. 218-225.

133. Ignatenko, O., A. van Schalk, and M.A. Reuter, *Recycling system flexibility: the fundamental solution to achieve high energy and material recovery quotas.* Journal of Cleaner Production, 2008. **16**(4): p. 432-449.

134. Islam, M.R., M.S.H.K. Tushar, and H. Haniu, *Production of liquid fuels and chemicals from pyrolysis of Bangladeshi bicycle/rickshaw tire wastes.* Journal of Analytical and Applied Pyrolysis, 2008. **82**(1): p. 96-109.

135. Mikulec, J. and M. Vrbova, *Catalytic and thermal cracking of selected polyolefins.* Clean Technologies and Environmental Policy, 2008. **10**(2): p. 121-130.

136. Mlynkova, B., E. Hajekova, and M. Bajus, *Copyrolysis of oils/waxes of individual and mixed polyalkenes cracking products with petroleum fraction.* Fuel Processing Technology, 2008. **89**(11): p. 1047-1055.

137. Subramani, V. and S.K. Gangwal, *A review of recent literature to search for an efficient catalytic process for the conversion of syngas to ethanol.* Energy & Fuels, 2008. **22**(2): p. 814-839.

138. Vasile, C., et al., *Feedstock recycling from the printed circuit boards of used computers.* Energy & Fuels, 2008. **22**(3): p. 1658-1665.

139. Venugopal, R., et al., *Additional feedstock for fluid catalytic cracking unit.* Petroleum Science and Technology, 2008. **26**(4): p. 436-445.

140. Achilias, D.S., et al., *Chemical recycling of polystyrene by pyrolysis: Potential use of the liquid product for the reproduction of polymer.* Macromolecular Materials and Engineering, 2007. **292**(8): p. 923-934.

141. Al-Salem, S.M., P. Lettieri, and J. Baeyens, *Recycling and recovery routes of plastic solid waste (PSW): A review.* Waste Management, 2009. **29**(10): p. 2625-2643.

142. Alston, S.M., et al., *Environmental Impact of Pyrolysis of Mixed WEEE Plastics Part 1: Experimental Pyrolysis Data.* Environmental Science & Technology, 2011. **45**(21): p. 9380-9385.

143. Garforth, A.A., et al., *Feedstock recycling of polymer wastes.* Current Opinion in Solid State & Materials Science, 2004. **8**(6): p. 419-425.

144. Hall, W.J. and P.T. Williams, *Pyrolysis of brominated feedstock plastic in a fluidised bed reactor.* Journal of Analytical and Applied Pyrolysis, 2006. **77**(1): p. 75-82.

145. Kaminsky, W., *RECYCLING OF POLYMERS BY PYROLYSIS.* Journal De Physique Iv, 1993. **3**(C7): p. 1543-1552.

146. Kaminsky, W., *CHEMICAL RECYCLING OF MIXED PLASTICS BY PYROLYSIS.* Advances in Polymer Technology, 1995. **14**(4): p. 337-344.

147. Kaminsky, W., *PYROLYSIS WITH RESPECT TO RECYCLING OF POLYMER.* Angewandte Makromolekulare Chemie, 1995. **232**: p. 151-165.

148. Kaminsky, W., M. Predel, and A. Sadiki, *Feedstock recycling of polymers by pyrolysis in a fluidised bed.* Polymer Degradation and Stability, 2004. **85**(3): p. 1045-1050.

149. Kaminsky, W., H. Schmidt, and C.M. Simon, *Recycling of mixed plastics by pyrolysis in a fluidised bed.* Macromolecular Symposia, 2000. **152**: p. 191-199.

150. Lopez, A., et al., *Influence of time and temperature on pyrolysis of plastic wastes in a semi-batch reactor.* Chemical Engineering Journal, 2011. **173**(1): p. 62-71.

151. Lopez, A., et al., *Pyrolysis of municipal plastic wastes II: Influence of raw material composition under catalytic conditions.* Waste Management, 2011. **31**(9-10): p. 1973-1983.

152. Mastellone, M.L., et al., *Fluidized bed pyrolysis of a recycled polyethylene.* Polymer Degradation and Stability, 2002. **76**(3): p. 479-487.

153. Sasse, F. and G. Emig, *Chemical recycling of polymer materials.* Chemical Engineering & Technology, 1998. **21**(10): p. 777-789.

154. Williams, P.T. and E.A. Williams, *Recycling plastic waste by pyrolysis.* Journal of the Institute of Energy, 1998. **71**(487): p. 81-93.

155. Williams, P.T. and E.A. Williams, *Fluidised bed pyrolysis of low density polyethylene to produce petrochemical feedstock.* Journal of Analytical and Applied Pyrolysis, 1999. **51**(1-2): p. 107-126.

156. Yoshioka, T., et al., *Pyrolysis of poly(ethylene terephthalate) in a fluidised bed plant.* Polymer Degradation and Stability, 2004. **86**(3): p. 499-504.

157. Sun, X., J.-Y. Hwang, and X. Huang, *The microwave processing of electric arc furnace dust.* Jom, 2008. **60**(10): p. 35-39.

158. Lam, S.S., A.D. Russell, and H.A. Chase, *Microwave pyrolysis, a novel process for recycling waste automotive engine oil.* Energy, 2010. **35**(7): p. 2985-2991.

159. Lam, S.S., A.D. Russell, and H.A. Chase, *Pyrolysis Using Microwave Heating: A Sustainable Process for Recycling Used Car Engine Oil.* Industrial & Engineering Chemistry Research, 2010. **49**(21): p. 10845-10851.

160. Ravella, A.M., William J;Achia, Biddanda V., *Conversion of C2 + hydrocarbons using microwave radiation (OP-3515)*. 1990, Exxon Research and Engineering Company: United States. p. 1-4.

161. Westerhout, R.W.J., J.A.M. Kuipers, and W.P.M. van Swaaij, *Experimental determination of the yield of pyrolysis products of polyethene and polypropene. Influence of reaction conditions.* Industrial & Engineering Chemistry Research, 1998. **37**(3): p. 841-847.

162. Peterson, J.D., S. Vyazovkin, and C.A. Wight, *Kinetics of the thermal and thermo-oxidative degradation of polystyrene, polyethylene and poly(propylene).* Macromolecular Chemistry and Physics, 2001. **202**(6): p. 775-784.

163. Nishizaki, H., K. Yoshida, and J.H. Wang, *Comparative study of various methods for thermogravimetric analysis of polystyrene degradation.* Journal of Applied Polymer Science, 1980. **25**(12): p. 2869-2877.

164. Shang, J., M. Chai, and Y. Zhu, *Photocatalytic Degradation of Polystyrene Plastic under Fluorescent Light.* Environmental Science & Technology, 2003. **37**(19): p. 4494-4499.

165. Madras, G., et al., *Molecular Weight Effect on the Dynamics of Polystyrene Degradation.* Industrial & Engineering Chemistry Research, 1997. **36**(6): p. 2019-2024.

166. Ren, J. and G.R. Hatfield, *Synthesis and Characterization of Poly(ethylene-co-styrene).* Macromolecules, 1995. **28**(7): p. 2588-2589.

167. Hlalele, L. and B. Klumperman, *In Situ NMR and Modeling Studies of Nitroxide Mediated Copolymerization of Styrene and n-Butyl Acrylate.* Macromolecules, 2011. **44**(17): p. 6683-6690.

168. Svatoš, A. and A.B. Attygalle, *Characterization of Vinyl-Substituted, Carbon−Carbon Double Bonds by GC/FT-IR Analysis.* Analytical Chemistry, 1997. **69**(10): p. 1827-1836.

169. *Practical Microwave Synthesis for Organic Chemists: Strategies, Instruments, and Protocols.* Journal of the American Chemical Society, 2009. **131**(20): p. 7204-7204.

170. Gharibeh, M., et al., *Microwave Synthesis of Zeolites: Effect of Power Delivery.* The Journal of Physical Chemistry B, 2009. **113**(26): p. 8930-8940.

171. Stinson, S., *Use of microwave heating to speed organic reactions continues to grow.* Chemical & Engineering News, 1996. **74**(21): p. 45-46.

172. Beyler, C.J. and M.M. Hirschler, *Sfpe Handbook of Fire Protection Engineering*, in *Sfpe Handbook of Fire Protection Engineering*, P.J. DiNenno, Editor. 2008, Natl Fire Protection Assn.

173. Costa, P., et al., *Study of the Pyrolysis Kinetics of a Mixture of Polyethylene, Polypropylene, and Polystyrene.* Energy & Fuels, 2010. **24**(12): p. 6239-6247.

174. Ward, P.G., et al., *A Two Step Chemo-biotechnological Conversion of Polystyrene to a Biodegradable Thermoplastic.* Environmental Science & Technology, 1980. **40**(7): p. 2433-2437.

175. Matyjaszewski K, D.T.P., *Handbook of Radical Polymerization*. 2002, New York: John Wiley and Sons Ltd.

176. Santos, R.D., B.G. Soares, and A.S. Gomes, *COPOLYMERIZATION OF STYRENE, MALEIC-ANHYDRIDE AND ACRYLONITRILE UP TO HIGH CONVERSION.* Macromolecular Chemistry and Physics, 1994. **195**(7): p. 2517-2521.

177. Alfrey, T. and E. Lavin, *THE COPOLYMERIZATION OF STYRENE AND MALEIC ANHYDRIDE.* Journal of the American Chemical Society, 1945. **67**(11): p. 2044-2045.

178. Cowie, J.M.G., *Alternating Copolymers*. Speciality Polymers, ed. J.M.G. Cowie. 1985, New York: Plenum Press.

179. Chen, S.A. and G.Y. Chang, *KINETICS OF THE COPOLYMERIZATION OF STYRENE WITH MALEIC-ANHYDRIDE IN ETHYL METHYL KETONE.* Makromolekulare Chemie-Macromolecular Chemistry and Physics, 1986. **187**(7): p. 1597-1602.

180. Deb, P.C. and G. Meyerhoff, *STUDY ON KINETICS OF COPOLYMERIZATION OF STYRENE AND MALEIC-ANHYDRIDE IN DIOXANE.* European Polymer Journal, 1984. **20**(7): p. 713-719.

181. Deb, P.C. and G. Meyerhoff, *STUDY ON KINETICS OF COPOLYMERIZATION OF STYRENE AND MALEIC-ANHYDRIDE IN METHYL ETHYL KETONE.* Polymer, 1985. **26**(4): p. 629-635.

182. Doiuchi, T. and Y. Minoura, *SOLVENT EFFECT ON THE ASYMMETRIC INDUCTION COPOLYMERIZATION OF STYRENE WITH MALEIC-ANHYDRIDE IN THE PRESENCE OF LECITHIN.* Makromolekulare Chemie-Macromolecular Chemistry and Physics, 1980. **181**(5): p. 1081-1088.

183. Hill, D.J.T., J.H. Odonnell, and P.W. Osullivan, *ANALYSIS OF THE MECHANISM OF COPOLYMERIZATION OF STYRENE AND MALEIC-ANHYDRIDE.* Macromolecules, 1985. **18**(1): p. 9-17.

184. Matyjaszewski, K., *Comparison and Classification of Controlled/Living Radical Polymerizations*, in *Controlled/Living Radical Polymerization*. 2000, American Chemical Society. p. 2-26.

185. cowie, J.M.G. and V. Arrighi, *Polymers:Chemistry & Physics of Modern Materials*. 3 ed. 2007, Florida: CRC Press.

186. Benoit, D., et al., *One-step formation of functionalized block copolymers.* Macromolecules, 2000. **33**(5): p. 1505-1507.

187. Chambard, G. and B. Klumperman, *Atom Transfer Radical Copolymerization of Styrene and Butyl Acrylate*, in *Controlled/Living Radical Polymerization*. 2000, American Chemical Society. p. 197-210.

188. De Brouwer, H., et al., *Controlled radical copolymerization of styrene and maleic anhydride and the synthesis of novel polyolefin-based block*

copolymers by reversible addition-fragmentation chain-transfer (RAFT) polymerization. Journal of Polymer Science Part a-Polymer Chemistry, 2000. **38**(19): p. 3596-3603.

189. Klumperman, B., *Mechanistic considerations on styrene-maleic anhydride copolymerization reactions.* Polymer Chemistry, 2010. **1**(5): p. 558-562.
190. Zaitseva, V.V., T.G. Tyurina, and S.Y. Zaitsev, *Copolymerization of Styrene with Acrylonitrile and Maleic Anhydride.* Polymer Science Series B, 2009. **51**(1-2): p. 13-19.
191. Zhu, M.Q., et al., *A unique synthesis of a well-defined block copolymer having alternating segments constituted by maleic anhydride and styrene and the self-assembly aggregating behavior thereof.* Chemical Communications, 2001(4): p. 365-366.
192. Lai, J.T. and R. Shea, *Controlled radical polymerization by carboxyl- and hydroxyl-terminated dithiocarbamates and xanthates.* Journal of Polymer Science Part a-Polymer Chemistry, 2006. **44**(14): p. 4298-4316.
193. Barner-Kowollik, C., et al., *Mechanism and kinetics of dithiobenzoate-mediated RAFT polymerization. I. The current situation.* Journal of Polymer Science Part a-Polymer Chemistry, 2006. **44**(20): p. 5809-5831.
194. Arita, T., M. Buback, and P. Vana, *Cumyl dithiobenzoate mediated RAFT polymerization of styrene at high temperatures.* Macromolecules, 2005. **38**(19): p. 7935-7943.
195. Chiefari, J., et al., *Thiocarbonylthio compounds (S=C(Z)S-R) in free radical polymerization with reversible addition-fragmentation chain transfer (RAFT polymerization). Effect of the activating group Z.* Macromolecules, 2003. **36**(7): p. 2273-2283.
196. Chong, Y.K., et al., *Thiocarbonylthio compounds S=C(Ph)S-R in free radical polymerization with reversible addition-fragmentation chain transfer (RAFT polymerization). Role of the free-radical leaving group (R).* Macromolecules, 2003. **36**(7): p. 2256-2272.

197. Moad, G., E. Rizzardo, and S.H. Thang, *Kinetics and mechanism of raft polymerization.* Abstracts of Papers of the American Chemical Society, 2002. **224**: p. 696-POLY.

198. Zhou, Y., et al., *Dependence of Thermal Stability on Molecular Structure of RAFT/MADIX Agents: A Kinetic and Mechanistic Study.* Macromolecules, 2011. **44**(21): p. 8446-8457.

199. Gao, X. and S. Zhu, *Modeling Analysis of Chain Transfer in Reversible Addition-Fragmentation Chain Transfer Polymerization.* Journal of Applied Polymer Science, 2011. **122**(1): p. 497-508.

200. Moad, G., et al., *Kinetics and mechanism of RAFT polymerization*, in *Advances in Controlled/Living Radical Polymerization*, K. Matyjaszewski, Editor. 2003, Amer Chemical Soc: Washington. p. 520-535.

201. Goto, A., et al., *Mechanism and kinetics of RAFT-based living radical polymerizations of styrene and methyl methacrylate.* Macromolecules, 2001. **34**(3): p. 402-408.

202. Moad, G., E. Rizzardo, and S.H. Thang, *Living radical polymerization by the RAFT process - A first update.* Australian Journal of Chemistry, 2006. **59**(10): p. 669-692.

203. Moad, G., E. Rizzardo, and S.H. Thang, *Living radical polymerization by the RAFT process.* Australian Journal of Chemistry, 2005. **58**(6): p. 379-410.

204. Barner-Kowollik, C. and S. Perrier, *The future of reversible addition fragmentation chain transfer polymerization.* Journal of Polymer Science Part a-Polymer Chemistry, 2008. **46**(17): p. 5715-5723.

205. Barner-Kowollik, C., et al., *RAFTing down under: Tales of missing radicals, fancy architectures, and mysterious holes.* Journal of Polymer Science Part a-Polymer Chemistry, 2003. **41**(3): p. 365-375.

206. Barner-Kowollik, C., et al., *Modeling the reversible addition-fragmentation chain transfer process in cumyl dithiobenzoate-mediated styrene homopolymerizations: Assessing rate coefficients for the*

addition-fragmentation equilibrium. Journal of Polymer Science Part a-Polymer Chemistry, 2001. **39**(9): p. 1353-1365.

207. Moad, G., E. Rizzardo, and S.H. Thang, *Living Radical Polymerization by the RAFT Process - A Second Update.* Australian Journal of Chemistry, 2009. **62**(11): p. 1402-1472.
208. Moad, G., E. Rizzardo, and S.H. Thang, *Toward living radical polymerization.* Accounts of Chemical Research, 2008. **41**(9): p. 1133-1142.
209. Oidian, G.G., *Principles of Polymerisation*. 4th ed. 2004: John Wiley and Sons.
210. Spirin, Y.L. and T.S. Yatsimirskaya, *The kinetics and mechanism of alternating copolymerization of styrene with maleic anhydride.* Polymer Science U.S.S.R., 1976. **18**(4): p. 857-862.
211. Barner, L. and S. Perrier, *Polymers with Well-Defined End Groups via RAFT – Synthesis, Applications and Postmodifications*, in *Handbook of RAFT Polymerization*. 2008, Wiley-VCH Verlag GmbH & Co. KGaA.
212. van den Dungen, E.T.A., et al., *Investigation into the Initialization Behaviour of RAFT-Mediated Styrene–Maleic Anhydride Copolymerizations.* Australian Journal of Chemistry, 2006. **59**(10): p. 742-748.
213. Pfeifer, S. and J.-F. Lutz, *A Facile Procedure for Controlling Monomer Sequence Distribution in Radical Chain Polymerizations.* Journal of the American Chemical Society, 2007. **129**(31): p. 9542-9543.
214. Benoit, D., et al., *One-Step Formation of Functionalized Block Copolymers.* Macromolecules, 2000. **33**(5): p. 1505-1507.
215. Moad, G., et al., *New Features of the Mechanism of RAFT Polymerization*, in *Controlled/Living Radical Polymerization: Progress in RAFT, DT, NMP & OMRP*. 2009, American Chemical Society. p. 3-18.
216. Mayo, F.R., *Chain Transfer in the Polymerization of Styrene: The Reaction of Solvents with Free Radicals1.* Journal of the American Chemical Society, 1943. **65**(12): p. 2324-2329.

217. K, I., *Auto-acceleration of radical polymerization rate in polymerization of styrene under the condition of predominant transfer.* European Polymer Journal, 1987. **23**(5): p. 409-413.

218. Glass, J.E. and N.L. Zutty, *Investigation of autoacceleration effects during the solution polymerization of styrene.* Journal of Polymer Science Part A-1: Polymer Chemistry, 1966. **4**(5): p. 1223-1243.

219. Rengarajan, R., et al., *N.m.r. analysis of polypropylene-maleic anhydride copolymer.* Polymer, 1990. **31**(9): p. 1703-1706.

220. Indira, S., *Evidence of essential disulfide bonds in angiotensin II binding sites of rabbit hepatic membranes. Inactivation by dithiothreitol.* Biochimica et Biophysica Acta (BBA) - Biomembranes, 1985. **813**(1): p. 103-110.

221. Liu, J.-D., et al., *Thiol antioxidant and thiol-reducing agents attenuate 15-deoxy-Δ12,14-prostaglandin J2-induced heme oxygenase-1 expression.* Life Sciences, 2004. **74**(19): p. 2451-2463.

222. Perera, I.N., et al., *Reductive decomposition of a diazonium intermediate by dithiothreitol affects the determination of NOS turnover rates.* Talanta, 2009. **78**(3): p. 910-915.

223. Bezdushna, E. and H. Ritter, *Microwave accelerated synthesis of N-phenylmaleimide in a single step and polymerization in bulk.* Macromolecular Rapid Communications, 2005. **26**(13): p. 1087-1092.

224. Pitsikalis, M., E. Siakali-Kioulafa, and N. Hadjichristidis, *Block Copolymers of Styrene and Stearyl Methacrylate. Synthesis and Micellization Properties in Selective Solvents.* Macromolecules, 2000. **33**(15): p. 5460-5469.

225. Shang, S., S.J. Huang, and R.A. Weiss, *Synthesis and characterization of itaconic anhydride and stearyl methacrylate copolymers.* Polymer, 2009. **50**(14): p. 3119-3127.

226. Lutz, J.-F., B.V.K.J. Schmidt, and S. Pfeifer, *Tailored Polymer Microstructures Prepared by Atom Transfer Radical Copolymerization of*

Styrene and N-substituted Maleimides. Macromolecular Rapid Communications, 2011. **32**(2): p. 127-135.

227. Baumgarten, E., *Organic Syntheses, Collective Volume*. 1 ed. 1973, New York: Wiley.
228. Greases, L.a., *Base Oil Report 2010*. 2010: Falls Church,Virginia
229. Lutz, J.F., B. Kirci, and K. Matyjaszewski, *Synthesis of well-defined alternating copolymers by controlled/living radical polymerization in the presence of Lewis acids.* Macromolecules, 2003. **36**(9): p. 3136-3145.
230. Rudnick, L.R., *Lubricant Additives: Chemistry and Applications*, in *Lubricant Additives: Chemistry and Applications*, L.R. Rudnick, Editor. 2009, CRC Press.
231. Villfort.Fj, J.W. Romberg, and S.F. Chien, *RHEOLOGY.* Lubrication, 1970. **56**(2): p. 25-&.
232. Kreuz, K.L., *DIESEL ENGINE CHEMISTRY - AS APPLIED TO LUBRICANT PROBLEMS.* Lubrication, 1970. **56**(6): p. 77-&.
233. Rein, S.W., *VISCOSITY .1.* Lubrication, 1978. **64**(1): p. 1-12.
234. Mohamed, M.M., H.H.A. Elnaga, and M.F. Elmeneir, *MULTIFUNCTIONAL VISCOSITY INDEX IMPROVERS.* Journal of Chemical Technology and Biotechnology, 1994. **60**(3): p. 283-289.
235. Valcho J, J., *Highly grafted, multi-functional olefin copolymer VI modifiers*. 2007.
236. Kukin, I., *Determination of Acids and Basic Nitrogen Compounds in Petroleum Products.* Analytical Chemistry, 1958. **30**(6): p. 1114-1117.
237. Papke, B.L., L.S. Bartley, and C.A. Migdal, *Adsorption of poly(isobutenyl)succinimide dispersants onto calcium alkylarylsulfonate colloidal dispersions in hydrocarbon media.* Langmuir, 1991. **7**(11): p. 2614-2619.
238. Papke, B.L. and L.M. Robinson, *Factors Affecting Poly(isobutenyl)succinimide Dispersant Adsorption onto Surfactant-Coated Colloidal Particles in Nonaqueous Media.* Langmuir, 1994. **10**(6): p. 1741-1748.

239. Won, Y.-Y., et al., *Effect of Temperature on Carbon-Black Agglomeration in Hydrocarbon Liquid with Adsorbed Dispersant.* Langmuir, 2004. **21**(3): p. 924-932.

240. Gallopoulos, N.E., *Hydrogen Bonding between Alcohols and Motor Oil Dispersants.* I&EC Product Research and Development, 1967. **6**(1): p. 36-39.

241. Hribernik, A. and B. Kegl, *Influence of Biodiesel Fuel on the Combustion and Emission Formation in a Direct Injection (DI) Diesel Engine.* Energy & Fuels, 2007. **21**(3): p. 1760-1767.

242. Seong, H.J. and A.L. Boehman, *Impact of Intake Oxygen Enrichment on Oxidative Reactivity and Properties of Diesel Soot.* Energy & Fuels, 2011. **25**(2): p. 602-616.

243. Yasutomi, S., Y. Maeda, and T. Maeda, *Kinetic approach to engine oil. 3. Increase in viscosity of diesel engine oil caused by soot contamination.* Industrial & Engineering Chemistry Product Research and Development, 1981. **20**(3): p. 540-544.

244. Landfester, K., F.J. Schork, and V.A. Kusuma, *Particle size distribution in mini-emulsion polymerization.* Comptes Rendus Chimie, 2003. **6**(11–12): p. 1337-1342.

245. Maroto, J.A., M. Quesada-Perez, and A.J. Ortiz-Hernandez, *Use of Kinematic Viscosity Data for the Evaluation of the Molecular Weight of Petroleum Oils.* Journal of Chemical Education, 2010. **87**(3): p. 323-325.

246. Azim, A., et al., *Multifunctional Additives Viscosity Index Improvers, Pour Point Depressants and Dispersants for Lube Oil.* Petroleum Science and Technology, 2009. **27**(1): p. 20-32.

247. Adamczewska, J.Z. and C. Love, *Oxidative stability of lubricants measured by PDSC CEC L-85-T-99 test procedure.* Journal of Thermal Analysis and Calorimetry, 2005. **80**(3): p. 753-759.

248. Kodali, D.R., *Oxidative stability measurement of high-stability oils by pressure differential scanning calorimeter (PDSC).* Journal of Agricultural and Food Chemistry, 2005. **53**(20): p. 7649-7653.

249. Aureli, R., et al., *PDSC and FTIR as tools for monitoring the oxidation process of poliolefinic base stocks*. Additives'97 - Additives in Petroleum Refinery and Petroleum Product Formulation Practice, Proceedings, ed. A. Kovacs. 1997, Budapest: Hungarian Chemical Soc. 8-14.